Summer 2024

MOISTURE AND GLASS TRANSITION TEMPERATURE KINETICS FROM LONG TERM HYGROTHERMAL AGING OF CARBON/EPOXY COMPOSITES

Behnaz Hassanpour
University of Texas at Arlington

MOISTURE AND GLASS TRANSITION TEMPERATURE KINETICS FROM LONG TERM HYGROTHERMAL AGING OF CARBON/EPOXY COMPOSITES

by

BEHNAZ HASSANPOUR

Presented to the Faculty of the Graduate School of

The University of Texas at Arlington in Partial Fulfillment

of the Requirements for the Degree of

DOCTOR OF PHILOSOPHY

THE UNIVERSITY OF TEXAS AT ARLINGTON

August 2024

ACKNOWLEDGMENTS

I would like to express my deepest gratitude to God. I am thankful for the strength, hope, and inspiration that have accompanied me throughout this journey. Your presence has been a source of comfort and motivation, guiding me in times of need.

I am profoundly grateful to my supervisor, Dr. Vistasp Karbhari. Your unwavering support, wisdom, and encouragement have been the cornerstone of my academic journey. Your mentorship has helped me grow not just as a researcher, but as a person. Thank you for believing in me and for providing countless opportunities that have shaped my path.

I also wish to extend my heartfelt thanks to my committee members, Dr. Paul J. Componation, Dr. Warda Ashraf, and Dr. Himan Hojat Jalali. Your insightful feedback and dedicated time have been invaluable to the completion of this dissertation. I deeply appreciate your commitment to my success and for pushing me to excel.

A special note of gratitude goes to Dr. Abolmaali. Thank you for giving me the opportunity to work with you and for introducing me to Dr. Karbhari. Your support has been instrumental in my journey, and I am sincerely thankful.

To my parents, this achievement belongs to you as much as it does to me. Your unwavering belief in me, along with your constant support and unconditional love, has been my greatest source of strength. You have stood by my side through every circumstance, making this journey much easier than it could have been. Your sacrifices and encouragement have been the foundation of my academic endeavors, and I am profoundly grateful and forever indebted to you for all you have done.

To my dear brother, your support and encouragement have meant so much to me. Thank you for always being there, for believing in me, and for the countless ways you have helped me along the way.

To my best friend, partner, colleague, and fiancé, Sunny—thank you from the bottom of my heart. Your unwavering love and support have been my rock. Through every challenge, you were there, lifting me up and believing in me even when I doubted myself. I am beyond grateful to have you by my side.

ABSTRACT

MOISTURE AND GLASS TRANSITION TEMPERATURE KINETICS FROM LONG TERM HYGROTHEMRAL AGING OF CARBON/EPOXY COMPOSITES

Behnaz Hassanpour, PhD

The University of Texas at Arlington, 2024

Supervising Professor: Vistasp M. Karbhari

The durability of fiber reinforced polymer composites used in civil infrastructure rehabilitation has become increasingly critical, especially under long-term hygrothermal aging conditions. This study focuses on the results of long-term (up to 6 years) hygrothermal aging of wet layup carbon/epoxy composites and investigates the effects of moisture, as well as accelerated aging at elevated temperatures with varying thicknesses and fabric areal weights. The primary objective is to establish a comprehensive understanding of moisture uptake kinetics and its subsequent effects on the glass transition temperature (T_g), mechanical performance, and the resulting implications for material durability. Four papers form the core of this work: a review of moisture uptake models, an analysis of T_g as a durability characteristic, the development of a two-stage model for moisture and T_g kinetics, and an examination of the effects of various aqueous environments on moisture kinetics, glass transition temperature and mechanical properties. The findings offer insights into the interactions between moisture-induced degradation and cure progression, providing a basis for predicting the long-term performance of FRP composites in real-world applications.

LIST OF FIGURES

LIST OF TABLES

TABLE OF CONTENTS

CHAPTER 1. INTRODUCTION

Fiber reinforced polymer (FRP) composites, composed of fibers embedded in a polymer matrix, are widely used in the rehabilitation and strengthening of aging and deteriorating structures. These materials, characterized by their high strength-to-weight ratio, light weight, stiffness attributes, corrosion resistance, and ease of installation and transportation, are increasingly used in applications in civil, marine, and naval infrastructure and structural systems. In these applications, they are exposed to a range of exposure conditions, including humidity and immersion, which are known to affect the durability of constituents of composites, and the fiber–matrix interface over extended periods.

FRP has been used in various field applications, but concerns persist regarding its long-term durability under changing environmental conditions. Non-autoclave processes, such as wet layup, are employed for their adaptability, cost considerations, and ability to conform to complex geometries. This method is widely adopted for the rehabilitation of structural elements, as well as for the repair and retrofitting of aging infrastructure, enabling rapid deployment and localized reinforcement without requiring extensive demolition or reconstruction [1]. However, despite its successful implementation, the ambient temperature curing process often leads to incomplete curing, increasing the vulnerability of these materials to environmental degradation. Furthermore, there are significant gaps in the understanding of long-term durability, especially over timescales of service life expected of civil infrastructure applications.

When composites are exposed to moisture, whether through humidity or immersion in solutions, they undergo a range of reversible and irreversible effects. These include plasticization,

swelling, degradation of molecular and network structure, saponification and deterioration of the fiber-matrix bond and interphase. These effects due to the interruption of hydrogen bond interchain by water molecules can significantly alter the properties of material, often leading to a decrease in glass transition temperature (T_g) [2-8]. Understanding the long-term performance of wet layup composites under these conditions is therefore essential to ensuring their durability and safety.

Although moisture uptake may result in both reversible and irreversible deterioration of resin characteristics, it can also cause an initial acceleration of cure progression, creating a competition between mechanisms that improve performance and increase the glass transition temperature and those that deteriorate due to uptake. While a significant number of laboratory studies have been conducted under controlled and accelerated conditions, most studies often have limited exposure periods of less than a year, and a lack of long-term in-service data does not capture the full effect of moisture uptake. The lack of long-term data has led to the use of conservative safety factors and design guidelines, resulting in inefficient material use and increased costs [9-11]. Additionally, current design coefficients are often time-invariant and do not consider variations in exposure severity or the degree of cure, making it difficult to predict long-term performance under real-world conditions. Furthermore, the use of ambient temperature cure systems leads to complex interactions between cure progression effects and environmental exposure effects that make it difficult to differentiate under short-term exposure conditions. Thus, the utilization of long-term exposure and development of a comprehensive understanding of long-term mechanisms of deterioration and effects, and durability is critical and offers valuable insights that were previously unattainable with short-term experiments, enabling a better understanding of

the competing mechanisms crucial for predicting the long-term behavior of such materials in real-world conditions.

Furthermore, given the notable impact of moisture uptake on performance characteristics and glass transition temperature, a comprehensive understanding of moisture uptake characteristics and kinetics is necessary for the prediction of long-term durability as well as to ensure accurate design, safety, and economic viability. Moreover, the relationship between moisture uptake and mechanical properties and performance requires more research.

1.1. RESEARCH OUTLINE

In order to investigate moisture uptake characteristics and key effects, such as on glass transition temperature and mechanical properties, an ambient cured epoxy and a wet layup carbon/epoxy composite at different thickness levels are subjected to immersion in water over a range of temperature. This thesis is presented in an article-based format and includes four papers, building on the understanding of long-term moisture uptake and its effects on the durability of wet layup carbon/epoxy composites. The aim of this research is to conduct a comprehensive study of ambient cured systems over a range of materials and exposure conditions over periods longer than 60 months.

The first part of the dissertation (Chapter 2) presents a paper titled "*Characteristics and Models of Moisture Uptake in Fiber-Reinforced Composite: A Topical Review*." This chapter provides a comprehensive literature review on mechanisms of moisture uptake, comparing

different models and providing insights into their lacunae and the steps that can be taken to address them.

Chapter 3 presents a paper titled "*Glass Transition Temperature as a Characteristic of the Durability of Fiber-Reinforced Polymer Composites."* This chapter reviews the effect of moisture on glass transition temperature including a review and presentation of relevant models. Glass transition temperature is a critical factor in design, serving as a threshold for operational limits, and is notably affected by moisture uptake. Previous work in this area predominantly modeled the deterioration of glass transition temperature as a linear process, suggesting a continuous decrease due to moisture uptake, even though some data indicated a transition. Short-term studies contributed to a limited understanding of the competing effects of moisture-activated post-cure on glass transition temperature and the transition of glass transition temperature kinetics from a steady decrease to an asymptotic regime. The transitions and their link to the moisture uptake characteristics specifically, the transition between the initial rapid diffusion-dominated regime and the second slower relaxation regime provide a mechanistic explanation for the phenomena. These insights were initially reported in the paper presented in Chapter 5, and further elucidated in this chapter, which posited the use of glass transition temperature as a characteristic of long-term durability.

Chapter 4 of the dissertation includes the paper titled "*Moisture and Glass Transition Temperature Kinetics of Ambient-Cured Carbon/Epoxy Composites."* The goal is to present the results of long-term hygrothermal aging of wet layup carbon/epoxy composites, including through acceleration using temperature of immersion, focusing on the development of a comprehensive

understanding of moisture uptake kinetics and its effects on glass transition temperature, interface, and inter-/intra-laminar dominated performance characteristics using a two-phase model for uptake that incorporates both diffusion- and relaxation-/deterioration-dominated regimes, as well as a transition regime. This model provides a mechanistic explanation for interacting phenomena that here to fore had been difficult to describe in an integrated fashion and provides the basis for accurate prediction of the long-term response of these materials. The model is validated using long-term experimental data.

Chapter 5 presents a paper titled "*Water, Saltwater, and Concrete Leachate Solution Effects on Durability of Ambient-Temperature Cure Carbon-Epoxy Composites."* This chapter delves into the impact of different environmental exposures, including water, seawater, and alkaline solutions, on the long-term performance of FRP composites. The chapter examines the competing influences of moisture-induced plasticization, post-curing, and other degradation mechanisms, such as fiber-matrix debonding and micro-cavitation, through comparisons of glass transition temperature and storage modulus. Additionally, the chapter investigates mechanical properties like tensile strength and modulus changes across the three different solutions.

Chapter 6 presents the concluding remarks and directions for future work.

1.2. REFERENCES

Helbling C, Abanilla M, Lee L, Karbhari VM. Issues of variability and durability under synergistic exposure conditions related to advanced polymer composites in the civil

infrastructure. Composites Part A: Applied Science and Manufacturing. 2006, 37(8), 1102-1110.

2. Nogueira P, Ramirez C, Torres A, Abad MJ, Cano J, Lopez J, López-Bueno I, Barral L. Effect of water sorption on the structure and mechanical properties of an epoxy resin system. Journal of Applied Polymer Science. 2001, 80(1), 71-80.

3. Hahn HT. Residual stresses in polymer matrix composite laminates. Journal of Composite Materials. 1976, 10(4), 266-278.

4. Xiao GZ, Delamar MA, Shanahan ME. Irreversible interactions between water and DGEBA/DDA epoxy resin during hygrothermal aging. Journal of Applied Polymer Science. 1997, 65(3), 449-458.

5. Zhou J, Lucas JP. Hygrothermal effects of epoxy resin. Part I: the nature of water in epoxy. Polymer. 1999, 40(20), 5505-5512.

6. Chateauminois A, Chabert B, Soulier JP, Vincent L. Dynamic mechanical analysis of epoxy composites plasticized by water: Artifact and reality. Polymer Composites. 1995, 16(4), 288-296.

7. Abanilla MA, Li Y, Karbhari VM. Durability characterization of wet layup graphite/epoxy composites used in external strengthening. Composites Part B: Engineering. 2005 Apr 1;37(2-3):200-12.

8. Nogueira P, Ramirez C, Torres A, Abad MJ, Cano J, Lopez J, López-Bueno I, Barral L. Effect of water sorption on the structure and mechanical properties of an epoxy resin system. Journal of Applied Polymer Science. 2001 Apr 4;80(1):71-80.

9. Spelter A, Bergmann S, Bielak J, Hegger J. Long-term durability of carbon-reinforced concrete: An overview and experimental investigations. Applied Sciences. 2019, 9(8), 1651.

10. Karbhari VM, Abanilla MA. Design factors, reliability, and durability prediction of wet layup carbon/epoxy used in external strengthening. Composites Part B: Engineering. 2007, 38(1), 10-23.

11. Karbhari VM. Long-term hydrothermal aging of Carbon-Epoxy materials for rehabilitation of civil infrastructure. Composites Part A: Applied Science and Manufacturing. 2022, 153, 106705.

CHAPTER 2. CHARACTERISTICS AND MODELS OF MOISTURE UPTAKE IN FIBER-REINFORCED COMPOSITES: A TOPICAL REVIEW

The study, titled "Characteristics and Models of Moisture Uptake in Fiber-Reinforced Composites: A Topical Review," has been published in Polymers in 2024.

Hassanpour B, Karbhari VM. Characteristics and Models of Moisture Uptake in Fiber-Reinforced Composites: A Topical Review. Polymers. 2024 Aug 9, 16(16), 2265. https://doi.org/10.3390/polym16162265

CHARACTERISTICS AND MODELS OF MOISTURE UPTAKE IN FIBER-REINFORCED COMPOSITES: A TOPICAL REVIEW

Behnaz Hassanpour [1], and Vistasp M. Karbhari [1,2]

[1]Department of Civil Engineering, University of Texas Arlington, Arlington, TX 76006, USA; vkarbhari@uta.edu

[2]Department of Mechanical and Aerospace Engineering, University of Texas Arlington, Arlington, TX 76006, USA

Abstract: Fiber-reinforced composites are commonly exposed to environments associated with moisture and solution, resulting in uptake, which causes changes in the bulk resin, the fiber–matrix interface, and even the fiber itself. Knowledge about uptake behavior and diffusion mechanisms and characteristics are critical to better understanding the response of these materials to environmental exposure faced through service to developing better materials through selection of constituents and to the prediction of long-term durability. This paper reviews aspects of uptake mechanisms and sub-sequent response, as well as models that describe the sorption process, with the aim of providing a comprehensive understanding of moisture-uptake-related phenomena and characteristics such as uptake rate, diffusion and relaxation/deterioration constants, transitions in regimes, and overall response.

Keywords: fiber; resin; composite; interface; degradation; hygrothermal; diffusion; moisture; Fickian; non-Fickian; humidity

2.1. INTRODUCTION

Fiber-reinforced polymer (FRP) composites are widely used in civil infrastructure in addition to their more common application in automotive, marine/naval, and aerospace sectors due to their favorable characteristics, such as being lightweight, their high specific strength and stiffness, and their tailorability. Despite their successful use in a large number of applications, there are still concerns related to the long-term durability of the materials in harsh and changing environmental conditions [1–5]. While FRP composites have potentially enhanced durability compared to conventional materials, they undergo various levels of degradation because of environmental exposure. The response of these materials is dependent on the level of void content, type of exposure, constituents of the composites, and on the fiber–resin interface [6–11], their volume fractions, fiber configuration [2], and the process used to fabricate the component, which can result in different levels of cure progression. This, in turn, can result in changes in propensity for moisture uptake and/or environment-induced microcracking. Furthermore, environmental exposure in the field is rarely due to a single isolated environment and is generally a synergistic effect of multiple conditions, which could change and accelerate the degradation process. In addition, most data are collected through short-term laboratory testing, which rarely covers the full range and extent of exposure in the field and resulting deterioration. The effects of moisture and solution through humidity and/or immersion are often the most common in civil infrastructure applications, and these conditions can result in significant mechanical degradation, potentially causing premature failure [12,13]. To ensure the safe design of FRP structures, it is necessary to address the long-term environmental effects on performance characteristics and service life. The degree of vulnerability to degradation depends on the environment's characteristics and the distinct

reactions of each constituent. Although some fibers, such as E-glass and aramid, are susceptible to moisture, others such as carbon and basalt remain unaffected by it. However, both the resin system and the fiber–matrix interphase are vulnerable to various environmental factors, with moisture being a significant concern since it can affect the integrity of the fiber–matrix bond, as well as degrade the constituents.

To predict the service life and durability of FRPs, it is essential to develop a comprehensive understanding of the mechanisms of environmental deterioration and aging. While several environmental exposure drivers exist, such as temperature, cycling, rain, sunshine, UV, etc., a substantial understanding can be gleaned from a closer examination of water's effects on different components within the system. Polymer-based materials exhibit variable water-absorption capacities, depending on factors such as their chemical composition, formulation, and the ambient humidity and temperature conditions [14–16]. Consequently, the extent of absorption is determined not only by the material's chemical compositions and formulation, but also by the hygrothermal conditions to which they are exposed [17]. Temperature fluctuations and moisture absorption, whether through humidity or solution, induce notable modifications in the physical and chemical attributes of the polymeric matrix, consequently leading to potential degradation in the polymers and at the interface between the polymer and fiber [18]. Moisture-induced changes involve the hydrolysis of the polymer matrix chain and interfacial bond, resulting from the interruption of interchain hydrogen bonds by water molecules. This can cause an increase in intersegmental hydrogen bond length [15], increased chain mobility [19], and even internal void formation accompanying saponification [20]. Physical degradation processes include swelling, plasticization, polymer relaxation, degradation of molecular and network structure, and weakening

of the fiber–matrix bond and interphase [9,15,19,21–29]. Swelling can lead to microcracking in the weakened resin that has undergone hydrolysis, contributing to further interfacial debonding at the hydrolyzed interface, which may result in accelerated physio-mechanical degradation [27,30–38]. The chemical and physical effects resulting from exposure to hygrothermal conditions can alter the properties of polymer matrix composites, with some changes being reversible, while others are irreversible and permanent [39,40]. It is emphasized, however, that reversibility is phenomenological and depends on the details of environmental exposure and material constituents. In some cases, such as when elevated ambient temperatures follow periods of high humidity or immersion, moisture uptake and its effect can be reversed. In other cases, long periods of immersion result in reversible mechanisms not being activated. There is thus a considerable difference between field and laboratory exposure effects, as well as between short-term testing (even under accelerated conditions) and long-term exposure and testing.

While numerous environmental conditions and factors can affect the durability of FRPs, the focus of this review is on generic effects of moisture and solution, highlighting the importance of understanding their transport into the composite and the subsequent effects on the substrates. While the aspects of mechanisms of deterioration and effects of environmental exposure that cause these, as well as that of overall durability, are extremely important, this paper focuses on a topical review of models of diffusion and moisture uptake, thereby providing readers with a nuanced view not just of models, but also of the complex interactions between short- and long-term phenomena that drive the consideration and use of different models and equations that describe them. In addition, the focus is strictly on the phenomena of moisture transport without detail on the chemical

reactions and changes in morphology that are also taking place that are best considered through more involved assessments of chemistry.

2.2. MECHANISMS AND CHARACTERISTICS DUE TO MOISTURE UPTAKE

In composite materials, the performance of the composite is determined by the properties of the polymer matrix, the reinforcing fibers, and the integrity of the interface between the fiber and polymer matrix. Comprehending the distinct yet interrelated effects of moisture on the matrix, fibers, and fiber–matrix interface is essential for understanding long-term behavior and reliability. The presence of moisture alters bulk polymeric properties through interactions with polymer chains [11,41–44]. Moisture transport in polymers depends on the presence of molecular-sized voids within the polymer structure and the affinity between the polymer and water. The availability of these voids is influenced by the polymer's structure, morphology, and crosslink density, while the polymer–water affinity is governed by the presence of hydrogen-bonding sites along the polymer chains, facilitating interactions with water molecules [19].

The process of water transfer within fiber-reinforced polymer composites involves various mechanisms. Water molecules primarily permeate the polymer matrix through diffusion. Additionally, absorbed water moves throughout the composites through capillary action along the fiber–matrix interface and along crack surfaces. This absorbed moisture induces expansion and swelling of the matrix, leading to plasticization and hydrolysis, thus promoting further crack formation and augmenting water diffusion within the composites [45]. To effectively study these

interactions, it is important to distinguish between reversible and irreversible changes in the properties of the polymer matrix. This requires clarifying the definition of absorption, adsorption, and desorption, along with an understanding of their role in determining the reversibility of moisture-induced effects [46–49]. The term "sorption" is a broad term encompassing generic moisture/solution transport mechanisms, typically used when the specific mechanism of uptake cannot be pinpointed.

As shown in Figure 2-1, absorption is a process where a liquid or vapor external to a solid (referred to as the sorbate) permeates the bulk solid (referred to as the sorbent). In the case of a composite, absorption involves capillary uptake through voids, microcracks, and interface gaps, filling free space without immediate plasticization or swelling of the resin, and generates very little heat. On the other hand, adsorption takes place when a liquid or vapor external to the solid adheres to the surface of the bulk solid, forming an adsorbed phase that is no longer part of the bulk fluid. This process generates heat (heat of solution) and can result in swelling [50,51].

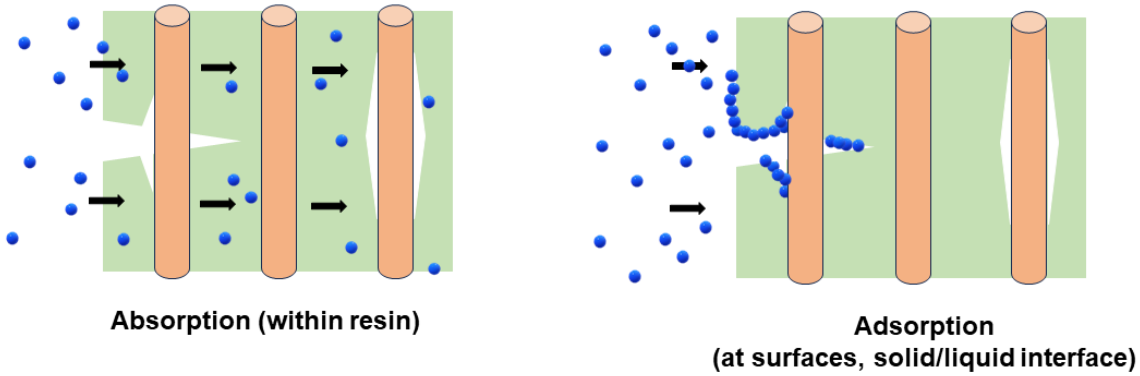

Figure 2-1. *Schematic representation of absorption into the resin and adsorption at surfaces.*

Physisorption and chemisorption are categories within adsorption, with physisorption indicating a weak interaction with the surface and chemisorption involving a strong interaction akin to chemical bonding [52]. The adsorption process is fundamental in the uptake of vapors into porous materials and is also applicable for describing vapor sorption, as well as fluid adsorption onto nonporous solid surfaces [53]. For a polymer free of voids or pores, the uptake of water is mainly an adsorption process. If a polymer contains pores, gaps, air bubbles, or other defects, both absorption and adsorption occur [51]. The pores or pathways must be of sufficient size for molecules to fill the gaps and adsorb/absorb onto the surfaces and into the material [54]. The presence of fibers results in interfacial areas resulting from the bond of the resin to the fiber, and this provides additional potential pathways for uptake. The process by which liquid molecules move randomly and the rate at which they move through the composite's bulk is known as diffusion [49]. The diffusion of moisture into polymer composites is generally perceived as a combination of absorption and adsorption processes. Liquid molecules penetrate the polymer surface upon direct contact with the composite, then progress through its bulk driven by concentration gradients, filling voids, cracks, and gaps, and subsequently reacting with the bulk polymer [38,55].

Desorption refers to the release of penetrant from the solid, to which it was previously adhered, into the surrounding vacuum or fluid. This occurs if a molecule has sufficient energy to surpass the activation barrier and the binding force. Thermal desorption involves heating the adsorbate to induce the detachment of atoms or molecules from the material. Detection and monitoring of desorption involve observing negative changes in weight, indicating a loss of weight, and complementing the positive values observed during uptake. In composite materials,

determination of the level of desorption, which is the release of previously adsorbed and absorbed moisture, helps assess the reversibility of water uptake and understand the effects of interfacial debonding and microcracking resulting from hygrothermal aging. It needs to be considered that desorption is usually difficult to achieve at the same temperature as initial immersion due to the strong interaction between the functional groups of the resin and water molecules, which disassociate only at higher temperatures [16]. For a specific mode of adsorption or absorption, it is assumed that the same mechanism is responsible for both the uptake and desorption, leading to the utilization of the same models for both phenomena. However, it is challenging to conclusively state that the desorption process is a complete reversal of the adsorption or absorption process. Studies indicate that sorption is not entirely reversible, and the diffusion coefficients, while generally assumed to be a single value for each temperature, may not be identical between the uptake and loss of a sorbate [25,26,56–58]. Thus, while the term "uptake" is generally assumed to represent the amount of solution that enters the composites, the level could be a combination of the increase in mass due to the sorption of water and the loss in mass due to mechanisms of desorption and loss of lower-molecular-weight species that leach out into the solution. The mass determined through gravimetric means, as commonly used to measure "uptake", is then the result of the competition between these mechanisms.

The exposure to moisture can result in reversible and irreversible changes, many of which are dependent on the time of exposure, temperature, and the state/type of water. Two types of water are involved in the absorption process. Free/unbound water and bound water [25]. Free water typically is the water that fills the matrix microcracks and voids without any chemical reaction with the polymer. This type of water consists of retained water molecules that can be easily

removed through thermal desorption at lower temperatures. On the other hand, bound water is chemically bonded to specific sites in the resin, such as the hydroxyl groups in the resin network. This type of water contains retained water molecules that are more difficult to remove by thermal desorption and require exposure to higher temperature levels to be removed from the resin network [59]. In the early stages of hygrothermal aging, especially during brief periods of lower temperature exposure, aging effects (such as softening), and plasticization may potentially be reversible through drying [60,61]. This reversibility is achievable if free water is involved, as it can be extracted without causing chemical reactions. Thus, reversible changes occur when moisture absorption by fiber-reinforced polymer composites (FRPs) temporarily reduces the physical properties of both the fiber–resin interface and resin. Once the free water undergoes desorption, the performance can return to its original state [60,62]. However, prolonged exposure to the environment, particularly at high temperatures, results in irreversible and permanent alterations in properties. When the resin in composites chemically reacts with bound water it can lead to hydrolysis, causing a plasticizing effect and reduction in properties. This may result in considerable damage, with desorption unable to completely reverse the absorption process. Irreversible changes can occur due to solution-induced degradation, micro-cavitation damage, deterioration of the bond between fiber and resin, and deterioration of the interface layer structure. This indicates that performance cannot be restored after removal of the solvent with irreversible degradation of the matrix, especially at temperatures well above the glass transition temperature (T_g) [27].

The glass transition temperature (T_g) holds great significance as a fundamental thermophysical property of polymers and fiber-reinforced polymer matrix composites. The glass

transition temperature is a characteristic temperature range at which an amorphous material undergoes a transformation from a rigid, brittle glassy state to a more viscous, rubbery state. It sets the upper bound for the use temperature of the material system and enables the characterization of both the cure and molecular state of the material since it depends intrinsically on chain extension and crosslinking, both of which increase T_g. As a parameter, it is also strongly dependent on chemical composition, phase morphology, and the presence of water within the polymer and hence serves to identify critical changes, both reversible and irreversible [63].

Moisture desorption is commonly performed to gauge the extent of reversibility in water absorption and to determine the potential effects of chemical and structural changes, interfacial debonding, and microcracking [64]. Desorption generally takes longer than absorption, and materials that have not reached a state of full polymerization might never completely dry because water molecules are chemically bonded to the resin at specific sites. Thus, to eliminate all water, heating above the glass transition temperature (T_g) is likely necessary, which causes deterioration [55,65].

Table 2-1 outlines degradation mechanisms, classifying them as reversible or irreversible in terms of chemical, physical, and physio-mechanical aspects. It is important to highlight that reversible processes can never achieve complete reversibility because the rearrangement of molecules inevitably results in an increased entropy of the system. Hydrolysis, typically regarded as irreversible [27], might exhibit some reversible traits through condensation or hydration reactions affecting hydrolyzed bonds [32,39,66–68].

Table 2-1. *Overview of degradation mechanisms in composites caused by moisture. (F = Fiber, M = Matrix, I = Interphase).*

Classification of Mechanism	Degradation Mechanism	Location			Reversible?
		F	M	I	Y/N
Chemical	Hydrolysis		×	×	N
	Pitting	×			N
	Chain Scission		×		N
	Debonding			×	N
Physical	Plasticization		×	×	Y
	Swelling		×		Y
	Leaching	×	×	×	N
	Relaxation (Physical Aging)		×		N
Physio-mechanical	Microcracking		×	×	N
	Micro voids		×	×	N

While there is a significant body of literature on the effect of moisture on resins and composites and of the viability, or lack thereof, of the Fickian diffusion model, there is a lack of a comprehensive review of uptake phenomena, the resulting mechanisms, and a range of models that would enable the reader to assess the suitability of models to best describe various regimes of uptake. This paper discusses that specific need.

Moisture sorption in a polymer matrix can occur through mechanisms of water dissolution within the polymer network and sorption in microscopic voids within the polymer matrix, contributing to the excess free volume in the structure and the formation of hydrogen bonds between water and the hydrophilic groups in the polymer [69]. Given the polar nature of water molecules, they bind to the polymer network through interactions, such as firmly bound direct

hydrogen bonds, multi-site interactions, dipole–dipole interactions, and van der Waals forces [70,71]. First-order hydrogen bonding involves water molecules bonding to a strongly polar region of the polymer network through its oxygen or hydrogen atoms. Dipole–dipole interactions are like hydrogen bonds, with lower dissociation energies. Van der Waals forces are characterized by very low dissociation energies. The polar characteristics of water molecules cause disruptions through these reactions, particularly disrupting Van der Waals bonds among polymer chains disturbing the existing interchain hydrogen bonds [71–74]. These lead to plasticization, enhancing chain segmental mobility [72,75] and swelling due to volumetric expansion as the interchain bond length extends [15,29,76,77], which can potentially result in a decrease in the glass transition temperature, T_g, and mechanical strength characteristics [19]. In addition, the accumulation of water molecules at polar sites on the polymer can further influence the material properties. The first-order effects of sorption, on a composite, are shown in Figure 2-2. Due to the tendency of water molecules to preferentially form hydrogen bonds with each other rather than with dissimilar polar sites on a polymer, multiple water molecules may accumulate at a single polar site through progressive hydrogen bonding, ultimately resulting in the formation of water clusters [62,78–82]. As water molecules disrupt interchain bonding through the formation of hydrogen bonds and the creation of water clusters, the distance between interchain bonds expands, leading to changes in the overall dimensions of the material [15,83].

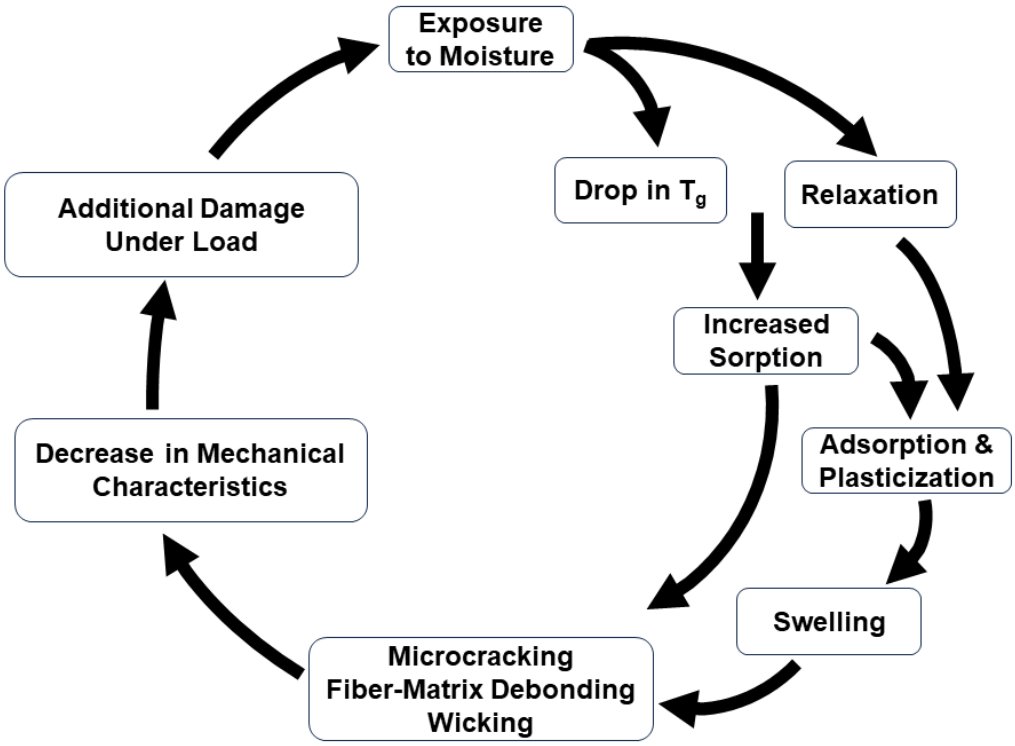

Figure 2-2. *Schematic showing first-order effects of sorption.*

The plasticization process is predominantly reversible, i.e., removing water leads to a subsequent T_g increase when transitioning from a "wet" state to a "dry" state [25]. The reversibility suggests that the polymer resin's mobility is enhanced by the presence of water due to weak interactions [19,84,85]. Water molecules that form multi-site interconnective bond complexes, however, do not contribute significantly to resin plasticization. Instead, these complexes create bridges between chain segments, leading to secondary crosslinking (pseudo crosslinking), which increases T_g [25]. An increase in exposure temperature contributes to a higher amount of multi-site interconnective bond water [25,84], thereby leading to higher T_g with increasing immersion temperatures.

Swelling resulting from water sorption increases relaxation and alters the network structure. As the polymer reacts to the swelling stress from absorbed moisture and dissipates the induced swelling stress initiated by plasticization, the network becomes more accessible to additional water [65]. The change in the polymer structure can become permanent and irreversible under certain conditions, particularly when the polymer undergoes chemical or physical aging. Physical aging occurs when polymer networks, upon cooling into a glassy state, remain in a nonequilibrium condition characterized by excess free volume or enthalpy. This state gradually diminishes over time as the polymer chains attempt to achieve a more stable, thermodynamic equilibrium. This phenomenon involves a gradual decrease in free volume and/or enthalpy, leading to adjustment in the morphology of the polymer chains towards thermodynamic equilibrium [86,87]. The presence of water within the epoxy accelerates the physical aging process due to plasticization, where water increases macromolecular chain mobility, resulting in a faster kinetic rate of physical aging [88]. Chemical aging, on the other hand, occurs when the polymer structure undergoes a chemical reaction, leading to the formation of aged polymer species [86,89]. Residual stresses developed within the polymer network during curing and subsequent cooling may undergo relaxation during the process of physical aging as a means of achieving equilibrium to balance stress disparities between areas with lower and higher crosslink density [86]. The presence of moisture further impacts this process by facilitating stress relaxation through increased chain mobility, thus altering the distribution and intensity of residual stresses. These forces arise due to the thermodynamic nonequilibrium of the glassy network and the internal stresses formed during cooling from higher temperatures. The contraction or shrinkage occurs predominantly in regions with higher crosslink density, where the polymer chains are more tightly bound and thus exhibit a higher tendency to shrink towards their centers of force [86]. With the aging of the polymer, highly

crosslinked regions ease towards a central nodular structure due to contractive forces developed during crosslinking [86]. As regions of lower density undergo physical aging, they become denser and consequently create higher levels of tortuosity in the water path. While both aging processes can initially result in an increase in T_g, the processes can also lead to degradation, where the polymer experiences a subsequent decrease in T_g [89].

Short-term plasticization can progress over time by hydrolysis, which causes chemical degradation, particularly of functional groups such as esters and ethers in polymers [43,90,91]. Alkaline hydrolysis, for instance, occurs when OH^- reacts with ester bonds, which are the weakest elements in the polymer's chemical structure. This reaction results in the formation of additional polar hydroxyl groups, potential chain scission, and exposure-related microcracking, and saponification, ultimately resulting in the fracture of the polymer molecular chain and leaching of lower-molecular-weight species (LMWS), with network linkages being attacked with increased exposure and moisture uptake [92–95]. When the polymer is exposed to water, degradation products with low molecular weight formed due to mechanisms such as chain scission may potentially diffuse out of the polymer matrix, particularly at elevated temperatures. This process can result in irreversible stiffening and embrittlement of the material [96–99]. Likewise, any remaining LMWS from the initial polymerization reaction and curing process may be driven out at higher temperatures, leading to an apparent weight loss in the polymer [100]. This phenomenon is evidenced by residual post-cure, accompanied by weight loss and some apparent increase in the glass transition temperature, followed by further degradation through chain scission [101]. Other LMWS components, such as plasticizers, mold release agents, and crosslinking agents, may also be desorbed [100,102].

While matrix degradation due to moisture is significant, the fibers themselves are also susceptible to moisture-related damage, impacting the overall integrity of polymer composites. Fibers play a critical role in bearing the loads in polymer composites, with the overall mechanical properties of the composite primarily reliant on fiber performance. Carbon and Basalt fibers show resistance to moisture, while glass and aramid fibers are prone to potential damage while exposed to moisture. Moisture attack on these fibers can lead to chemical degradation, particularly in glass fibers, even before interfacial deterioration occurs [103,104].

The phenomenon of stress corrosion cracking or, more generally, moisture-induced failure in glass fibers and glass fiber composites is recognized in both surface chemistry and fracture mechanics [104]. During the hygrothermal aging process, surface pitting and nanoscale voids can be observed on the glass fiber surface along with premature fiber failure (Figure 2-3). Initially, there is an induction period necessary for water to attain sufficient mobility on the glass surface [104]. Subsequently, water molecules interact with the silicon–oxide bonds near the glass surface, causing fiber weakening along with pitting and cracking [104]. This process occurs notably when moisture absorption is high, enabling water molecules to move freely on the glass surface and potentially initiate the hydrolysis reaction between silicon–oxide and water [105].

$$H_2O + Si\text{-}O\text{-}Si \rightarrow Si\text{-}OH + HO\text{-}Si \quad (1)$$

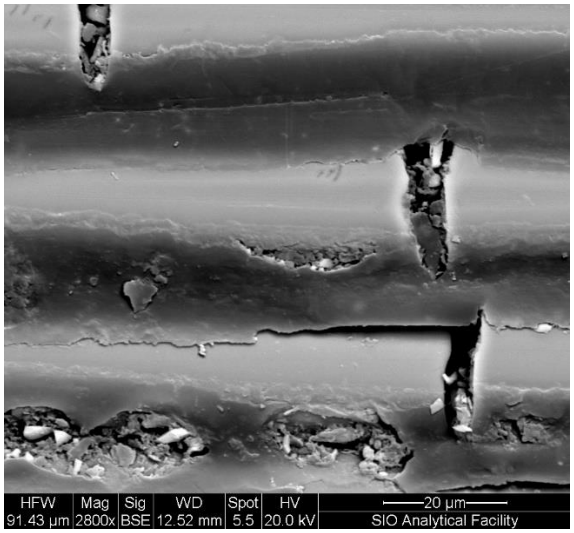

Figure 2-3. *SEM of E-Glass/Vinyl ester showing fiber level deterioration.*

This reaction occurs in three phases: adsorption, reaction, and separation. Adsorption is defined as a weak interaction between water molecules and Si-O bonds [105,106].

With glass fibers, degradation initiates as moisture draws out ions from the fiber, thus altering its structure. These ions react with water to form bases, which corrode and pit the fiber surface, creating flaws that significantly weaken strength and may cause premature fracture and failure of the fibers. Direct contact with basic solutions weakens glass fibers, leading to pitting, cracking, and leaching. This can result in rapid loss of the fiber's core and reactivity of the outer sheath, thereby accelerating the leaching process [20], although the introduction of metal ions in glass has been reported to mitigate degradation. Additionally, the hydrolysis reaction exhibits partial reversibility, with metal hydroxyls potentially forming a metal oxide layer on the fiber surface through condensation reactions or hydrations [67,107]. Therefore, employing a protective coating on the glass fiber surface is crucial to isolate the reinforcement from moisture and simultaneously enhance interfacial adhesion [34,68,107].

Aramid fibers absorb moisture, which can lead to accelerated fibrillation where a thin layer of fibrils is stripped from the fiber surface due to cohesive fiber failure. Solutions like sodium hydroxide and hydrochloric acid are known to significantly speed up hydrolysis, particularly when exposed to elevated temperatures and mechanical stress [20]. In contrast, carbon fiber exhibits stability; are highly inert and non-absorbent; and do not experience hydrolysis reactions [108,109].

The degradation of either the matrix or fiber can significantly weaken the interface, making it a region highly susceptible to deterioration and can lead to fiber–matrix debonding (Figure 2-4), which subsequently enables higher rates of moisture uptake through wicking. The interface in FRP serves as the boundary where fibers intersect with the polymer matrix, enabling load transfer based on strain compatibility. When this interface fails prematurely, the matrix's deformation or strain no longer matches that of the fibers, preventing effective load transfer from the matrix (the weaker component) to the fibers (the stronger component), thus negating the reinforcing effect of the fibers on the polymer matrix. Therefore, maintaining strain compatibility at the interface is crucial for FRP material integrity. However, achieving this compatibility is challenging under conditions of stress or environmental exposure to moisture and humidity due to mechanical (e.g., elastic modulus) and physical property differences (e.g., swelling ratio) between fibers and the matrix [110].

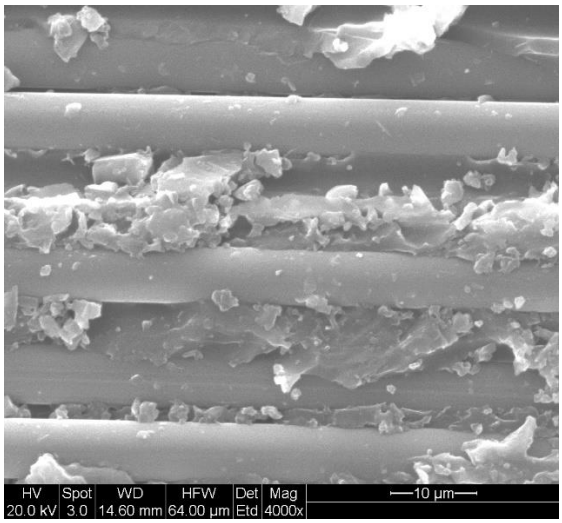

Figure 2-4. *SEM of carbon/epoxy showing regions of fiber–matrix debonding.*

Polymers commonly display a moisture uptake coefficient, denoted as β, which establishes a connection between the weight variation of the polymer due to the sorption of a solvent, like water, and corresponding volumetric alterations. This volume change is employed to calculate moisture-induced strain, using the moisture uptake values, where swelling remains negligible [43].

$$\varepsilon = \beta(M_t - M_0) \tag{2}$$

where ε is the moisture-induced strain, M_t is the moisture uptake value at time t, and M_0 refers to the reference moisture uptake level when no swelling occurs. Water molecules disrupt polymer interchain bonding via hydrogen bonds and clusters, causing dimensional changes in the material. In the case of composite materials, the moisture uptake coefficient of glass fibers is significantly lower than that of typical polymer composite matrices, while other fibers, such as carbon, exhibit negligible moisture uptake [111]. Consequently, in unidirectional composites where fibers are in the longitudinal direction, minimal swelling is observed. However, noticeable dimensional changes occur in the transverse and through-thickness directions with increased moisture uptake

[111]. The ingress of moisture induces a variable stress state before reaching saturation, and this stress distribution is contingent on the moisture concentration. According to Equation (2), delineating moisture-induced swelling strain, there exists a specific threshold moisture content that initiates a shift from compression to tension.

As water diffuses into the composite, stress gradients emerge at both macroscopic and interfacial levels. The layers with higher water concentration develop compressive moisture stresses, necessitating the development of tensile stresses further inward to maintain stress equilibrium within the bulk material [112]. These tensile stresses may induce microcracking, particularly in resin-rich areas surrounding voids [37]. Subsequently, these microcracks propagate through the resin toward interfaces, where the initiation of interfacial debonding may occur. Moisture-induced compressive stresses could contribute to the relaxation of residual tensile stresses established by thermal gradients during curing processes, potentially resulting in a strength increase before succumbing to moisture-induced resin and interfacial degradation [37]. The varying stress states occurring within the fiber–interphase–matrix region exert tensile forces on the fiber and compressive stresses on the matrix. Depending on the loading condition and material parameters [113], the interphase may experience either tensile or compressive stress, leading to significant internal stress gradients [113–115]. As the moisture content increases, the swelling strain progressively becomes more compressive. In unidirectional composites, the most substantial stresses emerge perpendicular to the reinforcing fiber. As moisture ingress takes place, the sum of forces through the thickness must equate to zero. Therefore, it is evident that the center of a sorbing species undergoes tensile loading, leading to microcracking, as polymers generally exhibit weakness in tension [116].

Additionally, differential swelling between the fiber and matrix can cause microcracks at their interface. For example, in carbon fiber polymer composites, the matrix absorbs moisture while carbon fibers do not, resulting in a mismatch in volumetric expansion. The swelling mismatch leads to microcracks during early exposure to moisture. Over longer-term exposure periods, these microcracks evolve into new paths for moisture transport, increasing morphological changes in the polymer and causing damage growth at the interface. Absorbed water can also generate osmotic pressure, potentially sufficient to cause debonding between the fiber and matrix along the interface, resulting in increased moisture sorption due to wicking [103,117,118].

Fiber–matrix debonding can lead to the potential dissolution of some matrix material into water and subsequent leaching along the interface due to hydrolysis [55,110,119–121]. Due to the interfacial debonding, the fiber reinforcement becomes vulnerable to hydrolytic attack. In carbon-fiber-reinforced polymers, the carbon fibers themselves are not affected by moisture or hydrolytic attack. However, the bond between the fibers and the matrix experiences a reduction in strength due to the decline in interfacial adhesion [122–124]. The combined effects of microcracking, high interfacial stress, and hydrolytic attack highlight the significant susceptibility of the interphasial region. As is discussed later, the presence of fibers causes a barrier to moisture transport with the passage being easier along the fiber than across it. This results in the diffusion coefficient along the length of fibers being higher than in the transverse direction [125,126]. A higher longitudinal diffusion coefficient is anticipated when interfacial debonding occurs, as water uptake through capillary action [116] resulting in an elevated rate of sorption along the interphase [67], where polymer characteristics may deviate from the bulk resin due to the resin's interaction with the fiber and sizing [67,127].

The simultaneous occurrence of physical and chemical degradation processes may impact the polymer at the surface of the composite and weaken the strength of the polymer, potentially leading to surface erosion [123,128–131]. The formation of basic micro-voids may even precede polymer blistering before surface erosion occurs. In structural composites, blistering can manifest when cracks develop within the polymer, forming macro-voids where water accumulates. The occurrence of surface erosion and cracking exacerbates the vulnerability of the fiber reinforcement, amplifying the overall degradation process.

Hygrothermal degradation due to moisture sorption can cause an increase in the molecular weight between crosslinks and a concurrent decrease in crosslink density of the polymer. The decline in crosslink density suggests that chain scission takes place in the presence of water at elevated temperatures. Classical rubber elasticity principles explain that the average molecular weight between crosslinks denoted as M_c (generally expressed in g/mol) can be effectively described as:

$$M_c = \frac{3RT\rho}{E'_{r\,p}} \tag{3}$$

where E'_{rp} represents the rubbery modulus of the polymer, R denotes the gas constant (8.3143 J/mol.K), T signifies the temperature in Kelvin, and ρ is the density of the polymer. This equation can be modified for use in composite materials as follows:

$$M_c = \frac{3RT\rho}{E'_{rp}\left(1 - V_f^n\right)} \tag{4}$$

where V_f is the fiber volume fraction, and the exponent, n, is 1/3 for fillers [132] and 1 for unidirectional composites, assuming the transverse direction is representative of the resin effect [101]. It is important to note that while the molecular weight calculations provide an acceptable order of magnitude [132], they should not be considered absolute values. Rather, these molecular weights should be understood as providing a qualitative indication of the changes occurring in the chemical structure of the composite matrix due to moisture sorption.

2.3. MOISTURE UPTAKE

Moisture uptake can occur when polymers and polymer composites come either directly or indirectly in contact with aqueous solutions or humidity. While the level of moisture content in a polymer or composite eventually reaches the maximum level when immersed in solution [55], this level (M_∞) can fluctuate through exposure to environments with varying levels of relative humidity [133].

The thermodynamic differences between saturated states of water vapor and liquid water are significant. The saturated state of water vapor, where the vapor pressure (e) equals the saturation pressure (e_s), differs thermodynamically from water. In this state, two independent phases of one molecule can coexist with equal chemical potential at equilibrium. It has been assumed that exposure to 100% relative humidity (RH) is comparable to immersion in water, to obtain isotherms for the material [36,133].

This leads to a consideration of Schroeder's paradox [134], which describes the inconsistency and difference observed in fully saturated moisture content when the material is

exposed to saturated vapor conditions compared to immersion in water at a specific temperature. Explanations for this paradox differ based on the material under consideration and include attribution of this behavior to capillary condensation in a presumed porous layer on the material surface [135], as an artifact of measurement techniques [136], or the existence of multiple solutions to a thermodynamic equilibrium equation [137].

Based on studies related to the penetration of rubber by water, it is hypothesized that a pressure gradient near the interface between water and rubber is responsible for the observed difference between exposure to the saturated vapor and water [57]. An early study on rubber treatment indicated that rubber submerged in a water solution absorbs more than when suspended in the saturated vapor above the solution. This is because the rubber seeks to achieve infinite dilution in water [41]. While a similar moisture absorption response has been observed in some polymer composites, showing reduced moisture absorption in saturated steam environments compared to water immersion at equivalent temperatures [138,139], others have been reported contrasting behavior. For example, Choi et al. [140] reported that carbon/epoxy systems can experience a greater moisture uptake in a 95% relative humidity environment than through immersion in water at the same temperature. Understanding these variations is crucial for assessing the sorption phenomena in polymer composites exposed to humid environments. It is emphasized that a single level of relative humidity can represent entirely different environments at different temperatures. In such cases, higher temperatures result in moist air containing a greater amount of water. Although water content in air is highly dependent on temperature, adsorption isotherms indicate that the relative pressure (or relative humidity for water vapor) determines the amount of vapor absorbed by a sorbent [80].

To better understand the role and effect of humidity on polymer/composite response it is important to have clarity on the phenomena itself. Relative humidity (RH) can be defined as the relationship between the actual water content in the air, indicated by its partial pressure *e*, and the maximum amount of water vapor the air can hold at the same temperature, known as saturation pressure e_s, as follows:

$$\%RH = \frac{e}{e_s(T)} \times 100\% \tag{5}$$

Alternatively, relative humidity can also be expressed in terms of the ratio between the actual water vapor dry mass mixing ratio, denoted as *w*, and the maximum (or saturation) mixing ratio, represented by w_s, at the ambient temperature and pressure conditions as follows:

$$\%RH = \frac{w}{w_s} \times 100\% \tag{6}$$

While relative humidity provides insights into atmospheric moisture levels, absolute humidity serves as a measure of the density of water vapor within a mixture of moist air and can be derived from fundamental principles [141]. The absolute humidity, denoted as d_v, is defined as follows:

$$d_v = \frac{m_v}{V} \tag{7}$$

where m_v is the mass of water vapor within a volume *V*, *e* is the partial pressure of the water vapor, n_v represents the moles of water vapor, *R* is the universal gas constant, and M_v as the molecular weight of water. The ideal gas law implies the following:

$$d_v = \frac{m_v}{n_v RT/e} = \frac{m_v e}{\frac{m_v}{M_v} RT} = \frac{eM_v}{RT} \tag{8}$$

leading to the following:

$$d_v = \left(217 \frac{\text{g} \cdot \text{K}}{\text{m}^3 \cdot \text{mbar}}\right) \frac{e}{T} \tag{9}$$

The constant 217 in this equation results from combining several constants (217 = M_v/R), where $M_v \approx 18.02$ g/mol and $R \approx 0.0831$ L·bar/mol. K). This equation shows how absolute humidity varies with temperature and relative humidity.

Isotherms are used to represent the maximum moisture content of a sorbent material as a function of partial pressure, defined as (P/P_0), where P and P_0 represent vapor pressure and saturation pressure, respectively, and represents how much moisture a substance can hold at equilibrium relative to its partial pressure [47,80]. With a basis in adsorption theory [47,80,142], isotherms, provide the theoretical basis for in the adsorption of molecules onto a surface. Incorporating thermal dependency into isotherm coefficients using isosteres [142] provides a means to introduce thermal dependency into the maximum moisture content and thus provides a means of assessing the effects of partial pressure (or humidity) and temperature on uptake.

Brunauer–Emmett–Teller (BET) [143] isotherms are used to graphically represent the relationship between the amount absorbed on a material's surface and the relative pressure at a

constant temperature. Despite the challenge of obtaining comprehensive data across relative pressures, existing studies indicate that the equilibrium moisture content does not reach a plateau at high relative pressures. Instead, the isotherms may take a range of forms as depicted in Figure 2-5. Under significantly high and low pressures, the dual sorption isotherm simplifies to a linear structure, featuring two distinct slopes at high and low relative pressures, connected by a nonlinear region.

The sorption curve follows a linear pattern at low activities, with the quantity of absorbed water at equilibrium rising nearly linearly across a broad spectrum of water activities, following Henry's law isotherm, except at low and high relative humidity. At low relative humidity, the deviation typically manifests as "type I" (curve (b) in Figure 2-5) isotherms, resembling Langmuir-type sorption isotherms (Brunauer–Emmett–Teller (BET) [143]. This type represents adsorption in a unimolecular layer. It is characterized by a rapid initial uptake of the adsorbate that quickly reaches a plateau, indicating the saturation of the adsorbent surface. Meanwhile, curve (c) in Figure 2-5 exhibits an S-shaped or sigmoid isotherm and is illustrative of a BET type II isotherm [143] under the dual sorption theory. The type II isotherm is the common type in BET analysis, showing a flatter region in the middle for monolayer formation, followed by multilayer formation at medium pressures. In curves (c) and (d) in Figure 2-5, adsorption increases as the vapor pressure of the adsorbed gas is approached, while in curves (e) and (f) in Figure 2-5, the maximum adsorption is attained, or almost attained, at some pressure lower than the vapor pressure of the gas [143]. Conversely, with high water activity, a deviation from this linearity occurs. The uptake of water at equilibrium increases markedly, potentially due to water clustering and the effect of temperature [144].

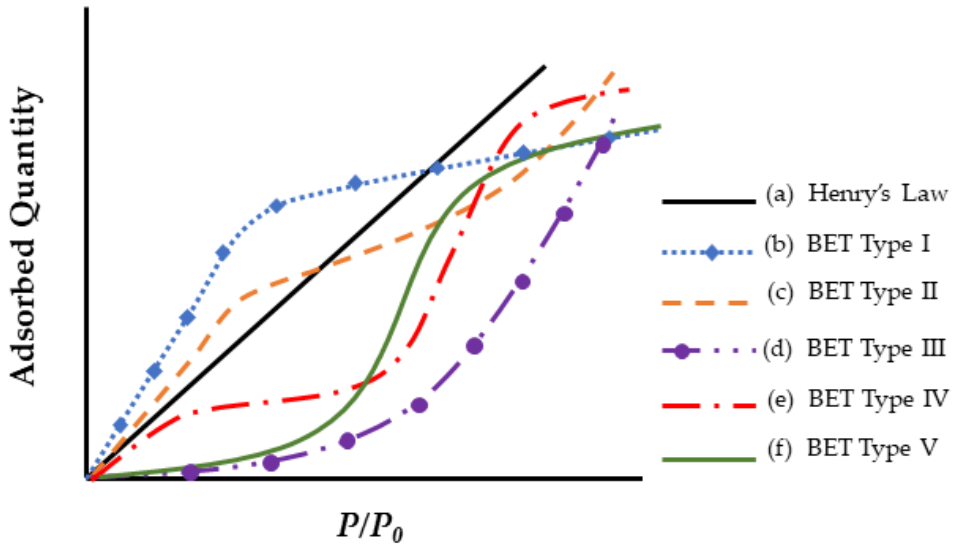

Figure 2-5. *Schematic representation of several types of isotherms. (Partial pressure (P/P_o) is shown in terms of $P \equiv$ vapor pressure and $P_o \equiv$ saturation pressure).*

It is generally accepted that the amount of sorbate absorbed is directly proportional to the partial pressure, indicative of the amount of sorbate in the air. Henry's law, in the context of equilibrium moisture content, explains this principle [145] as follows:

$$M_\infty = k\ (\%RH) \tag{10}$$

where M_∞ represents the equilibrium moisture content, (%RH) represents the percentage relative humidity level, and k is referred to as Henry's law constant, emphasizing that higher relative humidity corresponds to greater equilibrium/saturation mass uptake (M_∞) [139,146]. Henry's law has limited applicability to composites with a modified expression. Freundlich's equation can be expressed as:

$$M_\infty = a(\%RH)^b \quad (11)$$

where the constants *a* and *b* are specific to the material type, derived through a linear regression analysis of the moisture content data [147], which has been shown to have better applicability [133]. The exponent *b* has been reported to have values ranging between 1 and 4.3 [36,82,139,146], although it should theoretically be less than 1 [148]. Typical values of exponents are given as examples in Table 2-2 As can be seen, the values of a are higher for the neat resin than for the composite. Furthermore, both exponents increase with an increase in temperature of exposure, indicating the dependence of the values on temperature.

Table 2-2. *Typical values of Freundlich exponents.*

Material	a	b	Reference
Resin: 3501	6.3	1.7	[82]
Resin: NMD 2373	9.9	2.3	[82]
Composite: T300/1034	1.4	2	[133]
Composite: Glass/Epoxy	1	1	[139]
Composite: T300/1034	1.7	1	[146]
Composite: AS/3501-5	1.9	1	[146]
Composite: E-glass/epoxy at 20 °C	0.216	1.188	
Composite: E-glass/epoxy at 40 °C	0.496	1.752	
Composite: E-glass/epoxy at 60 °C	0.752	3.682	

Flory [149] and Huggins [150] developed a theory to describe polymer sorption, employing statistical analysis of polymer/solvent configurations using a lattice concept to model the random mixing of polymer and solvent, which was further developed by Apicella et al. [69]. The Flory–

Huggins theory is frequently applied to correlate penetrant activity with solution composition, formulated as follows:

$$ln\, a_s = ln\frac{P}{e} = ln\, v + (1 - v) + \chi(1 - v)^2 \quad (12)$$

where a_s denotes solvent activity, which is directly related to relative humidity; v indicates volume fraction of the solvent; χ signifies the interaction coefficient of polymer–solvent, which can be temperature dependent; and P is the equilibrium pressure, with e denoting partial pressure.

It is important that the role of these simple expressions (Henry's law and Freundlich's relation) is understood in the context of models developed for diffusion and hence a brief summary is provided herein. For example, the Langmuir model [151] is based on the following:

$$M_\infty = \frac{c(\%RH)}{1 + d(\%RH)} \quad (13)$$

whereas the dual sorption theory [144,152] addresses deviations from Henry's law by combining Langmuir sorption [151] with Henry's law [145], leading to the following:

$$M_\infty = k(\%RH) + \frac{c(\%RH)}{1 + d(\%RH)} \quad (14)$$

where k, c, and d can be expressed using Henry's law dissolution constant, determined through the statistical thermodynamic analysis of Langmuir's theory, such that

$$k = k_D p_0 \ , \quad c = C'_H b p_0 \ , \textit{and} \quad d = b p_0 \tag{15}$$

where k_D is the hole affinity constant, b is the hole saturation constant, $C_{H'}$ is the Langmuir capacity constant, and p_o is saturation vapor pressure.

Essentially, the dual sorption theory operates on the premise that water initially permeates the sorbent as free water through normal diffusion processes, following Henry's law, and can subsequently transform into an immobilized form as bound water at points within the micro-heterogeneous medium, characterized by its equilibrium conforming to the Langmuir isotherm [144]. When considering the kinetic aspect of dual sorption theory, known as Langmuir diffusion, additional assumptions come into play, which are further discussed in subsequent sections.

2.4. MOISTURE UPTAKE AND DIFFUSION

Gravimetric measurement techniques are commonly used to record moisture uptake of fiber-reinforced polymer (FRP) composites [153]. Samples are immersed in solution at a constant temperature and the absorption of water is monitored over time during immersion, enabling the observation of sorbate diffusion into a single sorbent specimen over time and providing the overall mass change due to sorbate uptake or loss, rather than concentrating solely on concentration [154,155]. The determination of moisture content at any time t, M_t, is specified as follows:

$$M_t = \frac{w_t - w_0}{w_0} \times 100 \tag{16}$$

where w_t is the mass of the sample immersed in water at time t, and w_0 refers to the initial mass of the specimen before immersion. In cases where there is no material degradation, water content

increases with immersion time an initial segment where moisture content increases linearly with time, followed by the attainment of an asymptote known as the equilibrium water content. The duration of immersion time significantly affects the uptake profile. However, there are cases where the moisture uptake does not reach equilibrium through the exposure period and instead continues to increase as polymer chains rearrange over time due to moisture penetrant molecules, resulting in further absorption at a slower rate than the initial uptake. This prolonged exposure to moisture significantly affects the physical, chemical, and mechanical properties of the composites, highlighting the importance of understanding its impact for assessing their long-term behavior and durability in these applications [95,156].

It is important to not just determine levels of uptake, but also the overall profile as represented by moisture content M_t plotted against the square root of time $t^{1/2}$, since these can provide rapid insight into the mechanisms and effects of uptake. A representative set of generic profile shapes is shown in Figure 2-6. These include the typical Fickian pattern, characterized by linear initial uptake up to around $0.6M_t/M_\infty$ and concave asymptotically towards the x-axis as M_t approaches the system's equilibrium content, M_∞. Alternatively, non-Fickian sorption may present itself with initial sigmoidal uptake, two-stage phenomena, or other anomalous features. Sigmoidal sorption, illustrated in Figure 2-6, represents characteristic non-Fickian behavior. The curves exhibit an S-shaped pattern, indicating a point of inflection. In the early 1960s, Long and Richman [157] introduced the variable surface concentration (VCS) model, which provided a detailed interpretation of experimental observations and was likely the first to reasonably explain two-stage sorption behavior [158]. They proposed that while the transport process follows Fickian principles, the delayed attainment of equilibrium at the material surface leads to unusual kinetics.

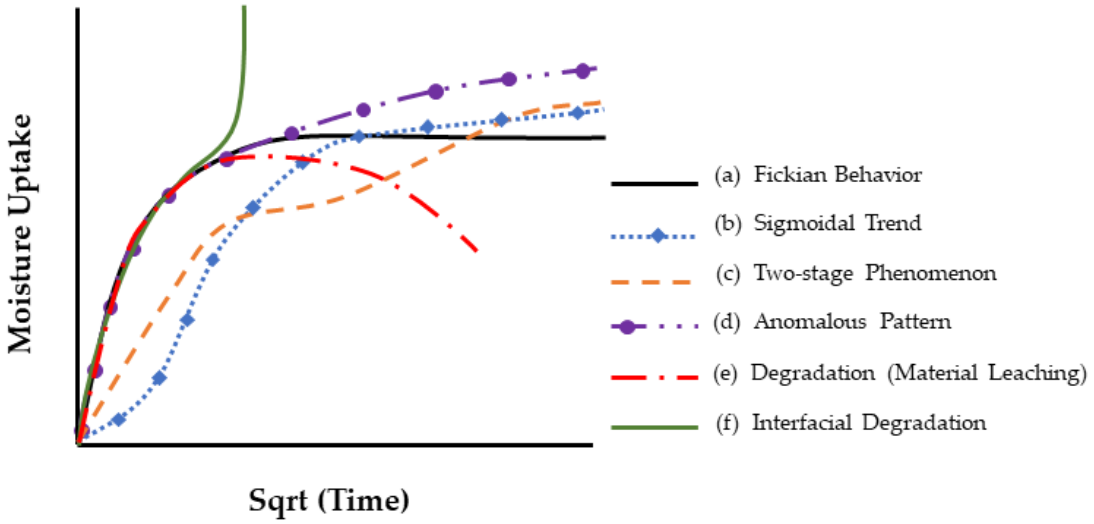

Figure 2-6. *Characteristic moisture uptake profile in polymeric composites.*

Two-stage sorption depicts a commonly reported profile for moisture uptake wherein the uptake curve consists of two distinct segments: (1) rapid Fickian absorption and (2) slower non-Fickian absorption. The curve initially follows a Fickian pattern until it starts to plateau. Instead of reaching the saturation level typical for Fickian absorption, the curve extends into a non-Fickian region. Ultimately, saturation is achieved over a longer period of exposure. A theory providing a satisfactory explanation for the characteristics of two-stage sorption was proposed in 1978 by Berens and Hopfenberg [159]. Severe departures from the commonly assumed Fickian response are shown in Figure 2-6, marked (e) and (f), and are associated with weight loss and a rapid increase in fluid content, respectively. Sorption patterns initially showing the uptake of sorbate may eventually decline after reaching a maximum uptake, as illustrated by curve (e), suggesting sorbent loss. Curves exhibiting sudden uptakes after an apparent equilibrium, like the one in curve (f), signify sorbent breakdown, such as interfacial wicking in composites, resulting in significant increases in moisture content. Weight gains along curves b-d, suggest reversible or, nearly

reversible, effects of fluids on polymeric composites, while weight gains along curves (e) and (f) indicate irreversible fluid-induced damage that may cause permanent material property degradation. Weight gain recordings along curve (f) are associated with extensive fiber–matrix debonding and degradation, while curve (e) indicates significant material loss due to the leaching of material (polymer or fiber), both exhibiting irreversible absorption behavior. It is emphasized that profiles obtained at one exposure condition could change dramatically through changes in exposure temperature, stress level, fluid acidity, or exposure duration [160,161].

Several foundational assumptions underlie the interpretation of moisture uptake curves. Primarily, it is presupposed that an increase in weight corresponds to an increase in the sorbate population within the sorbent. When the sorbate is extracted to retroactively calculate true weight gain post-degradation, the weight loss is considered to signify the removal of all sorbates and no sorbent. In other words, if LMWS are leached into the exposure environment, it is assumed that no additional LMWS are leached into the desorption environment. It is further assumed that impurities, such as metals or salts in solution, do not diffuse into the sorbent. Prior investigations indicate that solutions containing ions do indeed absorb into the specimen, but the modes of transport differ from those of water molecules [162].

Figures 2-5 and 2-6 present two different depictions of isotherm graphs for fiber-reinforced polymer (FRP) composites, illustrating different aspects of moisture interaction with the material. Figure 2-5 shows adsorbed quantity versus relative pressure, representing adsorption on the material's surface and how water vapor adheres as relative humidity increases. This graph typically displays relative pressure (P/P_0) on the x-axis and the amount of gas adsorbed (in cm^3/g or mol/g)

on the *y*-axis, providing insights into the composite's surface properties and porosity. Figure 2-6, on the other hand, depicts the bulk absorption of water into the material over time. The key differences between these isotherms include the physical processes they represent—surface adsorption in Figure 2-5 versus bulk absorption in Figure 2-6—their time dependency, and the information they provide. Adsorption isotherms, typically measured at equilibrium, offer insights into surface properties and porosity, while absorption isotherms, showing the kinetics of water uptake over time, inform about the material's overall moisture uptake capacity and rate.

The process of water uptake in polymers can be analyzed through the lens of diffusion, which is the process by which matter moves from one part of a system to another due to random molecular motions. Heat transfer by conduction also occurs because of random molecular motions, and there is a clear similarity between these two processes. Fick [163] recognized this and was the first to quantify diffusion by using the mathematical equation for heat conduction, assuming steady-state flow. The mathematical theory of diffusion in isotropic substances is thus based on the idea that the rate at which a substance diffuses through a unit area of a section is proportional to the concentration gradient measured perpendicular to the section [49]. Adolf Fick's first law [163] describes the diffusion process into a specific sorbing medium, as flux moving from regions of high concentration to those of low concentration as follows:

$$J = -D \cdot \nabla C = -D \cdot \frac{dC}{dx} \tag{17}$$

where *J* represents the total one-dimensional flux and rate of transfer per unit area of section, and *D* stands for the diffusion coefficient. The diffusion coefficient is defined in units of area per time, illustrating the rate of diffusion into or out of a sorbent medium. The concentration gradient along the *x*-axis is $\nabla C = dC/dx$, where *x* signifies distance through the sorbate, *C* represents the concentration of sorbate per unit of sorbent, and *t* represents time. The negative sign in the equation indicates that diffusion occurs in the direction of decreasing concentration.

Fick's second law [49] of diffusion explains how the concentration profile changes over time during diffusion. It states that the rate of change of concentration over time is proportional to the second derivative of concentration with respect to position in three dimensions, *x*, *y*, and *z*, with the diffusion coefficient *D* serving as the proportionality constant as follows:

$$\frac{dC}{dt} = D\left(\frac{d^2C}{dx^2} + \frac{d^2C}{dy^2} + \frac{d^2C}{dz^2}\right) \tag{18}$$

When diffusion is simplified to a single dimension, with a concentration gradient solely along the *x*-axis, then the equation reduces to the following:

$$\frac{dC}{dt} = \nabla \cdot [D(\overline{\nabla} C)] = D\left(\frac{d^2C}{dx^2}\right) \tag{19}$$

Adolf Fick's contribution to diffusion theory extends to recognizing diffusion as a dynamic molecular process and discerning the differences between a steady state and true equilibrium.

Fick's laws fundamentally necessitate a diffusion coefficient to express the rate of diffusion and commonly require achieving an equilibrium content, where the uptake rate gradually diminishes to zero as equilibrium is reached. Material characteristics, geometry, processing factors, and environmental exposures are factors that can influence and describe the parameters.

The influence of temperature on the diffusion coefficient, as widely recognized, is crucial in understanding moisture absorption in polymer composites. Studies have extensively explored how the rate of uptake, characterized in part by the diffusion coefficient varies with factors such as polymer type [100,102], crosslink density [164], degree of cure [165–167], filler type [82,168], and filler amount [45,169,170]. While the diffusion coefficient may vary over time [121,171], changes typically correlate with evolving concentration gradients, stress conditions, or reaction fronts. Increasing the temperature accelerates aging by modifying the diffusion rate, mechanism, and solubility [172–174]. Increased temperature leads to a higher diffusion rate due to increased molecular mobility and greater free volume [172]. According to the theory of free volume outlined in [175], available space between molecules increases as the temperature rises, starting from zero at absolute zero. When applied to viscoelastic polymers, the theory proposes that the viscosity and stiffness of the material depend on the amount of free volume within it [176]. Therefore, adding a diluent, such as water, to a polymer is expected to increase the overall free volume of the system, enhancing the movement of the polymer network [177].

It is noted that the temperature-dependent phenomenon [178] is frequently characterized through the Arrhenius relationship.

$$D = D_o \, exp\left[\frac{-E_a}{RT}\right] \tag{20}$$

where D_o represents temperature-independent empirical constant, E_a is the activation energy, R is the universal gas constant, and T represents temperature in degrees Kelvin. The activation energy, which represents the threshold that must be overcome to activate a mechanism/state, can be determined from the slope of a plot of $ln(D)$ versus $(1/T)$, and this is seen to vary not just with resin and type of composite, but also the thickness of the composite and the nuances of processing, especially as related to the degree of cure. Bonniau and Bunsell [139] reported activation energies of 47. 2 kJ/mol K and 43.9 kJ/mol K for E-glass/epoxy composites using diamine and dicyandiamide hardeners, respectively, wherein the former showed Fickian response and the latter with lower energy showed a two-stepped response. Karbhari [84] based on wet layup of carbon/epoxy reported activation energies of 71.02 kJ/mol K, 61.18 kJ/mol K, and 63.37 kJ/mol K, for the neat epoxy, one-layer composite, and two-layer composite, respectively, emphasizing that the decrease in activation energy for the composite was due to water-uptake-induced damage at the fiber–matrix interphase level.

However, the Arrhenius model may not always accurately describe the influence of temperature on degradation kinetics. Experiments have shown deviations from Arrhenius behavior, such as curvature instead of linear response, particularly in studies of polymer degradation [179], indicating that the overall lifetime of materials can be represented as the sum of individual processes, where the combined Arrhenius terms may exhibit non-Arrhenius behavior.

Thus, while the Arrhenius relationship is useful for describing the thermal dependency of D, by determining D_o and E_a, a dual Arrhenius model [179] can be expressed as:

$$D = D_{o1}\, exp\left[\frac{-E_{a1}}{RT}\right] + D_{o2}\, exp\left[\frac{-E_{a2}}{RT}\right] \tag{21}$$

where D_{o1} and E_{a1} represent the empirical diffusion coefficient and activation energy of the first phase, and D_{o2} and E_{a2} denote the corresponding values for the second phase.

While the Arrhenius model provides a reasonable approach for predicting the long-term behavior of FRP composites based on moisture uptake trends, it operates under the assumption that the dominant degradation mechanisms of the material remain constant over time and temperature during exposure, but the rate of degradation increases with the increase in temperature [180–182]. Zhou et al. [182], among others, presented an approach to calculate the time shift factor (TSF), between two solutions with the assumption that the Arrhenius time–concentration relationship remains applicable across the complete concentration range. Wu et al. [183] also recently employed a temperature shift factor (TSF) across various temperatures to forecast the prolonged effectiveness of Basalt fiber-reinforced polymer (BFRP) bars in an alkaline solution as follows:

$$\text{TSF} = exp\left[\frac{E_a}{R}\left(\frac{1}{T_0} - \frac{1}{T_1}\right)\right] \tag{22}$$

where T_0 and T_1 denote temperatures pertaining to Arrhenius plots.

The activation energy (E_a) for diffusion provides insight into the energy threshold needed for moisture diffusion. For instance, a lower activation energy of the resin suggests a weaker diffusion barrier and thus greater moisture absorption. The activation energy required for moisture diffusion depends on the type of water absorbed in the polymer. When water molecules enter a bulk polymer sorbent, they may exist in two states: free water and bound water [25,184]. Zhou and Lucas [62] investigated the mobility of water in different epoxy systems and reported that water molecules adhere to epoxy resins through hydrogen bonding, identifying two types of water in epoxy resins based on differences in the bond complex and activation energy. The quantity of bound water strongly depends on the exposure temperature, duration of exposure, and hygrothermal condition. Higher temperatures and longer exposure times result in a greater amount of bound water. Zhou and Lucas [25] observed a notable difference in activation energy required for desorbing bound water (around 15 kcal/mol) compared to free water (around 10 kcal/mol). This contrast in activation energies indicates variations in the binding strengths between water molecules and the resin and provides an explanation for deviation from the Fickian profile in Figure 2-6.

The understanding of effects of solution and humidity on moisture uptake in polymers highlights the importance of considering sample geometry in experiments. When measuring moisture absorption in materials, small plate-shaped samples are often used, because the time required for saturation increases with the square of the panel thickness. These samples are typically sized such that one dimension is much smaller than the other two, leading to moisture uptake

mainly through the broad faces of the plate. The moisture concentration can then be approximated using the solution for diffusion in an infinite plate, resulting in a linear increase in total moisture content with the square root of time ($t^{1/2}$) during the initial phase of absorption [133,170,185]. However, in practice, moisture uptake is not one dimensional. The width–thickness and length–thickness ratios of specimens, impact moisture absorption, resulting in the importance of accounting for edge effects. The edges of the composite samples are prone to localized moisture ingress due to surface flaws and exposed fibers known as the edge effect. Neglecting edge correction factors to account for this discrepancy can lead to inaccurate results and underestimate the overall moisture absorption characteristics of the composite material.

Figure 2-7, as an example, presents the distribution of moisture concentration $C(x,t)$ normalized by the initial concentration C_0 as a function of the position x/l in a symmetric, thin, unidirectionally reinforced composite sample of thickness $2l$, where the thickness coordinate x ranges from $-l$ to l, originating from the midplane. The curves are plotted for different time steps, with the direction of increasing time indicated by the arrow. Fluid absorption leads to material expansion, causing a non-uniform variation across the sample's thickness during the transient diffusion state. This results in time-dependent, non-uniform in-plane stress, denoted as $C(x,t)$. Higher moisture concentration exists near the edges until saturation is reached [186]. Furthermore, the presence of fibers at the edges facilitates a pathway for increased absorption, leading to more degradation in that area. The higher moisture uptake at the edges is accelerated by capillary action and interfacial wicking through microcracks and along debonded fiber–matrix interfaces, leading to a dramatic increase in moisture content. At saturation, the difference in moisture concentration across the specimen approaches zero, showing a uniform distribution. To compensate for water

penetrating through the edges, the “edge effect” must be considered, and adjustments must be made for moisture uptake through all surfaces and edges [187]. It needs to be considered that while thin specimens absorb moisture faster, thick specimens take longer to reach saturation, making the use of edge correction factors more important.

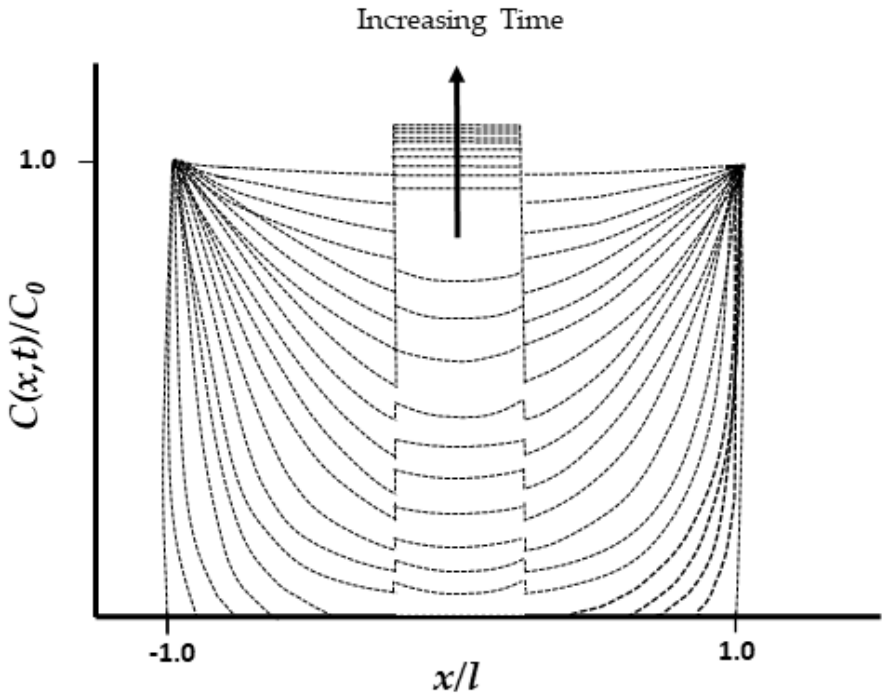

Figure 2-7. *Moisture concentration distribution at various times along the thickness direction.*

2.5. DIFFUSION MODELS

The discussion in the previous section focused on mechanisms of uptake and basic theories. However, what is needed is full models that describe uptake as a function of time and consider the various factors that influence rate, level, and maximum moisture uptake.

Uptake is representative of absorption, which involves both solubility and diffusivity, underlining the essential understanding of moisture diffusion mechanisms in polymer matrix composites. Upon direct contact with the composite, liquid molecules penetrate the polymer surface and move through its bulk, driven by concentration gradients [38,188]. This process is characterized by the random motion and the rate at which liquid molecules move within the composite's bulk. Polymers exhibit various diffusion behaviors, according to the relative rates of diffusion and polymer relaxation [49,51].

Selecting appropriate models for analyzing moisture uptake in fiber-reinforced polymer composites is important as the moisture uptake behavior often deviates from the Fick model as shown schematically in Figure 2-6.

The consequences of choosing an inappropriate model include premature termination of gravimetric monitoring of materials, failure to detect degradation phenomena that occur over longer absorption times, inaccurate estimates of maximum and saturation moisture uptake values, and misleading material characterization. Therefore, careful consideration in model selection is essential to accurately analyze moisture absorption behavior in polymer composites. Moreover, accurately determining diffusivity and moisture uptake within a polymer composite is crucial for predicting moisture-induced degradation effectively.

Among these models, one frequently utilized for steady-state one-dimensional diffusion is described by Fick's laws [163], owing to its simplicity. Case I Fickian diffusion entails a diffusion rate unaffected by concentration. This occurs in polymers when the mobility of polymer segments is greater than that of the diffusing molecules, allowing liquid molecules to have minimal impact

on the process. Rubbery polymers typically demonstrate Fickian diffusion due to their rapid response to environmental changes. Additionally, many glassy polymers also display Fickian diffusion under conditions where liquid solubility levels are relatively low. Case II Fickian diffusion, on the other hand, describes a situation where the diffusion rate is strongly influenced by concentration. This phenomenon is notable when absorbed liquid enhances polymer segment mobility via plasticization, thus easing diffusion. Case II Fickian diffusion commonly occurs when the diffusion rate exceeds polymer segment mobility, particularly observed in glassy polymers and with highly absorbent liquids. Non-Fickian or anomalous diffusion occurs when the mobility of polymer segments is comparable to the diffusion rate. This type of diffusion represents an intermediate state between the distinct behaviors observed in case I and case II diffusion.

The Fickian diffusion model offers a direct method to assess the water absorption of polymer composites. The conventional treatment of Fickian diffusion involves analyzing the one-dimensional aspect of Fick's second law shown by Equation (19) [155,166,189–194]. Fick's laws were developed based on fundamental heat-transfer equations, resulting in well-established solutions for the plane sheet case [49,195]. For an infinite plate, the moisture content in the isotropic ($D_x = D_y = D_z = D$) rectanguloid can be calculated assuming the materials follow 1-D Fickian behavior. The coefficient D is expected to remain constant regardless of time and position [196]. Considering a uniform initial distribution of sorbent, the solution to Fick's second law can be expressed as follows [48,49]:

$$\frac{C(x,t)-C_0}{C_1-C_0} = 1 - \frac{4}{\pi^2}\sum_{n=0}^{\infty}\frac{(-1)^n}{(2n+1)^2} exp\left[-\frac{Dt}{h^2}\pi^2(2n+1)^2\right] cos\left[\frac{(2n+1)\pi x}{h}\right] \qquad (23)$$

where D is the diffusion coefficient, C_0, is the initial distribution of sorbent within a plane sheet with surfaces held at a constant concentration, C_1. This describes the moisture concentration distribution $C(x,t)$ through the thickness of the plate, x, spanning from $-h/2$ to $+h/2$ for a plate thickness h over time, t. M_t, the total moisture content over time, is determined by integrating $C(x,t)$ through the thickness from $-h/2$ to $+h/2$ [122,189,197–199]:

$$M_t = M_\infty \cdot \left\{1 - \frac{8}{\pi^2}\sum_{n=0}^{\infty}\frac{1}{(2n+1)^2}exp\left[-\frac{Dt}{h^2}\pi^2(2n+1)^2\right]\right\} \quad (24)$$

where M_∞ is the equilibrium moisture uptake level.

It is fundamentally assumed that the mechanisms governing the diffusion of moisture into and out of a material are identical, leading to diffusion coefficients and trends for absorption and desorption. However, it has been consistently proven that this assumption should not be strictly followed because desorption trends fail to replicate absorption trends in many cases due to the presence of bound water [26,56–58,62,121].

Crank [49] proposed a short-time approximation for Equation (24) as follows:

$$M_t = M_\infty \cdot \frac{4\sqrt{Dt}}{h} \cdot \left\{\frac{1}{\sqrt{\pi}} + 2\sum_{n=1}^{\infty}(-1)^n \text{ ierfc } \frac{2\sqrt{Dt}}{nh}\right\} \quad (25)$$

which can be further simplified when M_t/M_∞ < 0.6 as suggested in [49,57,200,201] to the following:

$$M_t = \frac{4M_\infty}{h} \cdot \sqrt{\frac{Dt}{\pi}} \tag{26}$$

emphasizing that the initial level of moisture absorption is directly proportional to the square root of time. This correlation is commonly used to determine if moisture uptake is Fickian [77,202–204], in addition to the requirement for attainment of an equilibrium level. Intrinsically, this suggests that an increase in temperature results in a higher rate of uptake and faster attainment of equilibrium as shown in Figure 2-8.

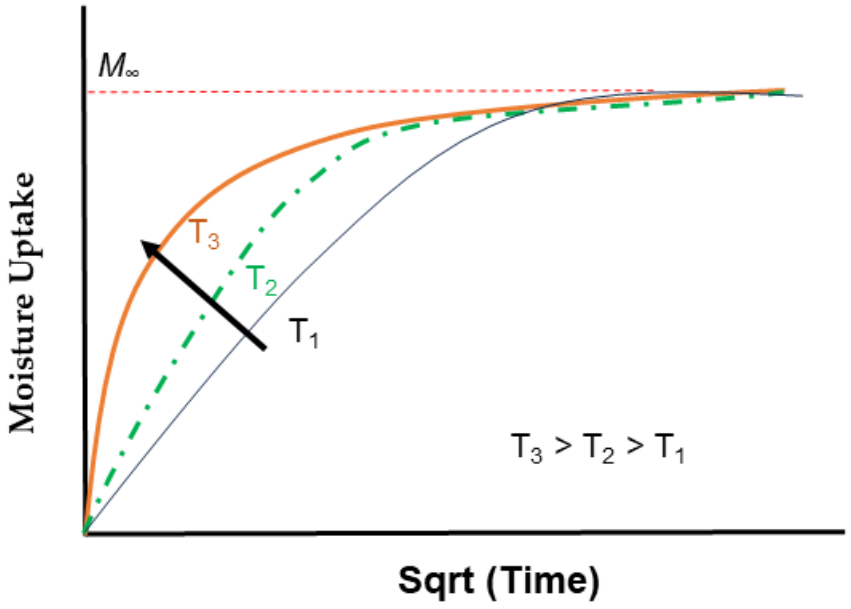

Figure 2-8. *Schematic showing the effect of temperature on rate and attainment of equilibrium for Fickian uptake.*

It should be noted that the use of Equation (26) is comparable to assuming that, during short times of uptake, a plane sheet can be regarded as a semi-infinite medium, exhibiting a uniform concentration within the sorbent, and a constant and consistently uniform concentration at the surface [49,57,133,195]. Grammatikos et al. [33] suggest that Equation (25) can be used to calculate moisture content over both long-term and short-term periods of exposure as follows:

$$\frac{M_t}{M_\infty} = \frac{4}{\pi^2}\sqrt{\frac{Dt}{h^2}} \qquad \text{when} \qquad Dt/h^2 < 0.04 \tag{27}$$

and

$$\frac{M_t}{M_\infty} = 1 - \frac{8}{\pi^2} exp\left(\frac{-Dt}{h^2}\pi^2\right) \qquad \text{when} \qquad Dt/h^2 > 0.04 \tag{28}$$

Shen and Springer [133], based on a consideration of variation of the part of Equation (24) in parentheses with dimensionless time $t^* = \frac{D_x t}{s^2}$, suggested that:

$$M_t \approx M_\infty \cdot \left\{1 - exp\left[-7.3\left(\frac{Dt}{h^2}\right)^{0.75}\right]\right\} \tag{29}$$

with diffusivity obtained from the initial slop of the uptake curve as shown in Figure 2-9.

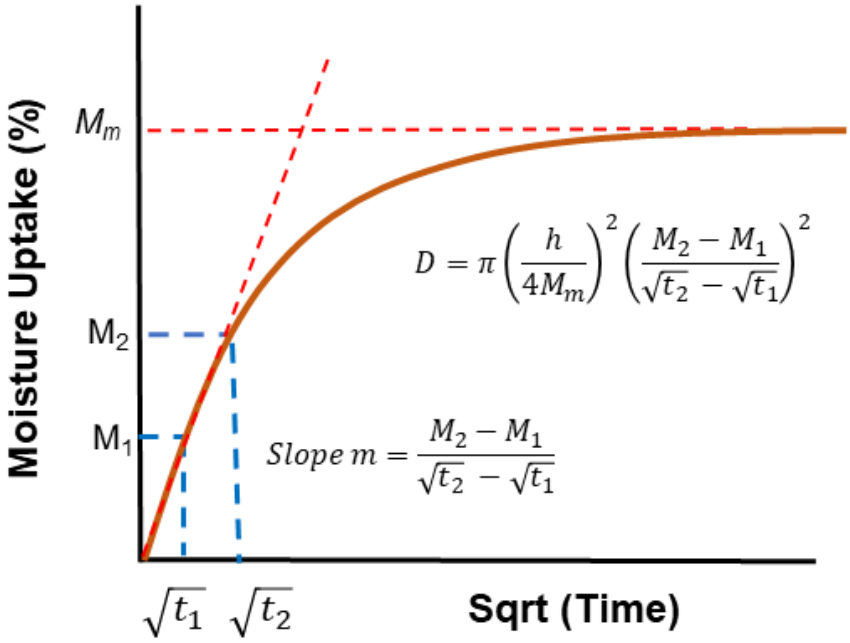

Figure 2-9. *Schematic showing determination of diffusivity for Fickian uptake (following [133]).*

Equation (29) is widely used for composites. The model, which is used extensively, overlooks the contribution of edge diffusion while providing reasonable estimates of *D* in the direction of fastest solution transport. However, edge diffusion becomes significant when the fastest diffusion direction aligns with the plate's plane. Using a 1-D model can then potentially introduce significant errors, with discrepancies of up to 50% in derived diffusion coefficients [55]. Consequently, a 3-D Fickian model is often used with anisotropic diffusion coefficients following [204,205] as follows:

$$\frac{M_t}{M_\infty} = 1 - \left(\frac{8}{\pi^2}\right)^3 \sum_{i=0}^{\infty}\sum_{j=0}^{\infty}\sum_{k=0}^{\infty} \frac{exp\left[-\pi^2 t\left[D_x\left(\frac{2i+1}{a}\right)^2 + D_y\left(\frac{2j+1}{b}\right)^2 + D_z\left(\frac{2k+1}{c}\right)^2\right]\right]}{\left((2i+1)(2j+1)(2k+1)\right)^2} \quad (30)$$

where *a*, *b*, and *c* represent the plate dimensions along the *x*-, *y*-, and *z*-axes, respectively, and D_x, D_y, and D_z denote the diffusion coefficients along the corresponding axes. When experimentally determining diffusion coefficients, if the plate's thickness is significantly smaller than its other dimensions, neglecting the edges is acceptable, and Equation (29) can be used to determine *D* values. Conversely, if edge effects on all six surfaces need to be considered, particularly when the sample's thickness is comparable to its length and width, then edge correction factors, *f*, must be considered. For the case of anisotropic materials, Fick's second law Equation (19), can be presented in Cartesian coordinates, incorporating distinct diffusion coefficients D_x, D_y, and D_z, along the global *x*, *y*, and *z* directions, respectively [48]. In such cases, Equation (19) takes the following form:

$$\frac{\partial C}{\partial t} = D_x \frac{\partial^2 C}{\partial x^2} + D_y \frac{\partial^2 C}{\partial y^2} + D_z \frac{\partial^2 C}{\partial z^2} \quad (31)$$

Assuming that diffusion coefficients are independent of time and concentration, an effective diffusion coefficient can be introduced, analogous to approaches in heat transfer [195] as follows:

$$\frac{\partial C}{\partial t} = D\left(\frac{\partial^2 C}{\partial \varepsilon^2} + \frac{\partial^2 C}{\partial \eta^2} + \frac{\partial^2 C}{\partial \zeta^2}\right) \tag{32}$$

where C is the equilibrium concentration, and ε, η, and ζ represent the transformed coordinates defined as follows:

$$\varepsilon = x\sqrt{\frac{D}{D_x}} \ , \eta = y\sqrt{\frac{D}{D_y}} \text{ and } \zeta = z\sqrt{\frac{D}{D_z}} \tag{33}$$

and D_x, D_y, and D_z are diffusion coefficients along x, y, and z directions, respectively. In the case of non-steady-state diffusion into a thin plate with dimensions l, w, and h along the x, y, and z directions, respectively, where h is significantly smaller than l and w, a simplified relation between dimensions and diffusion coefficients was proposed by Jost [48]:

$$\frac{l}{w} = \sqrt{\frac{D_x}{D_y}} \tag{34}$$

Given the fundamental assumption for diffusion into a thin plate of non-interference diffusion along the different directions, a supplementary derivation of the effective anisotropic diffusion coefficient, denoted as D, following the approach in [133] for a thin plate, leads to the following:

$$\frac{\sqrt{D}}{h} = \frac{\sqrt{D_x}}{l} + \frac{\sqrt{D_y}}{w} + \frac{\sqrt{D_z}}{h} \tag{35}$$

where D_x, D_y, and D_z rely on the orientation of the anisotropic medium under consideration, and l, w, and h, as before, are length, width, and thickness, respectively. In the case of unidirectional continuous fiber-reinforced composites, Shen and Springer [133] suggest the following:

$$D_a = D_x \left(1 + \frac{h}{l}\sqrt{\frac{D_z}{D_x}} + \frac{h}{w}\sqrt{\frac{D_y}{D_x}}\right)^2 \tag{36}$$

where D_x, D_y, and D_z represent the diffusion coefficients in the x, y, and z directions, respectively, with z designated as the fiber direction. Additionally, h, w, and l represent the specimen's thickness, width and length, respectively, with length corresponding to the fiber direction. Transverse diffusivities, in this case are typically considered equal i.e., $D_x = D_y$, resulting in:

$$\sqrt{D_a} = \left(1 + \frac{h}{w}\right)\sqrt{D_x} + \frac{h}{l}\sqrt{D_z} \tag{37}$$

This method can be employed to ascertain the longitudinal and transverse diffusivities [16,206] by graphing $\sqrt{Da}$ versus h/l. This plot typically yields a straight line, where the slope corresponds to D_z and the intercept to $(1 + (h/w))\sqrt{D_x}$, where D_x represents the adjusted 1-D

diffusion coefficient, and D_a represents the apparent coefficient determined through experimental data. In a homogenous material where $D = D_x = D_y$, Equation (35) can be expressed as follows:

$$D = D_x \left(1 + \frac{h}{l} + \frac{h}{w}\right)^2 \tag{38}$$

In the most cases, the experimentally determined apparent diffusion coefficients use a one-dimensional approximation, neglecting additional diffusion through the edges. Various approximations have been proposed to alleviate this complexity in determining coefficients for true 3-D flow. Building on the approach of Shen and Springer [133], the studies by Bao and Yee [207] suggest that, in the early stage, the diffusion in the *x*, *y*, and *z* directions could be treated independently, assuming that the total mass of absorbed moisture equals the cumulative amount absorbed from each surface independently. Consequently, the moisture uptake can be expressed [192,208] as follows:

$$\frac{M_t}{M_\infty} = \sqrt{\frac{16t}{\pi}} \left(\frac{\sqrt{D_x}}{l} + \frac{\sqrt{D_y}}{w} + \frac{\sqrt{D_z}}{h}\right) \tag{39}$$

While effective, this approximation overlooks diffusion at the sample edges. Therefore, Starink et al. [187] proposed an improved approximation, further discussed in [209–212]:

$$\frac{M_t}{M_\infty} = \sqrt{\frac{16t}{\pi}}\left(\frac{\sqrt{D_x}}{l} + \frac{0.54\sqrt{D_y}}{w} + \frac{0.54\sqrt{D_z}}{h} + \frac{0.33l}{wh}\sqrt{\frac{D_y D_z}{D_x}}\right) \tag{40}$$

It should be noted that in an orthorhombic system, such as the case with unidirectional composite laminae, there exist three principal diffusivities—D_1, D_2, and D_3, where D_1 aligns with the fiber axis, D_2 extends transversely across the width of the composite (longitudinal and transverse directions), and D_3 represents the through-thickness diffusivity. Following the methodology of Jaeger and Carslaw [195], determination of principal diffusivities involves a translation from global *x*-*y*-*z* coordinates to local 1–2–3 coordinates, considering a fiber orientation described by angles α, β, and γ between the 1 axis and the *x*, *y*, and *z*-axes, respectively. In the context of laminar composites, where through-thickness properties closely resemble transverse properties across the width, it is reasonable to assume $D_2 = D_3$ [133,195], such that

$$D_x = D_1 \cos^2\alpha + D_2 \sin^2\alpha \tag{41}$$

$$D_y = D_1 \cos^2\beta + D_2 \sin^2\beta \tag{42}$$

$$D_z = D_1 \cos^2\gamma + D_2 \sin^2\gamma \tag{43}$$

For unidirectional laminated composites, where D_1 and D_2 denote the diffusivities parallel and perpendicular to the fibers, respectively, and where D_x is not known, diffusivity can be determined using the diffusivity of the bulk resin, D_r, and the fiber volume fraction, V_f, as follows:

$$D_x = D_r \left[\left(1 - v_f\right) cos^2\, \alpha + \left(1 - 2\sqrt{v_f/\pi}\right) sin^2\, \alpha \right] \tag{44}$$

The diffusivity in the composite parallel to the direction of the fibers, D_1, can then be determined by the rule of mixtures where the diffusivities of the resin and fibers within a composite are D_r and D_f, respectively:

$$D_1 = \left(1 - V_f\right) D_r + V_f D_f \tag{45}$$

Further, following [213], Shen and Springer [133] develop an analogy for diffusivity as follows:

$$D_2 = \left(1 - 2\sqrt{\frac{V_f}{\pi}}\right) D_r + \frac{D_r}{B_D} \left[\pi - \frac{4}{\sqrt{1 - B_D^2 V_f/\pi}} tan^{-1} \left(\frac{\sqrt{1 - B_D^2 V_f/\pi}}{1 + \sqrt{B_D^2 V_f/\pi}} \right) \right] \tag{46}$$

where

$$B_D = 2\left(\frac{D_r}{D_f} - 1\right) \tag{47}$$

For composites in which the fiber's diffusivity is lower than that of the resin, such as in the case of as carbon and basalt fibers, Equations (45) and (46) can be simplified for $V_f < 0.785$ as follows:

$$D_1 \cong \left(1 - V_f\right)D_r \tag{48}$$

$$D_2 \cong \left(1 - 2\sqrt{\frac{V_f}{\pi}}\right)D_r \tag{49}$$

where D_1 and D_2 denote the diffusivities parallel and perpendicular to the fibers, respectively, and D_r is the diffusivity of the bulk resin. The value 0.785 originates from the packing efficiency of a hexagonally close-packed structure, in which the maximum possible volume fraction that spheres (or fibers in composite materials) can occupy within a given space is denoted. Consequently, the integration of Equation (35) results in the following:

$$\frac{\sqrt{D}}{h\sqrt{D_r}} = \frac{\sqrt{1 - V_f\, cos^2\,\alpha + 2\sqrt{\frac{V_f}{\pi}}\, sin^2\,\alpha}}{l} + \frac{\sqrt{1 - V_f\, cos^2\,\beta + 2\sqrt{\frac{V_f}{\pi}}\, sin^2\,\beta}}{w} + \frac{\sqrt{1 - V_f\, cos^2\,\gamma + 2\sqrt{\frac{V_f}{\pi}}\, sin^2\,\gamma}}{h} \quad (50)$$

Or

$$D = D_r \left[(1 - V_f)\, cos^2\,\alpha + (1 - 2\sqrt{\frac{V_f}{\pi}})\, sin^2\,\alpha \right] \times \left[1 + \frac{h}{l} \sqrt{\frac{(1 - V_f)\, cos^2\,\beta + (1 - 2\sqrt{\frac{V_f}{\pi}})\, sin^2\,\beta}{(1 - V_f)\, cos^2\,\alpha + (1 - 2\sqrt{\frac{V_f}{\pi}})\, sin^2\,\alpha}} + \frac{h}{w} \sqrt{\frac{(1 - V_f)\, cos^2\,\gamma + (1 - 2\sqrt{\frac{V_f}{\pi}})\, sin^2\,\gamma}{(1 - V_f)\, cos^2\,\alpha + (1 - 2\sqrt{\frac{V_f}{\pi}})\, sin^2\,\alpha}} \right]^2 \quad (51)$$

where α, β, and γ represent the angles between the fiber direction and the x, y, and z-axes, respectively, and h, l, and w indicate the thickness, length, and width of the specimen. In the case of a unidirectional composite represented by Equation (50) with a fiber volume exceeding $V_f >$ 0.785, a simplified approximation can be expressed as follows:

$$D \cong D_r h^2 \left[\frac{\sqrt{1 - 2\sqrt{V_f/\pi}}}{h} + \frac{\sqrt{1 - V_f}}{l} + \frac{\sqrt{1 - 2\sqrt{V_f/\pi}}}{w} \right]^2 \quad (52)$$

Although these statements theoretically hold true for $V_f >$ 0.785, it is important to note that practical V_f values generally fall below 0.785. Theoretically calculated fiber volume fractions range from 78.5% for square packing of circular fibers to 90.7% for hexagonal packing of circular

fibers [100]. Shen and Springer [133] and Starink et al. [187] derived correction factors for diffusivity coefficients based on dimensions and flow directions and these are given below:

$$f_{S\&S} = 1 + \frac{a}{b} + \frac{a}{c} \tag{53}$$

$$f_{SSC} = 1 + \lambda_1 \frac{a}{b} + \lambda_1 \frac{a}{c} + \lambda_2 \frac{a^2}{bc} \tag{54}$$

where a, b, c are the dimensions of a rectangular solid ($a \leq b \leq c$), and λ_1 and λ_2 are the average moisture concentration based on the direction of exposure. Several methods exist to derive λ_1 and λ_2, with the most accurate obtained by fitting their values using the complete 3-D diffusion Equation (30) and calculating the slope of the initial part across a range of rectanguloid sample shapes, as recommended by Starink et al. [187] such that

$$f_{SSC} = 1 + 0.54 \frac{a}{b} + 0.54 \frac{a}{c} + 0.33 \frac{a^2}{bc} \tag{55}$$

It should be noted that both correction factors assume that the average concentration is a constant, irrespective of specimen size. Based on a study of rectangular specimens of different sizes, Starink et al. [187] reported that Equation (55) is more accurate than Equation (53) with deviations in the diffusion coefficient being between 16 and 37% for the latter compared to less than 2% for the former.

In unidirectional composites, the diffusion rates can, in general, be expected to be direction dependent, and can be elucidated in three different cases:

Case 1: $D_f = 0$ and $\alpha = 0$

$$D_{eff}(\alpha = 0) \quad \simeq D_r \left[1 + \lambda_1 \left(\frac{a}{b} + \frac{a}{c}\right) \sqrt{\frac{1 - 2\sqrt{v_f/\pi}}{1 - v_f}}\right]^2 \tag{56}$$

Case 2: $D_f = 0$ and $\beta = 0$

$$D_{eff}(\beta = 0) \cong D_r \frac{1 - 2\sqrt{v_f/\pi}}{1 - v_f} \times \left[1 + \lambda_1 \left(\frac{a}{b} \sqrt{\frac{1 - v_f}{1 - 2\sqrt{v_f/\pi}}} + \frac{a}{c}\right)\right]^2 \tag{57}$$

Case 3: $D_f = 0$ and $\gamma = 0$

$$D_{eff}(\gamma = 0) \cong D_r \frac{1 - 2\sqrt{v_f/\pi}}{1 - v_f} \quad \times \left[1 + \lambda_1 \left(\frac{a}{b} + \frac{a}{c} \sqrt{\frac{1 - v_f}{1 - 2\sqrt{v_f/\pi}}}\right)\right]^2 \tag{58}$$

Although the Fickian model is used extensively for polymers and fiber-reinforced polymer matrix composites, it must be noted that the model does not consider swelling and assumes that the rate of uptake/diffusion is significantly faster than that of relaxation and thus is unable to address effects of volumetric change induced by moisture uptake, nor those of stresses. Furthermore, there is also an implicit assumption that the equilibrium moisture content is insensitive to temperature. While the initial stages of water diffusion in polymer and polymer matrix composites typically follow Fickian behavior, there is a significant body of literature

showing deviation over longer periods of exposure [49,110,120,121,124,132,139,171,184,199,200,204,214–228]. Anomalous diffusion, which occurs when deviations from Fickian behavior occur, is influenced by factors such as material type, environmental conditions, and the material's exposure history and level of degradation [49,119]. It should be remembered that the movement and ingress of water molecules into a polymer depends not only on water sorption into the free volume but also on the complex interactions between the polymer network and water. Factors such as polar groups within the structure, crosslink density, available free volume, and the outcomes of water–polymer interactions (including segmental relaxation, swelling, plasticization, and structural degradation) result in complexities and competing phenomena, which cause deviation from the ideal response represented by Fick's laws [66,229,230].

Mubashar et al. [231], Karbhari and Xian [16], and Jiang et al. [232] proposed that under low temperatures and when materials are exposed to humid air, the diffusion process typically follows a Fickian pattern. However, at higher temperatures and when materials are immersed in solutions, the diffusion process often diverges from Fickian behavior due to relaxation of the glassy polymer network and filling of debonded zones and voids through wicking [16,232]. As temperature or humidity increases, the predominance of Fickian diffusion mechanisms decreases, allowing other mechanisms to have a greater impact on moisture transport.

It should be remembered that moisture absorption in composite materials is through three different mechanisms: (1) diffusion of water molecules within the micro-gaps between polymer chains; (2) capillary transport into the gaps and defects at the interfaces between fibers and matrix;

and (3) transport through microcracks within the matrix due to swelling [233]. The presence of polar functional groups within cured epoxy resins, along with the relaxation processes induced by interactions with water molecules, leads to a deviation from classical Fick's law over time. Thus, the detailed understanding of diffusion mechanisms is important for modeling of uptake. In glassy polymers, the diffusion of small molecules often deviates from simple Fickian diffusion, as noted in numerous studies [49,227,228]. Consequently, several models have been introduced to address anomalous diffusion in resin [231,234–237]: two phase diffusion model (Jacobs–Jones model) [154,184,203,218,219,228,235,238–242], coupled diffusion–relaxation model (Berens–Hopfenberg model) [159,234], time-varying diffusion coefficient model [171,236,243], and the Langmuir-type model (Carter–Kibler model) [184,220,231], which was extended to the hindered diffusion model (HDM) [125,171,244,245], structural modification diffusion model [207], the stress-dependent model [49,227,228], and the history-dependent theory [49,228], thickness-dependent moisture absorption model [246], and barrier models [247,248]. These models incorporate additional factors, such as bound and unbound/free water phases, relaxation effects from swelling, various polymer-formed phase structures, and changes in diffusion coefficients over time. Empirical and experimental observations are used to determine their parameters and coefficients. It is widely accepted that transport in glassy polymers involves both concentration-gradient-driven Fickian diffusion and time-dependent relaxation processes [49,159,227,228,249]. Depending on the relative contributions of these two processes, a diverse range of behaviors has been observed [228].

As a means of addressing the discrepancy, Jacobs and Jones developed a model based on an assumption of simultaneous sorption initiation by two distinct Fickian phases [238]. One phase is denser, characterized by high crosslinking, while the other is less dense, with low crosslinking, thus indicating moisture uptake through two separate and independent diffusion phenomena, represented as follows:

$$\frac{M_t}{M_\infty} = V_d \cdot \left\{1 - exp\left[-7.3\left(\frac{D_d t}{h^2}\right)^{0.75}\right]\right\} + (1 - V_d) \cdot \left\{1 - exp\left[-7.3\left(\frac{D_l t}{h^2}\right)^{0.75}\right]\right\} \quad (59)$$

where M_t represents the moisture uptake at time t, M_∞ is the moisture content at saturation, V_d is the volume fraction of the denser phase, D_d is the diffusion coefficient of the denser phase, and D_l is the diffusion coefficient of the less dense phase. The initial phase of water uptake is characterized by rapid uptake, and the rate of uptake is expected to be additive, where diffusion occurs in both the highly crosslinked and lower crosslinked phases. Subsequently, the diffusion process decelerates as water is absorbed primarily into the highly crosslinked phase, while the less dense phase is assumed to be saturated and approaches equilibrium [154,238]. Maggana and Pissis [154] generalized the concept of denser and less dense phases into two arbitrary and independent phases, wherein the primary phase (referred to as phase I), that is, homogeneous and nonpolar, is responsible for the majority of water absorption, alongside a secondary phase (referred to as phase II), characterized by varying density and/or hydrophilic properties compared to phase I. Assuming that water diffusion occurs independently within each phase according to Fick's second law, the diffusion coefficient D and the saturation water content M for each phase can be determined separately [154], leading to a modification of Equation (59) as follows:

where M_1 and M_2 denote the maximum moisture content for phases I and II, respectively; D_1 and

$$M_t = M_1 \cdot \left\{1 - \frac{8}{\pi^2}\sum_{n=0}^{\infty}\frac{1}{(2n+1)^2} exp\left[-\frac{D_1 t}{h^2}\pi^2(2n+1)^2\right]\right\} + M_2 \cdot \left\{1 - \frac{8}{\pi^2}\sum_{n=0}^{\infty}\frac{1}{(2n+1)^2} exp\left[-\frac{D_2 t}{h^2}\pi^2(2n+1)^2\right]\right\} \quad (60)$$

D_2 are the diffusion coefficients for phases I and II, respectively; h represents the thickness; and t is the time. Since the uptakes are additive,

$$M_\infty = M_1 + M_2 \quad (61)$$

where M_∞ is the total moisture content at saturation of two stages, while the diffusion coefficient of each stage follows the Arrhenius relationship with independent values for the factor D_o and activation energy E_a. Equation (60) can be modified following the approach of Shen and Springer [133]:

$$M_t = M_1 \cdot \left\{1 - exp\left[-7.3\left(\frac{D_1 t}{h^2}\right)^{0.75}\right]\right\} + M_2 \cdot \left\{1 - exp\left[-7.3\left(\frac{D_2 t}{h^2}\right)^{0.75}\right]\right\} \quad (62)$$

It is emphasized that the existence of two stages can follow directly from the existence of two distinct water phases within a resin subjected to hygrothermal conditions. The sorption of phase I is influenced by the atmospheric water content, while the sorption of phase II is governed by temperature and time [62]. Mikols et al., for example [21], propose a simplified model that considers water sorption in the free volume, characterized by maximum moisture content, and accounts for additional water sorption resulting from changes in the polymer structure due to hygrothermal interactions and changes in free volume [21]. The process of determining diffusion coefficients for Equation (59) involves employing linear curve fitting of regions predominantly

governed by each phase. As shown in Figure 2-10, the initial slope of the uptake curve provides an approximate value for the diffusion coefficient, D_x, following the conventional Fickian approach [238] such that

$$\left[\frac{\partial M_t}{\partial \sqrt{t}}\right]_x = \frac{4M_\infty}{h} \cdot \sqrt{\frac{D_x}{\pi}} \tag{63}$$

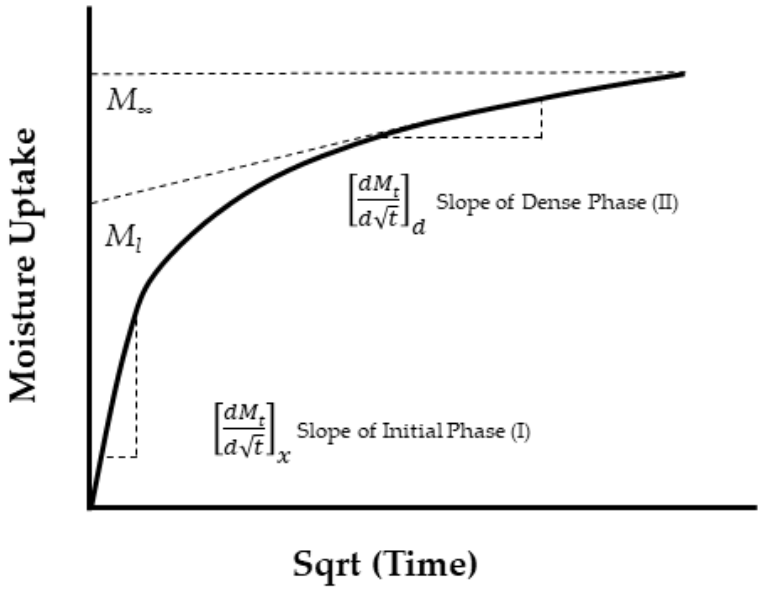

Figure 2-10. *Schematic showing determination of parameters in the two-phase Fickian model. (*x = l+d*, l represents the less dense phase and* d *represents denser phase).*

Since that uptake is additive as described by Equation (61) [238]:

$$\left[\frac{\partial M_t}{\partial \sqrt{t}}\right]_x = \left[\frac{\partial M_t}{\partial \sqrt{t}}\right]_d + \left[\frac{\partial M_t}{\partial \sqrt{t}}\right]_l \tag{64}$$

where the subscripts *d* and *l* represent the denser and less dense phases, respectively, while *x* is the combination of *l* and *d.*

At later stages, the slope indicates the uptake in the denser phase, while the uptake in the less dense phase approaches equilibrium. By extending a line from the region characterized by sorption of the denser phase to the ordinate axis, the equilibrium content for the less dense phase, denoted as M_l, can be determined from the intercept [238], as depicted in Figure 2-10. Subsequently

$$M_\infty = M_l + M_d \tag{65}$$

enables the determination of the diffusion coefficients associated with it [238]:

$$\left[\frac{\partial M_t}{\partial \sqrt{t}}\right]_d = \frac{4M_d}{h} \cdot \sqrt{\frac{D_d}{\pi}} \tag{66}$$

and

$$\left[\frac{\partial M_t}{\partial \sqrt{t}}\right]_l = \frac{4M_l}{h} \cdot \sqrt{\frac{D_l}{\pi}} \tag{67}$$

such that,

$$D_d = \pi \left(\frac{h}{4[M_\infty - M_l]}\right)^2 \left[\frac{\partial M_t}{\partial \sqrt{t}}\right]_d^2 \tag{68}$$

and

$$D_l = \pi \left(\frac{h}{4M_l}\right)^2 \left\{\left[\frac{\partial M_t}{\partial \sqrt{t}}\right]_x - \left[\frac{\partial M_t}{\partial \sqrt{t}}\right]_d\right\}^2 \tag{69}$$

From Equations (59) and (60), it can be deduced that the volume fraction of both the more and less dense phases can be expressed as follows:

$$V_d = \frac{M_d}{M_\infty} \tag{70}$$

and

$$1 - V_d = \frac{M_l}{M_\infty} \tag{71}$$

Jacobs and Jones [238] introduced a correlation for V_d derived from a universal formula for thermal conductivity in two-component systems exhibiting orthorhombic symmetry, where

$$V_d = \frac{\left(\frac{D_d}{D_l} + 2\right)\left(\frac{D_x}{D_l} - 1\right)}{\left(\frac{D_d}{D_l} - 1\right)\left(\frac{D_x}{D_l} + 2\right)} \tag{72}$$

where V_d represents the volume fraction of the dense phase relative to the total system (highly crosslinked), while D_d and D_l denote the diffusion coefficients associated with the denser and less dense phases, respectively, and D_x is the diffusion coefficient of the first stage of uptake.

In considering the influence of temperature on equilibrium moisture content, various approaches can be considered. One possibility involves a material capable of sorbing a finite amount of sorbate, where the volume percentage of one phase increases with temperature, resembling the model proposed in [21]. This implies that M_∞ remains constant over temperature while V_d varies. On the other hand, one could posit that there is no alteration in the relative volume percentage of either phase, but the equilibrium content of each phase increases proportionally with temperature. This suggests that M_∞ varies with temperature while V_d stays constant. A consideration in this vein is that of the levels of free and bound water within the polymer or composite as a function of period of exposure and details of the environmental conditions.

The Langmuir model and its variations consider the chemical interactions between water molecules and the polar groups of the resin, through assumption of the presence of two states for absorbed water molecules (expressed as two separate probabilities of state) and presents a framework where water sorption involves both the diffusion of free species into the sorbent and the simultaneous adsorption of water molecules to the polymer, forming a bound structure [144,184]. Carter and Kibler [184] proposed a non-steady-state diffusion model that integrated diffusion and Langmuir adsorption theory [46,144,203,231] such that

$$\frac{dC_D}{dt} = -\frac{dq}{dx} - \sigma \tag{73}$$

where x represents position, t signifies time, $C_D(x,t)$ denotes the concentration of the free diffusion phase, $q(x,t)$ indicates the mass flux of the free phase, and $\sigma(x,t)$ represents the rate at which the free phase transitions into a site-bound state. It is crucial to emphasize that only the free phase undergoes diffusion, while both free and bound water molecules possess the capability to bind to and free themselves from sorbent molecules. By introducing the Langmuir diffusion coefficient, D, along with the parameters α and β, and considering the concentration of site-bound molecules, $C_S(x,t)$, the ensuing fundamental equations can be formulated as follows [184]:

$$q = -D\frac{dC_D}{dx} \tag{74}$$

$$\sigma = \beta C_D - \alpha C_S \tag{75}$$

where α signifies the probability of a bound molecule transitioning to a free state, β represents the probability of a free molecule becoming bound, C_D is the concentration of the free diffusion phase, C_s is the concentration of bound molecules, and σ represents the rate at which the free phase transitions into a bound phase. Therefore,

$$\frac{\partial C_D}{\partial t} = D\frac{\partial^2 C_D}{\partial x^2} - \beta C_D + \alpha C_S \tag{76}$$

At equilibrium, the conversion rate is indicated as follows [144,184]:

$$\sigma = 0, \qquad \beta C_D = \alpha C_S \tag{77}$$

and the maximum moisture content, M_∞, at equilibrium can be described in terms of the equilibrium concentration $C_{D\infty}$ and $C_{S\infty}$ as follows:

$$M_\infty = C_{D\infty} + C_{S\infty} = C_{D\infty} + \frac{\beta}{\alpha} C_{D\infty} \tag{78}$$

where $C_{D\infty}$ is the equilibrium concentration of the free diffusion phase, and $C_{S\infty}$ is the equilibrium concentration of bound molecules. Subsequently, the expression for moisture content M_t, can be formulated as follows [184,203]:

$$M_t = M_\infty \cdot \left\{1 - \frac{\beta}{\alpha+\beta} exp(-\alpha t) - \frac{\alpha}{\alpha+\beta} exp(-\beta t) \cdot \frac{8}{\pi^2} \sum_{n=0}^{\infty} \frac{1}{(2n+1)^2} exp\left[-\frac{Dt}{h^2}\pi^2(2n+1)^2\right]\right\} \quad (79)$$

where t represents time in seconds, D stands for the Langmuirian diffusion coefficient, and h denotes the thickness of the specimen. When both α and β, representing the probability of a bound molecule transitioning to a free state and a free molecule becoming bound, respectively, are small compared to the parameter governing the rate of saturation of a one-dimensional specimen with thickness h, Carter and Kibler introduced the term κ [184], such that

$$\kappa = D\left(\frac{\pi}{h}\right)^2 \quad (80)$$

and indicated that Equation (79) is applicable only when α, $\beta << \kappa$. Since the conversion rate between the two phases is expected to be significantly less than κ, Equation (79) can be restated without the exp(-βt) term as follows [38,139,203,250]:

$$M_t = M_\infty \cdot \left\{1 - \frac{\beta}{\alpha+\beta} exp(-\alpha t) - \frac{\alpha}{\alpha+\beta} \cdot \frac{8}{\pi^2} \sum_{n=0}^{\infty} \frac{1}{(2n+1)^2} exp\left[-\frac{Dt}{h^2}\pi^2(2n+1)^2\right]\right\} \quad (81)$$

This structure essentially divides the uptake regime into three stages as shown in Figure 2-11: (a) the initial linear regime that is similar to Fickian diffusion; (b) the longer transitional regime; and (c) the final plateau representative of attainment of equilibrium. Figure 2-11 differentiates between moisture levels, M_1 and M_∞, representing the uptake levels at the pseudo-plateau (Fickian) level and the final equilibrium level, respectively. Simple expressions

representing moisture uptake as a function of time in the first two stages are also provided for comparison.

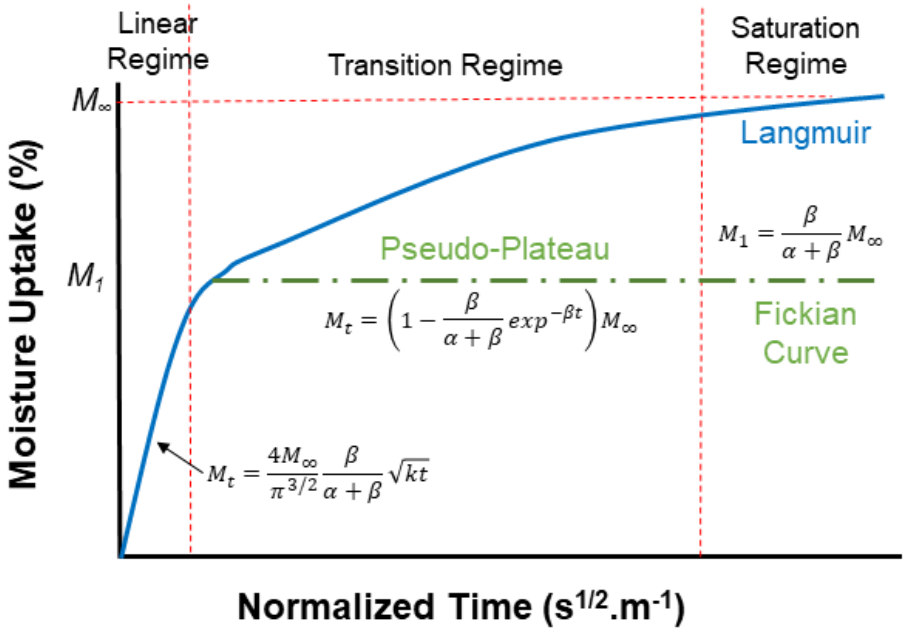

Figure 2-11. *Schematic showing the three stages representative of changes in Langmuir diffusion.*

Furthermore, Popineau et al. [220] provide approximate formulations that connect moisture uptake with time, using spatial distribution expressions as follows:

$$\frac{m_{free}(t)}{M_\infty} = \frac{\alpha}{\alpha+\beta}\left(1 - \frac{8}{\pi^2} e^{-\kappa t}\right) \tag{82}$$

$$\frac{m_{\text{bound}}(t)}{M_\infty} = \frac{\alpha\beta}{\alpha+\beta} e^{-\alpha t}\left(\frac{1}{\alpha}(e^{\alpha t}-1) - \frac{8}{\pi^2\kappa}(e^{-\kappa t}-1)\right) \quad (83)$$

Following [184,251], Equation (81) can be further simplified for short times as follows:

$$M_t = M_\infty\left[\left(\frac{\alpha}{\alpha+\beta}\right)\sqrt{\frac{16Dt}{h^2\pi^2}}\right], \quad t \leq 0.7/\kappa \quad (84)$$

and for prolonged exposure times as follows:

$$M_t = M_\infty\left[1 - \left(\frac{\beta}{\alpha+\beta}\right)exp(-\alpha t)\right], \quad t \gg 1/\kappa \quad (85)$$

The characterization of pseudo-equilibrium, denoted as $M_{ps\infty}$, can be characterized as follows:

$$M_{ps\infty} = M_\infty\left(\frac{\alpha}{\alpha+\beta}\right) \quad (86)$$

α can be calculated through differentiation of Equation (79), and subsequently, β can be derived using experimental data on mass uptake with time, where [252]

$$-\left(\frac{dM_t}{dt}\right)^{-1}\frac{d^2M_t}{dt^2} \approx \ constant \ = \alpha \tag{87}$$

$$exp(-\alpha t)\left[\alpha\left(\frac{dM_t}{dt}\right)^{-1} M_t + 1\right] \approx \ constant \ = 1 + \alpha/\beta \tag{88}$$

This state of pseudo-equilibrium signifies the fraction of mobile water within the sorbent and becomes noticeable as a plateau under conditions of sufficiently elevated temperatures and low specimen thicknesses, where the assumption $\alpha, \beta << \kappa$ holds true.

Among the models discussed for non-Fickian diffusion in resins, the Langmuir-type model has been reported to demonstrate good correspondence to uptake data [124,198,220,229,248,250,252–257]. Glaskova et al. [250] evaluated the performance of several models for a selected commercial epoxy resin and found that both the Langmuir-type and relaxation models yielded results that matched the experimental data. Similarly, other researchers [220,252,257] reported that Langmuir-type models produced highly consistent results and accurately predicted further mass increases based on collected experimental data. Nevertheless, there still exists a high level of concern related to accurately determining α and β that accurately correspond with levels of bound and free water in the material [8]. Various algorithms for curve fitting have been employed to determine values for D, α, β, and even M_∞. As an example, a commonly used method involves selecting a moisture content from an apparent pseudo-equilibrium plateau in the empirical moisture sorption curve to define $M_{ps\infty}$. This enables the determination of the ratio of α to $\alpha + \beta$ from Equation (86). Employing an exponential curve fit

based on Equation (85) yields β, facilitating the calculation of α using Equation (86) [220]. The slope of the initial uptake curve of M_t plotted against $t^{1/2}$ for times less than $0.7/\kappa$ is then utilized to ascertain the diffusion coefficient, D, through Equation (84) [220].

Li et al. [258], on the other hand, used a curve-fitting approach to determine the diffusion coefficient by fitting the simplified solution to Fick's Law, as outlined in Equation (24), and subsequently constrained D in Equation (79) to this determined value [258]. Following this, M_∞, α, and β are obtained through a curve-fitting algorithm. If β is assumed to be 0, it suggests no conversion, and consequently, the diffusion coefficient would be equivalent to Fickian diffusion. However, if β is greater than 0, water has the potential to convert from free to bound, and vice versa, allowing for a higher maximum moisture content in the sorbent compared to Fickian diffusion. It should, however, be mentioned that these fits can, at times, result in negative values of α and/or β, which would indicate invalidity of the model since α and β are probabilities of change in state of water, and hence positive.

To describe the anomalous absorption behavior, where the diffusion rate undergoes temporal changes in composite materials, a time-varying Langmuir diffusion model was proposed by Yu and Xing [259]. This model incorporates an equivalent time parameter, t^*, replacing the physical time t, to establish the relationship between the variation rate of the diffusion coefficient and time, such that

$$D = D_0 e^{-\lambda t} \tag{89}$$

$$t^* = \frac{1 - e^{-\lambda t}}{\lambda} \tag{90}$$

where D_0 is the initial diffusion coefficient, while λ is the rate at which the moisture diffusion coefficient changes over time. Thus, the time varying Langmuir diffusion model can be described as follows:

$$\frac{M_t}{M_\infty} = \frac{\alpha}{(\alpha+\beta)} e^{-\beta t^*} y(t^*) - \frac{\alpha}{(\alpha+\beta)} \left(e^{-\alpha t^*} - e^{-\beta t^*}\right) + 1 - e^{-\alpha t^*} \tag{91}$$

where

$$y(t^*) = 1 - \frac{8}{\pi^2} \sum_{n=0}^{\infty} \frac{1}{(2n+1)^2} e^{-\kappa(2n+1)^2 t^*} \tag{92}$$

and

$$\kappa = \pi^2 D_L / l^2 \tag{93}$$

where D_L represents the diffusion obtained from the Langmuir diffusion model at the initial time, α signifies the bounding rate of molecules in the free phase, and β denotes the transition rate of molecules from the bound to the free state.

While Langmuir-type models address mechanism changes through the state of water and can be used to assess the effects of non-negligible volume changes in materials resulting from uptake and diffusion, they do not explicitly account for combinations of short-term and long-term effects, the former of which is diffusion-dominated, whereas the latter could be affected by polymer relaxation. A two-stage diffusion pattern, with the initial stage being primarily characterized by Fickian diffusion, succeeded by a gradual relaxation of the polymer, was proposed by Bagley and Long [188]. This two-stage phenomenon initially developed for cellulose acetate, is applicable to various polymer-penetrant systems, including moisture absorption in thermoset resins and composites. This model identifies two distinct stages: an initial rapid diffusion phase driven by concentration gradients, following Fickian behavior, and a subsequent phase characterized by slow polymer relaxation, allowing for additional absorption, approaching to a true final equilibrium. This latter process involves the rearrangement of polymer chains over time due to the presence of moisture penetrant molecules, resulting in further absorption at a slower rate than the initial uptake. This model can be viewed as a modified Fickian model, incorporating a time-dependent maximum moisture content, as the polymer undergoes a gradual relaxation process allowing for increased moisture sorption over time [207]. Long and Richman [157] further refined the model by including an exponential dependence on time in the consideration of surface concentration [157].

The non-dimensional form of an equation is particularly advantageous because it excludes any dimensional variable properties, making it especially useful for managing more complex systems influenced by multiple dimensional variables, and can potentially provide a clearer description of absorption behavior, revealing underlying principles. The non-dimensional form of the Langmuir-type diffusion model was used to derive an approximate solution for the three-dimensional hindered diffusion model (HDM) resulting in the dimensionless form [184,260,261]:

$$D_x^* \frac{\partial^2 n^*}{\partial (x^*)^2} + D_y^* \frac{\partial^2 n*}{\partial (y^*)^2} + D_z^* \frac{\partial^2 n^*}{\partial (z^*)^2} = \mu \frac{\partial n^*}{\partial t^*} + (1-\mu)(n^* - N^*) \tag{94}$$

where

$$n^* = \frac{n(t)}{n_\infty} \quad N^* = \frac{N(t)}{N_\infty} \quad t^* = \beta t \tag{95}$$

$$x^* = \frac{x}{l} \quad y^* = \frac{y}{w} \quad z^* = \frac{z}{h} \tag{96}$$

$$D_x^* = \frac{D_x}{l^2(\gamma+\beta)} \quad D_y^* = \frac{D_y}{w^2(\gamma+\beta)} \quad D_z^* = \frac{D_z}{h^2(\gamma+\beta)} \quad \mu = \frac{\beta}{\gamma+\beta} \tag{97}$$

In the above, n^*, N^*, and t^* are dimensionless concentration of diffusing molecules at time t, the dimensionless reference concentration, and dimensionless time, respectively. Parameters x^*, y^*, and z^* are the dimensionless x-coordinate, y-coordinate, and z-coordinate, respectively. D_x^*, D_y^*,

and D_z^* are dimensionless diffusion coefficients in the *x*-, *y*-, and *z*-directions, respectively. Meanwhile, β and γ represent the probability of a bound molecule transitioning to a free state and a free molecule becoming bound, and *l*, *w*, and *h* are the length, width, and thickness, respectively. The analytical solution of the 3-D HDM can be restated as follows [125,184,244]:

$$M^* = 1 - \frac{512\mu}{\pi^6}\sum_{P=0}^{\infty}\sum_{Q=0}^{\infty}\sum_{k=0}^{\infty}\frac{1}{(2P+1)^2(2Q+1)^2(2R+1)^2}\mathrm{e}^{-\alpha t^*} - (1-\mu)\mathrm{e}^{-t^*} \quad (98)$$

where

$$\alpha = (A_1(2P+1)^2 + A_2(2Q+1)^2 A_3(2R+1)^2) \quad (99)$$

$$M^* = \frac{M(t)}{M_x} \quad t^* = \beta t \quad \mu = \frac{\beta}{\gamma+\beta} \quad (100)$$

where

$$A_1 = \frac{\pi^2 D_x}{\beta l^2} \quad A_2 = \frac{\pi^2 D_y}{\beta w^2} \quad A_3 = \frac{\pi^2 D_z}{\beta h^2} \quad (101)$$

At the simplest level, assuming a linear relationship between weight gain and time suggests representing saturation concentration as a linear function of time as well, such that

$$c_s = c_0 + k\sqrt{t} \tag{102}$$

where c_s is saturation concentration and c_0 is the initial moisture concentration. Thus, the weight gain for a specimen of thickness h is given as follows:

$$M = \int_{-h}^{h} c\,dx = 2hc_s = 2hc_0 + 2hk\sqrt{t} = M_0\left(1 + k'\sqrt{t}\right) \tag{103}$$

Given that the initial diffusion follows Fick's law, the moisture uptake over the entire experimental time scale can be approximated following [65] as follows:

$$M_t = M_{0\infty} \cdot \left[1 + k\sqrt{t}\right] \cdot \left\{1 - \frac{8}{\pi^2}\sum_{n=0}^{\infty}\frac{1}{(2n+1)^2}exp\left[-\frac{Dt}{h^2}\pi^2(2n+1)^2\right]\right\} \tag{104}$$

where M_t represents the water uptake at time t, $M_{\infty 0}$ is the level of quasi-equilibrium water uptake, k is a constant related to the relaxation of the polymer structure in the second diffusion stage, D is the diffusion coefficient, and h is the thickness of the specimen.

Using the Shen and Springer [133] approximation,

$$M_t = M_{0\infty}\left(1 + k\sqrt{t}\right)\left(1 - exp\left[-7.3\left(\frac{Dt}{h^2}\right)^{0.75}\right]\right) \quad (105)$$

where $M_{o\infty}$ represents the pseudo-equilibrium moisture content, and k is designated as a "relaxation coefficient" [207]. In the second phase, this relaxation is characterized by an asymptote that forms an increasing linear relationship with $t^{1/2}$ instead of a constant $M_{o\infty}$. Similar patterns have been observed where the asymptote takes the form of a decreasing linear function of $t^{1/2}$. A declining linear asymptotic pattern, indicating the attainment of a maximum moisture content followed by subsequent weight loss, may suggest sorbent degradation, which can be identified through permanent weight loss after redrying. Thus, k may signify either relaxation or degradation phenomena with a simple change in sign and is thus representative of structural modification rather than just relaxation.

It is emphasized that the determination of $M_{o\infty}$ is not a straightforward task and goes beyond merely assigning a maximum moisture content since $M_{o\infty}$ specifically denotes the equilibrium moisture content related to the Fickian component within Equation (104). Consequently, the sorption pattern of M_t versus $t^{1/2}$ needs to be categorized into three distinct sets. As shown in Figure 2-12 in these sets, Fickian diffusion and structural modification play dominant roles in influencing sorption during early and later times, respectively. The remaining phase characterizes an intermediate transition region. This approach offers a comprehensive perspective on the complex interplay of Fickian diffusion and structural modifications throughout various stages of sorption.

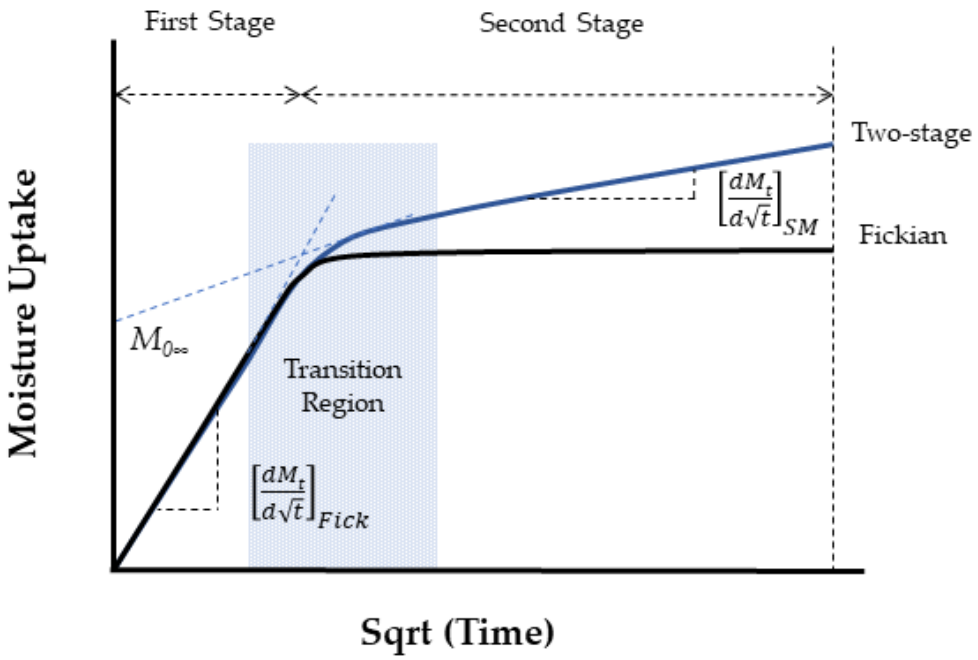

Figure 2-12. *Schematic of moisture uptake in a two-stage Fickian model.*

Conducting linear fits on both sets enables the determination of $M_{o\infty}$, k, and D. The ideal fit line for the Fickian-dominated phase is expected to intersect at the origin. $M_{o\infty}$, representing the pseudo-equilibrium moisture content, is obtained from the intercept of the best fit line that characterizes the gravimetric data dominated by structural modification. Once $M_{o\infty}$ is established, the values for D and k can be determined from the slopes of the respective line fits as follows:

$$\left[\frac{\partial M_t}{\partial \sqrt{t}}\right]_{Fick} = \frac{4M_{0\infty}}{h} \cdot \sqrt{\frac{D}{\pi}} \tag{106}$$

$$\left[\frac{\partial M_t}{\partial \sqrt{t}}\right]_{SM} = M_{0\infty} k \tag{107}$$

where the term with the subscript SM indicates the influence of structural modification.

In the context of the two-phase Fickian model, there exists an intermediate time where D_2 can be assessed. This is grounded in the assumption that the first phase has attained an equilibrium moisture content, while the second phase is still in the initial phases of sorption. Specifically, during this intermediate time, Equation (60) can be approximated as follow:

$$M_t \approx M_1 + M_2 \left[\frac{4}{h}\sqrt{\frac{D_2 t}{\pi}}\right] \tag{108}$$

Similarly, the model incorporating structural modification can be applied to later time intervals. In this phase, the Fickian component has attained its equilibrium moisture content, and the subsequent phase undergoes modification as dictated by the parameter *k*. Specifically, in this later timeframe, Equation (104) can be approximated as follows:

$$M_t \approx M_\infty + M_{0\infty}\sqrt{t} \tag{109}$$

From Equations (108) and (109),

$$M_{0\infty} \approx M_1 \tag{110}$$

and

$$M_{0\infty} k \approx \frac{4M_2}{h}\sqrt{\frac{D_2}{\pi}} \tag{111}$$

By employing the simplified model for structural modification, the diffusion coefficient of the second phase within the dual-phase Fickian model can be determined as follows:

$$D_2 \approx \pi\left[\frac{M_{0\infty} kh}{(M_\infty - M_{0\infty})4}\right]^2 \tag{112}$$

Hassanpour and Karbhari [262] proposed a modified model using a two-phase framework that integrates diffusion and relaxation/deterioration stages, alongside a transitional phase describing the full moisture absorption in composites and explicitly accounting for deterioration and damage that could occur during both phases. These effects can be differentiated based on discrepancies between "ideal" and "actual" diffusion and relaxation/deterioration coefficients; furthermore, the relaxation and diffusion coefficients are adjusted with modification factors L_1 and L_2 to effectively capture the changes. Moisture uptake in the composite can then be described as follows:

M_t= (Uptake due to diffusion-dominated regime) + (Uptake due to relaxation and longer-term deterioration) + (Uptake in the transitional regimes) (113)

i.e.,

$$\frac{M_t}{M_{trans}} = \left(1 + L_1 k_r \left[1 + \lambda\left(\frac{a}{b} + \frac{a}{c}\right)\sqrt{\frac{1 - 2\sqrt{V_f/\pi}}{1 - V_f}}\right]^2 \sqrt{t}\right)\left(1 - exp\left[-7.3\left(\frac{L_2 D_r \left[1 + \lambda\left(\frac{a}{b} + \frac{a}{c}\right)\sqrt{\frac{1 - 2\sqrt{V_f/\pi}}{1 - V_f}}\right]^2}{h^2} t\right)^{0.75}\right]\right) \quad (114)$$

where M_{trans} is the equilibrium moisture uptake level, M_t is the moisture uptake at time t, b and c represent the planar dimensions of the moisture uptake specimen, a is the thickness, and $\lambda = 0.54$ following Starink et al. [187]. D_r and D_f refer to the diffusion and relaxation coefficient in the resin, respectively, L_1 and L_2 are damage terms, and V_f is the fiber volume fraction. The modification factors indicate the changes in relaxation and diffusion characteristics beyond what would be expected if a direct transition from resin to composite response, based solely on fiber volume fraction, were feasible. This approach evaluates the changes at the interface and in the resin caused by temperature, distinguishing them from the characteristics of the bulk resin, as well as the bulk resin modified by fiber volume fraction, and offers a more comprehensive understanding of the local response, and can be rewritten as follows:

$$M_t = M_{trans}\left(1 - exp\left[-7.3\left(\frac{D_{eff}L_2 t}{h^2}\right)^{0.75}\right]\right) + M_{trans}k_{eff}L_1\sqrt{t} + M_{trans}\left(k_{eff}L_1\sqrt{t}\right)\left(-exp\left[-7.3\left(\frac{D_{eff}L_2 t}{h^2}\right)^{0.75}\right]\right) \quad (115)$$

where D_{eff} and k_{eff} are the effective diffusion and relaxation/deterioration coefficients, modified through correction factors as in Equation (56), with h representing the thickness.

Based on this analysis, it is reasonable to propose that the structural modification factor, denoted as k, is intricately linked to the uptake of a secondary phase. The diffusion process within this secondary phase progresses at a slower time scale, posing challenges in precisely determining the secondary equilibrium moisture content within the time constraints of most experimental investigations [69,126,159,207,221,235,249,263–268].

Berens and Hopfenberg [159] suggested use of a linear combination of distinct contributions from Fickian diffusion and polymeric relaxation, considered independently. The Behrens–Hopfenberg model [159] is founded upon the relaxation phenomena that occur as a result of polymer swelling during diffusion. In a glassy polymer, the diffusion of water is facilitated by Fickian diffusion, alongside changes in relaxation within the polymer network as the free volume undergoes alterations [159,269]. The total amount of absorption at time t, M_t, can be expressed as follows:

$$M_t = M_{F,t} + M_{R,t} \quad (116)$$

where M_t is the moisture uptake at time t, $M_{F,t}$ denotes the moisture uptake for the Fickian diffusion stage and $M_{R,t}$ represents the moisture uptake corresponding to the relaxation- dominant stage. After a period of diffusion primarily governed by Fick's law, swelling of the polymer leads to a gradual and significant increase in moisture sorption due to volume expansion. Simultaneously, physical or chemical degradation processes, such as polymer hydrolysis, chain breakage, the formation of small molecules, and their extraction from the composite, also take place, resulting in mass loss of the composite. If the mass loss resulting from physical or chemical degradation surpasses the increase in moisture due to swelling, it leads to a gradual reduction in moisture sorption, and vice versa. This phenomenon, encompassing swelling and initial chemical reactions, is referred to as the relaxation-dominated process and is assumed to follow first-order kinetics [159,270], such that

$$\frac{\mathrm{d}M_{R,t}}{\mathrm{d}t} = k\left(M_{R,\infty} - M_{R,t}\right) \tag{117}$$

where k stands for the relaxation rate constant, $M_{R,\infty}$ denotes the equilibrium uptake level related to the relaxation process and $M_{R,t}$ is the moisture uptake corresponding to the relaxation-dominant stage. On this basis, Berens and Hopfenberg [270] introduced a more comprehensive expression to incorporate multiple viscoelastic processes in the following form:

$$M_{R,t} = \sum_{i=1}^{N}\left(M_{R_i,\infty}\right)\left(1 - e^{-k_i t}\right) \tag{118}$$

leading to

$$M_t = M_{F,t} + M_{R,t} = M_{F,\infty}\left(1 - exp\left[-7.3\left(\frac{Dt}{l^2}\right)^{0.75}\right]\right) + M_{R,\infty}(1 - exp(-kt^2)) \qquad (119)$$

where M_F represents the amount of absorbed water attributed to the Fickian diffusion process, M_R corresponds to the amount of absorbed water linked to relaxation phenomena, $M_{F,\infty}$ denotes the saturation level of water absorption attained in the first stage disregarding stress relaxation, $M_{R,\infty}$ represents the equilibrium moisture uptake amount related directly to the relaxation process, and D is the diffusion coefficient. Studies on absorption in polymers indicate that the rate-controlling mechanism depends on the size of the penetrant [238]. If absorption starts rapidly but slows down in the later stages, it suggests that diffusion exceeds relaxation. However, when these processes occur simultaneously, differentiating them based on the absorption curve becomes challenging. For a more comprehensive understanding of diffusion behavior, a modified diffusion model was introduced by Du et al. [162], outlining three distinct stages of diffusion as shown schematically in Figure 2-13.

In this model, stage I is primarily governed by concentration gradients, while stage II is characterized by polymer relaxation. Stage III, on the other hand, is mainly affected by aging temperatures [162], such that:

$$M(t) = M_{m,I}(t) + M_{m,II}(t) + M_{m,III}(t) \qquad (120)$$

where $M(t)$ is the moisture content at time t, $M_I(t)$, $M_{II}(t)$, and $M_{III}(t)$ represent the moisture contents over time in Stage I, Stage II, and Stage III, respectively, and can be determined as:

$$M_I(t) = M_{m,I}\left\{1 - exp\left[-7.3\left(\frac{D_I t_I}{h^2}\right)^{0.75}\right]\right\} \tag{121}$$

$$M_{II}(t) = M_{m,II}\left\{1 - exp\left[-7.3\left(\frac{D_{II} t_{II}}{h^2}\right)^{\phi}\right]\right\} \tag{122}$$

$$M_{III}(t) = M_{\infty}\left\{1 - exp\left[-(\alpha\langle t_{III} - t_{II}^{\infty}\rangle)^{\beta}\right]\right\} + \varphi(T) \tag{123}$$

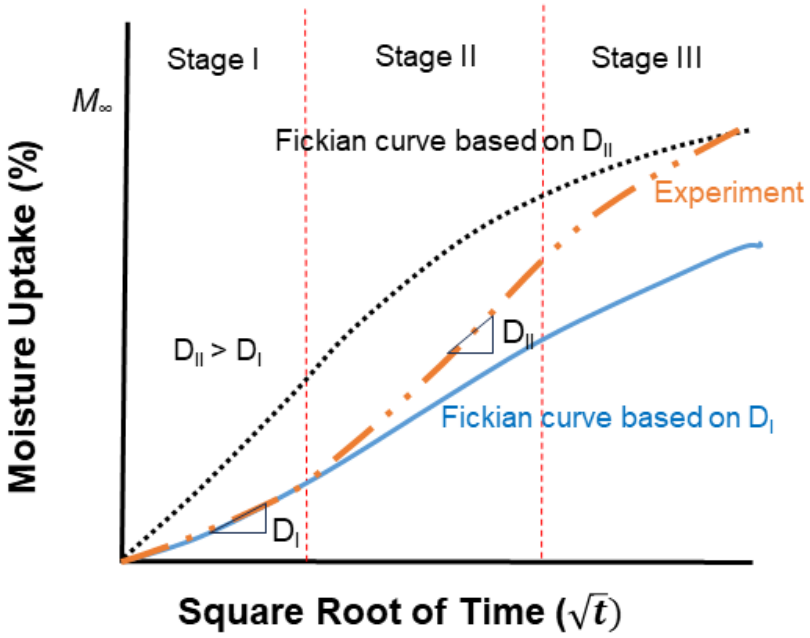

Figure 2-13. *Schematic showing three stages of uptake and bounding curves following [162].*

$M_{m,I}$ and $M_{m,II}$ represent the moisture content accrued in Stage I and Stage II, respectively, while M_∞ is the saturated moisture content. Similarly, D_I and D_{II} are the diffusion coefficient for Stage I and Stage II, respectively. Additionally, t_I, t_{II}, and t_{III} denote the moisture absorption time for each stage, while t_{II}^{∞} signifies the maximum absorption time at Stage II. Parameters ϕ, α, and β remain to be determined experimentally, and h denotes the thickness. The Macaulay bracket, < >, used for the time delay term, t_{III} - t_{II}^{∞}, signifies that third stage behavior occurs only when t_{III} is greater than or equal to t_{II}^{∞}. Additionally, $\varphi(T)$ functions as a dependency on aging temperature and is expressed as follows:

$$\varphi(T) = a\{1 - [exp(-k(T - T_{room}))]\} \tag{124}$$

where a and k denote parameters to be determined through experiments, with T representing temperature, and T_{room} indicating room temperature.

Another model, proposed by Gavril'eva et al. [271], introduces an additive model of moisture diffusion with a time-dependent diffusion coefficient and relaxational boundary conditions to address the challenges in achieving agreement between experimental and calculated results, emphasizing complex interactions of factors affecting moisture absorption kinetics in fiber-reinforced polymer composites. These factors involve redistribution of free volume, plasticization effect of water on the composite, damage formation, changes in stress concentration distribution, anisotropy, and swelling. It is difficult to develop integrated mechanistic models for each of these. In contrast, developing additive models that incorporate multiple processes is entirely feasible. The time-dependent nature of diffusion is expressed as follows:

$$D(t) = D_0 h(t) \tag{125}$$

where D_0 represents the initial diffusion coefficient, which remains constant, the function $h(t)$ denotes the time dependence of the diffusion coefficient, with $h(t)$ being greater than zero, and t signifies the time variable. By introducing a new time scale as τ

$$d\tau = h(t)dt, \text{ where } \tau = \int_0^t h(t)\, dt \tag{126}$$

a one-dimensional diffusion equation can be obtained [49,243]:

$$\frac{\mathrm{d}c(x,\tau)}{\mathrm{d}\tau} = D_0 \frac{\mathrm{d}^2 c(x,\tau)}{\mathrm{d}^2 x} \tag{127}$$

where τ is time, and the concentration of diffusing material at a point with coordinate x and time τ is denoted by $c(x,\tau)$, with D_0 representing the initial diffusion coefficient. In the new time scale, τ, the assumption is made that the boundary condition for Equation (127) takes the following form:

$$\mu(\tau) = \mu_1 + (\mu_0 - \mu_1)e^{-r\tau} \tag{128}$$

where parameters μ_0 and μ_1 denote the initial and limiting solubility, respectively, while r represents the relaxation constant ($r \geq 0$). Equation (128) defines the boundary condition, illustrating the structural relaxation of the polymer binder influenced by moisture [271]. Moisture

absorbed is then determined by measuring the mass of body at a specific time, τ, and is represented as follows:

$$M(t) = \widehat{M}(\tau) = \int_0^t c(x,\tau)\,\mathrm{d}\,x \tag{129}$$

such that the quantity of moisture absorbed at time by an initially dry plate is as follows [272]:

$$M(\tau) = M_1 + (M_0 - M_1)e^{-r\int_0^t h(t)dt} - 8\sum_{k=0}^{\infty} S_k \tag{130}$$

where M_0 and M_1 represent the limiting moisture content before, and after, stress relaxation due to moisture absorption in a plate with thickness l. r is the relaxation constant, and $h(t)$ denotes the time dependence of the diffusion coefficient. The term S_k is expressed as follows:

$$S_k = \frac{(M_0 n_k^2 D_0/l^2 - M_1 r)e^{-n_k^2 D_0/l^2 \int_0^t h(t)dt} + r(M_1 - M_0)e^{-r\int_0^t h(t)dt}}{n_k^2(n_k^2 D_0/l^2 - r)} \tag{131}$$

where l is the thickness of the plate, and $n_k = 2\pi(2k + 1)$. The model incorporates relaxation with Fickian diffusion, and when the relaxation term, r, is zero, the structure is basically that of Fickian diffusion.

Another version of the Fickian model, proposed by Upadhyay and Mishra [273], accounts for the impact of temperature on moisture absorption. In this equation, modifications have been proposed through the introduction of empirical parameters into the one-dimensional Fickian solution itself. To account for the concentration dependency of moisture absorption, the diffusion coefficient is described in relation to the instantaneous moisture concentration as follows:

$$D_{eff}(t) = D[1 + d \cdot M^2(t)] \tag{132}$$

where *D* is the coefficient of diffusion in a moisture-free condition, while *d*, a constant determined empirically, denotes the moisture sensitivity of the diffusion coefficient. It should be noted that when materials are exposed to moisture, not all water molecules in the environment are free; rather, they are weakly hydrogen-bonded. Therefore, they are not readily available for diffusion. A molecule cannot diffuse until it detaches from surrounding molecules. Consequently, the environmental moisture concentration is reduced by a factor, denoted as *b*, such that

$$M_{m\,eff} = b \cdot M_m \tag{133}$$

where M_m stands for the apparent atmospheric moisture concentration, and *b* represents a dimensionless constant, with its value falling between 0 and 1. Unlike the classical assumption, that assumes the composite can absorb moisture to its full capacity instantaneously, in reality, a finite amount of time is always required to attain the boundary conditions, which refers to the time taken to account for time delays and lags between the actual process and the idealized assumption of instantaneous boundary conditions. This discrepancy implies that the actual time taken to reach

a given concentration level within the material will always exceed the classical model's predictions. This aspect can be considered by introducing a time-shift factor t_s, such that

$$t_{eff} = (t - t_s) \ , \ t_s < t \tag{134}$$

where the variable t_s indicates the duration necessary for the establishment of the boundary condition within the material. Elevated temperatures result in increased kinetic energy and mobility of molecules, leading to higher coefficients of moisture diffusion. Considering the temperature dependency of the diffusion coefficient, the coefficient of diffusion can be formulated as follows:

$$D(T) = D_R \, exp[(\frac{E}{KT_R} - \frac{E}{KT})] \tag{135}$$

where $D(T)$ represents the diffusion coefficient at absolute temperature T, D_R denotes the diffusion coefficient at absolute reference temperature T_R, E represents a constant (activation energy for the process), and K is the Boltzmann constant, with a value of 1.38×10^{-23} joules per kelvin (J/K). Using Equations (133)–(135), Upadhyay and Mishra [273] concluded that moisture content can be determined as follows:

$$M(t) = \frac{2}{\sqrt{\pi}} \cdot b \cdot (M_m) \cdot \left[\frac{D_R \, exp\left(\frac{A}{T_R} - \frac{A}{T}\right) \cdot (t - t_s)}{L^2} \right]^{1/2} \tag{136}$$

where $M(t)$ represents the moisture uptake at time t, M_m is the apparent atmospheric moisture concentration, b is a dimensionless constant, D_R denotes the coefficient of diffusion at the absolute

reference temperature T_R, T represents the absolute temperature, L is the thickness of the specimen, and t_s measures the time required for the establishment of the boundary concentration in the material. Furthermore, A is another constant replaced by E/K, for simplicity.

As previously mentioned, with increasing temperature or humidity, Fickian diffusion mechanisms lose dominance, enabling other mechanisms to play a more significant role in moisture transport. To model concurrent diffusive, relaxation, and chemical degradation sorption or damage mechanisms, Xin et al. [196] considered the contribution of moisture absorbed by each as superimposable with the total moisture sorption M_t, divided into a diffusion-dominated uptake $M_{F,t}$, a polymer relaxation-dominated uptake $M_{R,t}$, and a composite damage-dominated uptake $M_{D,t}$, expressed as follows:

$$M_t = M_{F,t} + M_{R,t} + M_{D,t} \tag{137}$$

where $M_{F,t}$, $M_{R,t}$, and $M_{D,t}$ represent the individual contributions of the Fickian, relaxation, and damage processes at time t as introduced by Behrens and Hopfenberg [159], corresponding to the factors. Microcracks and/or voids can be formed at the interface [274] between the fiber and polymer or between layers/laminae as a consequence of environmental exposure resulting in chemical degradation and water pressure. All these mechanisms would potentially result in a significant, and rapid, increase in moisture uptake levels, especially over the composite damage-dominated regime, which is represented through an exponential form based on the trends seen in experimental data. The composite damage-dominated uptake, which is initiated after a specific aging time is expressed through the introduction of a Macauley bracket as follows:

$$M_{D,t} = M_{D,i} e^{\Omega \langle t - t_D \rangle} \tag{138}$$

where t_D represents the initial time when damage is initiated, Ω is a parameter associated with the uptake influenced by damage, $M_{D,i}$ is the mass sorption at the onset of damage, and $\langle\ \rangle$ denotes the Macauley bracket operator. Xin et al. express moisture absorption [196] as follows:

$$M_t = M_{F,\infty} \left(1 - exp \left[-7.3 \left(\frac{Dt}{h^2} \right)^{0.75} \right] \right) + \sum_{i=1}^{N} \left(M_{\mathrm{R},\infty} \right) (1 - e^{-k_i t}) + M_{D,i} e^{-\Omega \langle t - t_D \rangle} \tag{139}$$

where $M_{F,\infty}$ is the saturation level of water absorption disregarding stress relaxation, $M_{R,\infty}$ is the equilibrium moisture uptake amount related to the relaxation process, $M_{D,i}$ is the mass sorption at the onset of damage, k stands for the relaxation rate constant, and D is the diffusion coefficient.

A function characterized by three parameters, the equilibrium moisture content, initial diffusion coefficient, and the rate of diffusion variation over time can be employed to describe the absorption dynamics associated with non-Fickian diffusion. In contrast to the Fickian model, this approach [259] introduces an equivalent time parameter, denoted as t^*, rather than the physical time, to establish the relationship between the variation rate of the diffusion coefficient and time. The diffusion coefficient D is extremely sensitive to temperature in the context of moisture absorption and can be empirically expressed as follows:

$$D = D_0 e^{-\lambda t} \tag{140}$$

$$t^* = \frac{1 - e^{-\lambda t}}{\lambda} \tag{141}$$

leading to a solution in the form of a trigonometrical series for the Fickian model:

$$\frac{M_t}{M_\infty} = 1 - \sum_{n=0}^{\infty} \frac{8}{(2n+1)^2 \pi^2} e^{\frac{-D\,(2n+1)\pi^2 t^2}{l^2}} \tag{142}$$

where, at time t, M_t represents the amount of moisture absorbed, M_∞ is the maximum amount of moisture that can be absorbed, n is an integer indicating the number of terms in the series, D is the diffusion coefficient, and l is the thickness of the sample. Incorporating an equivalent parameter, t^* and D into Equation (142), where D_0 represents the initial diffusion coefficient and λ signifies the rate at which the moisture vapor diffusion coefficient changes over time, yields the time-varying diffusion model as follows:

$$\frac{M_t}{M_\infty} = 1 - \sum_{n=0}^{\infty} \frac{8}{(2n+1)^2 \pi^2} e^{\frac{-D_0\,(2n+1)\pi^2 t^*}{l^2}} \tag{143}$$

The time-varying diffusion coefficient model can be presented by modifying the classic Fickian model, with the diffusion coefficient treated as a function of time as suggested by Weitsman [243], such that

$$\frac{\partial C}{\partial t} = D_0 \, exp\left[-\frac{B}{\theta(t)}\right]\frac{\partial^2 C}{\partial x^2} \tag{144}$$

where D_0 and B represent material constants, while $\theta(t)$ signifies the absolute temperature, and results in the following:

$$C(x,t) = C_0\left\{1 + \frac{4}{\pi}\sum_{n=1}^{\infty}\frac{(-1)^n}{2n-1}cos\left[\frac{(2n-1)\pi x}{2L}\right]exp\left[-\left(\frac{(2n-1)\pi}{2}\right)^2 t^*\right]\right\} \tag{145}$$

where

$$t^* = \frac{D_0\int_0^t exp\left[-\frac{B}{\theta(s)}\right]ds}{L^2} \tag{146}$$

If the integral in Equation (145) equals *t*, diffusion is independent of time and simplifies to Fickian diffusion.

Roy et al. [171] suggested that viscoelastic effects influencing moisture absorption in polymers could be addressed by introducing a time-dependent diffusion coefficient and showed that moisture absorption can be effectively represented by incorporating a diffusion coefficient that increases exponentially to a plateau in the form of a Prony series, such that

$$D(t) = D_0 + \sum_r D_r \left[1 - exp\left(-\frac{t}{\tau_r}\right)\right] \quad (147)$$

leading to

$$\frac{M_t}{M_\infty} = 1 - \frac{8}{\pi^2}\sum_{n=0}^{\infty}\frac{1}{(2n+1)^2} exp\left\{\frac{-(2n+1)^2\pi^2}{l^2} \times \left[D_0 t + \sum_{r=1}^{R} D_r \left[t + \tau_r\left(e^{-\frac{t}{\tau_r}} - 1\right)\right]\right]\right\} \quad (148)$$

where the primary factors, M_∞, D_0, D_r, and τ_r, are determined through the process of fitting equation to the experimental data. M_t denotes the total amount of diffusing substance that has entered the material at time t, and M_∞ is the corresponding quantity after infinite time. D_0 and D_r are the unknown temperature-dependent Prony coefficients, τ_r is the time constant governing the time variation of D, corresponding to the retardation times, and n is the number of terms in the series.

The models discussed inherently assume that moisture uptake is based on resin characteristics and damage/defects in the composite including fiber–matrix debonding which can lead to increased moisture uptake due to wicking. Fibers cause anisotropy in the composite and thus also cause diffusion to be anisotropic with diffusion being fastest in the direction of fibers and slowest through the thickness. Fiber volume fraction, as seen through the formulation of some of the models, plays an important role both in terms of acting as a barrier to uptake and in increasing the tortuosity of the path of moisture ingress. Moisture uptake kinetics as a function of fiber volume fraction have been studied by Ray [115] and Kondo and Taki [275], who reported that diffusion kinetics were not affected. However, other studies have reported significant dependence on fiber

structure with directional diffusion ratios changing based on fabric type and fiber orientation [16,140,207,276–278] with a typical range of 25 to 53%. Korkees [55] and Dana et al. [279] presents an extensive review of fiber structure effects on diffusion in carbon/epoxy composites, emphasizing that the moisture uptake and diffusivity are significantly influenced by factors such as fiber volume fraction, fabric architecture, layup orientation, void content, and integrity of the fiber–matrix interfacial bond. Further details on directional diffusion are also reported by Korkees et al. [200], who reported that diffusion along fibers was three times faster than across them, and seven times faster than that in the through-thickness direction, In addition, they further emphasized the need to consider a two-stage response with an initial rapid Fickian response being, followed by a much slower second-stage that could extend for over 3.7 years.

These considerations, however, assume that the fibers themselves do not absorb moisture. In the case of aramid fibers, and others with similar morphologies, models need to consider two additional factors: (a) the uptake within the fiber itself and its contribution to overall diffusional response, and (b) the effect of fiber anisotropy, which extends to uptake and hence results in axial and radial diffusivities in the fiber itself. While these are not the focus of the current review, the interested reader is referred to the work by Aronhime et al. [170], Allred and Lindross [280], Cervenka et al. [281], and Wang et al. [282].

Thus, a large number of models have been developed to address diffusion taking into account a range of mechanisms and approaches, often differentiating moisture uptake into phases, where at least one is considered to be diffusion-dominated. The choice of method depends on the details of the material and exposure condition and must be considered carefully prior to selection.

2.6. CONCLUSIONS

FRP composites used in civil, marine, and offshore infrastructure applications are exposed to a range of environmental conditions, among which those of humidity and immersion are of specific interest because of their commonality and the complexity of resulting mechanisms in the polymer and composite. Based on a focused review, the following generic conclusions can be drawn:

- Transport of moisture into a polymer composite is affected through a range of mechanisms, including through interaction with the polymer chain itself and sorption into the volume. Rates of transport can be accelerated through damage in the composite in the form of microvoids/microcracks and fiber–matrix debonding. The interactions between the sorbed moisture and the constituents of the FRP composite are complex and can change through the service life of the structure.
- Uptake of solution into a composite can result in a range of reversible and irreversible mechanisms, which are affected by factors such as exposure environments, including temperature, constituent materials, extent of cure progression, and pre-existing damage.
- The effect of humidity levels on moisture uptake is dependent not just on the level of the humidity, but also on the temperature of exposure. Although levels of equivalence are often used between saturated humidity and immersion, the effect of both on the rate of uptake and maximum uptake are significantly different.
- Moisture uptake profiles can range from the extremes of linear to exponential with sigmoidal and stepped profiles in between. These can often be characterized by

diffusion coefficients and levels of moisture uptake equilibrium, both of which may have multiple phases based on the mechanics of sorption and the resulting shape of the uptake.

- Both rate coefficients and levels of equilibrium (transition, intermediate, and maximum) are affected by the temperature and humidity of exposure, as well as conditions of immersion. Increases in temperature generically increase rates of uptake through increases in molecular mobility. However, temperature increases, as well as initial exposure to moisture, can accelerate cure progression in FRP composites that have not attained complete polymerization prior to exposure, leading to a competition between phenomena that increase performance while decreasing capacity for sorption and those that increase sorption and deterioration.
- The Fickian diffusion model is most commonly used to describe moisture uptake and assumes that the diffusion coefficient is independent of moisture concentration and of its through thickness location, and that an equilibrium level of moisture uptake is attained which is independent of temperature of humidity exposure/immersion. Research has, however, shown that there are significant deviations from Fickian response, resulting in the development and use of stepped and phased models.
- In considering the appropriate model to describe the uptake response of a FRP composite, it is important to consider mechanisms of change in the constituents, as well as effects of aspects such as concentration at saturation and solvent activity. In this regard, the range of responses can be summarized below.

- Henry's law, where

$$C_{sat} = SP$$

- Freundlich's relation (power law), where

$$C_{sat} = a\left(\frac{P}{P_{sat}}\right)^{b}$$

- Fick's law, where

$$C_{sat} = \frac{-\frac{J}{D}\,P_{sat}}{\frac{dP}{dx}}$$

- Langmuir response, where

$$C_{sat} = \frac{cP}{1 + dP}$$

- Dual phased sorption, where

$$C_{sat} = SP + \frac{cP}{1 + dP}$$

in which C_{sat} is the water concentration at saturation, S is the solubility of water in the material (i.e., Henry's constant), P is the water partial pressure, P_{sat} is the saturation water pressure (such that $\%RH = 100\frac{P}{P_{sat}}$), J is the amount of moisture per unit area per unit time (defined as diffusion flux), D is the diffusion coefficient (which is a constant) and a, b, c, and d are constants that represent solvent activity.

- The Langmuir model intrinsically relates changes to the probability of conversion between two states of water, free and bound, and thus captures changes in uptake based on the stage of moisture uptake. This addresses some of the deviations from Fickian response but does not address longer-term effects, such as relaxation.

- Phased and stepped models assume that inherent changes in the material are due to the effects of uptake catalyze/initial additional/new mechanisms as the level of uptake increases, representing the changes through steps/phases.
- While the two-phased Fickian and the two-step (structural modification) models share the basic setup characteristics of dividing uptake into three regimes with the initial being diffusion-dominated and the second being a transition, they differ in the consideration of the third, with the former positing diffusion with a contribution to the first stage through two simultaneous mechanisms of diffusion and the latter considering two distinct mechanisms, initially a faster diffusion-dominated regime, and then a slower relaxation/deterioration-dominated regime. The two-step models are thus able to better capture response when there is apparent mass loss due to leaching of lower-molecular-weight species and/or constituents of the FRP composites.
- While the material provided in the review covers a range of models, it is cautioned that selection of a model depends on factors such as details of the material and its constituents, length of assessment, aspects of environmental exposure, and operative mechanisms. In many cases, experimental/field data are only available for short periods of time, thus obscuring/neglecting materials level changes that cause diffusional deviations from the simple Fickian response. It is emphasized that more research needs to be conducted to develop a comprehensive understanding not only of mechanisms and methods of describing uptake, but of directly linking these to the prediction of long-term response and durability.

2.7. REFERENCES

1. Gkikas, G.; Douka, D.D.; Barkoula, N.M.; Paipetis, A.S. Nano-enhanced composite materials under thermal shock and environmental degradation: A durability study. *Compos. Part B Eng.* **2015**, *70*, 206–214.

2. Machello, C.; Bazli, M.; Rajabipour, A.; Rad, H.M.; Arashpour, M.; Hadigheh, A. Using machine learning to predict the long-term performance of fibre-reinforced polymer structures: A state-of-the-art review. *Constr. Build. Mater.* **2023**, *408*, 133692.

3. Liu, T.Q.; Liu, X.; Feng, P. A comprehensive review on mechanical properties of pultruded FRP composites subjected to long-term environmental effects. *Compos. Part B Eng.* **2020**, *191*, 107958.

4. Tatar, J.; Milev, S. Durability of externally bonded fiber-reinforced polymer composites in concrete structures: A critical review. *Polymers* **2021**, *13*, 765.

5. Alsuhaibani, E.; Yazdani, N.; Beneberu, E. Durability and long-term performance prediction of carbon fiber reinforced polymer laminates. *Polymers* **2022**, *14*, 3207.

6. Airale, A.G.; Carello, M.; Ferraris, A.; Sisca, L. Moisture effect on mechanical properties of polymeric composite materials. In *AIP Conference Proceedings*; AIP Publishing: Naples, Italy, 2016; Volume 1736, p. 020020.

7. Khotbehsara, M.M.; Manalo, A.; Aravinthan, T.; Ferdous, W.; Nguyen, K.T.Q.; Hota, G. Ageing of particulate-filled epoxy resin under hygrothermal conditions. *Constr. Build. Mater.* **2020**, *249*, 118846.

8. Bratasyuk, N.A.; Latyshev, A.V.; Zuev, V.V. Water in epoxy coatings: Basic principles of interaction with polymer matrix and the influence on coating life cycle. *Coatings* **2023**, *14*, 54.

9. Ray, B.C. Effects of crosshead velocity and sub-zero temperature on mechanical behaviour of hygrothermally conditioned glass fibre reinforced epoxy composites. *Mater. Sci. Eng. A* **2004**, *379*, 39–44.

10. Meurs, P.F.; Schreurs, P.J.; Peijs, T.; Meijer, H.E. Characterization of interphase conditions in composite materials. *Compos. Part A Appl. Sci. Manuf.* **1996**, *27*, 781–786.

11. Selzer, R.; Friedrich, K. Mechanical properties and failure behaviour of carbon fibre-reinforced polymer composites under the influence of moisture. *Compos. Part A Appl. Sci. Manuf.* **1997**, *28*, 595–604.

12. Boubakri, A.; Elleuch, K.; Guermazi, N.; Ayedi, H.F. Investigations on hygrothermal aging of thermoplastic polyurethane material. *Mater. Des.* **2009**, *30*, 3958–3965.

13. Grammatikos, S.A.; Evernden, M.; Mitchels, J.; Zafari, B.; Mottram, J.T.; Papanicolaou, G.C. On the response to hygrothermal aging of pultruded FRPs used in the civil engineering sector. *Mater. Des.* **2016**, *96*, 283–295.

14. Yilmaz, T.; Sinmazcelik, T. Effects of hydrothermal aging on glass–fiber/polyetherimide (PEI) composites. *J. Mater. Sci.* **2010**, *45*, 399–404.

15. Adamson, M.J. Thermal expansion and swelling of cured epoxy resin used in graphite/epoxy composite materials. *J. Mater. Sci.* **1980**, *15*, 1736–1745.

16. Karbhari, V.M.; Xian, G. Hygrothermal effects on high V_F pultruded unidirectional carbon/epoxy composites: Moisture uptake. *Compos. Part B Eng.* **2009**, *40*, 41–49.

17. Pavlidou, S.; Papaspyrides, C.D. The effect of hygrothermal history on water sorption and interlaminar shear strength of glass/polyester composites with different interfacial strength. *Compos. Part A Appl. Sci. Manuf.* **2003**, *34*, 1117–1124.

18. Akbar, S.; Zhang, T. Moisture diffusion in carbon/epoxy composite and the effect of cyclic hygrothermal fluctuations: Characterization by dynamic mechanical analysis (DMA) and interlaminar shear strength (ILSS). *J. Adhes.* **2008**, *84*, 585–600.

19. Nogueira, P.; Ramírez, C.; Torres, A.; Abad, M.J.; Cano, J.; López, J.; López-Bueno, I.; Barral, L. Effect of water sorption on the structure and mechanical properties of an epoxy resin system. *J. Appl. Polym. Sci.* **2001**, *80*, 71–80.

20. Karbhari, V.M.; Chin, J.W.; Hunston, D.; Benmokrane, B.; Juska, T.; Morgan, R.; Lesko, J.J.; Sorathia, U.; Reynaud, A.D. Durability gap analysis for fiber-reinforced polymer composites in civil infrastructure. *J. Compos. Constr.* **2003**, *7*, 238–247.

21. Mikols, W.J.; Seferis, J.C.; Apicella, A.; Nicolais, L. Evaluation of structural changes in epoxy systems by moisture sorption-desorption and dynamic mechanical studies. *Polym. Compos.* **1982**, *3*, 118–124.

22. Birger, S.; Moshonov, A.; Kenig, S. The effects of thermal and hygrothermal ageing on the failure mechanisms of graphite-fabric epoxy composites subjected to flexural loading. *Composites* **1989**, *20*, 341–348.

23. Levy, R.L.; Fanter, D.L.; Summers, C.J. Spectroscopic evidence for mechanochemical effects of moisture in epoxy resins. *J. Appl. Polym. Sci.* **1979**, *24*, 1643–1664.

24. Costa, M.L.; Almeida, S.F.; Rezende, M.C. Hygrothermal effects on dynamic mechanical analysis and fracture behavior of polymeric composites. *Mater. Res.* **2005**, *8*, 335–340.

25. Zhou, J.; Lucas, J.P. Hygrothermal effects of epoxy resin. Part I: The nature of water in epoxy. *Polymer* **1999**, *40*, 5505–5512.

26. Mijović, J.; Lin, K.F. The effect of hygrothermal fatigue on physical/mechanical properties and morphology of neat epoxy resin and graphite/epoxy composite. *J. Appl. Polym. Sci.* **1985**, *30*, 2527–2549.

27. Antoon, M.K.; Koenig, J.L. The structure and moisture stability of the matrix phase in glass-reinforced epoxy composites. *J. Macromol. Sci.—Rev. Macromol. Chem.* **1980**, *19*, 135–173.

28. Pipes, R.B.; Vinson, J.R.; Chou, T.W. On the hygrothermal response of laminated composite systems. *J. Compos. Mater.* **1976**, *10*, 129–148.

29. Hahn, H.T. Residual stresses in polymer matrix composite laminates. *J. Compos. Mater.* **1976**, *10*, 266–278.

30. Sousa, J.M.; Correia, J.R.; Cabral-Fonseca, S. Durability of glass fibre reinforced polymer pultruded profiles: Comparison between QUV accelerated exposure and natural weathering in a mediterranean climate. *Exp. Tech.* **2016**, *40*, 207–219.

31. Cabral-Fonseca, S.; Correia, J.R.; Rodrigues, M.P.; Branco, F.A. Artificial accelerated ageing of GFRP pultruded profiles made of polyester and vinylester resins: Characterisation of physical–chemical and mechanical damage. *Strain* **2012**, *48*, 162–173.

32. Starkova, O.; Buschhorn, S.T.; Mannov, E.; Schulte, K.; Aniskevich, A. Water transport in epoxy/MWCNT composites. *Eur. Polym. J.* **2013**, *49*, 2138–2148.

33. Grammatikos, S.A.; Zafari, B.; Evernden, M.C.; Mottram, J.T.; Mitchels, J.M. Moisture uptake characteristics of a pultruded fibre reinforced polymer flat sheet subjected to hot/wet aging. *Polym. Degrad. Stab.* **2015**, *121*, 407–419.

34. Schutte, C.L. Environmental durability of glass-fiber composites. *Mater. Sci. Eng. R Rep.* **1994**, *13*, 265–323.

35. Jones, F.R. Durability of reinforced plastics in liquid environments. In *Reinforced Plastics Durability*, 1st ed.; Pritchard, G., Ed.; Woodhead Publishing: Cambridge, UK, 1999; Volume 10, Chapter 3, pp. 70–110.

36. McKague, E.L., Jr.; Reynolds, J.D.; Halkias, J.E. Swelling and glass transition relations for epoxy matrix material in humid environments. *J. Appl. Polym. Sci.* **1978**, *22*, 1643–1654.

37. Wood, C.A.; Bradley, W.L. Determination of the effect of seawater on the interfacial strength of an interlayer E-glass/graphite/epoxy composite by in situ observation of transverse cracking in an environmental SEM. *Compos. Sci. Technol.* **1997**, *57*, 1033–1043.

38. Ghorbel, I.; Valentin, D. Hydrothermal effects on the physico-chemical properties of pure and glass fiber reinforced polyester and vinylester resins. *Polym. Compos.* **1993**, *14*, 324–334.

39. Lassila, L.V.; Nohrström, T.; Vallittu, P.K. The influence of short-term water storage on the flexural properties of unidirectional glass fiber-reinforced composites. *Biomaterials* **2002**, *23*, 2221–2229.

40. Zheng, Q.; Morgan, R.J. Synergistic thermal-moisture damage mechanisms of epoxies and their carbon fiber composites. *J. Compos. Mater.* **1993**, *27*, 1465–1478.

41. Lowry, H.H.; Kohman, G.T. The mechanism of the absorption of water by rubber. *J. Phys. Chem.* **1927**, *31*, 23–57.

42. Adams, R.D.; Singh, M.M. The dynamic properties of fibre-reinforced polymers exposed to hot, wet conditions. *Compos. Sci. Technol.* **1996**, *56*, 977–997.

43. Lee, M.C.; Peppas, N.A. Water transport in epoxy resins. *Prog. Polym. Sci.* **1993**, *18*, 947–961.

44. Wright, W.W. The effect of diffusion of water into epoxy resins and their carbon-fibre reinforced composites. *Composites* **1981**, *12*, 201–205.

45. Lekatou, A.; Faidi, S.E.; Ghidaoui, D.; Lyon, S.B.; Newman, R.C. Effect of water and its activity on transport properties of glass/epoxy particulate composites. *Compos. Part A Appl. Sci. Manuf.* **1997**, *28*, 223–236.

46. Brunauer, S. *Gases and Vapors, The Adsorption of Gases and Vapors—Physical Adsorption*; Princeton University Press: Princeton, NJ, USA, 1943; Volume 1.

47. Tvardovskiy, A.V. *Sorbent Deformation*, 1st ed.; Elsevier, Academic Press: Amsterdam, The Netherlands, 2006; Volume 13, Chapter 1, pp. 5–28.

48. Jost, W. Diffusion in solids, liquids, gases. *Z. Für Phys. Chem.* **1952**, *201*, 319–320.

49. Crank, J. *The Mathematics of Diffusion*, 2nd ed.; Clarendon press: Oxford, UK, 1975; pp. 104–137.

50. Karbhari, V.M. E-glass/vinylester composites in aqueous environments: Effects on short-beam shear strength. *J. Compos. Constr.* **2004**, *8*, 148–156.

51. Chin, J.W.; Nguyen, T.; Aouadi, K. Sorption and diffusion of water, salt water, and concrete pore solution in composite matrices. *J. Appl. Polym. Sci.* **1999**, *71*, 483–492.

52. Clunie, J.S.; Ingram, B.T. Adsorption of nonionic surfactants. In *Adsorption from Solution at the Solid/Liquid Interface*; Parfitt, G.D., Rochester, C.H., Eds.; Academic Press: New York, NY, USA, 1983; pp. 105–152.

53. Brunauer, S.; Skalny, J.; Bodor, E.E. Adsorption on nonporous solids. *J. Colloid Interface Sci.* **1969**, *30*, 546–552.

54. Hagymassy, J., Jr.; Brunauer, S.; Mikhail, R.S. Pore structure analysis by water vapor adsorption: I. t-curves for water vapor. *J. Colloid Interface Sci.* **1969**, *29*, 485–491.

55. Korkees, F. Moisture absorption behavior and diffusion characteristics of continuous carbon fiber reinforced epoxy composites: A review. *Polym.-Plast. Technol. Mater.* **2023**, *62*, 1789–1822.

56. Cotugno, S.; Larobina, D.; Mensitieri, G.; Musto, P.; Ragosta, G. A novel spectroscopic approach to investigate transport processes in polymers: The case of water–epoxy system. *Polymer* **2001**, *42*, 6431–6438.

57. Van Amerongen, G.J. Diffusion in elastomers. *Rubber Chem. Technol.* **1964**, *37*, 1065–1152.

58. Weinmüller, C.; Langel, C.; Fornasiero, F.; Radke, C.J.; Prausnitz, J.M. Sorption kinetics and equilibrium uptake for water vapor in soft-contact-lens hydrogels. *J. Biomed. Mater. Res. Part A* **2006**, *77*, 230–241.

59. Pérez-Pacheco, E.; Cauich-Cupul, J.I.; Valadez-González, A.; Herrera-Franco, P.J. Effect of moisture absorption on the mechanical behavior of carbon fiber/epoxy matrix composites. *J. Mater. Sci.* **2013**, *48*, 1873–1882.

60. Hinkley, J.A.; Connell, J.W. Resin system and chemistry: Degradation mechanisms and durability. In *Long-Term Durability of Polymeric Matrix Composites*, 1st ed.; Pochiraju, K.V., Tandon, G.P., Schoeppner, G.A., Eds.; Springer Science & Business Media: New York, NY, USA, 2011; Chapter 1, pp. 1–37.

61. Hussnain, S.M.; Shah, S.Z.H.; Megat-Yusoff, P.S.M.; Hussain, M.Z. Degradation and mechanical performance of fibre-reinforced polymer composites under marine environments: A review of recent advancements. *Polym. Degrad. Stab.* **2023**, *215*, 110452.

62. Zhou, J.; Lucas, J.P. Hygrothermal effects of epoxy resin. Part II: Variations of glass transition temperature. *Polymer* **1999**, *40*, 5513–5522.

63. Hassanpour, B.; Karbhari, V.M. Glass transition temperature as a characteristic of the durability of fiber-reinforced polymer composites. In *Aging and Durability of FRP Composites and Nanocomposites*; Uthaman, A., Thomas, S., Mayookh Lal, H., Eds.; Woodhead Publishing, Elsevier: London, UK, 2024; Chapter 15, pp. 341–362.

64. Mercier, J.; Bunsell, A.; Castaing, P.; Renard, J. Characterisation and modelling of aging of composites. *Compos. Part A Appl. Sci. Manuf.* **2008**, *39*, 428–438.

65. Bao, L.-R.; Yee, A.F.; Lee, C.Y.-C. Moisture absorption and hygrothermal aging in a bismaleimide resin. *Polymer* **2001**, *42*, 7327–7333.

66. Léger, R.; Roy, A.; Grandidier, J.C. Non-classical water diffusion in an industrial adhesive. *Int. J. Adhes. Adhes.* **2010**, *30*, 744–753.

67. Ishida, H.; Koenig, J.L. The reinforcement mechanism of fiber-glass reinforced plastics under wet conditions: A review. *Polym. Eng. Sci.* **1978**, *18*, 128–145.

68. Bunker, B.C. Molecular mechanisms for corrosion of silica and silicate glasses. *J. Non-Cryst. Solids* **1994**, *179*, 300–308.

69. Apicella, A.; Nicolais, L.; De Cataldis, C. Characterization of the morphological fine structure of commercial thermosetting resins through hygrothermal experiments. In *Characterization of Polymers in the Solid State I: Part A: NMR and Other Spectroscopic Methods Part B: Mechanical Methods*, 1st ed.; Kaush, H.H., Zachman, H.G., Eds.; Advances in Polymer Science; Springer: Berlin/Heidelberg, Germany, 1985; pp. 189–207.

70. Takeshita, Y.; Becker, E.; Sakata, S.; Miwa, T.; Sawada, T. States of water absorbed in water-borne urethane/epoxy coatings. *Polymer* **2014**, *55*, 2505–2513.

71. Mijović, J.; Zhang, H. Molecular dynamics simulation study of motions and interactions of water in a polymer network. *J. Phys. Chem. B* **2004**, *108*, 2557–2563.

72. Nissan, A.H. H-bond dissociation in hydrogen bond dominated solids. *Macromolecules* **1976**, *9*, 840–850.

73. Kwei, T.K. Strength of epoxy polymers. *I. Eff. Chem. Struct. Environ. Cond. J. Appl. Polym. Sci.* **1966**, *10*, 1647–1655.

74. Wolff, E.G. Environmental effects—Mass Absorption. In *Introduction to the Dimensional Stability of Composite Materials*; DEStech Publications: Lancaster, PA, USA, 2004; Chapter 5, pp. 155–200.

75. Abusafieh, A.; Kalidindi, S.R. Effect of water absorption on the izod impact energy of crosslinked poly (methyl methacrylate-acrylic acid) and their composites. *Polym. Compos.* **1998**, *19*, 23–30.

76. Chiang, M.Y.; Fernandez-Garcia, M. Relation of swelling and T_g depression to the apparent free volume of a particle-filled, epoxy-based adhesive. *J. Appl. Polym. Sci.* **2003**, *87*, 1436–1444.

77. Adams, D.F. Properties characterization—Mechanical/physical/hygrothermal properties test methods. In *Reference Book for Composites Technology*; Lee, S.M., Ed.; Technomic Publishing Company: Lancaster, PA, USA, 1989; Volume 2, Chapter 4, pp. 40–78.

78. Zimm, B.H.; Lundberg, J.L. Sorption of vapors by high polymers. *J. Phys. Chem.* **1956**, *60*, 425–428.

79. Starkweather, H.W., Jr. Clustering of water in polymers. *J. Polym. Sci. Part B Polym. Lett.* **1963**, *1*, 133–138.

80. Van der Wel, G.K.; Adan, O.C.G. Moisture in organic coatings—A review. *Prog. Org. Coat.* **1999**, *37*, 1–14.

81. Karad, S.K.; Jones, F.R. Mechanisms of moisture absorption by cyanate ester modified epoxy resin matrices: The clustering of water molecules. *Polymer* **2005**, *46*, 2732–2738.

82. Delasi, R.; Whiteside, J.B. Effect of moisture on epoxy resins and composites. In *ASTM STP 658, Advanced Composite Materials—Environmental Effects*; Vinson, J.R., Ed.; American Society for Testing and Materials: Philadelphia, PA, USA, 1978; pp. 2–20.

83. Papanicolaou, G.C.; Kosmidou, T.V.; Vatalis, A.S.; Delides, C.G. Water absorption mechanism and some anomalous effects on the mechanical and viscoelastic behavior of an epoxy system. *J. Appl. Polym. Sci.* **2006**, *99*, 1328–1339.

84. Xian, G.; Karbhari, V.M. Segmental relaxation of water-aged ambient cured epoxy. *Polym. Degrad. Stab.* **2007**, *92*, 1650–1659.

85. Wedgewood, A.R.; Seferis, J.C.; Beck, T.R. Transport and related properties of paint films. II. Dynamic mechanical properties and humidity effects. *J. Appl. Polym. Sci.* **1985**, *30*, 111–133.

86. Mijovic, J.; Lin, K.F. Time-dependent changes in morphology of neat and reinforced epoxy resins part I. Neat epoxies. *J. Appl. Polym. Sci.* **1986**, *32*, 3211–3227.

87. Kong, E.S.; Adamson, M.J. Physical ageing and its effect on the moisture sorption of amine-cured epoxies. *Polym. Commun.* **1983**, *24*, 171–173.

88. Le Guen-Geffroy, A.; Le Gac, P.Y.; Habert, B.; Davies, P. Physical ageing of epoxy in a wet environment: Coupling between plasticization and physical ageing. *Polym. Degrad. Stab.* **2019**, *168*, 108947.

89. Leveque, D.; Schieffer, A.; Mavel, A.; Maire, J.F. Analysis of how thermal aging affects the long-term mechanical behavior and strength of polymer–matrix composites. *Compos. Sci. Technol.* **2005**, *65*, 395–401.

90. Ravve, A. Degradation of Polymers. In *Principles of Polymer Chemistry*, 2nd ed.; Kluwer Academic/Plenum Publishers: New York, NY, USA, 2000; pp. 581–616.

91. Apicella, A.; Migliaresi, C.; Nicolais, L.; Iaccarino, L.; Roccotelli, S. The water ageing of unsaturated polyester-based composites: Influence of resin chemical structure. *Composites* **1983**, *14*, 387–392.

92. Yi, Y.; Guo, S.; Li, S.; Rahman, M.Z.; Zhou, L.; Shi, C.; Zhu, D. Effect of alkalinity on the shear performance degradation of basalt fiber-reinforced polymer bars in simulated seawater sea sand concrete environment. *Constr. Build. Mater.* **2021**, *299*, 123957.

93. Nan, J.; Zhi, C.; Meng, J.; Miao, M.; Yu, L. Seawater aging effect on fiber-reinforced polymer composites: Mechanical properties, aging mechanism, and life prediction. *Text. Res. J.* **2023**, *93*, 3393–3413.

94. Bahrololoumi, A.; Morovati, V.; Shaafaey, M.; Dargazany, R. A multi-physics approach on modeling of hygrothermal aging and its effects on constitutive behavior of cross-linked polymers. *J. Mech. Phys. Solids* **2021**, *156*, 104614.

95. Karbhari, V.M. Long-term hydrothermal aging of carbon-epoxy materials for rehabilitation of civil infrastructure. *Compos. Part A Appl. Sci. Manuf.* **2022**, *153*, 106705.

96. Xiao, G.Z.; Shanahan, M.E.R. Swelling of DGEBA/DDA epoxy resin during hygrothermal ageing. *Polymer* **1998**, *39*, 3253–3260.

97. Boinard, E.; Pethrick, R.A.; Dalzel-Job, J.; Macfarlane, C.J. Influence of resin chemistry on water uptake and environmental ageing in glass fibre reinforced composites-polyester and vinyl ester laminates. *J. Mater. Sci.* **2000**, *35*, 1931–1937.

98. Mouzakis, D.E.; Zoga, H.; Galiotis, C. Accelerated environmental ageing study of polyester/glass fiber reinforced composites (GFRPCs). *Compos. Part B Eng.* **2008**, *39*, 467–475.

99. Mohammadi, H.; Morovati, V.; Poshtan, E.; Dargazany, R. Understanding decay functions and their contribution in modeling of thermal-induced aging of cross-linked polymers. *Polym. Degrad. Stab.* **2020**, *175*, 109108.

100. Lee, S.B.; Rockett, T.J.; Hoffman, R.D. Interactions of water with unsaturated polyester, vinyl ester and acrylic resins. *Polymer* **1992**, *33*, 3691–3697.

101. Karbhari, V.M. Dynamic mechanical analysis of the effect of water on E-glass-vinylester composites. *J. Reinf. Plast. Compos.* **2006**, *25*, 631–644.

102. Abeysinghe, H.P.; Edwards, W.; Pritchard, G.; Swampillai, G.J. Degradation of crosslinked resins in water and electrolyte solutions. *Polymer* **1982**, *23*, 1785–1790.

103. Bascom, W.D. The surface chemistry of moisture-induced composite failure. In *Interfaces Polymer Matrix Composites*, 1st ed.; Plueddeman, E.P., Ed.; Academic Press: New York, NY, USA; London, UK, 1974; Volume 6, pp. 79–108.

104. Bascom, W.D. Water at the interface. *J. Adhes.* **1970**, *2*, 161–183.

105. Michalske, T.A.; Freiman, S.W. A molecular mechanism for stress corrosion in vitreous silica. *J. Am. Ceram. Soc.* **1983**, *66*, 284–288.

106. Michalske, T.A.; Freiman, S.W. A molecular interpretation of stress corrosion in silica. *Nature* **1982**, *295*, 511–512.

107. Matthewson, M.J.; Kurkjian, C.R. Environmental effects on the static fatigue of silica optical fiber. *J. Am. Ceram. Soc.* **1988**, *71*, 177–183.

108. Kini, M.V.; Pai, D. The ageing effect on static and dynamic mechanical properties of fibre reinforced polymer composites under marine environment-a review. *Mater. Today Proc.* **2022**, *52*, 689–696.

109. Mirdehghan, S.A. Fibrous polymeric composites. In *Engineered Polymeric Fibrous Materials*, 1st ed.; Latifi, M., Ed.; Woodhead Publishing, Elsevier: Kidlington, UK, 2021; pp. 1–58.

110. Huang, S.; Fu, Q.; Yan, L.; Kasal, B. Characterization of interfacial properties between fibre and polymer matrix in composite materials–A critical review. *J. Mater. Res. Technol.* **2021**, *13*, 1441–1484.

111. Kaw, A.K. *Mechanics of Composite Materials*, 2nd ed.; CRC Press: Boca Raton, FL, USA, 2005.

112. Browning, C.E. The mechanisms of elevated temperature property losses in high performance structural epoxy resin matrix materials after exposures to high humidity environments. *Polym. Eng. Sci.* **1978**, *18*, 16–24.

113. Liao, K.; Tan, Y.M. Influence of moisture-induced stress on in situ fiber strength degradation of unidirectional polymer composite. *Compos. Part B Eng.* **2001**, *32*, 365–370.

114. Upadhyay, P.C.; Gupta, G.S.; Lyons, D.W. Plastic deformation of fiber coating in polymer matrix composites under hygrothermal loading. *J. Reinf. Plast. Compos.* **1999**, *18*, 985–1010.

115. Ray, B.C. Temperature effect during humid ageing on interfaces of glass and carbon fibers reinforced epoxy composites. *J. Colloid Interface Sci.* **2006**, *298*, 111–117.

116. Weitsman, Y.J.; Guo, Y.-J. A correlation between fluid-induced damage and anomalous fluid sorption in polymeric composites. *Compos. Sci. Technol.* **2002**, *62*, 889–908.

117. Yu, B.; Yang, J. Hygrothermal effects in composites. In *Comprehensive Composite Materials II*; Beaumont, P.W.R., Zweben, C.H., Eds.; Elsevier: Amsterdam, The Netherlands, 2018; Volume 1, pp. 502–519.

118. Gautier, L.; Mortaigne, B.; Bellenger, V. Interface damage study of hydrothermally aged glass-fibre-reinforced polyester composites. *Compos. Sci. Technol.* **1999**, *59*, 2329–2337.

119. Hahn, H.T. Hygrothermal damage in graphite/epoxy laminates. *ASME J. Eng. Mater. Technol.* **1987**, *109*, 3–11.

120. Kafodya, I.; Xian, G.; Li, H. Durability study of pultruded CFRP plates immersed in water and seawater under sustained bending: Water uptake and effects on the mechanical properties. *Compos. Part B Eng.* **2015**, *70*, 138–148.

121. Whitney, J.M.; Browning, C.E. Some anomalies associated with moisture diffusion in epoxy matrix composite materials. In *Advanced Composite Materials—Environmental Effects ASTM STP 658*; Vinson, J., Ed.; American Society for Testing and Materials: Philadelphia, PA, USA, 1978; pp. 43–60.

122. Pineda, A.F.; Garcia, F.G.; Simoes, A.Z.; da Silva, E.L. Mechanical properties, water absorption and adhesive properties of diepoxy aliphatic diluent-modified DGEBA/Cycloaliphatic amine networks on 316L stainless steel. *Int. J. Adhes. Adhes.* **2016**, *68*, 205–211.

123. Xiao, G.Z.; Delamar, M.A.; Shanahan, M.E.R. Irreversible interactions between water and DGEBA/DDA epoxy resin during hygrothermal aging. *J. Appl. Polym. Sci.* **1997**, *65*, 449–458.

124. Gillet, C.; Tamssaouet, F.; Hassoune-Rhabbour, B.; Tchalla, T.; Nassiet, V. Parameters influencing moisture diffusion in epoxy-based materials during hygrothermal ageing—A review by statistical analysis. *Polymers* **2022**, *14*, 2832.

125. Aktas, L.; Hamidi, Y.K.; Altan, M.C. Combined edge and anisotropy effects on Fickian mass diffusion in polymer composites. *J. Eng. Mater. Technol.* **2004**, *126*, 427–435.

126. Dewimille, B.; Bunsell, A.R. The modelling of hydrothermal aging in glass fibre reinforced epoxy composites. *J. Phys. D Appl. Phys.* **1982**, *15*, 2079.

127. Arvanitopoulos, C.D.; Koenig, J.L. Infrared spectral imaging of the interphase of epoxy-glass fiber-reinforced composites under wet conditions. *Appl. Spectrosc.* **1996**, *50*, 11–18.

128. Göpferich, A. Mechanisms of polymer degradation and erosion. *Biomaterials* **1996**, *17*, 117–128.

129. Göpferich, A. Erosion of composite polymer matrices. *Biomaterials* **1997**, *18*, 397–403.

130. Von Burkersroda, F.; Schedl, L.; Göpferich, A. Why degradable polymers undergo surface erosion or bulk erosion. *Biomaterials* **2002**, *23*, 4221–4231.

131. Lyu, S.; Sparer, R.; Untereker, D. Analytical solutions to mathematical models of the surface and bulk erosion of solid polymers. *J. Polym. Sci. Part B Polym. Phys.* **2005**, *43*, 383–397.

132. De'Nève, B.; Shanahan, M.E.R. Water absorption by an epoxy resin and its effect on the mechanical properties and infra-red spectra. *Polymer* **1993**, *34*, 5099–5105.

133. Shen, C.-H.; Springer, G.S. Moisture absorption and desorption of composite materials. *J. Compos. Mater.* **1976**, *10*, 2–20.

134. Schroeder, P.V. On the solidification and swelling phenomena of gelatine. *J. Phys. Chem.* **1903**, *45*, 75–117.

135. Choi, P.; Datta, R. Sorption in proton-exchange membranes: An explanation of Schroeder's paradox. *J. Electrochem. Soc.* **2003**, *150*, E601.

136. Onishi, L.M.; Prausnitz, J.M.; Newman, J. Water−Nafion equilibria. *Absence Schroeder's Parad. J. Phys. Chem. B* **2007**, *111*, 10166–10173.

137. Vallieres, C.; Winkelmann, D.; Roizard, D.; Favre, E.; Scharfer, P.; Kind, M. On Schroeder's paradox. *J. Membr. Sci.* **2006**, *278*, 357–364.

138. Harper, J.F.; Naeem, M. A comparative study of the effect of moisture absorption on the mechanical properties of glass fibre reinforced plastics. In *Controlled Interphases in Composite Materials*; Ishida, H., Ed.; Springer: Dordrecht, Netherlands, 1990; pp. 801–808.

139. Bonniau, P.A.; Bunsell, A.R. A comparative study of water absorption theories applied to glass epoxy composites. *J. Compos. Mater.* **1981**, *15*, 272–293.

140. Choi, H.S.; Ahn, K.J.; Nam, J.D.; Chun, H.J. Hygroscopic aspects of epoxy/carbon fiber composite laminates in aircraft environments. *Compos. Part A Appl. Sci. Manuf.* **2001**, *32*, 709–720.

141. Harrison, L.P. Fundamental concepts and definitions relating to humidity. In *Humidity and Moisture, Measurement and Control in Science and Industry*; Wexler, A., Ed.; Reinhold Publishing Corporation: New York, NY, USA, 1965; Volume 3, Chapter 1.

142. Ponec, V.; Knor, Z.; Cerny, S. *Adsorption on Solids*; Smith, D., Adams, N.G., Eds.; Butterworth: London, UK, 1974.

143. Brunauer, S.; Deming, L.S.; Deming, W.E.; Teller, E. On a theory of the van der Waals adsorption of gases. *J. Am. Chem. Soc.* **1940**, *62*, 1723–1732.

144. Vieth, W.R.; Howell, J.M.; Hsieh, J.H. Dual sorption theory. *J. Membr. Sci.* **1976**, *1*, 177–220.

145. Henry, W. Experiments on the quantity of gases absorbed by water, at different temperaturees, and under different pressures. *Philos. Trans. R. Soc. Lond.* **1803**, *93*, 29–43.

146. Loos, A.C.; Springer, G.S. Moisture absorption of graphite-epoxy composites immersed in liquids and in humid air. *J. Compos. Mater.* **1979**, *13*, 131–147.

147. Weitsman, Y.J. Moisture in composites: Sorption and damage. In *Fatigue of Composite Materials*, 1st ed.; Reifsnider, K.L., Ed.; Composite Materials Series; Elsevier Science Publisher B: Amsterdam, Netherlands, 1991; pp. 385–429.

148. Henry, D.C. LX. A kinetic theory of adsorption. *Lond. Edinb. Dublin Philos. Mag. J. Sci.* **1922**, *44*, 689–705.

149. Flory, P.J. Thermodynamics of high polymer solutions. *J. Chem. Phys.* **1942**, *10*, 51–61.

150. Huggins, M.L. Thermodynamic properties of solutions of long-chain compounds. *Ann. N. Y. Acad. Sci.* **1942**, *43*, 1–32.

151. Langmuir, I. The constitution and fundamental properties of solids and liquids. Part I. Solids. *J. Am. Chem. Soc.* **1916**, *38*, 2221–2295.

152. Barrer, R.M.; Barrie, J.A.; Slater, J. Sorption and diffusion in ethyl cellulose. Part III. Comparison between ethyl cellulose and rubber. *J. Polym. Sci.* **1958**, *27*, 177–197.

153. Marshall, J.M.; Marshall, G.P.; Pinzelli, R.F. The diffusion of liquids into resins and composites. *Polym. Compos.* **1982**, *3*, 131–137.

154. Maggana, C.; Pissis, P. Water sorption and diffusion studies in an epoxy resin system. *J. Polym. Sci. Part B Polym. Phys.* **1999**, *37*, 1165–1182.

155. Zhang, D.; Li, K.; Li, Y.; Sun, H.; Cheng, J.; Zhang, J. Characteristics of water absorption in amine-cured epoxy networks: A molecular simulation and experimental study. *Soft Matter* **2018**, *14*, 8740–8749.

156. Garcia-Espinel, J.D.; Castro-Fresno, D.; Gayo, P.P.; Ballester-Muñoz, F. Effects of sea water environment on glass fiber reinforced plastic materials used for marine civil engineering constructions. *Mater. Des. (1980–2015)* **2015**, *66*, 46–50.

157. Long, F.A.; Richman, D. Concentration gradients for diffusion of vapors in glassy polymers and their relation to time dependent diffusion phenomena. *J. Am. Chem. Soc.* **1960**, *82*, 513–519.

158. Sun, Y.-M. Sorption/desorption properties of water vapour in poly (2-hydroxyethyl methacrylate): 2. Two-stage sorption models. *Polymer* **1996**, *37*, 3921–3928.

159. Berens, A.R.; Hopfenberg, H.B. Diffusion and relaxation in glassy polymer powders: 2. Separation of diffusion and relaxation parameters. *Polymer* **1978**, *19*, 489–496.

160. Weitsman, Y.J. Effects of Fluids on Polymeric Composites—Contract Technical Report, A Review; Prepared for Office of Naval Research, Arlington, Virginia: Knoxville, TN, 1995; Report MAES 95-1.0 CM.

161. Weitsman, Y.J. Anomalous fluid sorption in polymeric composites and its relation to fluid-induced damage. *Compos. Part A Appl. Sci. Manuf.* **2006**, *37*, 617–623.

162. Du, Y.; Ma, Y.; Sun, W.; Wang, Z. Effect of hygrothermal aging on moisture diffusion and tensile behavior of CFRP composite laminates. *Chin. J. Aeronaut.* **2023**, *36*, 382–392.

163. Fick, A. Ueber diffusion. *Ann. Phys.* **1855**, *170*, 59–86.

164. Diamant, Y.; Marom, G.; Broutman, L.J. The effect of network structure on moisture absorption of epoxy resins. *J. Appl. Polym. Sci.* **1981**, *26*, 3015–3025.

165. Shirrell, C.D. Diffusion of water vapor in graphite/epoxy composites. In *ASTM STP 658, Advanced Composite Materials—Environmental Effects*; Vinson, J.R., Ed.; American Society for Testing and Materials: Philadelphia, PA, USA, 1977; pp. 21–42.

166. Gupta, V.B.; Drzal, L.T.; Rich, M.J. The physical basis of moisture transport in a cured epoxy resin system. *J. Appl. Polym. Sci.* **1985**, *30*, 4467–4493.

167. Karad, S.K.; Attwood, D.; Jones, F.R. Moisture absorption by cyanate ester modified epoxy resin matrices. Part IV: Effect of curing schedules. *Polym. Compos.* **2003**, *24*, 567–576.

168. Kumosa, L.; Benedikt, B.; Armentrout, D.; Kumosa, M. Moisture absorption properties of unidirectional glass/polymer composites used in composite (non-ceramic) insulators. *Compos. Part A Appl. Sci. Manuf.* **2004**, *35*, 1049–1063.

169. Aktas, L.; Hamidi, Y.; Altan, M.C. Effect of moisture on the mechanical properties of resin transfer molded composites-part I: Absorption. *J. Mater. Process. Manuf. Sci.* **2002**, *10*, 239–254.

170. Aronhime, M.T.; Neumann, S.; Marom, G. The anisotropic diffusion of water in Kevlar-epoxy composites. *J. Mater. Sci.* **1987**, *22*, 2435–2446.

171. Roy, S.; Xu, W.X.; Park, S.J.; Liechti, K.M. Anomalous moisture diffusion in viscoelastic polymers: Modeling and testing. *J. Appl. Mech.* **2000**, *67*, 391–396.

172. Papanicolaou, G.C.; Pappa, A. Water sorption and temperature effects on the dynamic mechanical behaviour of epoxy-matrix particulates. *J. Mater. Sci.* **1992**, 27, 3889–3896.

173. Devi, L.U.; Bhagawan, S.S.; Nair, K.C.M.; Thomas, S. Water absorption behavior of PALF/GF hybrid polyester composites. *Polym. Compos.* **2011**, *32*, 335–346.

174. Arnold, C.; Alston, S.; Korkees, F.; Dauhoo, S.; Adams, R.; Older, R. Design optimisation of carbon fibre epoxy composites operating in humid atmospheres. In Proceedings of the 10th Annual Conference: Innovation in Composites, Birmingham, UK, 5–6 May 2010.

175. Doolittle, A.K.; Doolittle, D.B. Studies in Newtonian Flow. V. Further Verification of the Free-Space Viscosity Equation. *J. Appl. Phys.* **1957**, *28*, 901–905.

176. Williams, M.L.; Landel, R.F.; Ferry, J.D. The temperature dependence of relaxation mechanisms in amorphous polymers and other glass-forming liquids. *J. Am. Chem. Soc.* **1955**, *77*, 3701–3707.

177. Kelley, F.N.; Bueche, F. Viscosity and glass temperature relations for polymer-diluent systems. *J. Polym. Sci.* **1961**, *50*, 549–556.

178. Bao, L.-R.; Yee, A.F. Effect of temperature on moisture absorption in a bismaleimide resin and its carbon fiber composites. *Polymer* **2002**, *43*, 3987–3997.

179. Celina, M.; Gillen, K.T.; Assink, R.A. Accelerated aging and lifetime prediction: Review of non-Arrhenius behaviour due to two competing processes. *Polym. Degrad. Stab.* **2005**, *90*, 395–404.

180. Marru, P.; Latane, V.; Puja, C.; Vikas, K.; Kumar, P.; Neogi, S. Lifetime estimation of glass reinforced epoxy pipes in acidic and alkaline environment using accelerated test methodology. *Fibers Polym.* **2014**, *15*, 1935–1940.

181. Nakayama, M.; Hosokawa, Y.; Muraoka, Y.; Katayama, T. Life prediction under sulfuric acid environment of FRP using X-ray analysis microscope. *J. Mater. Process. Technol.* **2004**, *155*, 1558–1563.

182. Zhou, J.; Chen, X.; Chen, S. Durability and service life prediction of GFRP bars embedded in concrete under acid environment. *Nucl. Eng. Des.* **2011**, *241*, 4095–4102.

183. Wu, G.; Dong, Z.-Q.; Wang, X.; Zhu, Y.; Wu, Z.-S. Prediction of long-term performance and durability of BFRP bars under the combined effect of sustained load and corrosive solutions. *J. Compos. Constr.* **2015**, *19*, 04014058.

184. Carter, H.G.; Kibler, K.G. Langmuir-type model for anomalous moisture diffusion in composite resins. *J. Compos. Mater.* **1978**, *12*, 118–131.

185. Shanahan, M.E.; Auriac, Y. Water absorption and leaching effects in cellulose diacetate. *Polymer* **1998**, *39*, 1155–1164.

186. Zhang, Y.; Ma, J.; Wu, C.; Han, X.; Zhang, W. Effects of moisture ingress on the mesoscale mechanical properties of epoxy adhesives under elevated temperature. *Polym. Test.* **2021**, *94*, 107049.

187. Starink, M.J.; Starink, L.M.P.; Chambers, A.R. Moisture uptake in monolithic and composite materials: Edge correction for rectanguloid samples. *J. Mater. Sci.* **2002**, *37*, 287–294.

188. Bagley, E.; Long, F.A. Two-stage sorption and desorption of organic vapors in cellulose acetate. *J. Am. Chem. Soc.* **1955**, *77*, 2172–2178.

189. Zhang, Y.; Adams, R.D.; da Silva, L.F. Absorption and glass transition temperature of adhesives exposed to water and toluene. *Int. J. Adhes. Adhes.* **2014**, *50*, 85–92.

190. Li, L.; Yu, Y.; Wu, Q.; Zhan, G.; Li, S. Effect of chemical structure on the water sorption of amine-cured epoxy resins. *Corros. Sci.* **2009**, *51*, 3000–3006.

191. Frank, K.; Childers, C.; Dutta, D.; Gidley, D.; Jackson, M.; Ward, S.; Maskell, R.; Wiggins, J. Fluid uptake behavior of multifunctional epoxy blends. *Polymer* **2013**, *54*, 403–410.

192. Saidane, E.H.; Scida, D.; Assarar, M.; Ayad, R. Assessment of 3D moisture diffusion parameters on flax/epoxy composites. *Compos. Part A Appl. Sci. Manuf.* **2016**, *80*, 53–60.

193. Alam, P.; Robert, C.; Brádaigh, C.M. Tidal turbine blade composites—A review on the effects of hygrothermal aging on the properties of CFRP. *Compos. Part B Eng.* **2018**, *149*, 248–259.

194. Guzman, V.A.; Brøndsted, P. Effects of moisture on glass fiber-reinforced polymer composites. *J. Compos. Mater.* **2015**, *49*, 911–920.

195. Carslaw, H.S.; Jaeger, J.C. *Conduction of Heat in Solids*, 2nd ed.; Clarendon Press: Oxford, UK, 1959.

196. Xin, H.; Liu, Y.; Mosallam, A.; Zhang, Y. Moisture diffusion and hygrothermal aging of pultruded glass fiber reinforced polymer laminates in bridge application. *Compos. Part B Eng.* **2016**, *100*, 197–207.

197. Apeagyei, A.K.; Grenfell, J.R.; Airey, G.D. Application of Fickian and non-Fickian diffusion models to study moisture diffusion in asphalt mastics. *Mater. Struct.* **2015**, *48*, 1461–1474.

198. LaPlante, G.; Ouriadov, A.V.; Lee-Sullivan, P.; Balcom, B.J. Anomalous moisture diffusion in an epoxy adhesive detected by magnetic resonance imaging. *J. Appl. Polym. Sci.* **2008**, *109*, 1350–1359.

199. Legghe, E.; Aragon, E.; Bélec, L.; Margaillan, A.; Melot, D. Correlation between water diffusion and adhesion loss: Study of an epoxy primer on steel. *Prog. Org. Coat.* **2009**, *66*, 276–280.

200. Korkees, F.; Alston, S.; Arnold, C. Directional diffusion of moisture into unidirectional carbon fiber/epoxy composites: Experiments and modeling. *Polym. Compos.* **2018**, *39*, E2305–E2315.

201. Broughton, W.R.; Lodeiro, M.J. *Techniques for Monitoring Water Absorption in Fibre-Reinforced Polymer Composites*; Report number: NPL Measurement Note CMMT(MN)64; National Physical Laboratory (NPL): Teddington, UK, 2000; pp. 1–15.

202. Comyn, J. Introduction to polymer permeability and mathematics of diffusion. In *Polymer Permeability*, 1st ed.; Comyn, J. Ed.; Springer Nature: Dordrecht, Netherlands, 1985; Chapter 1, pp. 1–10.

203. Gurtin, M.E.; Yatomi, C. On a model for two phase diffusion in composite materials. *J. Compos. Mater.* **1979**, *13*, 126–130.

204. Arnold, C.; Korkees, F.; Alston, S. The long-term water absorption and desorption behaviour of carbon-fibre/epoxy composites. In Proceedings of the ECCM-15 Proceedings, ESCM: 15th European Conference on Composite Materials, Venice, Italy, 24–28 June 2012.

205. Vanlandingham, M.R.; Eduljee, R.F.; Gillespie, J.W., Jr. Moisture diffusion in epoxy systems. *J. Appl. Polym. Sci.* **1999**, *71*, 787–798.

206. Chateauminois, A.; Vincent, L.; Chabert, B.; Soulier, J.P. Study of the interfacial degradation of a glass-epoxy composite during hygrothermal ageing using water diffusion measurements and dynamic mechanical thermal analysis. *Polymer* **1994**, *35*, 4766–4774.

207. Bao, L.-R.; Yee, A.F. Moisture diffusion and hygrothermal aging in bismaleimide matrix carbon fiber composites—Part I: Uni-weave composites. *Compos. Sci. Technol.* **2002**, *62*, 2099–2110.

208. Springer, G.S. Environmental effects. In *Engineering Mechanics of Fibre Reinforced Polymers and Composite Structures*, 1st ed.; Hult, J., Rammerstorfer, F.G., Eds.; Springer: Vienna, Austria, 1994; Volume 348, pp. 287–314.

209. Bone, J.E.; Sims, G.D.; Maxwell, A.S.; Frenz, S.; Ogin, S.L.; Foreman, C.; Dorey, R.A. On the relationship between moisture uptake and mechanical property changes in a carbon fibre/epoxy composite. *J. Compos. Mater.* **2022**, *56*, 2189–2199.

210. Jain, D.; Kamboj, I.; Bera, T.K.; Kang, A.S.; Singla, R.K. Experimental and numerical investigations on the effect of alkaline hornification on the hydrothermal ageing of Agave natural fiber composites. *Int. J. Heat Mass. Transf.* **2019**, *130*, 431–439.

211. Lei, Y.; Zhang, T.; Zhang, J.; Zhang, B. Dimensional stability and mechanical performance evolution of continuous carbon fiber reinforced polyamide 6 composites under hygrothermal environment. *J. Mater. Res. Technol.* **2021**, *13*, 2126–2137.

212. Arnold, J.C.; Alston, S.M.; Korkees, F. An assessment of methods to determine the directional moisture diffusion coefficients of composite materials. *Compos. Part A Appl. Sci. Manuf.* **2013**, *55*, 120–128.

213. Springer, G.S.; Tsai, S.W. Thermal conductivities of unidirectional materials. *J. Compos. Mater.* **1967**, *1*, 166–173.

214. Karbhari, V.M.; Hassanpour, B. Water, saltwater, and concrete leachate solution effects on durability of ambient-temperature cure carbon-epoxy composites. *J. Appl. Polym. Sci.* **2022**, *139*, e52496.

215. Korkees, F.; Swart, R.; Barsoum, I. Diffusion mechanism and properties of chemical liquids and their mixtures in 977-2 epoxy resin. *Polym. Eng. Sci.* **2022**, *62*, 1582–1592.

216. Jarrett, W.; Korkees, F. Environmental impact investigation on the interlaminar properties of carbon fibre composites modified with graphene nanoparticles. *Polymer* **2022**, *252*, 124921.

217. Harper, B.D.; Staab, G.H.; Chen, R.S. A note on the effects of voids upon the hygral and mechanical properties of AS4/3502 graphite/epoxy. *J. Compos. Mater.* **1987**, *21*, 280–289.

218. Weitsman, Y.J. Effects of Fluids on Mechanical Properties and Performance. In *Fluid Effects in Polymers and Polymeric Composites*; Penumadu, D., Ed.; Mechanical Engineering Series; Springer: Boston, MA, USA, 2011, 123–144.

219. Placette, M.D.; Fan, X.; Zhao, J.-H.; Edwards, D. A dual stage model of anomalous moisture diffusion and desorption in epoxy mold compounds. In *Conference on Thermal, Mechanical & Multi-Physics Simulation and Experiments in Microelectronics and Microsystems*; IEEE Conference: Linz, Austria, 2011; pp. 1–8.

220. Popineau, S.; Rondeau-Mouro, C.; Sulpice-Gaillet, C.; Shanahan, M.E. Free/bound water absorption in an epoxy adhesive. *Polymer* **2005**, *46*, 10733–10740.

221. Cai, L.W.; Weitsman, Y.J. Non-Fickian moisture diffusion in polymeric composites. *J. Compos. Mater.* **1994**, *28*, 130–154.

222. Wan, Y.Z.; Wang, Y.L.; Cheng, G.X.; Han, K.Y. Three-dimensionally braided carbon fiber–epoxy composites, a new type of material for osteosynthesis devices. *I. Mech. Prop. Moisture Absorpt. Behav. J. Appl. Polym. Sci.* **2002**, *85*, 1031–1039.

223. Neumann, S.; Marom, G. Free-volume dependent moisture diffusion under stress in composite materials. *J. Mater. Sci.* **1986**, *21*, 26–30.

224. Neumann, S.; Marom, G. Prediction of moisture diffusion parameters in composite materials under stress. *J. Compos. Mater.* **1987**, *21*, 68–80.

225. Dhakal, H.N.; Zhang, Z. Polymer matrix composites: Moisture effects and dimensional stability. In *Wiley Encyclopedia of Composites*, 2nd ed.; Nicolais, L., Borzacchiello, A., Eds.; John Wiley & Sons: Hoboken, NJ, USA, 2012; Volume 1, pp. 1–7.

226. Marsh, L.L.; Lasky, R.; Seraphim, D.P.; Springer, G.S. Moisture solubility and diffusion in epoxy and epoxy-glass composites. *IBM J. Res. Dev.* **1984**, *28*, 655–661.

227. Fujita, H. Diffusion in polymer-diluent systems. In *Fortschritte der Hochpolymeren-Forschung*; Jayakumar, R., Ed.; Advanced in Polymer Science; Springer: Berlin/Heidelberg, Germany, 1961; Volume *3*, pp. 1–47.

228. Crank, J.; Park, G.S. *Diffusion in Polymers*; Academic Press: London, UK; New York, NY, USA, 1968; p. 452.

229. Kim, J.-K.; Hu, C.; Woo, R.S.; Sham, M.-L. Moisture barrier characteristics of organoclay–epoxy nanocomposites. *Compos. Sci. Technol.* **2005**, *65*, 805–813.

230. Coniglio, N.; Nguyen, K.; Kurji, R.; Gamboa, E. *Characterizing water sorption in* 100% solids epoxy coatings. *Prog. Org. Coat.* **2013**, *76*, 1168–1177.

231. Mubashar, A.; Ashcroft, I.A.; Critchlow, G.W.; Crocombe, A.D. Modelling cyclic moisture uptake in an epoxy adhesive. *J. Adhes.* **2009**, *85*, 711–735.

232. Jiang, X.; Kolstein, H.; Bijlaard, F.S. Moisture diffusion in glass–fiber-reinforced polymer composite bridge under hot/wet environment. *Compos. Part B Eng.* **2013**, *45*, 407–416.

233. Robert, M.; Roy, R.; Benmokrane, B. Environmental effects on glass fiber reinforced polypropylene thermoplastic composite laminate for structural applications. *Polym. Compos.* **2010**, *31*, 604–611.

234. Cotugno, S.; Mensitieri, G.; Musto, P.; Sanguigno, L. Molecular interactions in and transport properties of densely cross-linked networks: A time-resolved FT-IR spectroscopy investigation of the epoxy/H_2O system. *Macromolecules* **2005**, *38*, 801–811.

235. Wong, T.C.; Broutman, L.J. Moisture diffusion in epoxy resins Part I. Non-Fickian sorption processes. *Polym. Eng. Sci.* **1985**, *25*, 521–528.

236. Yeh, R.-J.; Lin, P.-W.; Lin, K.-F. Two-stage moisture absorption behavior and hydrolysis of cured dicyanate ester resins. *J. Polym. Res.* **2002**, *9*, 31–36.

237. Kotsikos, G.; Gibson, A.G.; Mawella, J. Assessment of moisture absorption in marine GRP laminates with aid of nuclear magnetic resonance imaging. *Plast. Rubber Compos.* **2007**, *36*, 413–418.

238. Jacobs, P.M.; Jones, F.R. Diffusion of moisture into two-phase polymers: Part 3 Clustering of water in polymer resins. *J. Mater. Sci.* **1990**, *25*, 2471–2475.

239. Meares, P. The solubilities of gases in polyvinyl acetate. *Trans. Faraday Soc.* **1958**, *54*, 40–46.

240. Paul, D.R. Effect of immobilizing adsorption on the diffusion time lag. *J. Polym. Sci. Part A-2 Polym. Phys.* **1969**, *7*, 1811–1818.

241. Paul, D.R.; Koros, W.J. Effect of partially immobilizing sorption on permeability and the diffusion time lag. *J. Polym. Sci. Polym. Phys. Ed.* **1976**, *14*, 675–685.

242. Post, N.L.; Riebel, F.; Zhou, A.; Keller, T.; Case, S.W.; Lesko, J.J. Investigation of 3D moisture diffusion coefficients and damage in a pultruded E-glass/polyester structural composite. *J. Compos. Mater.* **2009**, *43*, 75–96.

243. Weitsman, Y.J. Diffusion with time-varying diffusivity, with application to moisture-sorption in composites. *J. Compos. Mater.* **1976**, *10*, 193–204.

244. Grace, L.R.; Altan, M.C. Characterization of anisotropic moisture absorption in polymeric composites using hindered diffusion model. *Compos. Part A Appl. Sci. Manuf.* **2012**, *43*, 1187–1196.

245. Guloglu, G.E.; Altan, M.C. Moisture absorption of carbon/epoxy nanocomposites. *J. Compos. Sci.* **2020**, *4*, 21.

246. Wong, K.J.; Low, K.O.; Israr, H.A.; Tamin, M.N. Thickness-dependent non-Fickian moisture absorption in epoxy molding compounds. *Microelectron. Reliab.* **2016**, *65*, 160–166.

247. Sun, L.; Boo, W.-J.; Clearfield, A.; Sue, H.-J.; Pham, H.Q. Barrier properties of model epoxy nanocomposites. *J. Membr. Sci.* **2008**, *318*, 129–136.

248. Liu, W.; Hoa, S.V.; Pugh, M. Water uptake of epoxy–clay nanocomposites: Model development. *Compos. Sci. Technol.* **2007**, *67*, 3308–3315.

249. Berens, A.R. Diffusion and relaxation in glassy polymer powders: 1. Fickian diffusion of vinyl chloride in poly (vinyl choride). *Polymer* **1977**, *18*, 697–704.

250. Glaskova, T.I.; Guedes, R.M.; Morais, J.J.; Aniskevich, A.N. A comparative analysis of moisture transport models as applied to an epoxy binder. *Mech. Compos. Mater.* **2007**, *43*, 377–388.

251. Mensitieri, G.; Lavorgna, M.; Musto, P.; Ragosta, G. Water transport in densely crosslinked networks: A comparison between epoxy systems having different interactive characters. *Polymer* **2006**, *47*, 8326–8336.

252. Scott, P.; Lees, J.M. Water, salt water, and alkaline solution uptake in epoxy thin films. *J. Appl. Polym. Sci.* **2013**, *130*, 1898–1908.

253. Bratasyuk, N.A.; Ostanin, S.A.; Mokeev, M.V.; Zuev, V.V. Water transport in epoxy/polyurethane interpenetrating networks. *Polym. Adv. Technol.* **2022**, *33*, 3173–3191.

254. Melo, R.Q.C.; Santos, W.R.G.; Barbosa de Lima, A.G.; Lima, W.M.P.B.; Silva, J.V.; Farias, R.P. Water absorption process in polymer composites: Theory analysis and applications. In *Transport Phenomena in Multiphase Systems*; Delgado, J., Barbosa de Lima, A., Eds.; Advanced Structured Materials; Springer: Cham, Switzerland, 2018*;* Volume 93, pp. 219–249.

255. Gao, C.; Zhou, C. Moisture absorption and cyclic absorption–desorption characters of fibre-reinforced epoxy composites. *J. Mater. Sci.* **2019**, *54*, 8289–8301.

256. Sugiman, S.; Salman, S.; Maryudi, M. Effects of volume fraction on water uptake and tensile properties of epoxy filled with inorganic fillers having different reactivity to water. *Mater. Today Commun.* **2020**, *24*, 101360.

257. Suri, C.; Perreux, D. The effects of mechanical damage in a glass fibre/epoxy composite on the absorption rate. *Compos. Eng.* **1995**, *5*, 415–424.

258. Li, Y.; Miranda, J.; Sue, H.-J. Hygrothermal diffusion behavior in bismaleimide resin. *Polymer* **2001**, *42*, 7791–7799.

259. Yu, H.; Xing, P. Moisture absorption characterization of carbon fiber-reinforced polymer using Fickian and non-Fickian models. *Polym. Compos.* **2022**, *43*, 8935–8946.

260. Kumar, A.; Roy, S. Modeling of anomalous moisture diffusion in nanographene reinforced thermoset polymers. *Compos. Struct.* **2015**, *122*, 1–7.

261. Guloglu, G.E.; Hamidi, Y.K.; Altan, M.C. Moisture absorption of composites with interfacial storage. *Compos. Part A Appl. Sci. Manuf.* **2020**, *134*, 105908.

262. Hassanpour, B.; Karbhari, V.M. Moisture and glass transition temperature kinetics of ambient-cured carbon/epoxy composites. *J. Compos. Sci.* **2023**, *7*, 447.

263. Connelly, R.W.; McCoy, N.R.; Koros, W.J.; Hopfenberg, H.B.; Stewart, M.E. The effect of sorbed penetrants on the aging of previously dilated glassy polymer powders. *I. Low. Alcohol Water Sorpt. Poly (Methyl Methacrylate). J. Appl. Polym. Sci.* **1987**, *34*, 703–719.

264. Newns, A.C. The sorption and desorption kinetics of water in a regenerated cellulose. *Trans. Faraday Soc.* **1956**, *52*, 1533–1545.

265. Petropoulos, J.H.; Roussis, P.P. Diffusion of penetrants in organic solids accompanied by other rate processes. *Mol. Cryst. Liq. Cryst.* **1969**, *9*, 343–357.

266. Stewart, M.E.; Hopfenberg, H.B.; Koros, W.J.; McCoy, N.R. The effect of sorbed penetrants on the aging of previously dilated glassy polymer powders. *II. N-Propane Sorpt. Polystyr. J. Appl. Polym. Sci.* **1987**, *34*, 721–735.

267. Wong, T.C.; Broutman, L.J. Water in epoxy resins part II. Diffusion mechanism. *Polym. Eng. Sci.* **1985**, *25*, 529–534.

268. Johncock, P.; Tudgey, G.F. Epoxy systems with improved water resistance, and the non-fickian behaviour of epoxy systems during water ageing. *Br. Polym. J.* **1983**, *15*, 14–18.

269. Starkova, O.; Chandrasekaran, S.; Schnoor, T.; Sevcenko, J.; Schulte, K. Anomalous water diffusion in epoxy/carbon nanoparticle composites. *Polym. Degrad. Stab.* **2019**, *164*, 127–135.

270. Berens, A.R.; Hopfenberg, H.B. Induction and measurement of glassy-state relaxations by vapor sorption techniques. *J. Polym. Sci. Polym. Phys.* **1979**, *17*, 1757–1770.

271. Gavril'eva, A.A.; Kychkin, A.K.; Sivtseva, A.N.; Vasil'eva, A.A. Moisture absorption by a reinforced polymer composite (BFRP Rebar). *Russ. Eng. Res.* **2021**, *41*, 612–615.

272. Ray, B.C.; Rathore, D. Environmental damage and degradation of FRP composites: A review report. *Polym. Compos.* **2015**, *36*, 410–423.

273. Upadhyay, P.C.; Mishra, A. Modified one-dimensional fickian solution for moisture absorption in composites. *J. Reinf. Plast. Compos.* **1990**, *9*, 335–345.

274. Yu, Y.; Yang, X.; Wang, L.; Liu, H. Hygrothermal aging on pultruded carbon fiber/vinyl ester resin composite for sucker rod application. *J. Reinf. Plast. Compos.* **2006**, *25*, 149–160.

275. Kondo, K.; Taki, T. Moisture diffusivity of unidirectional composites. *J. Compos. Mater.* **1982**, *16*, 82–93.

276. Bao, L.R.; Yee, A.F. Moisture diffusion and hygrothermal aging in bismaleimide matrix carbon fiber composites—*Part* II: Woven and hybrid composites. *Compos. Sci. Technol.* **2002**, *62*, 2111–2119.

277. Loung, C.L.; Dynes, P.J.; Kaelble, D.H. Moisture diffusion analysis of micro-structure degradation in graphite epoxy composites. In *ASTM STP 696, Nondestructive Evaluation and Flaw Criticality for Composite Materials*; Pipes, R.B., Ed.; American Society for Testing and Materials: Philadelphia, PA, USA, 1979; pp. 298–315.

278. Arao, Y.; Koyanagi, J.; Hatta, H.; Kawada, H. Analysis of time-dependent deformation of CFRP considering the anisotropy of moisture diffusion. *Adv. Compos. Mater.* **2008**, *17*, 359–372.

279. Dana, H.R.; Perronnet, A.; Freour, S.; Casari, P.; Jacquemin, F. Identification of moisture diffusion parameters in organic matrix composites. *J. Compos. Mater.* **2013**, *47*, 1081–1092.

280. Allred, R.E.; Lindrose, A.M. The room temperature moisture kinetics of Kevlar 49 fabric/epoxy laminates. In *ASTM STP 674. Composite Materials: Testing and Design*; Tasai, S.W., Ed.; American Society for testing and Materials: Philadelphia, PA, USA, 1979; pp. 313–323.

281. Cervenka, A.J.; Bannister, D.J.; Young, R.J. Moisture absorption and interfacial failure in aramid/epoxy composites. *Compos. Part A Appl. Sci. Manuf.* **1998**, *29*, 1137–1144.

282. Wang, J.; Li, Y.; Yu, T.; Li, Q.; Li, Z. Anisotropic behaviors of moisture absorption and hygroscopic swelling of unidirectional flax fiber reinforced composites. *Compos. Struct.* **2022**, *297*, 115941.

CHAPTER 3. GLASS TRANSITION TEMPERATURE AS A CHARACTERISTIC OF THE DURABILITY OF FIBER REINFORCED POLYMER COMPOSITES

The study, titled "Glass Transition Temperature as a Characteristics of Durability of Fiber Reinforced Polymer Composites," is included in the chapter and is published as a chapter in the book "Aging and Durability of FRP Composites and Nanocomposites" in 2023.

Hassanpour, B.; Karbhari, V.M. Glass transition temperature as a characteristic of the durability of fiber-reinforced polymer composites. In Aging and Durability of FRP Composites and Nanocomposites; Uthaman, A., Thomas, S., Mayookh Lal, H., Eds.; Woodhead Publishing, Elsevier: London, UK, 2024; Chapter 15, pp. 341–362. https://doi.org/10.1016/B978-0-443-15545-1.00002-0

GLASS TRANSITION TEMPERATURE AS A CHARACTERISTIC OF THE DURABILITY OF FIBER-REINFORCED POLYMER COMPOSITES

Behnaz Hassanpour and Vistasp M. Karbhari

Department of Civil Engineering, University of Texas Arlington, Arlington, TX, United States

3.1. INTRODUCTION

Fiber-reinforced polymer matrix composites provide substantial advantages over traditional materials such as structural steel and concrete because of their inherently high specific strength and stiffness characteristics, lightweight, ease of forming in the field, multifunctionality, and potentially high durability under harsh and changing environments. With an appropriate selection of constituent materials and processing techniques, these materials can withstand most environmental regimes common in civil infrastructure sectors. The ability of a composite to provide high durability and extended service life depends intrinsically on the appropriate level of cure of the polymer and the effectiveness of the fiber-matrix bond as well as the integrity of the resin structure without significant voids and/or microcavities. The assessment of durability is often conducted through mechanical characterization after exposing the composites to a range of exposure conditions over extended periods of time and using mechanisms of time-temperature superposition to predict long-term durability. As part of these tests, or even in a stand-alone sense, the determination of glass transition temperature (T_g) and changes in its characteristics because of exposure plays a critical role in durability assessment. It is hence important to understand this

material characteristic, its measurement, relevance, and relation to durability, and how it can be used to assist in the prediction of service life, including remaining service life after exposure to deteriorative effects. It is assumed that other chapters in this book focus on specifics of degradation/deterioration mechanisms and on the effects of exposure on mechanical characteristics and hence the focus of the chapter is solely on the glass transition temperature.

The glass transition temperature (T_g) holds great significance as a fundamental thermophysical property of polymers and fiber-reinforced polymer matrix composites, especially of reactive thermosetting systems commonly used in civil infrastructure. It sets the upper bound for the use temperature of the material system and enables the characterization of both the cure and molecular state of the material since it depends intrinsically on chain extension and crosslinking, both of which increase T_g. As a parameter, it is also strongly dependent on chemical composition, phase morphology, and the presence of water/solution within the polymer and hence serves to identify critical changes, both reversible and irreversible in nature. When polymer materials are heated above T_g, they undergo a transition to a rubbery or viscous state, depending on factors such as molecular weight and the extent to which the temperature exceeds T_g. Conversely, below T_g, bulk polymers are intrinsically glassy, exhibiting varying degrees of brittleness depending on their structural complexity and cooling conditions. The glass transition is accompanied by a molecular-scale energy change that allows the macromolecular chains to shift from high-amplitude motions in the rubbery state to low-amplitude local molecular motions in the glassy state [1-4]. The glass transition temperature is distinct from the melting point. While glassification (also known as vitrification) is considered a pseudo-second-order phase transition, melting is a true first-order phase transition. Glassification results in a (pseudo) discontinuity in

the second derivative, impacting characteristics like heat capacity and expansion coefficient. Melting, on the other hand, induces a discontinuity in the first derivative of the Gibbs free energy, which includes volume and entropy [5].

As noted previously the intrinsic glass transition temperature can be influenced by a variety of parameters such as heating rate both during cure and later during use, aging history, morphology, molecular weight, flexibility of the main chain, side groups, degree of cure, curing conditions, the presence of plasticizers and other additives, and the polymer's aging history. The assessment of initial and in-service conditions is useful because the interactions between these components can differ across various polymer systems [6,7].

Below the glass transition temperature, the polymer's molecular dynamics are constrained, which implies that molecular motion is reduced to small-scale rearrangements like atomic vibrations and rotations. Translational motion is more prevalent than rotational motion above the glass transition temperature, just as in a liquid-like condition. When a material reaches its T_g, physicochemical properties such as electrical and heat conductivity, the dielectric constant, specific volume, and thermal capacity, among others, gradually change. Although the glass transition represents a temperature regime of reversible transition of an amorphous polymer from the molten or rubber-like state (very elastic) to the stiff and moderately brittle glassy state, a single temperature, is often used to represent the characteristic as a reference [8] and is used to represent a change in state and to establish a point at which a material can be assumed to start to degrade [9]. In this aspect, it is often utilized to set operational boundaries and to determine the acceptable service temperature and use regime [10,11]. It is noted that temperature has a significant impact

on both Young's and flexural moduli, as well as relaxation time because a rise in temperature results in the activation of greater internal degrees of freedom and rotational modes of the polymer chains in the network, making polymer materials softer and subject to greater deformations in less time for a given applied stress. On the other hand, temperatures below the range of the glass transition result in a strong increase in the Young's and flexural moduli as well as a sharp decrease in the ultimate strength [12].

Typically, when a material is subjected to a hygrothermal environment, the T_g decreases because of the sorption of moisture/solution resulting in a lowering of the threshold service temperature of the material. The degree of resin plasticization and water/resin interactions present in the material are reflected in this change in T_g. From an aspect of materials and structural design, it is hence crucial to be able to pinpoint the causes causing T_g change and to be able to anticipate T_g depression [13]. Furthermore, the link between the glass transition temperature and the moisture content of these materials is of interest because many amorphous solids spontaneously absorb water from their surroundings and water frequently functions as a potent plasticizer for such materials. It is crucial to comprehend the fundamental mechanisms driving the interactions between water and polymers since such sorbed water might affect the physical and/or chemical characteristics of the polymer, the fiber-matrix bond, and the composite. Sorbed water acts as a plasticizer, lowering the glass transition temperature, T_g, of the polymer, whereas an antiplasticizing effect results in an increase [14,15]. Given that exposure to conditions of humidity or contact with aqueous solutions is commonly seen in the environment and in service of structural systems it is important to better understand the relation between the glass transition temperature and moisture content in the polymer and composite, especially as related to the extent of lowering

T_g with increase in uptake [14,15]. It is noted that models of classical diffusion can be used to characterize the complex moisture absorption process in a resin below its glass transition temperature [16-18] enabling the development of better models to assess the critically needed effects of environmental exposure and aging on deterioration over the intended service-life and effects on the reliability of the material and structure [19–21].

3.2. METHODS OF DETERMINING GLASS TRANSITION TEMPERATURE

The determination of the glass transition temperature (T_g) is accomplished most commonly through methodologies such as differential scanning calorimetry (DSC), dynamic mechanical analysis (DMA), thermomechanical analysis (TMA), dielectric analysis (DEA), dielectric thermal analysis (DETA), synchronous scan spectra (SSS), and infrared spectroscopy (IR). Among these approaches, DMA is often preferred in scientific studies due to its ability to provide valuable information regarding both changes in modulus and glass transition temperature as well as provide insight into changes in morphology and network characteristics. Indirectly the extent of damage at the fiber-matrix bond level can also be assessed. In this case, the T_g is typically determined by locating the midpoint of the inclined region in the tangent plot [3,22–28].

In thermomechanical analysis (TMA), a popular thermal technique used with bulk samples, a probe in contact with the specimen to be assessed is subjected to a controlled application of force. Changes in the sample's length, including those brought on by softening during melting, are measured as the temperature rises. This technique can be used to gather useful data, including thermal expansion coefficients, transition temperatures, and the identification of thermal events. The linear isobaric expansivity can also be calculated using TMA. The glass transition temperature

(T_g) can be determined using the profiles showing dimensional changes with the temperature that were acquired using TMA as shown schematically in Fig. 3-1.

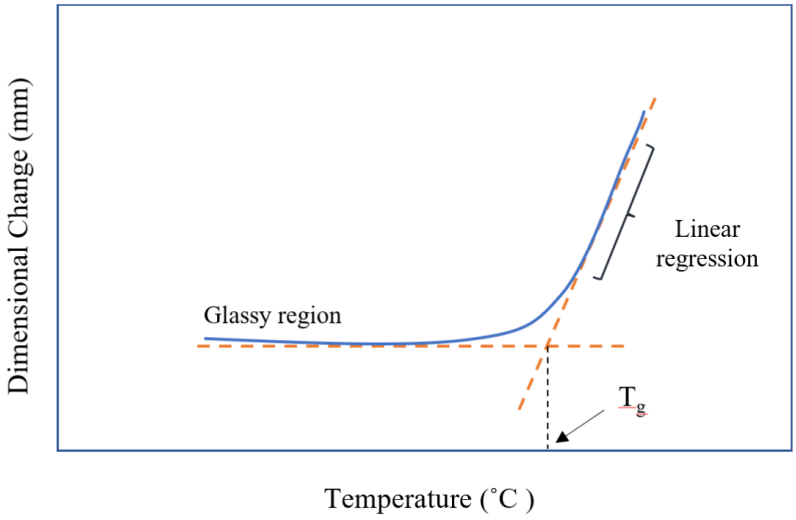

Figure 3-1. *Determination of glass transition temperature (T_g) using thermomechanical analysis (TMA).*

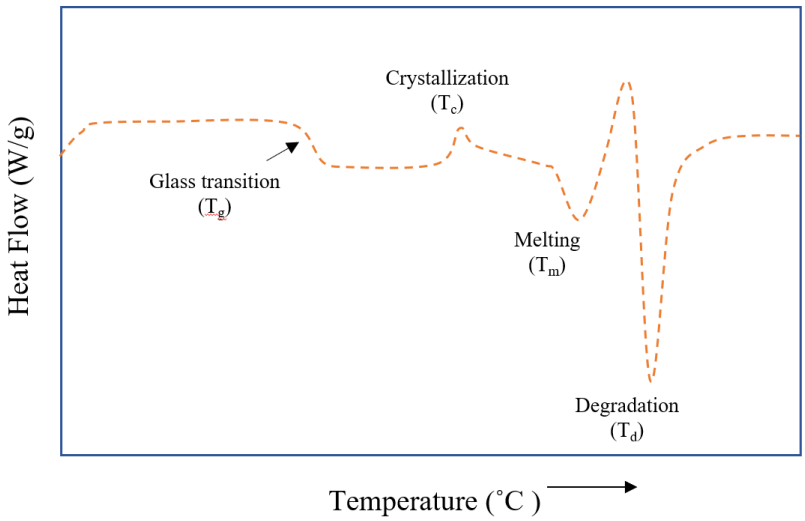

Figure 3-2. *Determination of glass transition temperature (T_g) using differential scanning calorimetry (DSC).*

Differential scanning calorimetry (DSC) is commonly employed for analyzing the thermal properties of materials. It is based on the measurement of specific heat changes and is particularly suitable for analyzing dry and small samples. DSC provides valuable information regarding endothermic and exothermic processes, allowing for the measurement of energy absorption or release and the characterization of temperature and heat flow changes associated with material transitions over time and temperature [29]. This technique enables the determination of the glass transition temperature (T_g) and the monitoring of cure progression. T_g is typically calculated from the temperature at which the first heat flow peak appears in the DSC curve, signifying the initiation of the glass transition as shown schematically in Fig. 3-2. Alternatively, T_g can be determined using the midpoint temperature of the heat flow peak upon second heating of the sample [9,13,30,31].

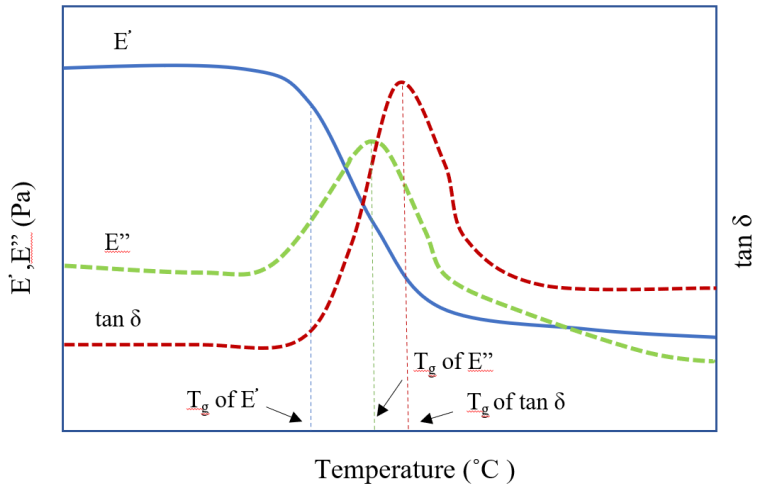

Figure 3-3. *Schematic of curves from dynamic mechanical analysis (DMA) and determination of glass transition temperature.*

Dynamic mechanical analysis (DMA) is a widely utilized technique for studying the mechanical behavior of materials in response to applied mechanical forces or displacements. When discussing the glass transition temperature (T_g) using DMA results, several significant curves are considered, including the dynamic or storage modulus (*E'*), loss modulus (*E''*), and loss factor (*E''/E' = tan(δ)*), as functions of temperature, which are indicative of T_g, as shown schematically in Fig. 3-3.

The storage modulus reflects a material's ability to store mechanical energy, the loss modulus indicates its ability to dissipate mechanical energy, and the ratio of the loss to storage modulus, or tan(δ), represents its damping properties. It should be noted that in DMA alone, different T_g values can be obtained from the storage modulus (*E'*), loss modulus (*E''*), or *tan(δ) = E''/E'* [11,26,32,33]. In the absence of a clear peak or step-like change in the loss modulus (*E''*) or storage modulus (*E'*) graphs, T_g can still be calculated using DMA. Typically, the temperature at which either the loss modulus or storage modulus exhibits a noticeable increase or decrease is used to determine T_g. This is because the glass transition is accompanied by a decrease in stiffness (increase in E'') and an increase in energy dissipation (increase in *E''*) as observed in the storage modulus and loss modulus graphs. As shown in Fig. 3-3 the appearance of a peak or step in these graphs represents the glass transition temperature (T_g) of the material. T_g can also be estimated by examining a significant increase in *tan δ*, which signifies an enhanced ability of the material to dissipate mechanical energy and transition from a glassy state to a rubbery or viscous state [34]. Three separate stages can be identified in the process: The storage modulus (*E'*) gradually

decreases during the initial stage as the temperature increases. This implies that the epoxy matrix remains glassy, and the laminates have a high storage modulus. A significant and quick fall in the value of *E'* during the second stage indicates the onset of the glass transition in the resin matrix. The last stage is distinguished by low modulus values, suggesting that the epoxy matrix has transitioned to a rubbery condition. At this stage, the mobility of polymer chains increases, resulting in increased energy dissipation inside the material [34]. These changes can be effectively used for the assessment of moisture uptake and its effects [35].

Additional techniques for measuring the glass transition temperature include dynamic mechanical thermal analysis (DMTA), dynamic vapor sorption (DVS), inverse gas chromatography (IGC), and process rheometer (PR), These methods enable the determination of the threshold relative humidity for moisture-induced glass transition at a specific temperature. Furthermore, several modes of scanning probe microscopy (SPM) have recently been employed as a non-destructive approach to detect thermal transitions in polymer films. In this method, the SPM probe serves both as a thermal actuator (heater) and a sensor. Thermal transitions within the material can be determined by detecting changes in thermal diffusivity or heat capacity while monitoring the resonance frequency of the heated probe during its oscillation over the surface of a polymer at various probe temperatures (T_p). Another non-destructive thermal SPM method, which relies on sample heating rather than probe heating, has also demonstrated potential in detecting glass transitions and melting points on the surface of polymer [8,36-38].

3.3. MODELS FOR THE DETERMINATION OF RELATIONS BETWEEN T_g AND MOSITURE

Glass transition characterizes the range of temperatures over which an amorphous material undergoes a transformation from a rigid, brittle state to a more flexible, rubbery state [39], during this transition, there is a noticeable shift in the molecular mobility of the amorphous compounds [40]. Moisture uptake is known to perceptibly affect a polymer's glass transition temperature. The impact of moisture absorption on the glass transition temperature (T_g) of polymers is a complex process influenced by alterations in molecular interactions and mobility within the polymer matrix. Plasticizers, often at a lower molecular weight than the bulk, are known to have an impact on the T_g of polymers. The extent of T_g depression depends on the concentration of the plasticizer and its interaction with the amorphous material. Water is a common plasticizer for a range of materials [40,41], thus the water content in amorphous polymers can have a significant lowering effect on the glass transition temperature and thus the glass transition temperature can be directly affected by the relative humidity of the environment [38].

The free volume, and consequently the molecular mobility, of the epoxy matrix macromolecules increases because of moisture absorption. The molecular mobility inside the polymer matrix is improved because of this increase in free volume since enhanced molecular mobility leads to a dissociation of the hydrogen bonds between the water molecules and the active sites within the resin matrix. Then, a general decrease of H-bonding develops and a consequent increase in the mobility of the water molecules, which requires a greater free volume than the H-bonds. This increase in the molecular mobility of epoxy matrix-moisture systems causes a lowering of the glass transition temperature.

Numerous models have been developed over time to clarify the nature of the glass transition phenomenon. Kinetic theories and equilibrium theories are the two basic classes into which these theories can be divided. According to kinetic theories, the relaxation of molecular movements is a dynamic process that contributes to the glass transition. Equilibrium theories, on the other hand, concentrate on the thermodynamic features of the glass transition.

Gibbs and DiMarzio proposed one of the earliest equilibrium theories of the glass transition. In this model, the conformational entropy is thought to reach zero at a thermodynamic second-order transition point. All molecular conformations effectively become “frozen” and exhibit restricted mobility below this transition temperature [42,43]. A variety of mechanical and phenomenological models and hypotheses have been employed to elucidate the underlying mechanisms and phenomena that influence the glass transition temperature. At temperatures above T_g, the molecular mobility is sufficient for the material to exhibit the properties (such as enthalpy, specific volume, etc.), that are inherent to the equilibrium rubbery or liquid state. So, using these mechanisms can aid in the development of models. These approaches not only shed light on the fundamental concepts and variables governing the glass transition phenomenon but also offer insights into the intricate changes in the physical and molecular behavior of materials during the transition from a glassy to a rubbery or viscous state. Among these mechanisms, free volume theories play a significant role in understanding the glass transition temperature. According to these theories, the availability of free space for molecular rearrangement is considered a critical factor in the behavior of polymers near and below their glass transition temperature. In the context of free volume theories applied to polymers, for the polymer backbone to undergo conformational changes, there must be space into which molecular segments can migrate. The fractional free

volume of the polymer represents the overall amount of unoccupied space per unit volume. As the temperature decreases, reduced free volume and sluggish molecular movements cause the polymer's volume to contract, resulting in solid-like characteristics with limited thermal expansion. This volume contraction occurs as the temperature decreases from a level well above T_g because the molecules can locally reorganize themselves to minimize the free volume. As the temperature approaches T_g, the material's volume contracts similarly to that of a solid, with an expansion coefficient typically around half of the value observed above T_g. This reduction in molecular motion hampers molecular rearrangement within the experimental time scale [7].

The free volume theory postulates that the glass transition temperature is closely related to the amount of unoccupied space or free volume between polymer chains. In this theory, the prediction of the glass transition temperature is based on the fraction of free volume and the activation energy required for molecular mobility. Examples of models based on free volume theory include the Cohen-Turnbull, WLF (Williams-Landel-Ferry), and Gordon-Taylor models [44-46]. The Cohen-Turnbull model, proposed independently by G. Cohen and D. Turnbull in the late 1940s, represents one of the earliest models that was used to assess the effects of changes on the glass transition temperature. It characterizes the glass transition temperature, as the temperature at which the rate of molecular relaxation becomes exceedingly slow, preventing the material from maintaining its amorphous, glassy state. Instead, it starts to exhibit properties resembling those of a supercooled liquid. According to the Cohen-Turnbull model, as the temperature decreases, the viscosity or resistance to flow of the glass-forming material increases significantly. While providing a qualitative understanding of the glass transition phenomenon, this model has served

as the foundation for further research and the development of more detailed models that describe the glass transition behavior of diverse materials.

In addition to the free volume theory, other mechanisms can be employed to explain the glass transition temperature. Factors such as the degree and extent of cure, mole and crosslink density information, molecular weight, plasticization, degree of crosslinking, heat capacity, and weight or mole fraction all contribute to the variation in the glass transition temperature of thermosetting polymers, and the resulting composites. To predict and comprehend the glass transition behavior in various materials, it is essential to understand these parameters [7,47-49]. Numerous approaches have been proposed to determine the glass transition temperature of mixtures by examining the properties of the individual pure components. These proposed correlations assume that fundamental characteristics exhibit additive behavior, while acknowledging potential variations in specific details. By considering the glass transition behavior of amorphous materials through the lens of polymer free volume theory, it is possible to establish more theoretically significant correlations. Under the assumption of complete volume additivity at the glass transition temperature (T_g) and the absence of any special interactions between the two components, the glass transition of a mixture (such as one developed by sorption of moisture into a polymer or composite) as [40]:

$$T_{g\,mix} = \emptyset_1 . T_{g1} + \emptyset_2 . T_{g2} \quad (1)$$

where $\emptyset$ represents each component's volume fraction. This relationship is based on a rule of mixtures used to describe behavior in ideal solutions. Similarly, the glass transition temperature of amorphous mixtures can be assessed as

$$T_{gm}^{eq} = \frac{\varphi_1 T_{g1} + k\varphi_2 T_{g2}}{\varphi_1 + k\varphi_2} \quad (2)$$

where *T* stands for the glass transition temperature of the mixture predicted by the equation of interest. The subscripts 1 and 2 refer to components 1 and 2 of the mixture, respectively. The concentration of the components is denoted by either a mole fraction (*x*) or a weight fraction (*w*). The parameter *k* is a parameter whose physical interpretation depends on the underlying physical model of the specific equation used [50]. A few important relations, used commonly to assess effects of environment on T_g are listed below:

The Gordon-Taylor (G-T) equation: The two fundamental premises upon which Gordon and Taylor [45] based their theory were volume additivity, or the ideal volume of mixing, and a linear change in volume with temperature. The Gordon-Taylor hypothesis is based on this assumption and relies on Eq. (2) as its foundation and can be expressed in terms of the weight fraction of each component since $\phi = [(\Delta\alpha.w/\rho)]$ where $\Delta\alpha$ signifies the change in thermal expansivity at T_g, and ρ corresponds to the actual density of the material. Their proposed expression is possibly the most used equation for calculating the glass transition temperature of amorphous mixtures [50]

$$T_{g\ mix} = \frac{w_1 T_{g1} + k w_2 T_{g2}}{w_1 + k w_2} \quad (3)$$

where *w* represents the weight fraction concentration in the mixture and subscripts 1 and 2 refer to components 1 and 2, respectively. Additionally, $W_2 = 1 - W_1$ [51] and *k* denotes the strength of the

interaction between the two components. By employing the Gordon-Taylor (GT) equation and analyzing experimental data, it becomes possible to assess the influence of moisture content on the glass transition temperature of an anhydrous substance. As anticipated, the glass transition temperature (T_g) exhibits a decrease in response to increasing moisture content [14,50,52]. There is variation in the scientific literature concerning the use of the G-T equation, particularly in the determination of *k*. Some researchers propose that *k* can be derived as the ratio of free volumes of the two components. The concept of polymer-free volume formed the foundation for the initial formulation of the parameter *k*, which was employed in the computation of polymer mixtures and polymer-plasticizer (diluent) blends. The equation can be expressed as follows, where *V* represents the specific volume at the corresponding temperature (*T*):

$$k = (V_2.V_1)/(\Delta\alpha_2.\Delta\alpha_1) \quad (4)$$

Other researchers have suggested that in order for such a theory to compute *k* accurately, knowledge of the true densities of the plasticizer and polymer, as well as their respective thermal expansivity is required [27,50,53] such that

$$k = (\rho_1.T_{g1})/(\rho_2.T_{g2}) \quad (5)$$

The Simha-Boyer equation provides an alternative method by stating that the changes in the thermal expansion coefficient maintain a constant value in relation to temperature ($\Delta\alpha \times T_g$ = *constant*) such that [54]

$$k = (V_2.T_{g1})/(V_1.T_{g2}) \quad (6)$$

In a study conducted to establish an equation that describes the correlation between *k* and T_g, where *k* represents a fitting parameter that demonstrates sensitivity to the plasticizing effect of water and is influenced by variations in the thermal expansion coefficient, the glass transition temperature (T_g) was shown to increase as the value of *k* is raised [55] with the relationship effectively demonstrating by an empirical linear equation between these two parameters [56] in the form of $k = 0.0293\ T_g + 3.61$.

The Kelley and Bueche equation: The T_g of a miscible mixture, such as one including a plasticizer and a polymer, is ideally predictable in practice based on the characteristics of the individual components. Many methods have been put forth to calculate the glass transition temperatures of mixes using the thermo-physical characteristics of the individual pure components. All of these connections have in common the presumption that certain qualities at the T_g are additive and continuous. Kelley and Bueche [57] and Williams et al. [46] proposed that the glass transition temperature behavior in plasticized systems can be attributed to a critical volume fraction at the glass transition. The Kelley and Bueche discovered polymer-diluent model can be described as:

$$T_{g\,mix} = \frac{\sum \varphi_i T_{gi} \Delta\alpha_i}{\sum \varphi_1 \Delta\alpha_i} \tag{7}$$

where ϕ_i is the volume fraction of component *i*, ($T_{g,i}$) $\Delta\alpha_i$ is the change in the coefficient of thermal expansion (CTE) while moving from the glass to the liquid (rubber) state, and $T_{g,mix}$ and $T_{g,i}$ are the glass transition temperatures of the mixture and of the components. If no experimental data are available, the constant *k* can be made to equal the change in heat capacity from the glass to rubber

state, C_{pi}, as a substitute for experimental data represented for mixtures with two or more components as:

$$T_{g\,mix} = \frac{\sum w_i T_{gi} \Delta C_{pi}}{\sum w_1 \Delta C_{pi}} \tag{8}$$

The Kelley-Bueche equation is based on the viscosity and proportionate increase in free volume caused by diluent and plasticizer effects on a polymeric system. By examining the correlation between viscosity and glass transition temperature, as well as the segmental motion of a polymer, Kelley and Bueche formulated a technique for evaluating the impact of a diluent on the polymer. This method involves assessing the relative increase in free volume contributed by the diluent. The consideration of free volume enables the estimation of the glass transition temperature of a polymer-diluent mixture based on its constituents and composition. A combination of the Cohen and Turnbull expression, WLF constant, and equation for the viscosity-molecular mobility relationship [44,46] results in the modified Doolittle relationship which relates the molecular transport on free volume [57]:

$$\emptyset = A\ exp\ [-\frac{bv_0}{v_f}]\ ,\ v_f = v_g[0.025 + \alpha(T - T_g)]$$

In the given equation, ϕ is fluidity when it has a reverse relationship with viscosity $\eta(\phi = 1/\eta)$, v_o denotes the van der Waals volume of the molecule, v_f represents the average free volume per molecule, b is a constant of order unity, v_g corresponds to the volume at the glass transition temperature T_g, and a represents the difference between the thermal expansion coefficients of the liquid and the glass. By recognizing the influence of moisture uptake on the glass transition

temperature and its subsequent reduction, the Kelley-Bueche equation can be extended to incorporate moisture content data [58,59]. This allows for the prediction of T_g changes associated with the diffusion of a diluent medium in a polymer or polymer-diluent model. The equation can be derived following expressions [13,57,60] as

$$T_{gwet} = \frac{\alpha_p V_p T_{gp} + \alpha_d (1 - V_p) T_{gd}}{\alpha_p V_p + \alpha_d (1 - V_p)} \tag{9}$$

where ρ_p represents the density of the dry polymer, ρ_d represents the density of the diluent, V_p denotes the volume fraction of the polymer in the system, α_p and α_d are the coefficients of volume expansion for the polymer in the glassy state and the diluent in the liquid state, respectively while polymer volumetric expansion coefficient is $\alpha_p = 3(\alpha_{re} - \alpha_{ge})$ where α_{re} and α_{ge} are rubbery and glassy linear thermal expansion coefficients, respectively, and are determined by dimensional change trace obtained from TMA, DMA, or other experimental procedures. When M_m is the equilibrium water content, in the case where the diluent is water.

$$V_p = \frac{1}{1 + 0.01\, M_m (\rho_p / \rho_w)} \tag{10}$$

In the case of a polymer-water system, a simplified version of the Kelley-Beuche equation can be employed. The coefficient of expansion of amorphous water within the temperature range from its glass transition temperature (T_g) to its melting point (T_m) at 0°C is not known. By assuming the coefficient of expansion of the amorphous phase (α_p) is equal to the coefficient of expansion of the water or other diluent ($\alpha_p = \alpha_w$), the Kelley-Beuche equation can be expressed in a simplified form [5]:

$$T_g = V_p\, T_{gp} + \left(1 - V_p\right) T_{gw} \tag{11}$$

The Fox equation: Application of the Gordon-Taylor/Kelley-Bueche equations, for two components [14] is often known as the Fox equation [61,62]. The Fox or Gordon-Taylor/Kelley-Buche equations can be made simpler by employing the Simha-Boyer rule, which allows us to determine the constant *k* from the densities of the two components. Using the general equation provided by Equations provided by Eqs. 1 and 2, and the Simha-Boyer rule ($\Delta\alpha \cdot T_g$ = constant), which was applied to the Gordon-Taylor equation, and assuming that the component specific volumes are identical presented in the Eq. 5: $k = (\rho_1 . T_{g1})/(\rho_2 . T_{g2})$ will result in $k = T_{g1}/T_{g2}$ and the representation of the Fox equation [50]. This form is beneficial in circumstances where Δα is ambiguous, especially when measuring in water due to the low T_g and the complexity in determining Δα. Therefore, when both components have comparable densities, the Gordon-Taylor/Kelley-Bueche equations can be used [14]. Furthermore, when the differences in densities are large for most low molecule weight glass formers, the Fox equation will not be appropriate. The calculation of the parameter *k* is where the Fox equation and Kelley-Bueche equation diverge. In the Kelley-Bueche equation, *k* is based on the concept of free volume, whereas the Fox equation does not explicitly consider factors such as free volume or thermal expansion coefficients.

The weighted average relationship between T_g and mass fraction is described by this model, and it is applied to the case when *k = 1*.

$$\frac{1}{T_g} = \sum \frac{w_i}{T_{gi}} \tag{12}$$

where w_i is the mass fraction of component i, T_g is the mixture's glass transition temperature, T_{gi} is the component's glass transition temperature [55]. The Fox equation has garnered significant interest among various models due to its explicit and simplified form, specifically employing an inverse rule-of-mixture. In contrast, the Gordon-Taylor equation simplifies directly to $T_g = w_1T_{g,1} + w_2T_{g,2}$, which represents the conventional expression of a direct rule-of-mixture. Notably, in comparison to the Fox equation, the application of the Gordon-Taylor equation necessitates a regression analysis of experimental data [65].

William, Landel and Ferry and Fox-Flory equations: The William, Landel and Ferry equation is based on the relationship between viscosity of the polymer and glass transition temperature. The transition from glass to rubber or liquid is accompanied by very sudden changes in the material's physical properties, such as a rise in entropy, heat capacity, and volume and a decrease in stiffness and viscosity. The glass transition temperature of the material can be calculated using these changes in the substance's physical properties. The change of the physical properties with temperature is better represented by the Williams Landel Ferry (WLF) [46] formula. When used to describe viscosity, the term looks like this:

$$\frac{log\,\eta}{log\,\eta_g} = \frac{-C_1(T-T_g)}{C_2+T-T_g} \tag{13}$$

In this equation, the parameter C_1, and C_2 are the fitting parameters, and variable η and η_g represent the viscosities at temperature T and T_g, respectively. The values of C_1 and C_2 may vary slightly around certain “universal values" (C_1=17.4 and C_2=51.6) determined by Williams, Landel and Ferry in 1955 [59,64-66]. It should be noted that these universal values can depend on the

specific material being considered, as discussed by Ferry in 1980 [4]. The glass transition temperature T_g of a polymer is well known to vary with chain length molecular weight. Fox and Flory proposed one of the equations that is frequently used to investigate this relationship [64,67-69].

$$1/T_g = 1/T_{g,\infty} + constant/M \tag{14}$$

i.e.,

$$T_g = T_{g\infty} - \frac{Kg}{MW} \tag{15}$$

When the prior equation cannot match the data, a stretched exponential function is used where n is a non-exponential parameter varying between 0 and 1 such that

$$1 - \frac{T_g}{T_{g(\infty)}} = exp\left(-\left(\frac{A}{MW}\right)^n\right) \tag{16}$$

In these equations, $T_{g(\infty)}$ is a maximum anhydrous T_g, MW is molecular weight and kg is the characteristic parameter of the dependency between T_g and MW in Eq. 15. A(g/mol) which is a characteristic parameter of the T_g and molecular weight relationship in Eq. 16 and is a constant. The Fox-Flory equation is based on experimental results. However, if we assume that the product of the glass transition temperature and the change in specific heat, $\Delta C_{pi}\, T_{g,i}$ is the same for all compounds, it can be directly obtained from the Gordon-Taylor equation.

The Couchman Equation: An equation for characterizing the T_g behavior of polymer-plasticizer blends has been developed by Couchman and Karasz based on thermodynamic considerations. This equation is identical to the Gordon-Taylor/Kelley-Bueche equations except for one key difference [68]:

$$k = {\Delta C_{p2}}\Big/{\Delta C_{p1}} \tag{17}$$

The Couchman-Karasz equation is based on thermodynamic theory, which connects entropy and heat capacity and relates them to glass transition temperature. Using the mole/weight fraction and heat capacity information we will have the formula of this model [68]. The Couchman-Karasz equation, which assumes the glass transition to be a thermodynamic condition, evaluates the T_g of components by the change in heat capacity (ΔC_p) rather than the change in volume at the glass transition. The liquid-glass transition can be viewed as a second order phase transition process in this manner, where the heat capacity of the sample varies during the transition from liquid to glass [69] such that:

$$\Delta C_P = C_p^{liquid} - C_p^{glass} \tag{18}$$

Using the assumption that ΔC_p is temperature-independent [70] the relationship can be expressed following [71] as

$$ln(T_{CK}) = \frac{\Delta C_{p1} x_1 \, ln(T_{g1}) + \Delta C_{p2} x_2 \, ln(T_{g2})}{\Delta C_{p1} x_1 + \Delta C_{p2} x_2} \tag{19}$$

Couchman and Karasz (1978) presented a modified version of Eq. 19, assuming that C_p is proportional to temperature rather than independence. Ten Brinke et al. suggested that the modified equation should be used and questioned the validity of the premise that C_p and temperature are independent of one another [72]. This is the most often used version of the Couchman-Karasz equation:

$$T_{CK} = \frac{\sum \Delta C_{pi} x_i T_{gi}}{\sum \Delta C_{pi} x_i} \tag{20}$$

$$T_{g12} = \frac{\Delta C_{p1} x_1 T_{g1} + \Delta C_{p2} x_2 T_{g2}}{\Delta C_{p1} x_1 + \Delta C_{p2} x_2} \tag{21}$$

Ten Brinkle et al. also argued against the assumption of the independence of ΔC_{pi} from temperature and proposed an alternative assumption where the change in heat capacity is proportional to the temperature (T). Under this condition, they introduced what is known as the "modified" C-K equation as well as modified Fox equation [27]. The Couchman-Karasz equation has undergone more complicated modifications, such as those made by Pinal [50], which takes the entropy of mixing the components in the blend shown by Eq. (21) into account, and by Kwei [73], which added a term to take the interaction of hydrogen bonds between polymeric components into account.

$$T_{gm} = T_{CK} exp\left[- \frac{{}^{\Delta H_{mix}}/_{T_{CK}} + \delta S^{c}_{mix}}{\Delta C_{p,m}} \right] \tag{22}$$

where ΔS_{mix} is entropy and show by: $\Delta S_{mix} = {}^{\Delta H_{mix}}/_{T_{CK}} + \delta S^{c}_{mix}$ and the mixture's glass transition temperature is represented as T_{gm} while T_{CK} is the glass transition temperature predicted by the Couchman-Karasz model, ${}^{\Delta H_{mix}}/_{T_{CK}}$ is representing heat/temperature and $\Delta C_{p,m}$ is heat capacity of mixture. Both the Gordon-Taylor and Couchman-Karasz equations rely on the free volume theory and are applicable when the mixing partners possess similar shapes and sizes and are ideally mixed. These equations assume that the free volume of the substances exhibits additive behavior, and no interactions occur between the mixing partners [74].

The Jenkel-Heusch and Kwei Equations: In some cases, there are likely to be significant particular interactions between the materials in a two-component combination. The typical Gordon-Taylor-type equation should be modified in this instance, according to several authors [75], by including a new quadratic parameter [14]. This type of equation was introduced by Jenkel-Heusch. When taking into account systems with significant interactions, the Jenkel-Heusch equation provides a useful method for defining the behavior of amorphous blends. Because of its usefulness in recording composition-dependent fluctuations in $T_{g.}$ Even though it is less well-known than some other equations, the Jenkel-Heusch equation [76], which takes into account monotonic (all positive or all negative) deviations from the linear combination [77], demonstrated good agreement with experimental data [78] in the following form

$$T_g = w_1 T_{g1} + w_2 T_{g2} + q w_1 w_2 \tag{23}$$

where T_g is the glass transition temperature of the blend, T_{g1} is the glass transition temperature of component 1, T_{g2} is the glass transition temperature of component 2, w_1 is the weight fraction of

component 1, w_2 is the weight fraction of component 2, and q is a measure of the interaction between the two components 1 and 2. Here, the empirical "interaction parameter" q indicates the nature and strength of the interactions that take place. A modification of the Jenkel-Heusch equation, known as the Kwei equation [73], uses the constants k_i computed using the Simha-Boyer rule [54] can be represented in a form where the term qw_1w_2 is proportional to the number of interactions present in the mixture, and q is a measure of interaction between two components [79,80] as

$$T_{g\,mix} = \frac{w_1 T_{g1} + k w_2 T_{g2}}{w_1 + k w_2} + q w_1 w_2 \tag{24}$$

If $q = 0$, the Kwei equation reduces to the Gordon-Taylor equation even though k is not equal to one.

The DiBeneditto Equation: A further factor that may affect the glass transition temperature (T_g) is cross-link density. When a polymer undergoes cross-linking, it can experience a substantial increase in T_g. However, the effect on T_g is limited and not very noticeable at lower cross-linking levels. The shift in T_g, however, becomes significant when the cross-linking intensity rises and exhibits sensitivity to only modest changes in the cross-linking density (M_c). This adds difficulty to the analysis because, in the majority of systems, the change in T_g depends on the polymer's chemical composition. The network structure of the polymer gradually changes as additional cross-linking agents are added to it. The cross-linking agent can be thought of as a specific kind of copolymerizing unit, which has a combined effect on T_g. As a result, two separate yet related factors—the degree of cross-linking, or 1/Mc—and the copolymer effect—influence the change

in the glass-transition temperature. The cross-linking effect consistently increases T_g and appears to be unaffected by chemical composition. However, depending on the chemical properties of the cross-linking agent, the copolymer effect can either increase or decrease T_g. To investigate the connection between the level of cross-linking and the accompanying change in T_g, numerous research has been conducted [81]. Divergent results are produced by this research because there is a lack of agreement among them. However, by averaging the outcomes, the shift in T_g can be used to obtain the following equation, which provides rough estimations of M_c:

$$T_g - T_{g0} = \frac{3.9\times10^4}{M_c} \tag{25}$$

where T_{g0} is the polymer's uncross-linked glass transition temperature. It must be kept in mind that this equation only takes into account the shift caused by cross-linking; the shift caused by the copolymer effect is not taken into account.

In the literature, several theoretical and empirical formulas exist that establish a connection between the glass transition temperature (T_g) and the degree of cure. One of the noteworthy formulations is the original DiBenedetto equation [82,83]. This equation describes the relationship between the shift in the glass-transition temperature and the level of cross-linking, and it was developed by DiMarzio [42] and, more recently, DiBenedetto. It is important to mention that, according to Nielson [84], this particular study has not been published. The equation proposed by DiBenedetto is as follows:

$$\frac{T_g - T_{gu}}{T_{gu}} = \frac{X\left(\frac{E_X}{E_m} - \frac{F_X}{F_m}\right)}{1 - X\left(1 - \frac{F_X}{F_m}\right)} \quad (26)$$

The fraction of all segments that are crosslinked is known as the crosslink density, or *X*. T_{gu} stands for the uncrosslinked polymer's glass transition temperature, whereas E denotes lattice energy. The subscripts x and m stand for fully crosslinked and uncrosslinked polymers, respectively, and the letter *F* stands for segmental mobility. The ratio E_x/E_m has frequently been proposed to be close to 1.0 or slightly greater, implying a similar amount of lattice energy between the crosslinked and uncrosslinked states (according to the unpublished DiBenedetto study cited by Neilson [84]). On the other side, the ratio F_x/F_m is predicted to get closer to zero, showing that segmental mobility is significantly reduced after crosslinking. Some researchers [83,85,86] have treated the crosslink density X as α, where stands for the degree of conversion because it was difficult to measure the crosslink density X quantitatively. Similarly, T_{gu} has been regarded as T_{g0}, which represents the glass transition temperature at $\alpha = 0$, corresponding to the state of the entire monomer. By defining $T_{g\infty}$ as the glass transition temperature at α=1, the relationship $(E_x/E_m)/(F_x/F_m) = T_{g\infty}/T_{g0}$ can be derived from the aforementioned equation. Setting $F_x/F_m = \lambda'$ and rearranging equation (1) yields:

$$\frac{T_g - T_{g0}}{T_{g\infty} - T_{g0}} = \frac{\lambda'}{1 - (1 - \lambda')\alpha} \quad (27)$$

The development of an understanding of how different models predict the glass transition temperature (T_g) and determining the most reliable and appropriate model for a given material is of utmost importance. Comparative investigations typically involve the collection of experimental

T_g data across various materials, and subsequently comparing the predictions of different models against these experimental values. Statistical analyses are then conducted to assess the agreement between the predicted and experimental T_g values, aiming to identify the model that best captures the observed T_g behavior.

3.4. SUMMARY AND DISCUSSION

Moisture is known to be a major environmental factor in civil infrastructure and is known to detrimentally affect the long-term performance of polymers and composites. While performance characteristics can be measured through mechanical tests these take significant material and can be inconclusive as related to the characterization of effects and the determination of rationale for changes at a phenomenological basis although correlations can be drawn between mechanical performance changes over time and changes in microstructural features as seen through microscopy. The assessment of glass transition temperature, however, provides an effective means of assessing changes since it not only decreases with increase in moisture content, but the shape and extent change based on the effects of the uptake on molecular mobility and cross-link density. The determination of change in glass transition temperature and its relation to other dynamic characteristics can yield critical information that enables the specific assessment of performance change and prediction of long-term durability. Exposure of thermosetting resins such as epoxies and composites when exposed to moisture, either in the form of humidity or through solution immersion, is known to induce plasticization, resulting in a decrease in the glass transition temperature (T_g). This plasticization occurs due to the water molecules interrupting the interchain hydrogen bonds within the material. For example, in a study by Suh D et al. [87], the T_g of a dry composite specimen was measured to be 208.3°C. However, as the equilibrium water uptake

increased, the T_g decreased. At a temperature of 35°C, the equilibrium water uptake reached 1.07%, causing a reduction in the T_g to 178.7°C. Moreover, during hygrothermal conditioning from 95°C to 35°C, when the water uptake reached 1.67%, there was a significant decrease in T_g of 49.2°C. Similarly in a study on long-term hydrothermal aging of wet layup carbon/epoxy fabricated by the wet layup process Karbhari [20] reported lower rates of decrease in the glass transition with increases in moisture content than previously reported with prepreg-based materials with the attainment of a threshold after which further decrease was either extremely slow or not noted. This was correlated with the attainment of asymptotic thresholds in the performance characteristics. The interested reader is referred to [20] for further discussion of correlations with storage modulus as well as the use of both the loss factor peak and storage modulus as a means of differentiating between effects of postcure, plasticization, and deterioration. The use of multi-frequency DMTA to assess durability has been demonstrated in [88] providing further links between the glass transition temperature and activation energy which can be used as an indicator of materials degradation and differences in rates depending on the exposure condition temperature and type of solution). While the glass transition temperature has been used in the past as a characteristic of state of the material, there is growing use of it as a means of assessing changes in durability and in prediction of service life and long-term durability. This is not only due to the ease of determining activation energies and the use of time-temperature superposition based on true indicators of phenomenological change but also the ability to use changes in T_g and dynamic moduli to differentiate between mechanisms that are critical for the interpretation of material state and remaining service life. It is proposed that the use of techniques based on these are far more accurate than the use of extrapolation of performance characteristics even when based on acceleration of aging through use of higher temperatures of exposure (and immersion).

3.5. REFERENCES

[1] R. Overney, C. Buenviaje, R. Luginbühl, F. Dinelli, Glass and structural transitions measured at polymer surfaces on the nanoscale, J. Therm. Anal. Calorim. 59 (1–2) (2000) 205–225.

[2] B. Cuq, F. Gonçalves, J.F. Mas, L. Vareille, J. Abecassis, Effects of moisture content and temperature of spaghetti on their mechanical properties, J. Food Eng. 59 (1) (2003) 51–60.

[3] J. Rieger, The glass transition temperature Tg of polymers—Comparison of the values from differential thermal analysis (DTA, DSC) and dynamic mechanical measurements (torsion pendulum), Polym. Test. 20 (2) (2001) 199–204.

[4] J.D. Ferry, Viscoelastic Properties of Polymers, John Wiley & Sons, 1980.

[5] R.J. Morgan, J.E. O'neal, The durability of epoxies, Polym.-Plast. Technol. Eng. 10 (1) (1978) 49–116.

[6] M.J. Adamson, Thermal expansion and swelling of cured epoxy resin used in graphite/epoxy composite, J. Mater. Sci. 15 (1980) 1736–1745.

[7] D.I. Bower, An Introduction to Polymer Physics, Cambridge University Press, New York, 2002.

[8] J. Tomaszewska, T. Sterzynski, A. Wo ´ zniak-Braszak, M. Banaszak, Review of recent ´ developments of glass transition in PVC nanocomposites, Polymers 13 (24) (2021) 4336.

[9] V.M. Karbhari, G. Xian, S.K. Hong, Effect of thermal exposure on carbon fiber reinforced composites used in civil infrastructure rehabilitation, Composites A 149 (2021) 106570.

[10] V.M. Karbhari, Durability of FRP composites for use in civil infrastructure: from materials to application, Fiber Reinforced Polymeric Materials and Sustainable Structures, Springer, 2023, pp. 33–45.

[11] J. Michels, R. Widmann, C. Czaderski, R. Allahvirdizadeh, M. Motavalli, Glass transition evaluation of commercially available epoxy resins used for civil engineering applications, Composites B 77 (2015) 484–493.

[12] A.A. Alqahtani, V. Bertola, Polymer and composite materials in two-phase passive thermal management systems: a review, Materials. 16 (3) (2023) 893.

[13] J. Zhou, J.P. Lucas, Hygrothermal effects of epoxy resin. Part II: variations of glass transition temperature, Polymer 40 (20) (1999) 5513–5522.

[14] B.C. Hancock, G. Zografi, The relationship between the glass transition temperature and the water content of amorphous pharmaceutical solids, Pharm. Res. 11 (1994) 471–477.

[15] C.A. Oksanen, G. Zografi, The relationship between the glass transition temperature and water vapor absorption by poly (vinylpyrrolidone), Pharm. Res. 7 (1990) 654–657.

[16] C.H. Shen, G.S. Springer, Moisture absorption and desorption of composite materials, J. Compos. Mater. 10 (1) (1976) 2–20.

[17] A. Hale, C.W. Macosko, H.E. Bair, Glass transition temperature as a function of conversion in thermosetting polymers, Macromolecules 24 (9) (1991) 2610–2621.

[18] S. Lunak, J. Vladyka, K. Dušek, Effect of diffusion control in the glass transition region ˇ on critical conversion at the gel point during curing of epoxy resins, Polymer 19 (8) (1978) 931–933.

[19] V.M. Karbhari, M.A. Abanilla, Design factors, reliability, and durability prediction of wet layup carbon/epoxy used in external strengthening, Composites B 38 (1) (2007) 10–23.

[20] V.M. Karbhari, Long-term hydrothermal aging of carbon-epoxy materials for rehabilitation of civil infrastructure, Composites A 153 (2022) 106705.

[21] A. Spelter, S. Bergmann, J. Bielak, J. Hegger, Long-term durability of carbon-reinforced

concrete: an overview and experimental investigations, Applied Sciences 9 (8) (2019) 1651.

[22] J. Yang, X. Chen, Y. Li, W. Luo, R. Fu, M. Zhang, Glass transition in polymers monitored by synchronous scan spectra, Polym Test 28 (2) (2009) 165–168.

[23] B. Zimmermann, D. Vrsaljko, IR spectroscopy based thermal analysis of polymers, Polym. Test. 29 (7) (2010) 849–856.

[24] A. Bayatpour, M. Hojjati, Moisture effect on properties of out-of-autoclave laminates with different void content, Int. J. Compos. Mater. 10 (1) (2020) 1–9.

[25] M.J. Richardson, Thermal analysis of polymers using quantitative differential scanning calorimetry, Polym. Test. 4 (2–4) (1984) 101–115.

[26] H.M. Pollock, A. Hammiche, Micro-thermal analysis: techniques and applications, J. Phys. D, Appl. Phys. 34 (9) (2001) R23.

[27] I.I. Katkov, F. Levine, Prediction of the glass transition temperature of water solutions: comparison of different models, Cryobiology 49 (1) (2004) 62–82.

[28] M. Kunaver, J. Zadnik, O. Planinsek, S. Srcic, Inverse gas chromatography: a different approach to characterization of solids and liquids, Acta Chim. Slov. 51 (3) (2004) 373–394.

[29] C. Leyva-Porras, P. Cruz-Alcantar, V. Espinosa-Solís, E. Martínez-Guerra, C.I. PiñónBalderrama, I. Compean Martínez, et al., Application of differential scanning calorimetry (DSC) and modulated differential scanning calorimetry (MDSC) in food and drug industries, Polymers 12 (1) (2019) 5.

[30] A. Majumdar, J.P. Carrejo, J. Lai, Thermal imaging using the atomic force microscope, Appl. Phys. Lett. 62 (20) (1993) 2501–2503.

[31] Q. Yang, G. Xian, V.M. Karbhari, Hygrothermal ageing of an epoxy adhesive used in FRP strengthening of concrete, J. Appl. Polym. Sci. 107 (4) (2008) 2607–2617.

[32] Humboldt Universitat zu Berlin, Investigation of polymers with differential scanning calorimetry, in: Advanced Lab: DSC Investigation Polymer, Humboldt University of Berlin, 2009. Available from https://polymerscience.physik.hu-berlin.de/docs/manuals/DSC.pdf.

[33] W. Brostow, R. Chiu, I.M. Kalogeras, A. Vassilikou-Dova, Prediction of glass transition temperatures: binary blends and copolymers, Material Letters 62 (17–18) (2008) 3152–3155.

[34] K. Chen, G. Zhao, J. Chen, X. Zhu, S. Guo, Improvements in temperature uniformity in carbon fiber composites during microwave-curing processes via a recently developed microwave equipped with a three-dimensional motion system, Materials 16 (2) (2023) 705.

[35] G. Xian, V.M. Karbhari, Segmental relaxation of water-aged ambient cured epoxy, Polym. Degrad. Stab. 92 (9) (2007) 1650–1659.

[36] M. Meincken, R.D. Sanderson, Advantages of scanning probe microscopy in polymer science: research in action, S. Afr. J. Sci. 100 (5) (2004) 256–260.

[37] K. Backfolk, R. Holmes, P. Ihalainen, P. Sirviö, N. Triantafillopoulos, J. Peltonen, Determination of the glass transition temperature of latex films: comparison of various methods, Polym. Test. 26 (8) (2007) 1031–1040.

[38] D.J. Burnett, F. Thielmann, J. Booth, Determining the critical relative humidity for moisture-induced phase transitions, Int. J. Pharm. 287 (1–2) (2004) 123–133.

[39] T.K. Kwei, Introduction to physical polymer science, by LH Sperling, J. Polym. Sci. A

Polym. Chem. 31 (4) (1993) 1097.

[40] Y.H. Roos, S. Drusch, Phase Transitions in Foods, Academic Press, 2015.

[41] V.M. Karbhari, B. Hassanpour, Water, saltwater, and concrete leachate solution effects on durability of ambient-temperature cure carbon-epoxy composites, J. Appl. Polym. Sci. 139 (27) (2022) e52496.

[42] E.A. DiMarzio, On the second-order transition of a rubber, J. Res. Natl. Bur. Stand. – A. Phys. Chem. 68 (6) (1964) 611–617.

[43] J.H. Gibbs, E.A. DiMarzio, Nature of the glass transition and the glassy state, J. Chem. Phys. 28 (1958) 373–383.

[44] M.H. Cohen, D. Turnbull, Molecular transport in liquids and glasses, J. Chem. Phys. 31 (5) (1959) 1164–1169.

[45] M. Gordon, J.S. Taylor, Ideal copolymers and the second-order transitions of synthetic rubbers. I. Non-crystalline copolymers, J. Appl. Chem. 2 (9) (1952) 493–500.

[46] M.L. Williams, R.F. Landel, J.D. Ferry, The temperature dependence of relaxation mechanisms in amorphous polymers and other glass-forming liquids, J. Am. Chem. Soc. 77 (14) (1955) 3701–3707.

[47] B. Koo, Y. Liu, J. Zou, A. Chattopadhyay, L.L. Dai, Study of glass transition temperature (Tg) of novel stress-sensitive composites using molecular dynamic simulation, Model. Simul. Mater. Sci. Eng. 22 (6) (2014) 065018.

[48] Y. Park, J. Ko, T. Ahn, S. Choe, Moisture effects on the glass transition and the low temperature relaxations in semiaromatic polyamides, J. Polym. Sci. B. Polym. Phys. 35 (5) (1997) 807–815.

[49] R. Lin, A. Su, J. Hong, Glass transition temperature versus conversion relationship in the

polycyclotrimerization of aromatic dicyanates, Polym. Int. 49 (4) (2000) 345–357.

[50] R. Pinal, Entropy of mixing and the glass transition of amorphous mixtures, Entropy 10 (3) (2008) 207–223.

[51] P.G. Royall, D.Q.M. Craig, C. Doherty, Characterisation of moisture uptake effects on the glass transitional behaviour of an amorphous drug using modulated temperature DSC, Int. J. Pharm. 192 (1) (1999) 39–46.

[52] E. Penzel, J. Rieger, H.A. Schneider, The glass transition temperature of random copolymers: 1. Experimental data and the Gordon-Taylor equation, Polymer 38 (2) (1997) 325–337.

[53] H.A. Schneider, J. Rieger, E. Penzel, The glass transition temperature of random copolymers: 2. Extension of the Gordon-Taylor equation for asymmetric Tg vs composition curves, Polymer 38 (6) (1997) 1323–1337.

[54] R. Simha, R.F. Boyer, On a general relation involving the glass temperature and coefficients of expansion of polymers, J. Chem. Phys. 37 (5) (1962) 1003–1007.

[55] M.M. Bertotto, A. Gastón, M.J. Rodríguez Batiller, P. Calello, Comparison of mathematical models to predict glass transition temperature of rice (cultivar IRGA 424) measured by dynamic mechanical analysis, Food Sci. Nutr. 6 (8) (2018) 2199–2209.

[56] S. Fongin, K. Kawai, N. Harnkarnsujarit, Y. Hagura, Effects of water and maltodextrin on the glass transition temperature of freeze-dried mango pulp and an empirical model to predict plasticizing effect of water on dried fruits, J Food Eng 210 (2017) 91–97.

[57] F.N. Kelley, F. Bueche, Viscosity and glass temperature relations for polymer-diluent systems, J. Polym. Sci. 50 (154) (1961) 549–556.

[58] P.S. Theocaris, E.A. Kontou, G.C. Papanicolaou, The effect of moisture absorption on the

thermomechanical properties of particulates, Colloid. Polym. Sci. 261 (1983) 394–403.

[59] C.E. Browning, C.E. Husman, J.M. Whitney, Moisture Effects in Epoxy Matrix Composites, Air Force Materials Laboratory, Wright Patterson Air Force Base, OH, 1977 AFMLTR-77-17.

[60] M.A. Abanilla, Y. Li, V.M. Karbhari, Durability characterization of wet layup graphite/epoxy composites used in external strengthening, Composites B 37 (2–3) (2005) 200–212.

[61] T.G. Fox, Influence of diluent and of copolymer composition on the glass temperature of a polymer system, Bull. Am. Phys. Soc. 1 (1952) 123.

[62] T.G. Fox Jr, P.J. Flory, Second-order transition temperatures and related properties of polystyrene. I. Influence of molecular weight, J. Phys. A 21 (6) (1950) 581–591.

[63] T.Q. Liu, R. Wang, S. Zhen, P. Feng, A binary resin system of epoxy and phenolformaldehyde for improving the thermo-mechanical behavior of FRP composites, Constr. Build. Mater. 389 (2023) 131790.

[64] G. Roudaut, D. Simatos, D. Champion, E. Contreras-Lopez, M. Le Meste, Molecular mobility around the glass transition temperature: a mini review, Innovative Food Sci. Emerg. Technol. 5 (2) (2004) 127–134.

[65 Kawai K., Fukami K., Thanatuksorn P., Viriyarattanasak C., Kajiwara K. Effects of moisture content, molecular weight, and crystallinity on the glass transition temperature of inulin. Carbohydr. Polym. 83(2): 934–939.

[66] T.G. Fox, P.J. Flory, The glass temperature and related properties of polystyrene. Influence of molecular weight, J. Polym. Sci. 14 (75) (1954) 315–319.

[67] S. Montserrat, P. Colomer, The effect of the molecular weight on the glass transition temperature in amorphous poly (ethylene terephthalate), Polym. Bull. 12 (2) (1984) 173–

180.

[68] P.R. Couchman, F.E. Karasz, A classical thermodynamic discussion of the effect of composition on glass-transition temperatures, Macromolecules 11 (1) (1978) 117–119.

[69] I.I. Katkov, F. Levine, Prediction of the glass transition temperature of water solutions: comparison of different models, Cryobiology 49 (1) (2004) 62–82.

[70] M.G. Abiad, M.T. Carvajal, O.H. Campanella, A review on methods and theories to describe the glass transition phenomenon: applications in food and pharmaceutical products, Food Eng. Rev. 1 (2009) 105–132.

[71] E.J. Mayhew, C.H. Neal, S.Y. Lee, S.J. Schmidt, Glass transition prediction strategies based on the Couchman-Karasz equation in model confectionary systems, J. Food Eng. 214 (2017) 287–302.

[72] G. Ten Brinke, F.E. Karasz, T.S. Ellis, Depression of glass transition temperatures of polymer networks by diluents, Macromolecules 16 (2) (1983) 244–249.

[73] T.K. Kwei, The effect of hydrogen bonding on the glass transition temperatures of polymer mixtures, J. Polym. Sci.: Polym. Lett. Ed. 22 (6) (1984) 307–313.

[74] M. Schugmann, P. Foerst, Systematic investigation on the glass transition temperature of binary and ternary sugar mixtures and the applicability of Gordon–Taylor and Couchman–Karasz equation, Foods 11 (12) (2022) 1679.

[75] T.K. Kwei, E.M. Pearce, J.R. Pennacchia, M. Charton, Correlation between the glass transition temperatures of polymer mixtures and intermolecular force parameters, Macromolecules 20 (5) (1987) 1174–1176.

[76] E. Jenckel, R. Heusch, Die Erniedrigung der Einfriertemperatur organischer Gläser durch Lösungsmittel, Kolloid-Zeitschrift 130 (2) (1953) 89–105.

[77] M.M. Bertotto, A. Gastón, M.J. Rodríguez Batiller, P. Calello, Comparison of mathematical models to predict glass transition temperature of rice (cultivar IRGA 424) measured by dynamic mechanical analysis, Food Sci. Nutr. 6 (8) (2018) 2199–2209.

[78] A. Dubault, L. Bokobza, E. Gandin, J.L. Halary, Effects of molecular interactions on the viscoelastic and plastic behaviour of plasticized poly (vinyl chloride), Polym. Int. 52 (7) (2003) 1108–1118.

[79] B. Grönniger, E. Fritschka, I. Fahrig, A. Danzer, G. Sadowski, Water sorption in rubbery and glassy polymers, nifedipine, and their ASDs, Mol. Pharmaceutics 20 (4) (2023) 2194–2206.

[80] A.T. Slark, Application of the Kwei equation to the glass transition of dye solute-polymer blends, Polymer 40 (8) (1999) 1935–1941.

[81] T.G. Fox, S. Loshaek, Influence of molecular weight and degree of crosslinking on the specific volume and glass temperature of polymers, J. Polym. Sci. 15 (80) (1955) 371–390.

[82] R. Lin, A. Su, J. Hong, Glass transition temperature versus conversion relationship in the polycyclotrimerization of aromatic dicyanates, Polym. Int. 49 (4) (2000) 345–357.

[83] J.P. Pascault, R.J.J. Williams, Glass transition temperature versus conversion relationships for thermosetting polymers, J. Polym. Sci. B. Polym. Phys. 28 (1) (1990) 85–95.

[84] L.E. Nielsen, Cross-linking–effect on physical properties of polymers, J. Macromol. Sci., Part C. 3 (1) (1969) 69–103.

[85] C. Feger, W.J. MacKnight, Properties of partially cured networks. 2. The glass transition, Macromolecules 18 (2) (1985) 280–284.

[86] H.E. Adabbo, R.J.J. Williams, The evolution of thermosetting polymers in a conversion–

temperature phase diagram, J. Appl. Polym. Sci. 27 (4) (1982) 1327–1334.

[87] D.W. Suh, M.K. Ku, J.D. Nam, B.S. Kim, S.C Yoon, Equilibrium water uptake of epoxy/carbon fiber composites in hygrothermal environmental conditions, J. Compos. Mater. 35 (3) (2001) 264–278.

[88] V.M. Karbhari, Q. Wang, Multi-frequency dynamic mechanical thermal analysis of moisture uptake in E-glass/vinylester composites, Composites B 35 (2004) 299–304.

CHAPTER 4. MOISTURE AND GLASS TRANSITION TEMPERATURE KINETICS OF AMBIENT-CURED CARBN/EPOXY COMPOSITES

This chapter contains a paper titled “Moisture and Glass Transition Temperature Kinetics of Ambient-Cured Carbon/Epoxy Composites” published in Journal of Composites Science in 2023.

Hassanpour B, Karbhari VM. Moisture and Glass Transition Temperature Kinetics of Ambient-Cured Carbon/Epoxy Composites. Journal of Composites Science. 2023 Oct 27, 7(11), 447. https://doi.org/10.3390/jcs7110447

MOISTURE AND GLASS TRANSITION TEMPERATURE KINETICS OF AMBIENT CURED CARBON/EPOXY COMPOSITES

Behnaz Hassanpour[1] and Vistasp M. Karbhari[1,2 *]

[1] Department of Civil Engineering; University of Texas Arlington; Arlington, TX 76006, USA

[2] Department of Mechanical and Aerospace Engineering; University of Texas Arlington; Arlington, TX 76006; USA

Abstract: Carbon fiber reinforced polymer composites are widely used in the rehabilitation, repair, and strengthening of civil, marine and naval infrastructure and structural systems. In these applications they are exposed to a range of exposure conditions including humidity and immersion which are known to affect the durability of the resin and the fiber-matrix interface over long periods of time. This paper presents results of long-term hygrothermal aging of wet layup carbon/epoxy composites including through acceleration by temperature focusing on the development of a comprehensive understanding of moisture uptake kinetics and its effects on glass transition temperature and interface and inter-/intra-laminar dominated performance characteristics. A two-phase model for uptake that incorporates both diffusion and relaxation/deterioration dominated regimes as well as a transition regime is shown to describe uptake well. Effects of uptake, including at elevated temperatures reflective of accelerated aging, on glass transition temperature and flexural strength are correlated emphasizing a three-stage progression of overall response in line with the moisture uptake changes. It is shown that both glass transition temperature and flexural strength show steep initial decreases followed by a regime

with slower decrease and then an asymptotic or near-asymptotic response with time of immersion suggesting close correlation with moisture uptake which forms the basis for future modeling.

Keywords:
Carbon/epoxy composite; hygrothermal aging; diffusion; relaxation; interface; glass transition temperature; flexural strength; durability; water.

4.1. INTRODUCTION

The rehabilitation of deteriorating, and under-strength, civil infrastructure elements is increasingly implemented through the external bonding of prefabricated or wet layup composites under field conditions. While these materials have been used successfully in the field in applications ranging from pipelines and tunnels to buildings and bridges, the lack of long-term durability data and concerns related to long-term durability under harsh and changing environmental conditions including due to the hygrothermal exposure has resulted in the development of design guidelines and codes incorporating extremely conservative reduction and partial safety factors [1, 2]. While carbon fibers per se are not affected by the environmental regimes likely to be faced in routine use, the resin and the interface are susceptible to degradation and change by a range of exposure conditions among which moisture, in the form of high humidity and/or immersion, is of significant concern. The use of non-autoclave manual processes such as wet layup which also incorporate ambient temperature cure increase susceptibility to moisture and temperature induced changes over their life cycle [3, 4]. Exposure of epoxies and related carbon/epoxy composites to moisture in the form of humidity and/or solution immersion is known to result in plasticization [5-7] which causes a decrease in glass transition temperature through

interruption of interchain hydrogen bonds by water molecules [8, 9], swelling [8-10], degradation of molecular and network structure [11, 12], saponification and degradation of the fiber-matrix bond and interphase [3,13-15]. While moisture uptake can result in reversible and irreversible deterioration of resin characteristics, it can also cause an initial acceleration in cure progression thereby setting up a competition between mechanisms of performance enhancement and increased glass transition temperature and those of deterioration due to uptake [6].

Moisture uptake in an epoxy is related to the presence of molecular sized holes and on polymer-water affinity, in addition to debond-based paths at the fiber-matrix interface in a composite. The holes depend on structure, morphology, and degree of polymerization whereas the affinity is related to the presence of hydrogen bonding sites along the polymer chain. Apicella et al. [16,17] hypothesized three modes for sorption (a) bulk dissolution, (b) moisture sorption onto surface holes in free volume, and (c) hydrogen bonding between hydrophilic polymer groups and water. The existence of two forms of water, free and bound was proposed by Moy and Karasz [18] and Pethrick et al. [19] among others bringing the recognition of multiple phenomena and mechanisms affecting diffusion and leading to the development of two-staged and multiphase models for uptake in contrast to the traditional Fickian mode wherein uptake is characterized by two parameters, diffusivity and uptake level of saturation [20], with diffusion being characterized in polymers and composites with a constant diffusion coefficient [21, 22], a concentration-dependent diffusion coefficient [23] or a stress-dependent diffusion coefficient [24]. Dual stage sorption models have been proposed for several cases of moisture uptake by Behrens and Hoptenberg [25], Bagley and Long [26], Peppas and Sahlin [27], Carter and Kibler [28], and Bao et al. [29] among others.

These models focus on addressing aspects of anomalous (non-Fickian) diffusion that is comprised of additional physical and physicochemical processes particularly as related to phenomena such as molecular relaxation, segmental mobility retardation, interaction of the penetrant with macromolecules, wicking, micro-cracking, and other deterioration mechanisms that modify the diffusion process. These also attempt to address the slow increase in uptake levels after a transition point which results in a saturation level not being attained within shorter-term time frames, as well as the effect of cure progression on changes in network structure which in turn results in changes in diffusion. Since moisture uptake has a significant influence on performance characteristics and glass transition temperature, a deep understanding of moisture uptake characteristics and kinetics is essential for the prediction of long-term durability, and to ensure accurate design, safety, and economic viability [30, 31]. Despite significant efforts in this area the complexity of mechanisms inherent in a composite which depend on the constituent materials and the bond between them, both of which are affected by moisture uptake, has resulted in a lack of comprehensive knowledge of durability especially under long-term service conditions. This severely limits the use of these materials in areas where catastrophic failure could lead to severe damage not just to the structure itself but also the environment [32] and emphasizes the need for more accurate modeling of moisture uptake and understanding the mechanisms associated with diffusion [33].

The short-time frames used for study of moisture and solution related aging and degradation has been shown to be insufficient to attain saturation, especially for systems such as ambient and moderate-temperature cured composites [31,33] emphasizing the need for longer term studies for the comprehensive understanding of mechanisms and prediction of durability of these

systems [34]. This paper is part of a comprehensive study on the long-term durability of ambient-cured systems over a range of materials and exposure conditions. In this study, an ambient-cured epoxy and wet layup carbon/epoxy composites, at different thickness levels, used extensively in the rehabilitation of civil infrastructure, are subjected to immersion in deionized water over a range of temperatures for periods up to 5 years to investigate moisture uptake characteristics and key effects, including on glass transition temperature, and to distinguish between mechanisms of Fickian diffusion and longer-term relaxation-/deterioration-based uptake. The longer-term goal is to not only provide the basis for accurate characterization and prediction of durability at a fundamental level so that it can be modeled based on constituent material and processing combinations based on exposure conditions, but to also ensure the development of appropriate design/safety factors for use in the field. Specifically, the investigation focuses on the development of a model to describe moisture kinetics in composites that is based on resin kinetic characteristics and is able to identify levels of difference in these based on composite constituents, configuration, and moisture induced damage/changes across both stages of uptake, while also taking into account the effect of temperature of immersion. In addition, the goals were to further assess the effects on trends in glass transition temperature and flexural strength, emphasizing resin- and interface-dominating effects.

4.2. MATERIALS AND TEST METHODS

To ensure that wet layup and the ambient cure process similar to those used in the field were used the resin system was designed with a viscosity of 700-900 cps and a gel time of approximately 60 minutes using a 4,4′-isopropylidenephenol-epichlorohydrin (similar to a DGEBA Epon 828 type system) with an aliphatic amine hardener in a 2:1 ratio. Unidirectional

fabric of 12k untwisted T700 Carbon fibers having a nominal strength, modulus, and density of 4900 MPa, 230 GPa, and 1.80 g/cm3 were used as the reinforcement. To assess effects of fabric and overall thickness on uptake mechanisms two areal weights of fabric at 300 and 600 grams per square meter (gsm) were used to fabricate composites of 1 and 2 layer thicknesses, with the latter being from both fabrics, with nominal thicknesses of 0.72 mm (1 layer of the 300 gsm fabric, designated in the paper as 300/1), 1.34 mm (2 layers of 300 gsm fabric, designated in the paper as 300/2) and 1.8 mm (2 layers of 600 gsm fabric, designated in the paper as 600/2). The use of 2 areal weights of the same fabric type enables both a change in the fiber volume fraction and assessment of greater intralaminar intermingling /compaction between layers without changes in overall constituent and process characteristics. The panels were fabricated using the wet layup process with only manual roller-based pressure and without vacuum bags or pressure plates to mimic field conditions as closely as possible. Fiber mass fractions were determined through acid digestion to be 35%, 39% and 44% for the 300/1, 300/2 and 600/2 composites, respectively, resulting in effective fiber volume fractions of 26%, 29% and 34%, respectively, with void fractions ranging from 2-3%. Flat panels of resin of 5 mm thickness were also cast under ambient temperature conditions resulting in a density of 1.22 g/cm^3. Details are also provided in Table 4-1 for ease of reference.

Table 4-1. *Summary of characteristics for the composite specimens.*

Composite	**Fabric Areal Weight (gsm)**	**Number of Layers**	**Thickness (mm)**	**Fiber Mass Fraction (%)**
300/1	300	1	0.72	35
300/2	300	2	1.34	39
600/2	600	2	1.80	44

All specimens were conditioned for 30 days at 20–23 °C prior to exposure and testing to ensure a reasonable level of cure progression based on prior investigation of the same resin system [35,36], for which the glass transition temperature prior to exposure was noted to be 92 °C [35].

Moisture uptake was determined on specimens of 25.4 mm × 25.4 mm size cut from resin plaques and composite plates at the actual thickness of each specimen thereby keeping surface conditions consistent. Five specimens were used for each measurement with specimens immersed in temperature-controlled baths at 23±1℃, 37.8±1℃ and 60±1℃, with continuous monitoring of both water levels and temperature. Specimens were placed ensuring no contact between adjacent specimens so as to preclude any difference in exposure conditions. A set of specimens was also stored under controlled conditions of 23℃ and 30% RH as reference controls and to assess the progression of cure over time. Specimens were removed periodically, over a period exceeding 5 years, using padded tweezers to ensure minimal pressure and no transfer of oils or substances from human hands that could inadvertently contaminate the specimens and/or the solutions, patted dry with tissue paper and then weighed to measure uptake after which they were reinserted into the baths. The time period for the operation was standardized for consistency and to avoid effects of varying levels of evaporating through the specimens.

Dynamic Mechanical Thermal Analysis (DMTA)-based characterization was conducted in three-point bending mode on specimens of 9 mm width with a span: thickness ratio of 16:1 at a frequency of 1 Hz with a strain of 0.0025% and a heating rate of 5℃/minute. Specimens were placed in the three temperature baths with the moisture uptake specimens, and similar care was taken to ensure that the time period between the removal of specimens from the temperature-

controlled baths and the initiation of DMTA testing was standardized. A minimum of three specimens were tested for each set at periodic intervals up to 60 months.

To correlate changes in moisture uptake and glass transition temperature with mechanical performance flexure tests following ASTM D790 were conducted at periodic levels, on specimens placed in the 3 temperature-controlled baths using the same precautions as used with DMTA specimens. A minimum of 5 specimens were tested in three-point-flexure mode at each time period (up to 60 months) and immersion condition. A span-to-depth ratio of 16:1 was used with a nominal width of 12.5 mm. The test was specifically chosen to assess performance of the number of layers and fabric weight which result in difference in fiber and bundle interactions and compaction, causing tortuosity in flow and increased interlaminar and interlaminar interaction components. The 3-point flexure test incorporates both shear and bending components and, hence, enables a focus on resin- and interface-dominated effects. Photographs of test equipment for the DMTA and flexure tests are shown in Figure 4-1(a)-(b), respectively.

(**a**) (**b**)

Figure 4-1. *Test equipment: (a) DMTA, (b) flexure.*

4.3. RESULTS AND DISCUSSIONS

4.3.1. MOISTURE UPTAKE AND KINETICS

While moisture uptake in polymers and composites is often described by the process of Fickian diffusion it has been shown that many of these materials do not attain saturation over extended periods of time with uptake continuing to increase due to aspects such as moisture-induced changes at the resin and fiber-interface levels including within the polymer network and from relaxation and deterioration processes which are slower than the initial diffusion processes [29, 37]. Following Bao et al. [29], moisture uptake, M_t, at time t, can be expressed as:

$$\frac{M_t}{M_{trans}} = \left(1 + k\sqrt{t}\right)\left(1 - exp\left[-7.3\left(\frac{Dt}{h^2}\right)^{0.75}\right]\right) \quad (1)$$

where M_{trans} and D are the equilibrium moisture uptake level and diffusion coefficient associated with uptake in the first stage as shown in the schematic in Figure 4-1, k is a time dependent coefficient characteristic of the rate of polymer relaxation and second stage damage due to the moisture absorbed and h is the thickness of the specimen.

The second stage in Figure 4-2 is associated with slower relaxation processes, as polymer chains slowly rearrange in the presence of penetrants, with the uptake in this stage being due to coupling of diffusion and macromolecular relaxation. Moisture parameters, including the level of M_{trans}, which indicates the level of transition uptake between Stage I and Stage II, for the resin are listed in Table 4-2 with a comparison of experimental data with results based on the use of Equation (1) shown in Figure 4-3. As seen from Table 4-2 and Figure 4-3, there is very small

variation in the level of M_{max} at the end of the time period, with similar levels being obtained at all three temperatures of immersion, suggesting a common threshold that is attained faster by elevating the temperature of immersion. As is noted later in the paper, the three composites do not show this similarity in attainment due to differences in mechanisms at the fiber–matrix interphase and at the intra- and interlaminar levels.

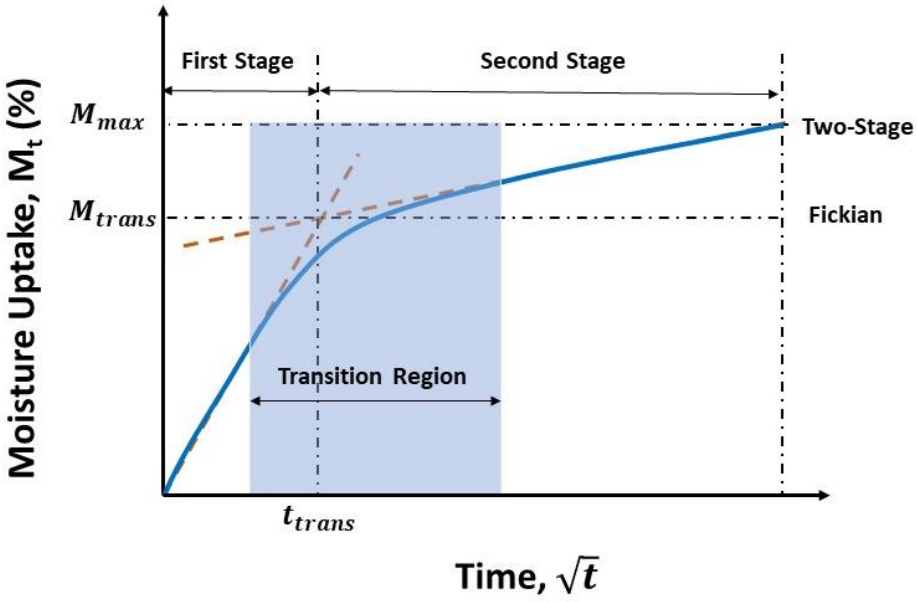

Figure 4-2. *Schematic of moisture uptake curves and stages following different models.*

Table 4-2. *Moisture uptake parameters for resin.*

Temperature of Immersion (℃)	**D_r (x 10^{-7} mm^2/s)**	**k_r (x 10^{-4} mm^2/s)**	**M_{trans} (%)**	**M_{max} (%)**
23	1.04	0.280	3.274	4.338
37.8	3.77	0.236	3.435	4.496
60	25.4	0.216	3.532	4.546

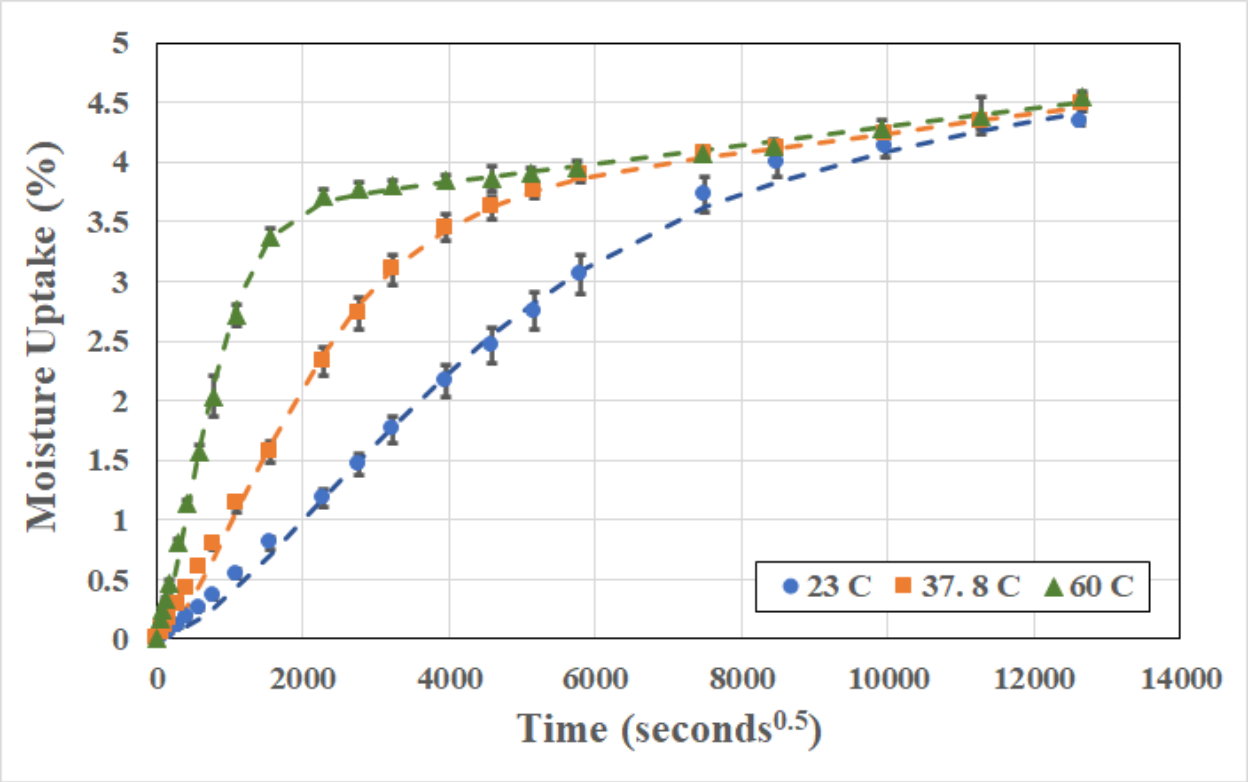

Figure 4-3. *Moisture uptake curves for resin specimens. Dashed lines indicate model predictions.*

As is expected the diffusion coefficient increases with temperature of immersion indicating early mass increase at high rates associated with classical Fickian processes in stage I with more complex interactions due to hydrolysis and relaxation-based processes including an increase in network hydrophilicity and reduction in crosslink density in stage II resulting in the variation in values of *k*. The levels of M_{trans} and M_{max} are affected by the temperature of immersion further emphasizing the non-Fickian nature of uptake in line with [6] since strict Fickian diffusion should result in the same saturation level, M_{max}, irrespective of immersion temperature.

In an attempt to compare moisture uptake in a resin to that in a composite formed of that resin, consideration has to be provided to the change in volume of resin through which diffusion occurs as well as the paths for uptake along fiber-matrix interfaces, network areas of change locally due to fiber interactions, and effects of tortuosity because of modified flow paths around fibers. In the current case since carbon fibers are effectively inert to influence of moisture, effects due to absorption into the fiber and changes in the fiber do not have to be considered. These effects in a two-stage model can be then differentiated based on differences between the "ideal" and "actual" diffusion and relaxation/deterioration coefficients. In the case of unidirectional composites wherein diffusion is direction dependent Shen and Springer [21] drew an analogy from heat conduction to express diffusivity in a unidirectional composite in a direction normal to the fibers, D_N, as:

$$D_N \cong \left(1 - 2\sqrt{\frac{V_f}{\pi}}\right) D_r + \frac{D_r}{B_D}\left[\pi - \frac{4}{\sqrt{1-\left(\frac{B_D^2 V_f}{\pi}\right)}}.\tan^{-1}\left(\frac{\sqrt{1-B_D^2 V_f/\pi}}{\sqrt{1+B_D^2 V_f/\pi}}\right)\right] \tag{2a}$$

where

$$B_D = 2\left(\frac{D_r}{D_f} - 1\right) \tag{2b}$$

and the diffusivity in the composite parallel to the direction of the fibers, D_f, is given by the rule of mixtures as:

$$D_f = \left(1 - V_f\right)D_r + V_f D_f \tag{2c}$$

where D_r and D_f are the diffusivities in the resin and fiber, respectively, and V_f is the fiber volume fraction. Following Starink et al. [38] for the specific case where $D_f = 0$, the effective diffusivity in the composite can be expressed as

$$D_c = D_r\left[1 + \lambda\left(\frac{a}{b} + \frac{a}{c}\right)\sqrt{\frac{1-2\sqrt{V_f/\pi}}{1-V_f}}\right]^2 \tag{3}$$

where b and c are the planar dimensions of the moisture specimen, a is the thickness (h in equation 1) and $\lambda = 0.54$. Treating the relaxation coefficient in the same way and neglecting second order edge effects, moisture uptake in the composite can be determined through a combination of Equations (1) and (3) as:

$$\frac{M_t}{M_{trans}} = \left(1 + k_r\left[1 + \lambda\left(\frac{a}{b} + \frac{a}{c}\right)\sqrt{\frac{1-2\sqrt{V_f/\pi}}{1-V_f}}\right]^2\sqrt{t}\right)\left(1 - exp\left[-7.3\left(\frac{D_r\left[1+\lambda\left(\frac{a}{b}+\frac{a}{c}\right)\sqrt{\frac{1-2\sqrt{V_f/\pi}}{1-V_f}}\right]^2}{h^2}t\right)^{0.75}\right]\right) \tag{4}$$

Keeping in mind that the models used are approximations and do not account for interactions between fiber and matrix, changes in network structure and morphology due to moisture uptake, changes in reaction thermodynamics due to absorption (endothermic absorption resulting in an increase in uptake with temperature an exothermic with a decrease with temperature) as well as effects of tortuosity due to fiber entanglement and compaction, modification factors L_1 and L_2 are applied to the relaxation and diffusion coefficients of the resin, respectively, such that:

$$\frac{M_t}{M_{trans}} = \left(1 + L_1 k_r \left[1 + \lambda\left(\frac{a}{b} + \frac{a}{c}\right)\sqrt{\frac{1-2\sqrt{V_f/\pi}}{1-V_f}}\right]^2 \sqrt{t}\right)\left(1 - exp\left[-7.3\left(\frac{L_2 D_r\left[1+\lambda\left(\frac{a}{b}+\frac{a}{c}\right)\sqrt{\frac{1-2\sqrt{V_f/\pi}}{1-V_f}}\right]^2}{h^2} t\right)^{0.75}\right]\right) \quad (5)$$

The modification factors represent the specific changes in relaxation and diffusion characteristics over those that would be expected if a direct transition from resin to composite response, as represented by the inclusion of fiber volume fraction, were viable. This provides an assessment of interface and resin changes effected by temperature as differentiated from the bulk resin and fiber volume fraction modified bulk resin modified characteristics and provides a more thorough understanding of local response especially as affected by the fabric type, number of layers and compaction, and temperature of solution. Equation (5) effectively describes the response over the two regions and the transition zone between stage I and stage II uptake, and can be rewritten as

M_t= (Uptake due to diffusion dominated regime) + (Uptake due to relaxation and longer-term deterioration) + (Uptake in the transitional regimes) (6)

i.e.,

$$M_t = M_{trans}\left(1 - exp\left[-7.3\left(\frac{D_{eff}L_2 t}{h^2}\right)^{0.75}\right]\right)$$

$$+\ M_{trans}k_{eff}L_1\sqrt{t}$$

$$+\ M_{trans}\left(k_{eff}L_1\sqrt{t}\ \right)\left(-\ exp\left[-7.3\left(\frac{D_{eff}L_2 t}{h^2}\right)^{0.75}\right]\right) \quad (7a)$$

where:

$$D_{eff} \cong D_r\left[1 + \lambda\left(\frac{a}{b} + \frac{a}{c}\right)\sqrt{\frac{1-2\sqrt{V_f/\pi}}{1-V_f}}\right]^2 \quad (7b)$$

and

$$k_{eff} \cong k_r\left[1 + \lambda\left(\frac{a}{b} + \frac{a}{c}\right)\sqrt{\frac{1-2\sqrt{V_f/\pi}}{1-V_f}}\right]^2 \quad (7c)$$

The first term in equation (7a) represents Fickian diffusion whereas the second is that of longer-term relaxation/deterioration which as expected is linear in structure. When the relaxation term, k_{eff}, is zero the structure is basically that of Fickian diffusion. Thus, a comparison of the terms and of the diffusion and relaxation/ deterioration coefficients and deterioration modification factors L_1 and L_2 can be used to further understand differences, not just in moisture uptake and rates, but also in the extent of phenomena changing response from that of the matrix and/or the idealized composite.

Figures 4-4(a)-(c) show traces of moisture uptake experiments for the three composites (300/1, 300/2 and 600/2) over 3 temperatures of immersion each, along with the results from the use of equation (5), showing close correspondence between them. The increase in uptake level

with temperature confirms the trends reported earlier [29,31,34,39] in contrast to the temperature independence of equilibrium moisture content reported through shorter-term exposure [40] and on bulk resins rather than composites [41]. Values for the kinetic parameters for diffusion and relaxation/deterioration coefficients determined directly from resin data following Equations (7b) and (7c), respectively, as well as the final coefficients, determined through the use of Equation (4), are listed in Table 4-3.

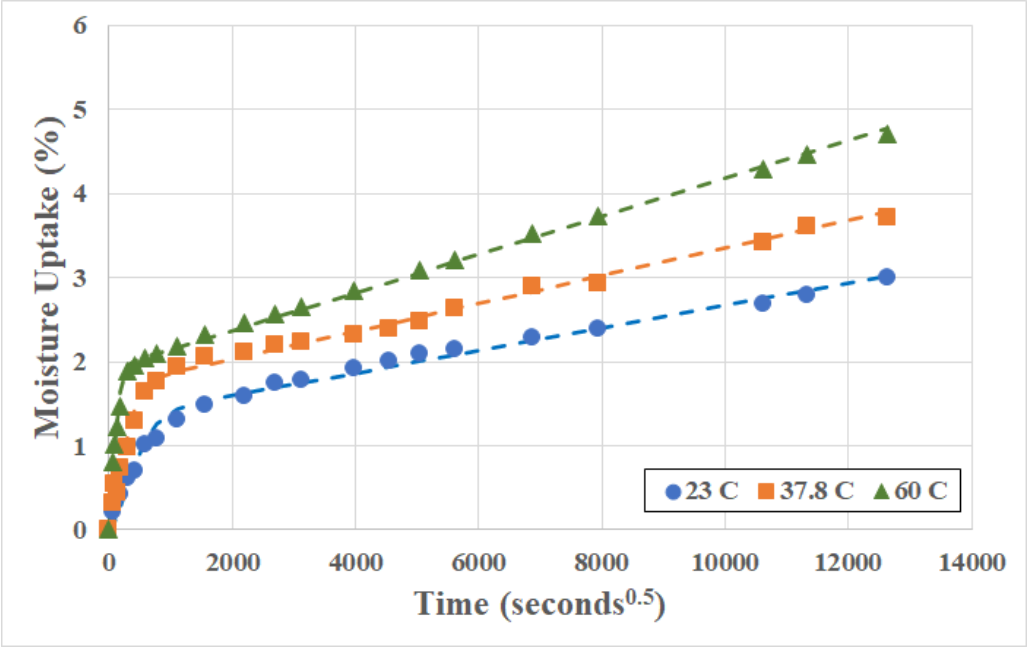

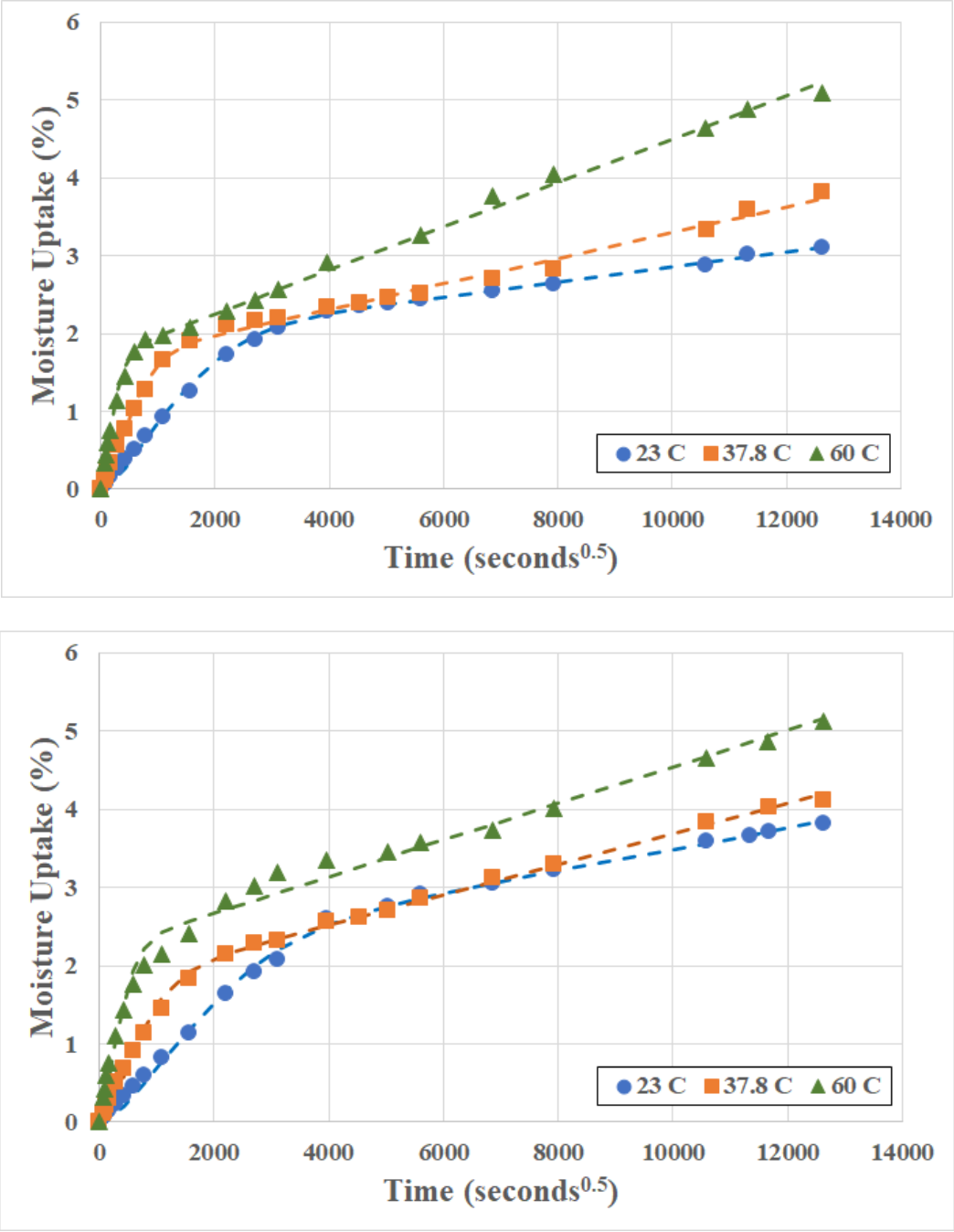

Figure 4-4. *Comparison of experimental data and model predictions for moisture uptake in composites: (a) 300/1 composite, (b) 300/2 composite, (c) 600/2 composite. Dashed lines indicate model predictions.*

Table 4-3*. Moisture kinetics parameters for the modified two-stage uptake process.*

Material	**Temperature of Immersion (℃)**	D_{eff} **(x 10^{-7} mm^2/s)**	k_{eff} **(x 10^{-4} mm^2/s)**	D **(=D_{eff} x L_2) (x 10^{-7} mm^2/s)**	k **(=k_{eff} x L_1) (x 10^{-4} mm^2/s)**	M_{trans} **(%)**	M_{max} **(%)**
300/1	23	1.089	0.293	1.648	1.015	1.326	3.008
	37.8	3.947	0.247	4.174	0.969	1.702	3.809
	60	26.59	0.226	28.41	1.172	1.922	4.702
300/2	23	1.130	0.304	0.585	0.507	1.893	3.102
	37.8	4.096	0.256	3.502	0.992	1.655	3.804
	60	27.60	0.234	19.18	1.667	1.686	5.083
600/2	23	1.158	0.311	0.593	0.647	2.116	3.812
	37.8	4.197	0.262	3.796	1.133	1.729	4.115
	60	28.28	0.240	14.01	1.163	2.202	5.115

As can be seen from Figure 4-4(a)-(c) and Tables 4-2 and 4-3 the maximum moisture uptake, M_{max} increases with temperature of immersion for all specimens. The uptake in the composites is less than that of the neat resin at the two lower temperatures but at the highest temperature of immersion the levels in the composite are higher which can be correlated to the additional deterioration which causes wicking along the fiber-matrix interface resulting also in a substantially increased diffusivity coefficient, *D.* It is of interest to note that the level of uptake

increases with increase in fiber volume fraction again indicative of additional uptake paths along the debonded fiber-matrix interface regions. The transition moisture content associated with the transition between stage I and stage II uptake, M_{trans}, is lower for the composites than for the resin at all temperature. Although mechanisms of desorption and extent were not assessed in the current investigation, it is important to note that the transition also signifies the change in dominant mode from free to bound water, since the second stage effects which occur after transition are largely due to the latter. As can be seen in Figure 4-5(a) the transition point is attained substantially earlier in the composites than in the resin with time to attain M_{trans} increasing with volume fraction and decreasing with temperature of immersion. The rate of increase with fiber volume fraction is the highest at 23℃ with the rates at the two higher temperatures being substantially lower, again indicating the complex interaction between the effects of cure progression and diffusion in the first stage. Earlier attainment indicates a shorter dominance of stage I type mechanisms.

Given the importance of the extent of each regime, it is also of interest to assess the ratio M_{trans}/M_{max} since it provides insight into the relative influence and lengths of the initial diffusion-dominated initial regime and the subsequent relaxation/deterioration based regime that has slower rates of uptake but represents a complex set of competing phenomena including longer-term hydrolysis of the resin, irreversible network changes, and deterioration through increase in size and extent of microcavities and fiber-matrix debonding. As seen in Figure 4-5(b) the ratio is independent of temperature in the case of resin as should be expected since the maximum uptake is similar with the uptake at the highest temperature of immersion being only 4.8% greater than that at the lowest, and the mechanisms in the network being expected to be similar. In the composites, however, the ratio is lower, decreasing with temperature of immersion and for majority of the specimens (except for the two layered specimens immersed in water at 23℃) being

between 0.41-0.45 suggesting a similarity in overall behavior and extent of the diffusion dominated regime. In the case of the two layered specimens the higher level for the lower volume fraction at the lowest temperature of immersion can be related to greater paths for uptake along fiber-matrix interface regions and local areas of resin inhomogeneity in cure which are obviated at the higher temperatures of immersion which have been noted previously to lead to further progression of cure [31,42,43].

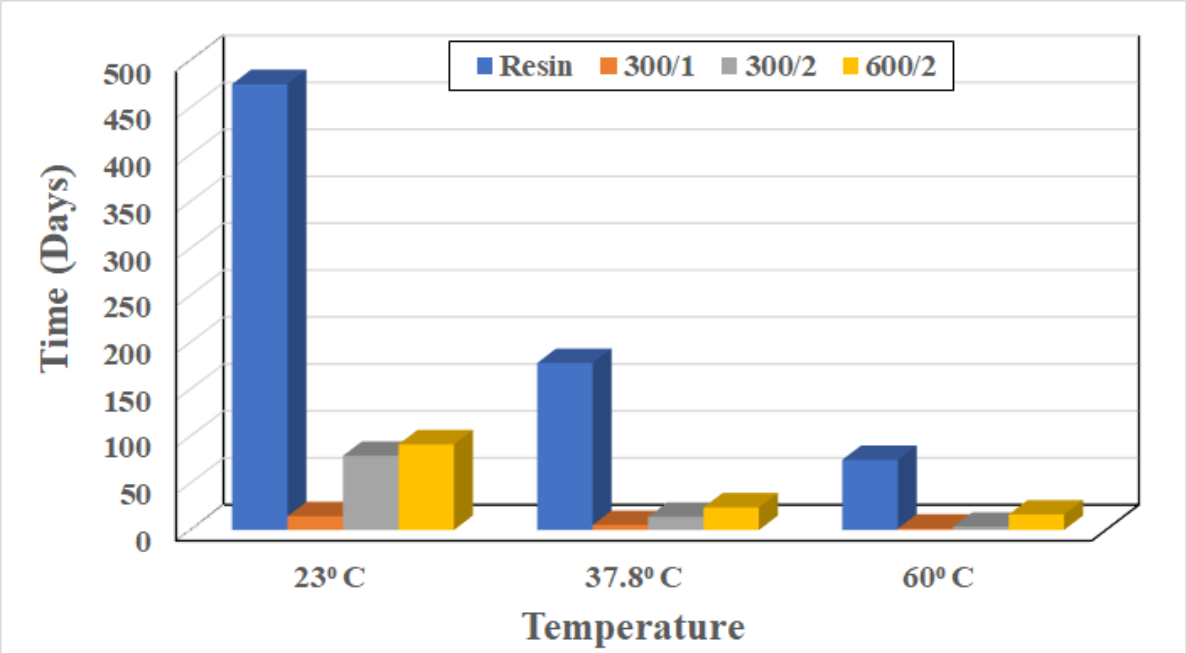

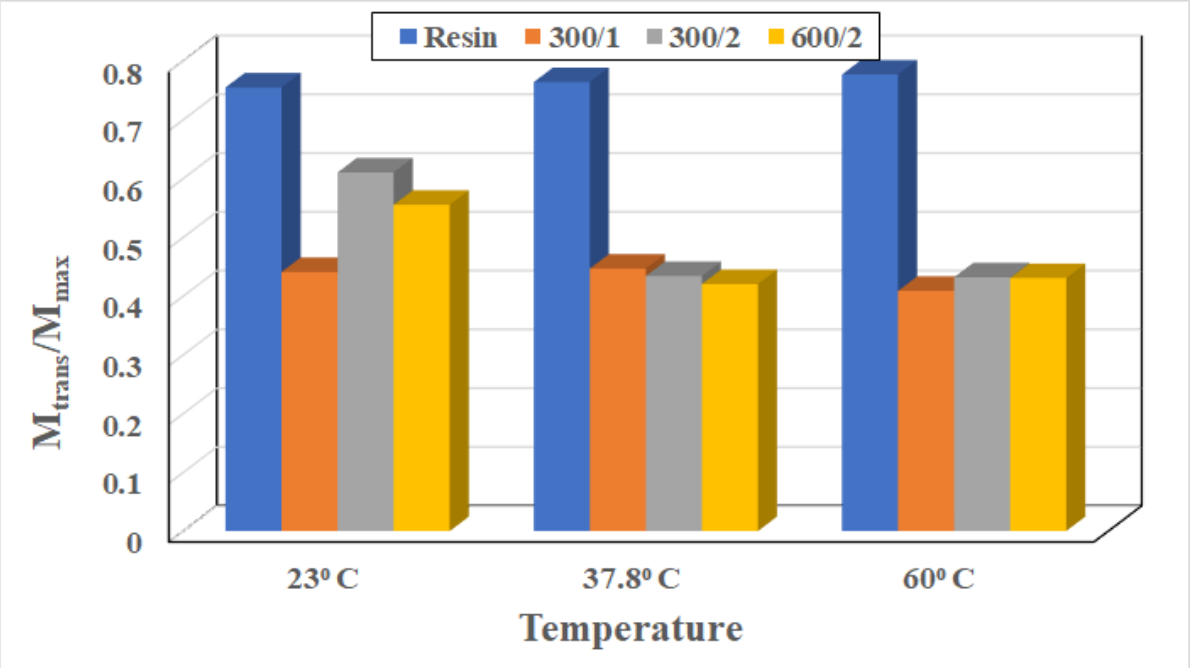

Figure 4-5. *(a). Time to transition as a function of material type and temperature of immersion. (b) Moisture transition ratio as a function of material type and temperature of immersion.*

As seen in Figure 4-2, uptake is characterized by the two parameters of M_{trans} and M_{max} and it is instructive to relate these to fundamental thermodynamic principles associated with heat of absorption, ΔH, when water uptake occurs in a polymer. Following van't Hoff's equation [44,45] the effect of temperature, T, on solubility (i.e., weight gain in this case) can be described by the change in enthalpy due to dissolution as

$$\frac{d\,ln(c_s)}{dT} = \frac{\Delta H}{RT^2} \tag{8a}$$

where c_s is the concentration at a point of equilibrium/threshold and R is the universal gas constant (=8.3143 J/mol K), and the heat of absorption is assumed to be constant over the temperature range used for moisture uptake experiments. Integrating equation (8a) we obtain

$$c_s = c_{s,ref}\, exp\left[\frac{-\Delta H}{R}\left(\frac{1}{T} - \frac{1}{T_{ref}}\right)\right] \quad (8b)$$

which can be rewritten as

$$c_s = c_{s0} exp\left(\frac{-\Delta H}{RT}\right) \quad (8c)$$

which is in the form of

$$M = A\, exp\left(\frac{-\Delta H}{RT}\right) \quad (8d)$$

where *M* is the uptake at equilibrium or the threshold level, and *A* is a temperature independent constant. Equation 8(d) indicates that for an endothermic reaction uptake due to absorption increases with temperature while it decreases with temperature in exothermic absorption. *ΔH* can be determined from the slope of the linear relation between *ln(M)* and *1/T* and values for the resin and 3 composites at the thresholds of M_{trans} and M_{max} are given in Table 4-4. As can be seen the heat of absorption is endothermic which is in line with results of increasing levels of uptake with temperature and respond with results determined for experiments conducted earlier by Apicella et al. [46] for Bisphenol A and B polyesters samples and their E-glass composites over a range of water immersion between 20 and 90℃, where the heats of absorption were 3.2 kJ/mol K and 5.98 kJ/mol K for the Bis A resin and its composite and 5.9 kJ/mol K and 10.9 kJ/mol K for the Bis B resin and its composite, respectively. Values at the level of M_{trans}, the equilibrium threshold for stage I absorption, are lower than those for the maximum uptake for all three composites.

Table 4-4. *Heat of Absorption at moisture uptake thresholds.*

Material	**Heat of Absorption (kJ/mol K)**	
	At M_{trans}	**At M_{max}**
Resin	1.65	1.0
300/1	8.04	9.81
300/2	2.39	10.95
600/2	1.34	6.62

The diffusion coefficient essentially represents the rate of uptake during the initial stage and thus serves as a useful indicator of overall response in Stage I. In all cases the diffusion coefficients of the composite specimens are higher than those of the unreinforced resin with the coefficients increasing with both time and fiber volume fraction indicating a temperature and interface-based rate response. The higher diffusion coefficients for the composite are in line with results reported earlier [40,47] and are largely due to fiber-matrix debonding which creates additional, and faster, paths for moisture uptake and interaction with the bulk resin. It should be emphasized that water absorbed into the composite results not just in plasticization of the resin but also microcavitation-type damage, including deterioration of fiber–matrix bonds and local bonds in the resin network. Both of these are irreversible and result in the formation of cavities that provide further volume for water uptake, i.e., a potential increase in free water content, which can lead to an increase in reactions with the polymer, causing enhanced molecular mobility of the epoxy molecules and disassociation of hydrogen bonds between the molecules of absorbed water and active sites in the epoxy network.

Given the complex interactions at play, especially as moisture uptake levels come close to the transition threshold, M_{trans}, it is of interest to assess the hypothetical values of the Fickian diffusion coefficient if M_{trans} were actually the level of equilibrium as seen in short-term response rather than a transition to the longer-term slower phenomena. In this case the diffusion coefficient can be determined from the initial slope of the uptake verses √t cure as

$$D_f = \pi \left(\frac{h}{4M_{f\infty}}\right)^2 \left(\frac{M_2 - M_1}{\sqrt{t_2} - \sqrt{t_1}}\right)^2 \tag{9}$$

where $M_{f\infty}$ is the short-term equilibrium level (= M_{trans}) and M_2 and M_1 are uptake levels at times t_2 and t_1, respectively. Results for D_f are shown in Figure 4-6 in comparison to the values of D using the two-stage model as well as equation (7b).

As can be seen all three characteristic measures of diffusion indicate an increase with temperature of immersion. D_{eff}, which is based directly on the resin characteristics represents the theoretically derived values accounting for the physical presence of fibers and use of edge correction but does not intrinsically account for moisture uptake effects such as wicking, debonding and network site-water reactions due to differential cure regimes, as expected indicates an increase in diffusivity with increase in fiber volume fraction. Fickian diffusion, which assumes a single set of uptake phenomena and a saturation point in the short-term, shows some variation with fiber volume fraction due to flow path tortuosity and compaction differences between layers but not the larger interaction with longer-term and relaxation/irreversible deterioration that is captured by the two-stage model emphasizing the inadequacy of the Fickian diffusion model for carbon fiber reinforced polymer matrix composites as mentioned earlier by Bone et al. [30] and indicating the need to more closely assess the complex and interacting phenomena even in Stage I

of the uptake. A measure of this can be approximated by estimation of permeability, which indicates the ease with which a fluid will flow through the material and can be determined as the product of *D* and *M*, following the general method reported in [7, 48], using the two thresholds of transition and end of the time period.

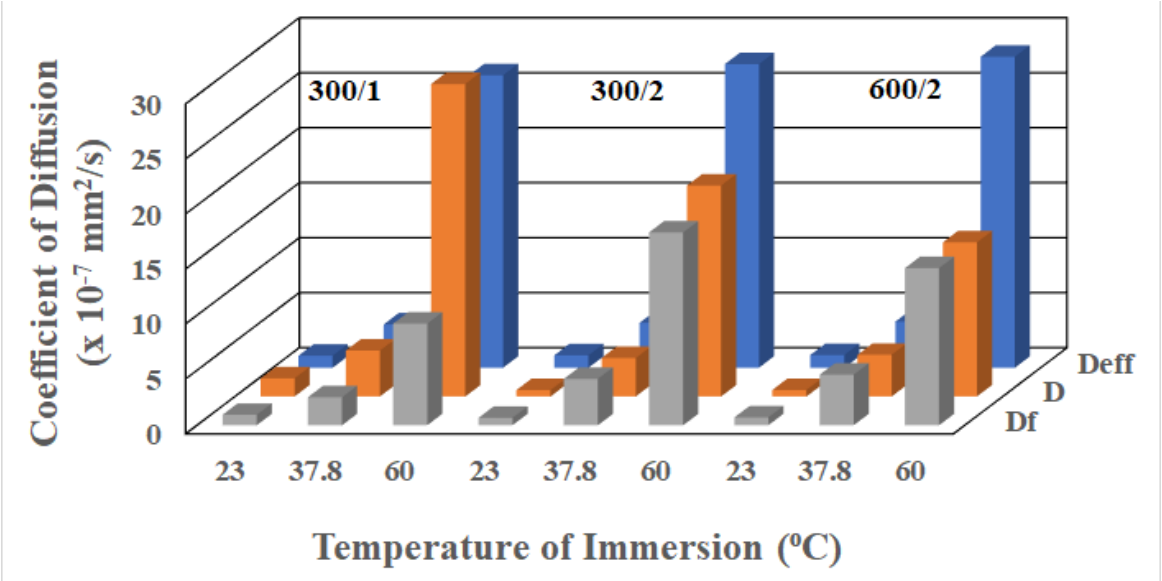

Figure 4-6. *Comparison of diffusion characteristics.*

Table 4-5 lists the permeabilities for the composites at the different temperatures of immersion at the two moisture uptake thresholds from which it can be seen that while the permeability for each composite increases with temperature, the relation across temperatures as a function of fiber volume fraction is more complex and is dependent on phenomena that take place at different stages of uptake. At the transition level the permeability at a given temperature is lower in the 2-layered composites than in the single-layered composite as would be expected with an increase in fiber volume fraction. However, the permeability for the lower weight fabric is lower than that with the higher weight fabric at the two lower temperatures due to greater integrity of the

interlaminar region between plies in this set. At the highest temperature, however, the fiber volume fraction effect, gained through intralaminar intermingling, dominates. This is repeated at the M_{max} threshold indicating that the effects are from Stage I phenomena rather than Stage II and are due to damage at the fiber-matrix interphase level and due to free, rather than bound, water.

Table 4-5. *Permeability in composites at moisture uptake thresholds.*

Composite	**Temperature of Immersion (℃)**	**Permeability (x 10^{-9} mm^2/s)**	
		At M_{trans}	**At M_{max}**
300/1	23	2.19	4.96
	37.8	7.09	15.89
	60	54.60	133.59
300/2	23	1.11	1.81
	37.8	5.79	13.35
	60	32.34	97.49
600/2	23	1.25	2.26
	37.8	6.56	15.62
	60	30.85	71.66

Since diffusion is a thermally activated process, a measure of the differences in phenomena can also be assessed through the use of an Arrhenius type relationship for the determination of activation energy, E_a, that must be overcome for moisture uptake [49]:

$$D = D_0 exp\left(\frac{-E_a}{RT}\right) \quad (10)$$

where D_0 is a temperature independent constant, R is the universal gas constant and T is the temperature of immersion on the Kelvin scale. Plotting $ln(D)$ v/s $(1/T)$ values of activation energies can be determined to be 71.02, 63.73, 76.78, and 69.06 kJ/mol K for the neat resin, single layered, and two-layered composites, respectively, indicating fairly close levels for the materials with the lowest being for the single layer composite. In general, the composites show a lower level of required activation energy due to the propensity for damage at the fiber-matrix interface level which results in wicking and capillary action. The higher level for the 300/2 composite is related to the increased compression between fiber layers leading to increased tortuosity as well as due to cure progression and local inhomogeneity as is discussed in the next section.

While the values of relaxation/deterioration coefficient determined following equation 7(c), k_{eff}, directly from the resin characteristics decreases with temperature and increases with fiber volume fraction, the experimentally determined second stage coefficient, k, for the composite for the most part increases with temperature, following trends reported earlier [29, 31], indicating increased molecular relaxation and damage with temperature of immersion. Given that the second stage is initiated at the threshold of the transition point, M_{trans}, (see Figure 4-2) it is of interest to assess the rate of change as a function of the extent of region II for the materials under consideration as

$$k = m\left(1 - \frac{M_{trans}}{M_{max}}\right) + k_0 \tag{11}$$

where the term $\left(1 - \frac{M_{trans}}{M_{max}}\right)$ represents the extent of the overall uptake which can be considered as being dominated by Stage II mechanisms. The slopes (rate of increase in k, as a function of extent of stage II uptake) determined as m = 2.79, 5.05, 4.0 and 3.44 for the resin, 300/1, 300/2 and 600/2 composites, respectively, show a decrease with increasing fiber volume fraction with

all being greater than that of the neat resin samples indicating the important role played by the presence of fibers in overall deterioration and relaxation in Stage II. The results further emphasize that water content has a similar effect to temperature on physical aging but with vastly different kinetics which is in line with results postulated earlier for unreinforced epoxies [50]. Arnold et al. [33] used a technique of removing long-term mass uptake and initial slow uptake to determine thew hypothetical Fickian behavior of carbon/epoxy composites exposed to 5 conditions of immersion and humidity. Using a similar technique, the response in Stage II uptake can be isolated to determine an effective coefficient of uptake in this stage. For the purposes of this assessment, we differentiate this characteristic from a diffusion coefficient since it is in the relaxation/deterioration regime. In this case the coefficient is determined between the uptake level of M_{trans} and M_{max} (i.e., $M_{f\infty}$ is M_{max}-M_{trans} in order to only consider Stage II response). And has to be considered in that vein as being a characteristic enabling assessment of relative behavior/rate of response with details shown in Figure 4-7.

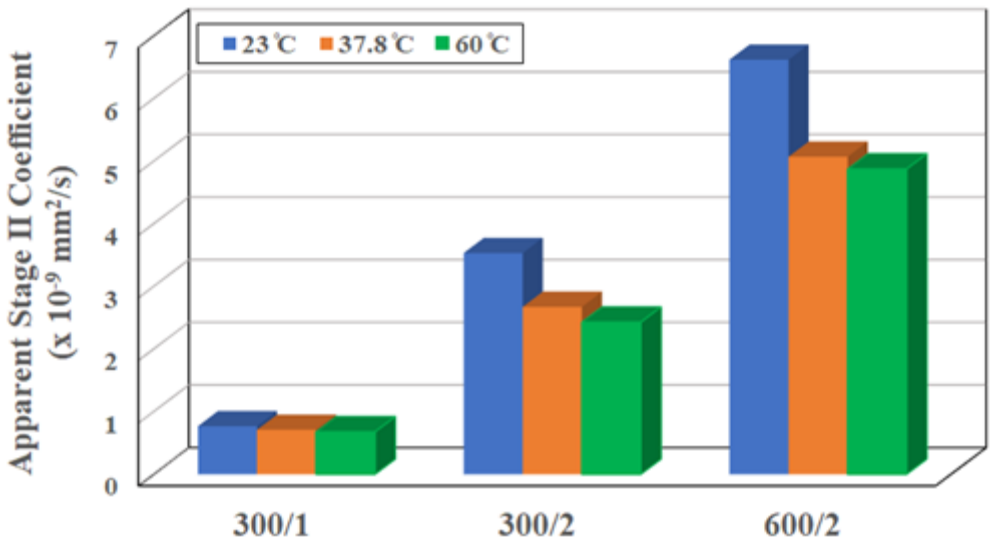

Figure 4-7. *Apparent stage II coefficients as a function of composite type and temperature of immersion.*

As can be seen, the apparent Stage II coefficient decreases with increasing temperature which can be related to increased cure progression and fiber-matrix deterioration resulting in less potential relaxation/creep type mechanisms at the higher temperatures. It is also of interest that the coefficient increases with fiber volume fraction which is in line with results reported by Papanicolaou et al. [51] using a hybrid viscoelastic interphase model to explain the change in interphase thickness with time and fiber loading. As the bulk resin between fibers and the fiber-matrix interphase region is affected by moisture uptake the relaxation increases, as determined directly through slope of the uptake curve, as discussed above.

4.3.2. CHARACTREIZATION OF GLASS TRANTION TEMPERATURE(T_g)

Moisture uptake is known to result in plasticization and reduction in the glass transition temperature through an increase in macromolecular mobility and weakening of hydrogen bonds in the network. The accurate determination, and prediction, of glass transition temperature is critical since it serves as a threshold for materials use in design, and in setting operational limits. It should be noted that in the case of epoxies and their composites cured under ambient, and moderate, temperature conditions, as is seen often in civil infrastructure rehabilitation and in naval/offshore repair, the degree of cure attained is less than 100% resulting in phases of partially reacted material within a more highly cross-linked network. These areas not only continue to cure over time but can also be affected by exposure to moisture with cure progression being initially accelerated by moisture [42,43] in conjunction with deteriorative phenomena such as moisture induced

plasticization, hydrolysis, saponification, fiber-matrix debonding and matrix micro-cavitation/microcracking making it difficult to isolate effects. For the purposes of the current investigation the T_g was determined from the peak of the loss tangent curve since this measure is independent of specimen dimensions and hence represents a material characteristic not affected by test setup [52]. Figures 4-8(a)-(c) shows the percentage change in T_g as a function of moisture content for the 3 composite specimens at 23, 37.8 and 60 ℃, from which it can be seen that response largely follows a two-stage process of an initial rapid decrease in T_g followed by a very slow and almost asymptotic regime at higher uptake levels corresponding to larger periods of immersion. The presence of an asymptotic regime was noted earlier [8, 9] through studies on epoxies wherein the T_g initially decreased with time of hygrothermal aging and then approached an asymptotic value with minor oscillations with the response being attributed to the effects of secondary crosslinking due to interactions of type II bound water with hydrophilic groups such as hydroxyls and amines. It should be noted that T_g depends on hygrothermal history and water-network interactions rather than solely on the presence of moisture. As pointed out earlier by Zhou and Lucas [6], type I bound water disrupts interchain Van der Waals forces and hydrogen bonds resulting in increased chain mobility and decreasing the glass transition temperature whereas type II water increases the T_g through the formation of a secondary cross-link network. This interaction and competition in effects results in cross link density approaching an asymptotic value over time and is hypothesized herein to result in the T_g approaching asymptotic values over extended periods of hygrothermal aging. Since DMTA testing was conducted only periodically with increasing intervals, it is not possible to accurately predict the threshold for the initiation of the slow change or asymptotic nature in the current study. However, the trends can clearly be seen in Figure 4-8 and further details are provided in Table 4-6. As can be seen from Figure 4-8, the decrease can be

described as a two-stage regime of an initial rapid drop transitioning to a slower decrease leading to an asymptotic level with some oscillation. The trend of an initial decrease followed by an increase and then a decrease to an asymptotic shown by specimens immersed in water at 23℃ relates to the progression of postcure as described through an earlier investigation on a similar system [31]. It can also be noted that at the higher temperatures of immersion the final state of the two layered specimens is similar and distinct from that of the single layered specimens which is due to the greater resin rich surfaces in the single layered specimens as compared to the interlaminar region in the two-layered specimens.

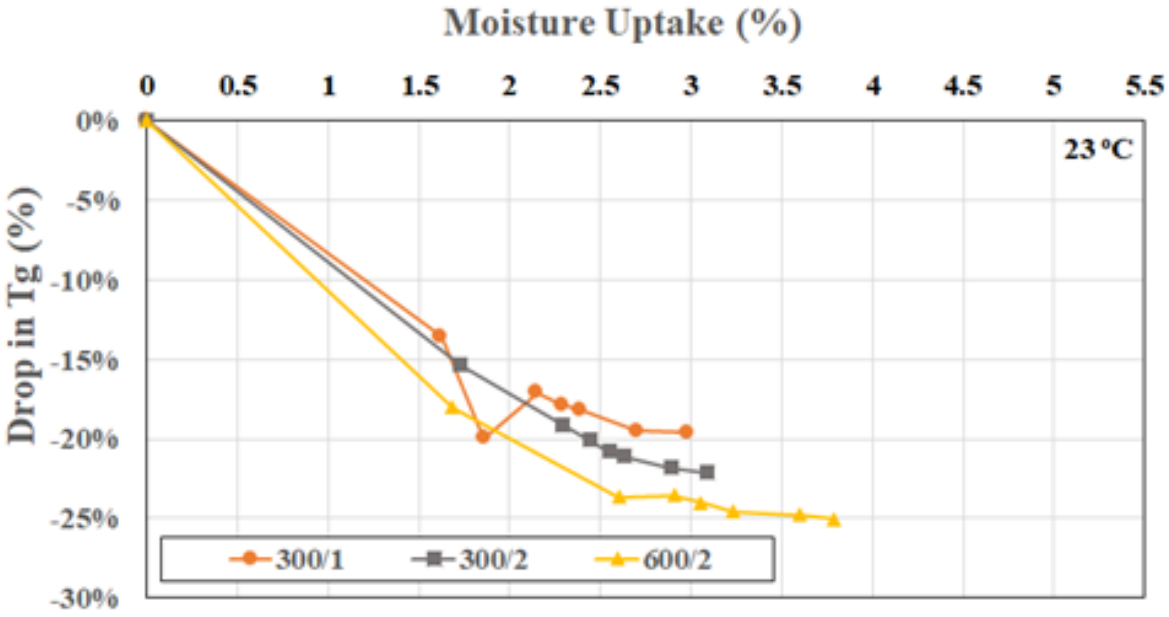

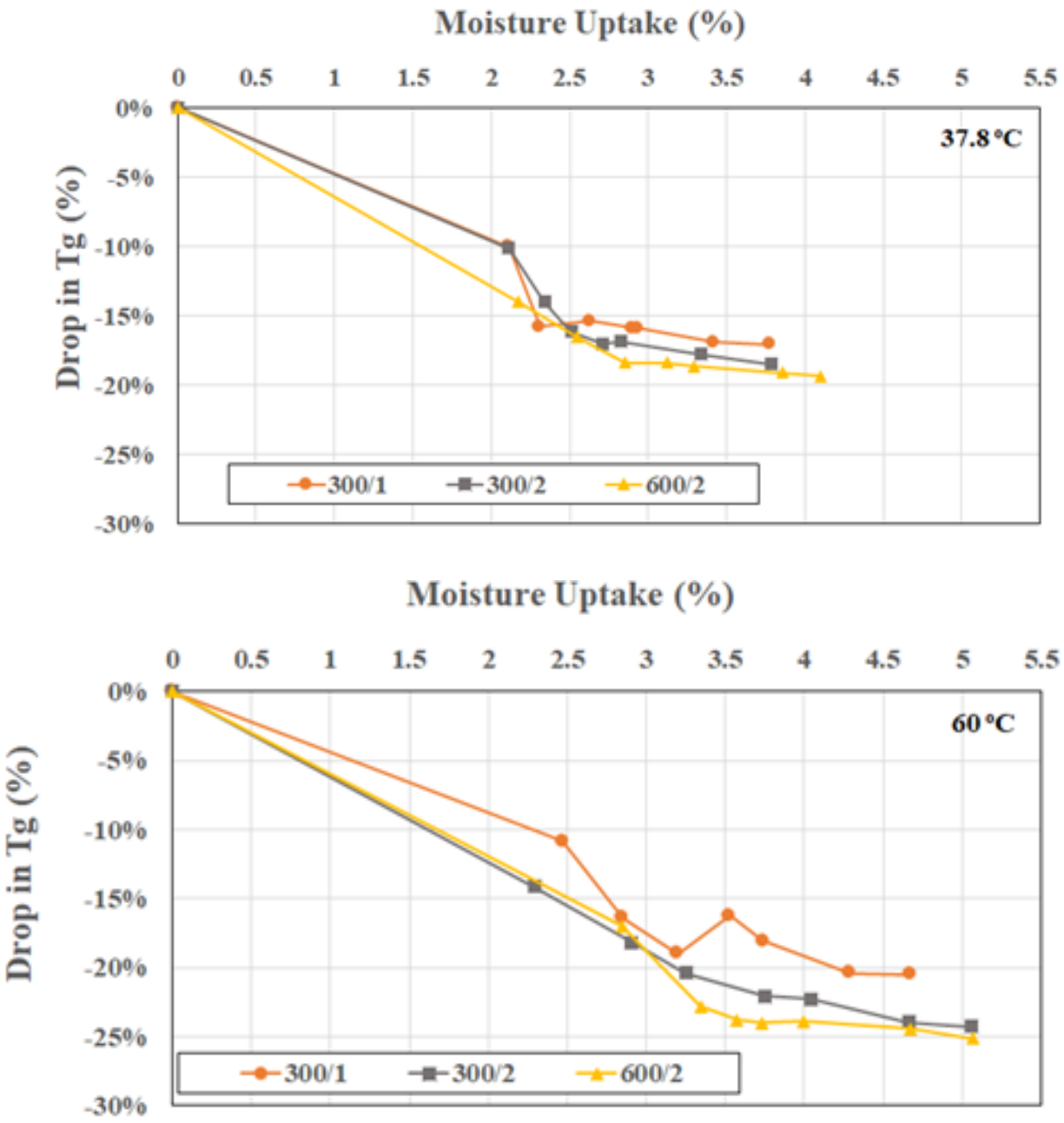

Figure 4-8. *Drop in T_g with increase in moisture uptake (a) Specimens immersed in water at 23 ℃, (b) Specimens immersed in water at 37.8 ℃, (c) Specimens immersed in water at 60 ℃.*

Table 4-6. *Characteristics Associated with T_g changes because of hygrothermal aging.*

Temperature of Immersion (℃)	**Composite**	**% drop in T_g at 60 months**	**Drop in T_g per % Moisture Uptake**
23	300/1	-19.6	6.82
	300/2	-22.1	6.95
	600/2	-25.0	6.37
37.8	300/1	-17.0	4.68
	300/2	-18.5	4.74
	600/2	-19.4	4.56
60	300/1	-20.5	4.55
	300/2	-24.3	4.65
	600/2	-25.1	4.38

It is of interest to compare the levels of decrease in T_g of the neat resin with those of the composites to assess the effects of the presence of fibers and inter- and intralaminar regions between layers and the consequent fiber- and interphase-related phenomena. Xian and Karbhari [35] reported drops of 23.9%, 15.2%, and 18.5% for the resin after immersion in water at the three temperatures of 23, 37.8, and 60 ˚C, respectively, for two years. At similar periods of time, the drop in the 300/1, 300/2, and 600/2 composites was 18.2%, 21.1%, and 24.6% after immersion in water at 23 ˚C, 15.9%, 16.8%, and 18.7% after immersion in water at 37.8˚C, and 18.1%, 22.3%, and 23.9% after immersion in water at 60 ˚C. The trend of the lowest drop being at the intermediate temperature of 37.8 ˚C is shown by the resin and all three composites and is thought to be linked to greater postcure that occurs at this temperature. This is also shown to a lesser extent at the highest temperature of immersion, in which the decrease is less than that due to immersion at 23 °C.

It is noted that theoretical models for the prediction of T_g based on moisture content such as the Gordon-Taylor model [53], the Kelley-Bueche model [54], the DiBenedetto equation [55] all show a decreasing trend for T_g with increasing moisture content but fail to predict the asymptotic regime. This is due to the complicated and competing macro- and micro-phenomena at play including as related to changes in the polymer network, viscoelastic response, and the interplay between free and bound water.

As can be seen in Table 4-6, the highest drop across all composites is at the highest temperature of immersion, with the reduction increasing with fiber volume fraction at each temperature of immersion, in line with effects expected due to fiber clusters, which can limit the extent of interphase percolation. As measured at the end of the 60-month period, the drop in glass transition temperature per percent of moisture uptake decreases with increasing temperature of immersion, with the maximum being 6.95 ºC/wt % of water for the 300/2 composite at the lowest temperature of immersion and 4.65 ºC/wt % of water at the highest temperature of immersion. However, given that the decrease approaches asymptotic levels over extended periods of immersion time, it is perhaps more instructive to determine the relation with moisture content at the threshold itself. For purposes of comparison, Figure 4-9 shows results for the drop per percent moisture uptake for the initial period, the 44-month period, which represents the beginning of the asymptote, and the 60-month level, which represents the end of the period of immersion.

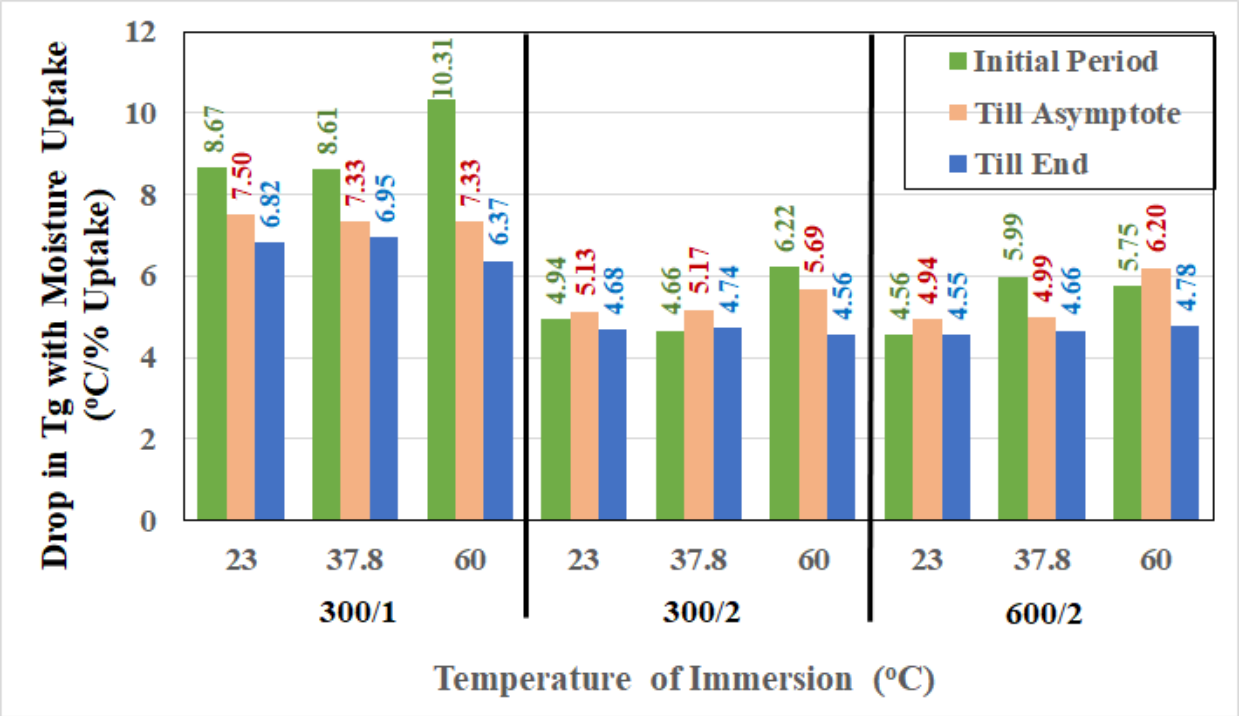

Figure 4-9. *Difference in change in T_g based on stage of moisture uptake.*

It should be noted that in some cases, especially for the two-layered composites, the asymptotic level is attained even prior to the 44-month level. The levels at both these periods are significantly lower than the decreases of 15℃ and 20℃ per percent of moisture uptake reported elsewhere [12, 56, 57]. It should be noted that T_g indicates a level of structural change between the glassy and rubbery regimes. Diffusion is affected by a combination of unoccupied molecular volume of the resin, free volume, and the polymer water affinity due to hydrophilic centers of the network. Increase in crosslink density results in decreased rates, and levels of moisture uptake and regions of high density can hinder further diffusion due, at least in part, to the inaccessibility of hydrogen bonding sites [18, 58] and thus it is expected that the attainment of a threshold in ambient cured materials in which cure progression is initially accelerated by immersion and temperature

will coincide with changes in the extent and rate of crosslink progression and transition in the two stages of uptake as described in the diffusion model used in this investigation.

4.3.3. CHARACTERIZATION OF FLEXURAL STRENGTH

Given that the study includes both single layered and two-layered composites, it is important to be able to test for residual characteristics a manner that would encompass both the interfacial reactions between the resin-rich surfaces on either side of the single reinforcement layer in the 300/1 specimens as well as the interlaminar phenomenon in the 2 layer (300/2 and 600/2) specimens in addition to keeping in mind that the use of the heavier fabric in the 600/2 case would result in greater fiber and bundle intermingling resulting in an increased interlaminar component. While the assessment of mechanisms between these is not the focus of this investigation the use of a single test to assess performance across those three types was critical and hence the 3-point flexure test incorporating both shear and bending components was selected. It should be noted that tensile tests while widely reported on in the literature are not ideal to assess resin and interface dominated effects such as would be expected through immersion for periods of time at different temperature in water since strength and modulus are fiber-dominated characteristics for unidirectional composites. The strength of the composite in three-point flexure is determined as:

$$\sigma_f = \frac{3PL}{2bh^2} \tag{12}$$

where P is the applied force, L is the support span and b and h are the width and thickness of the specimen. Results for flexure testing for the three materials as a function of time and temperature

of immersion are shown in Figures 4-10(a)-(c) from which it can be seen that strength retention can be described in terms of three stages- the first stage which has a rapid decrease in strength, followed by a more gradual and longer second stage, and the final stage where the drop over time is extremely slow and the performance appears to attain a near asymptotic regime. As can be seen from Figure 4-10 and Table 4-7, overall reductions over the 60-month period of immersion ranges from a low of 19.87% for the single-layered composite, 300/1, after immersion at 23 ◦C, to a maximum of 49.54% for the two-layered composite with the heavier fabric, 600/2, after immersion at 60 ◦C. It should be noted that the greater intralaminar phenomena in the heavier fabric leads to greater decreases when fiber–matrix interphases are deteriorated. Overall reduction increases with temperature J. Compos. Sci. 2023, 7, 447 18 of 23 of immersion and fiber volume fraction, with the latter effect being due to the increased surfaces for debonding, the initial drop, which is over a period of 2 months for the 300/1 and 300/2 composites and 4 months for the 600/2 composites, is related to effects of plasticization, noted earlier in terms of effect on glass transition temperature, and reported earlier [59,60]. The drop in glass transition temperature is less than that in flexural strength over the total period of study, suggesting that the water absorbed into the composite and found within the fiber–matrix interphasial region and accumulated in cracks and voids including within the debonded areas does not have as great an effect on glass transition as it does on the weakening of bonds, and thereby on flexural strength, as noted earlier by Bone et al. [30].

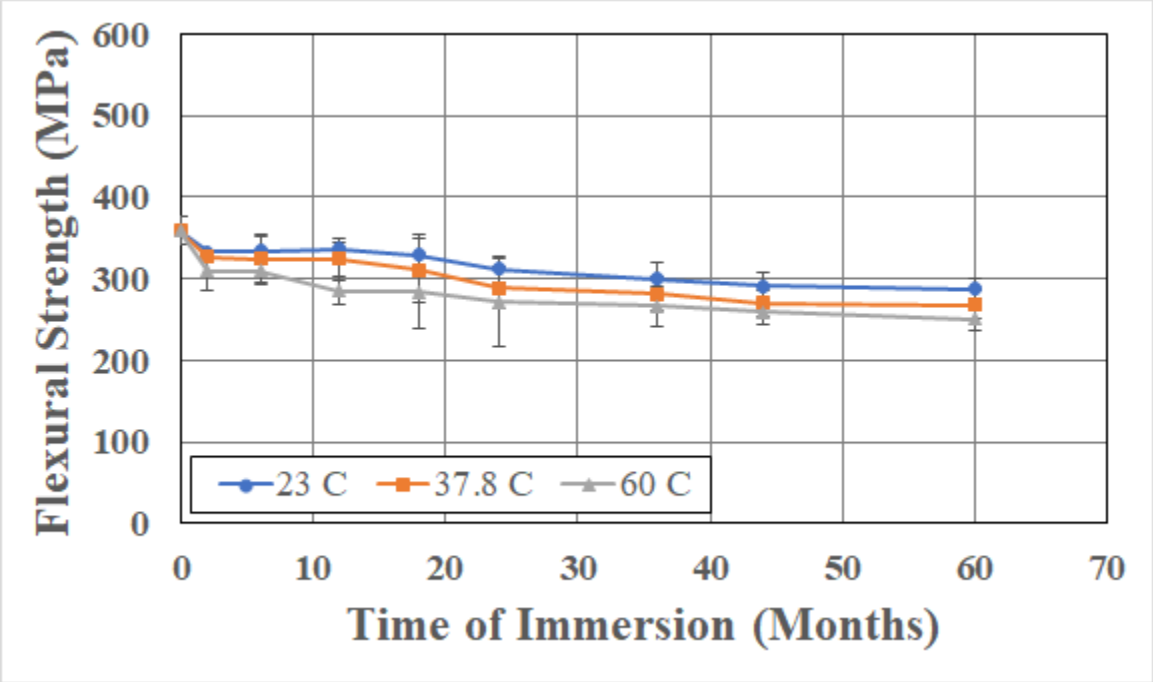
Flexural Strength (MPa)
600
500
400
300
200
100
0
23 C
37.8 C
60 C
0
10
20
30
40
50
60
70
Time of Immersion (Months)

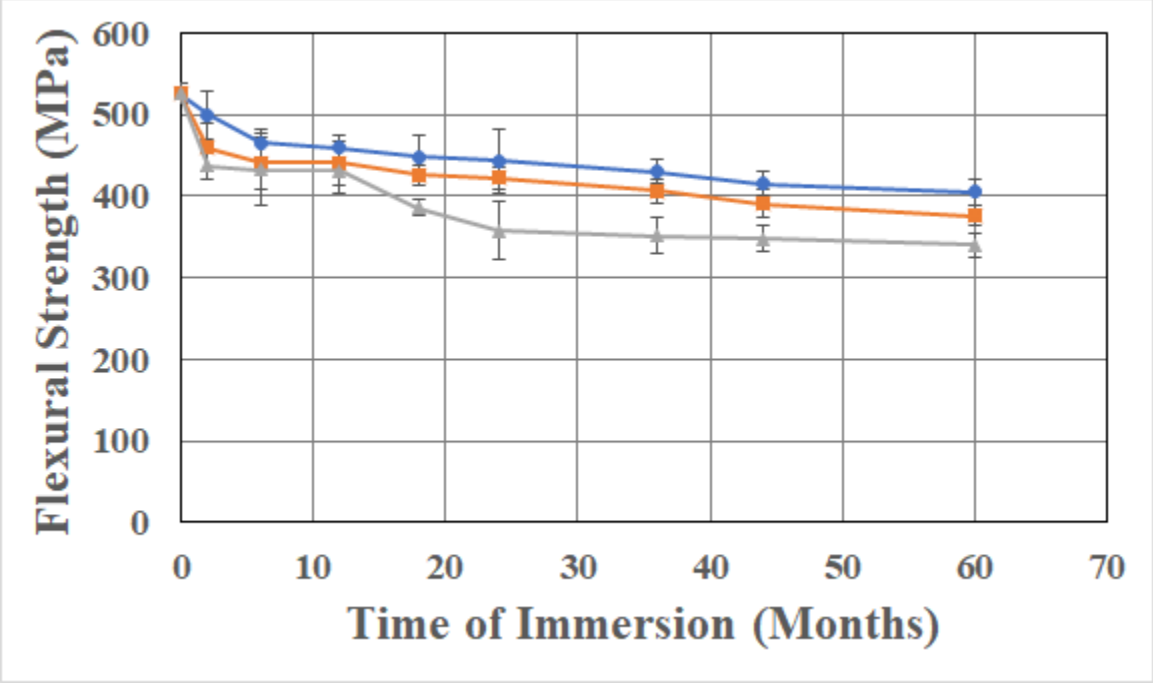
Flexural Strength (MPa)
600
500
400
300
200
100
0
0
10
20
30
40
50
60
70
Time of Immersion (Months)

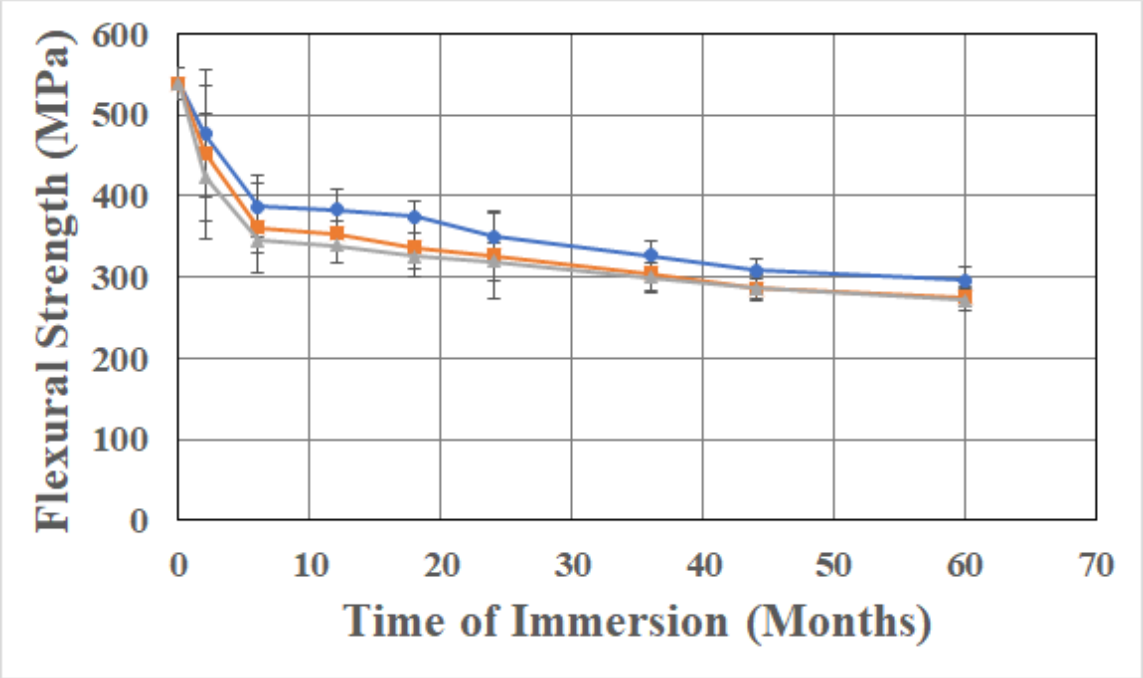

Figure 4-10. *Effect of time and temperature of immersion on flexural strength: (a) 300/1 composite, (b) 300/2 composite, (c) 600/2 composite.*

Table 4-7. *Percentage (%) decrease in flexural strength.*

Composite	**Temperature of Immersion (℃)**	**Time Period Under Consideration**		
		2 Months	**4 months**	**60 months**
300/1	23	7.27	6.69	19.87
	37.8	8.84	9.54	25.22
	60	13.60	13.78	30.15
300/2	23	5.02	11.57	22.98
	37.8	12.72	16.07	28.57
	60	16.85	17.75	32.25
600/2	23	11.55	28.19	44.98
	37.8	15.99	32.98	48.95
	60	21.39	35.93	49.54

The two-layered composites also show a greater level of reduction than the single layered composite, highlighting the effect of moisture uptake on the interlaminar region formed between adjacent layers of fabric, which, as noted earlier, results in a greater decrease in the glass transition temperature as well.

It is also of interest to note that the composites with the heavier fabric showed the greatest drop in both glass transition temperature and flexural strength indicating a level of correlation between the two characteristics, which can be further compared in Figure 4-11.

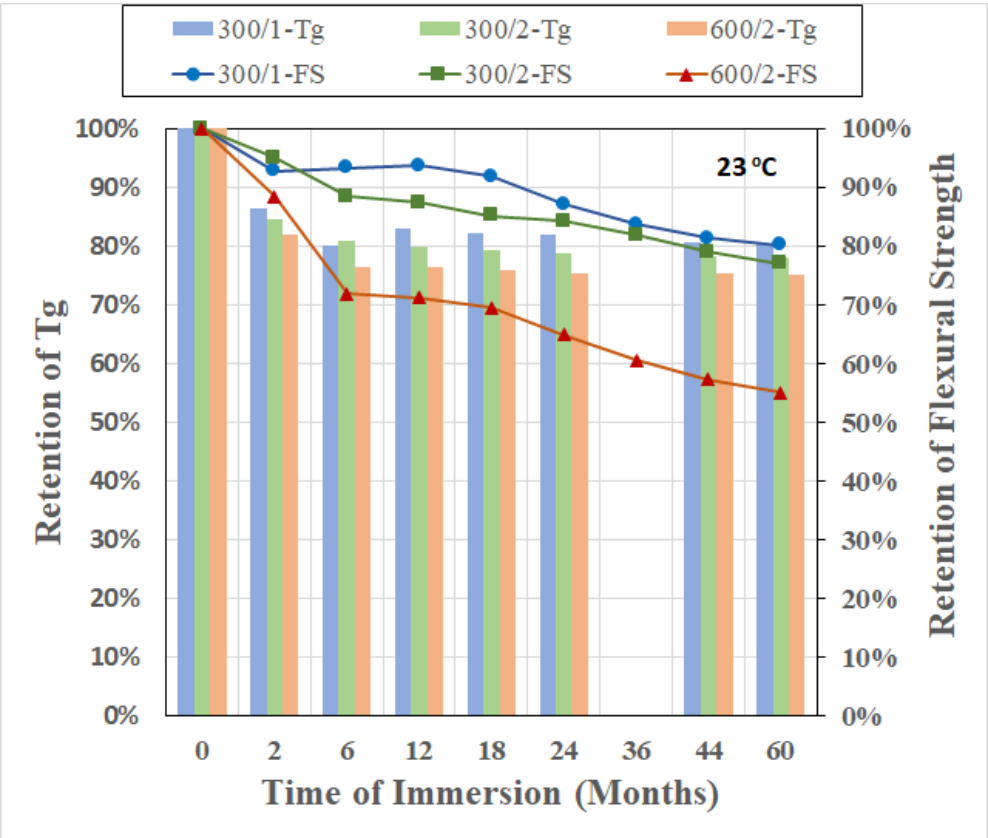
300/1-Tg
300/2-Tg
600/2-Tg
300/1-FS
300/2-FS
600/2-FS
23 °C
Retention of Tg
Retention of Flexural Strength
100%
90%
80%
70%
60%
50%
40%
30%
20%
10%
0%
0
2
6
12
18
24
36
44
60
Time of Immersion (Months)

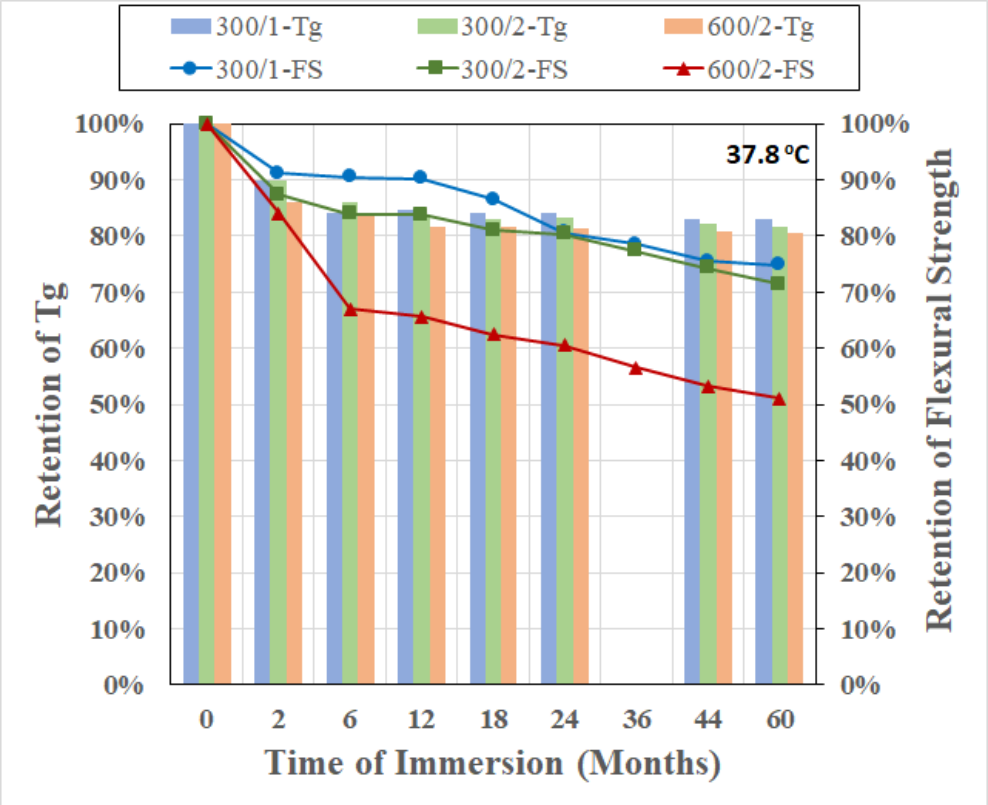
300/1-Tg
300/2-Tg
600/2-Tg
300/1-FS
300/2-FS
600/2-FS
37.8 °C
Retention of Tg
Retention of Flexural Strength
100%
90%
80%
70%
60%
50%
40%
30%
20%
10%
0%
0
2
6
12
18
24
36
44
60
Time of Immersion (Months)

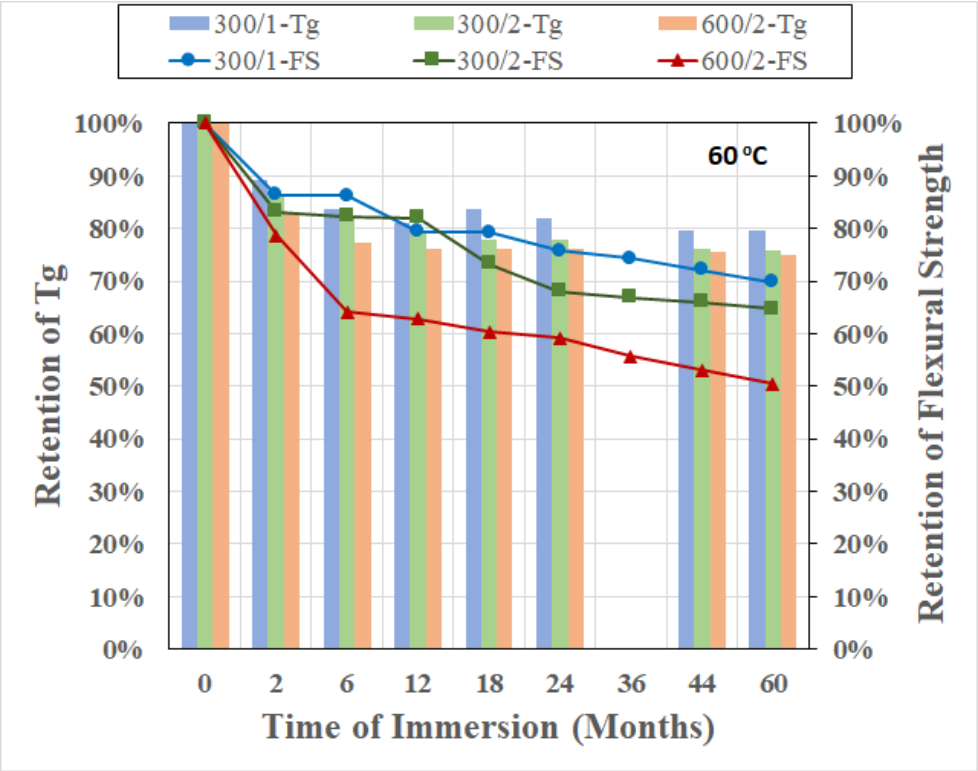

Figure 4-11. *Correlation of retention in T_g and flexural strength as a function of time of immersion: (Immersed in water at 23 ◦C, (b) immersed in water at 37.8 ◦C, (c) immersed in water at 60 ◦C.*

As can be seen for both, the overall response can be considered to fall into three regions. In the first, which is dominated by rapid moisture uptake by diffusion, there is a rapid drop in both characteristics, initiated by plasticization. The second region, which is the transition between the diffusion dominated and longer-term relaxation dominated regimes, is characterized by water bound at the interface and free water accumulating in cracks at the interlaminar level, resulting in a slow but steady reduction in both T_g and flexural strength. Changes in this region are dominated by interphasial phenomena as reported earlier by Guloglu et al. [61]. The third stage is one where the glass transition temperature reaches an asymptotic level and further reduction in flexural

strength is extremely slow with the regime being one where diffusivity has a much reduced effect as water transport is not rate limiting as suggested earlier by Bone et al. [30], suggesting that a more comprehensive model for performance prediction as a function of long-term moisture exposure (and uptake) could be developed through separate consideration of the three regions and consideration of the different effects of free and bound water and level of interphasial (including interlaminar) damage.

4.4. SUMMARY AMD CONCLUSIONS

The moisture uptake response of wet layup ambient cure processed carbon epoxy composites used in the rehabilitation of civil infrastructure and in naval/offshore structures is shown to be described by a two-stage model incorporating a diffusion-dominated regime, a longer-term regime wherein the primary considerations are those of material relaxation/deterioration and water transport is not rate-limiting, and a transition regime between them. Moisture uptake in the composites measured over extended periods of time exceeding five years after immersion in water at 23 and 37.8 ◦C is lower than that in the unreinforced resin but is greater at the highest temperature of immersion of 60 ◦C, suggesting that mechanisms change with temperature and that this needs to be further considered in the design of accelerated aging tests.

Glass transition temperature (T_g) is noted to initially decrease with increasing moisture content, with an initial stage exhibiting a rapid decrease in T_g, followed by a slower regime with some oscillation including increase as a result of postcure, and then an asymptotic regime at higher uptake levels. The greatest decrease in T_g occurs at the highest immersion temperature, and the decline becomes more apparent with an increase in the fiber volume fraction at each immersion temperature, which can be attributed to the effects of secondary crosslinking due to interactions of

bound water with hydrophilic groups. In a similar fashion, but at significantly higher levels of overall deterioration, changes in flexural strength behavior of the composites is also described by three distinct stages: a rapid decline in strength due to diffusion-driven moisture uptake and plasticization, a transition to a relaxation-dominated regime leading to gradual decreases in both glass transition temperature and flexural strength, and, finally, T_g approaching an asymptotic level with extremely gradual reduction in flexural strength. Additionally, composites with a higher fabric weight exhibited the most significant decline in both T_g and flexural strength, indicating a noteworthy correlation between these two characteristics due to increased deterioration at the interphasial and intralaminar regions. The correlation of regimes and levels of deterioration provides a basis for continued research into correlating increases in moisture content with degradation at the interface levels and through interaction between absorbed water molecules and the polymer network, since both flexural performance and glass transition temperature are affected in similar fashion. The development of an integrated model based on mechanistic principles at the micro- and macromechanical levels provides a potential means of not just more accurate predictions of long-term performance but also of better design parameters for ensuring efficient and durable design of composite systems. Further, the deviation in response between the two lower temperatures of immersion and the highest, albeit still below the wet glass transition, temperature provides caution for the use of higher-temperature exposure as a means of shortening periods of evaluation through accelerated testing. In order to develop a comprehensive model for prediction of long-term durability based on constituent materials and exposure conditions, further research into changes at the level of fiber–matrix bond degradation that results in wicking as well as changes in resin network and morphology is needed in addition to a more complete assessment of moisture-related plasticization and postcure phenomena which affect both uptake and glass transition

temperature. The incorporation of these changes into a single model is the focus of ongoing research.

4.5. REFERENCES

1. Spelter A; Bergmann S; Bielak J; Hegger J. Long-term durability of carbon reinforced concrete. An overview and experimental investigation. Applied Sciences, **2019**, 9, 1651-1665.

2. Karbhari VM; Abanilla MA. Design factors, reliability, and durability prediction of wet layup carbon/epoxy used in external strengthening. Composites B, **2007**, 38(1), 10-23.

3. Abanilla MA; Karbhari VM; Li Y. Interlaminar and intralaminar durability characterization of wet layup carbon/epoxy used in external strengthening. Composites B, **2006**, 37(7/8), 650-661.

   Abanilla MA; Li Y; Karbhari, VM. Durability characterization of wet layup graphite/epoxy composites used in external strengthening. Composites B, **2005**, 37(2/3), 200-212.

5. Adamson MJ. Thermal expansion and swelling of cured epoxy resin used in graphite/epoxy composite materials. Journal of Materials Science, **1980**, 15, 1736–45.

6. Zhou, J; Lucas, J.P. Hygrothermal effects of epoxy resin. Part I: The nature of water in epoxy. Polymer **1999**, 40, 5505–5512.

7. Nogueira, P.; Ramirez, C.; Torres, A.; Abad, M.J.; Cano, J.; Lopez, J.; Lopez-Bueno, I.; Barral, L. Effect of water sorption on the structure and mechanical properties of an epoxy system. J. Appl. Polym. Sci. **2001**, 80, 71–80.

8. Xiao GZ; Shanahan MER. Swelling of DGEBA/DDA epoxy resin during hygrothermal aging. Polymer, **1998**, 39, 3253-3260.

9. De'Nève B; Shanahan MER. Water absorption by an epoxy resin and its effect on the mechanical properties and infra-red spectra. Polymer, **1993**, 34(24), 5099–105.

10. Hahn, H.T. Residual stresses in polymer matrix composite laminates. Journal of Composite Materials. **1976**, 10, 266–278.

11. Xiao, G.Z.; Delmar, M.; Shanahan, M.E.R. Irreversible interactions between water and DGEBA/DDA epoxy resin during hygrothermal aging. J. Appl. Polym. Sci. **1977**, 65, 449–458.

12. Chateauminois, A.; Chabert, B.; Soulier, J.P.; Vincent, L. Dynamic-mechanical analysis of epoxy composites plasticized by water—Artifact and reality. Polym. Compos. **1995**, 16, 288–296.

13. Abanilla, M.A.; Li, Y.; Karbhari, V.M. Interlaminar and intralaminar durability characterization of wet layup carbon/epoxy used in external strengthening. Compos. B **2006**, 37, 650–661.

14. Mazor, A.; Broutman, L.J.; Eckstein, B.H. Effect of long-term water exposure on the properties of carbon and graphite fiber reinforced epoxies. Polym. Eng. Sci. **1978**, 18, 341–349.

15. Costa ML; Almeida SFM de; Rezende MC. Hygrothermal effects on dynamic mechanical analysis and fracture behavior of polymeric composites. Materials Research. 2005, 8(8), 335–340.

16. Apicella, A.; Nicolais, L.; de Cataldis, C. Characterization of the morphological fine structure of commercial thermosetting resins through hygrothermal exposure. Adv. Polym. Sci. **1985**, 66, 189–207.

17. Apicella, A.; Tessieri, R.; de Cataldis, C. Sorption modes of water in glassy epoxies. J. Membr. Sci. **1984**, 18, 211–225.

18. Moy, P.; Karasz, F.E. Epoxy-water interactions. Polym. Eng. Sci. **1980**, 20, 315–319.

19. Pethrick, R.A.; Hollins, E.A.; McEwan, L.; Pollock, A.; Hayward, D.; Johncock, P. Effect of cure temperature on the structure and water absorption of epoxy/amine thermosets. Polym. Int. **1996**, 39, 275–288.

20. Crank J. The Mathematics of Diffusion. Cambridge University Press, NY, **1975**.

21. Shen, C.-H.; Springer, G.S. Moisture absorption and desorption of composite materials. J. Compos. Mater. **1976**, 10, 2–20.

22. Boll DJ; Bascom WD; Motiee B. Moisture absorption by structural epoxy-matrix carbon-fiber composites. Composites Science and Technology. **1985**, 24(4), 253–273.

23. Shirrell CD. Diffusion of water vapor in graphite/epoxy composites. In ASTM STP 658, Advanced Composite materials – Environmental Effects. American Society for Testing and Materials, Philadelphia, PA, **1977**, 21-42.

24. Neumann S; Marom G. Stress dependence of the coefficient of moisture diffusion in composite materials. Polymer Composites, **1985**, 6(1), 9–12.

25. Berens, A.R.; Hopfenberg, H.B. Diffusion and relaxation in glassy polymer powders: 2 Separation of diffusion and relaxation parameters. Polymer **1978**, 19, 489–496.

26. Bagley, E.; Long, F.A. Two-stage sorption and desorption of organic vapors in cellulose acetate. J. Am. Chem. Soc. **1955**, 77, 2172–2182.

27. Peppas NA, Sahlin JJ. A simple equation for the description of solute release. III. Coupling of diffusion and relaxation. International Journal of Pharmaceutics. **1989**, 57, 169-172.

28. Carter HG; Kibler KG. Langmuir-type model for anomalous moisture diffusion in composite resins, Journal of Composite Materials, **1978**, 12, 118-131.

29. Bao, L.-R.; Yee, A.F.; Lee, C.Y.-C. Moisture absorption and hygrothermal aging in a bismaleimide resin. Polymer **2001**, 42, 7327–7333.

30. Bone, J.E.; Sims, G.D.; Maxwell, A.S.; Frenz, S.; Ogin, S.L.; Foreman, C.; Dorey, R.A. On the relationship between moisture uptake and mechanical property changes in a carbon fibre/epoxy composite. J. Compos. Mater. **2022**, 56, 2189–2199.

31. Karbhari, V.M. Long-term hydrothermal aging of carbon-epoxy materials for rehabilitation of civil infrastructure. Compos. A **2022**, 153, 106705, 12 pp.

32. Capiel G; Uicich J; Fasce D; Montemartini PE. Diffusion and hydrolysis effects during water aging on an epoxy-anhydride system. Polymer Degradation and Stability. **2018**, 153, 165–171.

33. Arnold JC; Alston SM; Korkees F. An assessment of methods to determine the directional moisture diffusion coefficients of composite materials. Composites A, **2013**, 55, 120–128.

34. Scott, P.; Lees, J.M. Water, saltwater and alkaline solution uptake in epoxy thin films. J. Appl. Polym. Sci. **2013**, 130, 1898–1908.

35. Xian, G.; Karbhari, V.M. Segmental relaxation of water-aged ambient cured epoxy. Polym. Degrad. Stab. **2007**, 92, 1650–1659.

36. Xian, G.; Karbhari, V.M. DMTA based investigation of hygrothermal aging of an epoxy system used in rehabilitation. J. Appl. Polym. Sci. **2007**, 104, 1084–1094.

37. Karbhari, V.M.; Hong, S.K. Effect of sequential thermal aging and water immersion on moisture kinetics and SBS strength of wet layup carbon epoxy composites. J. Compos. Sci. **2022**, 6, 306, 23 pp.

38. Starink MJ; Starink LMP; Chambers AR. Moisture uptake in monolithic and composite materials: edge correction for rectanguloid samples. Journal of Materials Science. **2002**, 37, 287-294.

39. Chaplin A; Hamerton I; Herman H; Meudhar AK; Shaw SJ. Studying water uptake effects in resins based on cyanate ester/bismaleimide blends. Polymer. 2000, 41(11), 3945-3956.

40. Chateauminois A; Vincent L; Chabert B; Soulier JP. Study of the interfacial degradation of a glass-epoxy composite during hygrothermal ageing using water diffusion measurements and dynamic mechanical thermal analysis. Polymer, **1994**, 35(22), 4766–4774.

41. McKague EL Jr; Reynolds JD; Halkias JE. Swelling and glass transition relations for epoxy material in humid environments. Journal of Applied Polymer Science. **1978**, 22(6), 1643-1654.

42. Ghorbel, I.; Valentin, D. Hydrothermal effects on the physico-chemical properties of pure and glass fiber reinforced polyester and vinylester resins. Polym. Compos. **1993**, 14, 324–334

43. Marshall, J.M.; Marshall, G.P.; Pinzelli, R.F. The diffusion of liquids into resins and composites. Polym. Compos. **1982**, 3, 131–137.

44. Bao L-R; Yee AF. Effect of temperature on moisture absorption in a bismaleimide resin and its carbon fiber composite. Polymer. **2002**, 43(14), 3987-3997.

45. Sandler SI. Chemical and Engineering Thermodynamics. Wiley, New York, **1999**.

46. Apicella A; Migliaresi C; Nicolais L; Iaccarino L; Roccotelli S. The water ageing of unsaturated polyester-based composites: influence of resin chemical structure. Composites. **1983**, 14(4), 387–392.

47. Mijovic J; Lin K-F. The effect of hygrothermal fatigue on physical/mechanical properties and morphology of neat epoxy resin and graphite/epoxy composite. Journal of Applied Polymer Science, **1985**, 30(6), 2527-2549.

48. Mouzakis DE; Kager-Kocsis J. Effects of gasoline absorption on the tensile impact response of HDPE/Selar^{TM} laminar microlayer composites. Journal of Applied Polymer Science. **1998**, 68(4), 561-569.

49. Crank J; Park GS. Diffusion in Polymers, Academic Press, London, **1968**.

50. Zheng Y; Priestley RD; McKenna GB. Physical aging of an epoxy subsequent to relative humidity jumps through the glass concentration. Journal of Polymer Science. B. Polymer Physics. **2004**, 42(11), 2107–2121.

51. Papanicolaou GC; Portan DV; Kontaxis LC. Interrelation between fiber-matrix interphasial phenomena and flexural stress relaxation behavior of a glass fiber-polymer composite. Polymers, **2021**, 13, 978, 16 pp.

52. Hagen R; Salmén ; Lavebratt H; Stenberg B. Comparison of dynamic mechanical measurements and Tg determinations with two different instruments. Polymer testing. **1994,** 13(2), 113–128.

53. Gordon M; Taylor MS. Ideal copolymers and the second-order transitions of the synthetic rubbers. I. Non-crystalline copolymers. Journal of Applied Chemistry. **1952**, 2(9), 493–500.

54. Kelley FN; Bueche F. Viscosity and glass temperature relations for polymer-diluent systems. Journal of Polymer Science. **1961**, 50, 549–556.

55. Pascault JP; Williams JJ. Glass transition temperature versus conversion relationships for thermosetting polymers. Journal of Polymer Science. B. Polymer Physics. **1990**, 28(1), 85–95.

56. Wright WW. The effect of diffusion of water into epoxy resins and their carbon-fibre reinforced composites. Composites. **1981**, 12(3), 201–205.

57. Barton JM; Greenfield DCL. The Use of dynamic mechanical methods to study the effect of absorbed Water on temperature-dependent properties of an epoxy resin-carbon fibre composite. British Polymer Journal. **1986**, 18(1), 51–56.

58. Vanlandingham MR; Eduljee RF; Gillespie Jr JW. Moisture diffusion in epoxy systems. Journal of Applied Polymer Science. **1999**, 71(5), 787–798.

59. Karbhari VM. Dynamic mechanical analysis of the effect of water on E-glass-vinylester composites. Journal of Reinforced Plastics and Composites. **2006**, 25(6), 631-644.

60. Tual N; Carrer N; Davies P; Bonnemains T; Lolive E. Characterization of seawater aging effects on mechanical properties of carbon/epoxy composites for tidal turbine blades. Composites A, **2015**, 78, 380-389.

61. Bone JE; Sims GD; Maxwell AS; Frenz S; Ogin SL, Foreman C; Dorey RA. On the relationship between moisture uptake and mechanical property changes in a carbon fibre/epoxy composite. Journal of Composite materials, **2022**, 56(14), 2189-2199.

62. Guloglu GE; Hamidi YK; Altan MC. Moisture absorption of composites with interfacial storage. Composites A, **2020**, 134, 105908.

CHAPTER 5. WATER, SALTWATER, AND CONCRETE LEACHATE SOLUTION EFFECTS ON DURABILITY OF AMBIENT-TEMPERATURE CURE CARBON-EPOXY COMPOSITES

This chapter contains a paper published in the Journal of Applied Polymer Science in 2022.

Karbhari VM, Hassanpour B. Water, saltwater, and concrete leachate solution effects on durability of ambient-temperature cure carbon-epoxy composites. Journal of Applied Polymer Science. 2022 Jul 15, 139(27), e52496. https://doi.org/10.1002/app.52496.

Water, saltwater, and concrete leachate solution effects on durability of ambient-temperature cure carbon-epoxy composites

Vistasp M. Karbhari | Behnaz Hassanpour

Department of Civil Engineering, Department of Mechanical & Aerospace Engineering, University of Texas at Arlington, Arlington, Texas, USA

Civil Engineering Research Foundation; Federal Highway Administration.

California Department of Transportation; SCCI

Abstract

Wet layup carbon epoxy composites are extensively used for rehabilitation of civil infrastructure. This study focuses on foundation building for understanding durability of such materials through long term (up to five years) hygrothermal aging in water, saltwater, and concrete leachate, solutions. Moisture uptake is described using a two-stage model incorporating diffusion and relaxation/deterioration parameters with the concrete leachate solution showing further transitions and the highest value of the relaxation/deteriorative coefficient. Glass transition temperatures decreased with an increase in moisture content reaching an initial minimum followed by fluctuations and small increases with an increase in the time of exposure. Immersion in concrete leachate results in the largest decrease. Tan d height shows an initial decrease followed by an increase and then a continued decrease indicative of initial plasticization and post-cure followed by deterioration at the resin and fiber-matrix levels. Although short-term response in mechanical properties shows differences with immersion in water having the least effect, solution type had

very little difference on residual mechanical characteristics at the end of the 60-month period of immersion. The results emphasize the need for further understanding of competing effects in ambient cured composites and of the need for longer term testing for determination of design factors.

KEYWORDS carbon fiber, degradation, epoxy, polymer matrix composites, solution

5.1. INTRODUCTION

Fiber reinforced polymer matrix composites are routinely used for the rehabilitation of aging and understrength concrete infrastructure elements such as decks, girders, columns, piers, and pipes due to their high-performance characteristics with low thickness requirements in comparison to traditional materials. There are also advantages related to the relative ease of placement in the field, lightweight nature of the materials, and potential long-term durability. In a number of these applications the composites, either in prefabricated form or processed on site, are bonded onto concrete substrates to strengthen the existing structural concrete element and/or increase service life [1-3]. These materials are also increasingly used in applications in the marine and offshore domains [4-6]. Often, cure is attained under ambient conditions or at moderately elevated temperatures, and the materials are not processed in an autoclave nor required to meet the stringent aerospace qualification standards at the constituent level. These materials are subject to a wide range of environmental exposures including immersion in aqueous media ranging from water, seawater and alkaline solutions. While polymer composites have been noted to have a successful history of use in such applications there are significant gaps in the understanding of long-term durability [7-9] especially over the timescales of service life expected of civil

infrastructure elements. The lack of this data and fundamental understanding of mechanisms has led to the incorporation of excessively high factors of safety in design often resulting in inefficient use of the material [10]. Design values provided by different codes and guidelines also show significantly different recommendations that further differ from predictions based on accelerated testing procedures [11]. In addition, current design coefficients consider time-invariant coefficients and ignore a number of important aspects such as differences in severity of exposure and degree of cure due to resin and processing method used [8]. Thus, the development of a comprehensive understanding of long-term mechanisms of deterioration and effects, and durability, over a range of exposure conditions is critical to the greater, and more effective, use of polymer composites in applications in civil infrastructure and the marine and offshore sectors.

The in-field processing of composites for the strengthening of civil infrastructure elements including the bonding of these to the composite substrate generically involves ambient temperature cure of the resin, or adhesive, and the composite. In these cases, the crosslinking reactions in the polymer are not completed even over extended time periods resulting in incomplete cure and the consequent increased susceptibility to deterioration of mechanical performance characteristics, and a decrease in glass transition temperature when exposed to moisture [10, 12]. While carbon fibers are inert to most environmental exposure conditions likely to be faced by civil infrastructure the epoxy systems used as the matrix in the composite, and to effect a bond between the composite and the concrete substrate, are known to be affected by moisture adsorption and absorption resulting from exposure to humidity and aqueous solutions. The effects include decreases in glass transition temperature through interruption of hydrogen bonds by water molecules [13-15], decreases in strength characteristics [15], swelling [16], degradation of the molecular structure [17,

18], and increased interfacial deterioration [1, 19]. Nogueira et al. [15] showed that moisture uptake decreased with increase in degree of cure due to the higher crosslink density of the network which decreases the presence of molecular sized holes in the polymer structure resulting in lower free volume. In addition, the tensile strength and toughness of the epoxy decreases with increasing moisture content due to the plasticizing effect of the water [15, 20] emphasizing the effect of incomplete cure, which results in the existence of phases of unreacted and partially reacted material within a more highly crosslinked network. These local areas have a strong effect on overall moisture uptake and reduction in durability.

While the effects of moisture and solutions common in the aerospace domain on the durability of higher temperature cure epoxies and composites has been fairly well documented [21-25] the effects on ambient temperature cure epoxies and composites are not as well understood especially as related to solutions typical in civil engineering applications including salt water and concrete pore solutions [7]. Both Chin et al. [26] and Scott and Lees [7] focused on developing a basic understanding of phenomena related to solution uptake in the resin. While Chin at al [25] reported that diffusion followed a Fickian process, Scott and Lees [7] showed that the Fickian model did not provide a good representation at intermediate times and that Langmuir diffusion was more effective in modeling anomalous diffusion in an epoxy resin. Based on a review of literature, Scott and Lees [7] also concluded that differences in the chemical constituents of solutions, and aspects such as the specific resin chemistry, cure conditions, and exposure temperatures resulted in it not being possible to draw firm conclusions on effects with salt solutions being reported to both increase and decrease the rate of moisture uptake and equilibrium content. Wang et al. [27] suggested that a three-stage curve best modeled moisture uptake for an epoxy

immersed in water and alkaline solutions and showed that the solutions had an imperceptible difference on mechanical properties over the time period of study, whereas Xin et al. [28] introduced a three-stage process that included diffusion, relaxation, and damage dominated regimes. In a study on an epoxy and its carbon fiber composite immersed in water, acidic, and alkaline solutions Uthaman et al. [2] showed that the effect of immersion in acidic solution was the most severe with the alkaline exposure also having a more detrimental effect than that of water.

The discrepancies in results based on differences in epoxy formulation and hardener used, cure conditions, and even chemical makeup of the test solutions, makes it difficult to clearly differentiate between effects and form a fundamental understanding that could lead to the development of a rational basis for prediction of service life under a range of exposure conditions. Further, it is clear that the short time frames used for the study of ageing and degradation may not be sufficient to obtain saturation and hence raise questions regarding the viability of use of short-term exposure even under accelerated conditions for the comprehensive understanding of mechanisms and the prediction of durability of ambient cured systems [7]. To address these concerns a comprehensive investigation on ambient cured systems over a range of materials and exposure conditions is being undertaken over periods exceeding 36 months, which begin to cover the range of time necessary to study longer term effects.

In this article an ambient cured epoxy and its wet layup carbon epoxy composite used extensively in the rehabilitation of civil infrastructure are subjected to immersion in aqueous solutions for periods between 44 months and longer than five years in order to develop a fundamental understanding, and differentiation, of mechanisms and phenomena through the study

of moisture uptake, dynamic mechanical characterization, and mechanical testing. The longer-term goal is to not only provide the basis for accurate characterization and predictability of durability but to also enable the development of appropriate design factors across systems.

5.2. MATERIALS AND TEST METHODS

The resin system consisted of a 4,4'-isopropylidenephenol-epichlorohydrin (similar to a DGEBA Epon 828 type system) combined with an aliphatic amine hardener in a 2:1 ratio having a viscosity of 700 to 900 cps and a gel time of about 60 minutes at 23oC. The reinforcement was a unidirectional fabric of T700 carbon fibers in untwisted 12k form with fibers having nominal strength, modulus, and density of 4,900 MPa, 230 GPa, and 1.80 g/cm3, respectively. The fabric had an aerial weight of 300 grams per square meter and composites were fabricated with one and two layers using the wet layup process with thicknesses of 0.72 mm and 1.34 mm, respectively. Since the intent was to replicate overhead strengthening of beams and slabs in the field the panels were fabricated using a similar process with the application of only manual roller-based pressure and without the use of vacuum bags or pressure plates to increase compaction. Further cure progression was allowed under ambient conditions. Fiber volume fractions were determined through acid digestion to be 26% and 29%, respectively, with void fractions between 2 to 3%. This range is similar to that seen in the field, equivalent of fiber weight factions of 42-46% and similar ranges have been reported previously [29-31]. Neat resin panels were also cast under the same conditions. All specimens were conditioned for 30 days at 20-23^{o}C prior to exposure and testing, to ensure a reasonable level of cure progression based on previous investigations of the same resin system [32, 33]. In the field these systems are rarely subject to external heat sources to expedite cure and cure progression takes place under ambient conditions which are likely to be cooler on

the soffit of the deck/beam than on the top surface. The solutions studied were water, saltwater solution to simulate a marine or offshore environment using 5% NaCl following [26] and concrete leachate to duplicate the alkaline environment due to concrete following [34] ensuring that the solution contains salts from concrete rather than a simulated solution.

Moisture uptake was recorded on specimens of 25.4 mm x 25.4 mm size cut from resin plaques and composite plates at the actual thickness of each specimen thereby keeping surface conditions consistent. Five specimens were used for each measurement with specimens immersed in the three solutions in temperature-controlled baths at 23 ± 1^{o}C with continuous monitoring of both water levels and temperature. Specimens were placed ensuring no contact between adjacent specimens so as to preclude any difference in exposure conditions. A set of specimens was also stored under controlled conditions of 23^{o}C and 30% RH as reference controls and to assess the progression of cure over time. Specimens were removed periodically, over a period exceeding five years, using padded tweezers to ensure minimal pressure and no transfer of oils or substances from human hands that could inadvertently contaminate the specimens and/or the solutions, patted dry with tissue paper and then weighed to measure uptake after which they were re-inserted into the baths. The time period for the operation was standardized for consistency and to avoid effects of varying levels of evaporation through the specimens.

Dynamic Mechanical Thermal Analysis (DMTA) based characterization was conducted in three-point bending mode on specimens of 35 mm x 9 mm size with a span: thickness ratio of 16:1 at a frequency of 1 Hz with a strain of 0.0025% and a heating rate of 5^{o}C/minute. As with the moisture uptake specimens, care was taken to ensure that the time period between the removal of

specimens from the temperature controlled baths and the initiation of DMTA testing was standardized. A minimum of three specimens were tested for each set at periodic intervals up to 44 months.

Mechanical characterization was conducted using tension and three-point flexure tests following ASTM D3039 and D7264, respectively, with five specimens being tested at each time period and immersion condition for up to 60 months. Tension tests were conducted with untabbed specimens to reduce ambiguity related to environmental exposure effects between the tabbed and untabbed regions and the potential change in conditions caused by cure of the adhesive used for tabbing after completion of exposure. It was noted that all specimens failed within the gauge length and not in the grips. Flexure specimens used a span to thickness ratio of 16:1 with a minimum of five specimens for each time period and immersion solution.

5.3. RESULTS AND DISCUSSION

5.3.1 MOISTURE UPTAKE AND KINETICS

Kinetics of water diffusion into polymers and composites has been described through a range of models of which Fickian [21, 22, 35, 36] and Langmuir diffusion [37, 38] are the most common. Transport in glassy polymers involves both concentration and temperature gradient driven Fickian processes and time dependent relaxation/deteriorative mechanisms. In the latter, polymer chains rearrange over time in the presence of penetrant molecules resulting in further, but slower, absorption and adsorption. In addition, the competing effects of cure progression (which for ambient cure can initially be accelerated by water uptake) and effects of moisture on the structure of the polymer, effect of voids on increased absorption, and the accelerated deteriorative

effects of matrix microcracking and fiber matrix debonding increase the complexity of molecular interactions between the solution and resin. In such cases a two-stage diffusion model better describes the effects of phenomena of moisture uptake which at time, t, can be expressed following Bao et al. [39] as.

$$\frac{M_t}{M_\infty} = \left(1 + k\sqrt{t}\right)\left(1 - exp\left[-7.3\left(\frac{Dt}{h^2}\right)^{0.75}\right]\right) \quad (1)$$

where M_∞ and D are the equilibrium moisture uptake level and diffusion coefficient associated with stage 1 uptake, h is the specimen thickness, k is a time dependent coefficient characteristic of the rate of polymer relaxation and second stage damage due to moisture absorbed. When k equals 0 equation (1) reverts to the Fickian form of diffusion modeled by Shen and Springer [36].

Figures 5-1(a)-(c) show uptake curves for the resin, single-layered, and two-layered composites in the three solutions. As reported earlier [7, 26] the type of solution does not have a significant effect on overall uptake in the neat resin with the diffusion coefficients being within the range reported by previous studies [15, 26, 40, 41] of 0.5-3 x 10^{-7} mm^2/s. However, in the case of the composites the uptake in the alkaline solution is substantially higher than in the other two solutions showing an additional transition due to greater fiber matrix debonding providing channels for accelerated capillary flow. Similar behavior was noted at shorter time scales by Abanilla et al. [1] for ambient cured graphite/epoxy composites. The values of M_∞/M_{max} are reasonably close for the resin samples suggesting the prevalence of similar phenomena and transition between stages. The differences, however, are far greater in the case of the composite specimens. In all cases the ratios for the composites are significantly lower than the resin with ranges of 0.35-0.54 for the single layered composite and 0.36-0.58 for the two layered composites

as compared to 0.71-0.81 for the resin. The specimens immersed in the concreate leachate (i.e. alkali solution) show the lowest ratios 0.35 and 0.36 for the one and two layered specimens, respectively, indicating substantially earlier transition from stage 1 to stage 2 regimes, which is representative of earlier deterioration of the fiber-matrix interfaces and of resin network structure.

Diffusion parameters obtained through best fit curves solving for *M*, *D* and *k*, in equation (1), and moisture kinetic characteristics are listed in Table 5-1 for the neat resin and the two composites. The apparent diffusion coefficients determined experimentally use a one-dimensional approximation which ignores additional diffusion through the edges. Following Shen and Springer [36] an edge correction can be applied as follows:

$$D_x = D_a \left[1 + \frac{h}{l} + \frac{h}{b}\right]^{-2} \tag{2}$$

where D_x is the corrected coefficient, D_a is the apparent coefficient determined directly through experimental data, and *l*, *b*, and *h* are the length, width, and thickness of the specimens, respectively. Values of the corrected parameters are also provided in Table 5-1.

It is of interest to note that with the exception of the composites immersed in concrete leachate (i.e. alkali solution) the levels of moisture uptake at the end of the period of immersion is lower than that that of the resin, which is in keeping with the effect of the presence of fibers. In the case of immersion in the alkali solution greater fiber matrix debonding and matrix deterioration results in the increased uptake and as seen in Figures 5-1(b)-(c) there is an additional transition that results in this increase suggesting a three-phase uptake process. Importantly the level of M_∞, the equilibrium moisture content associated with phase one uptake, for the composites is lower than that of the resin emphasizing that the increased level of uptake takes place in the second stage

which is related to relaxation and deteriorative processes such as from fiber-matrix debonding and matrix microcracking. This is further borne out through a comparison of coefficients, *D* and *k*, from which it can be seen that there is a significantly higher value of *k* pertaining to composites immersed in concrete leachate solution with the values being similar at the one- and two-layer levels and about 4.2 times that of the neat resin. First-stage diffusion coefficients for the resin are fairly close across all three solutions and higher, although at the same magnitude than those reported for epoxies used in civil infrastructure [7, 26] and similar to that reported in [32] for the same system but conducted over a much shorter time period of immersion.

(a)

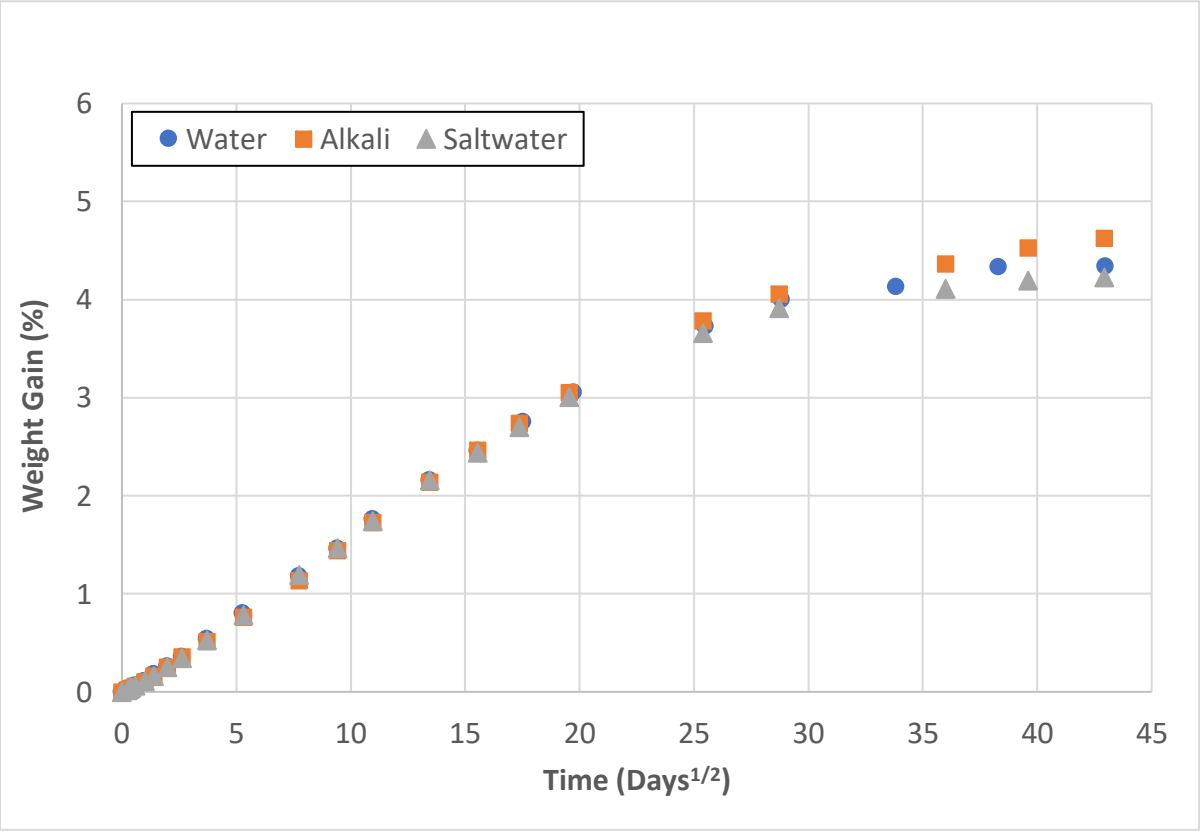

(b)

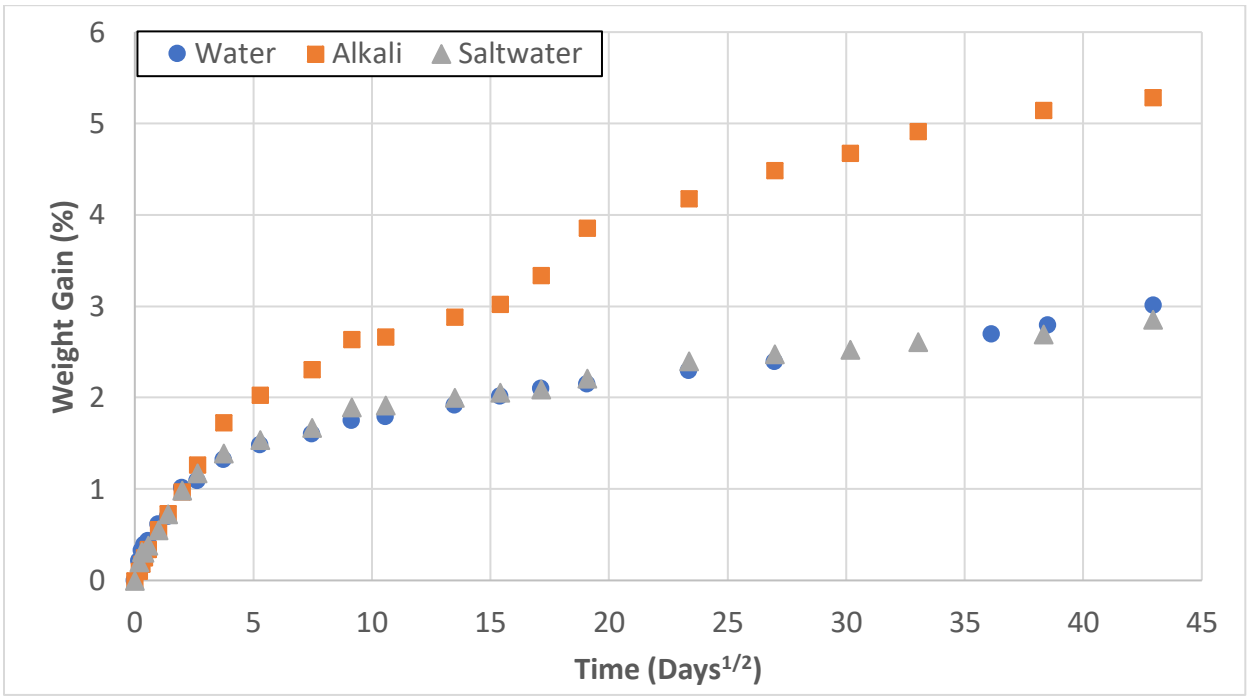
Water
Alkali
Saltwater
Weight Gain (%)
Time (Days^1/2)
0
1
2
3
4
5
6
0
5
10
15
20
25
30
35
40
45

(c)

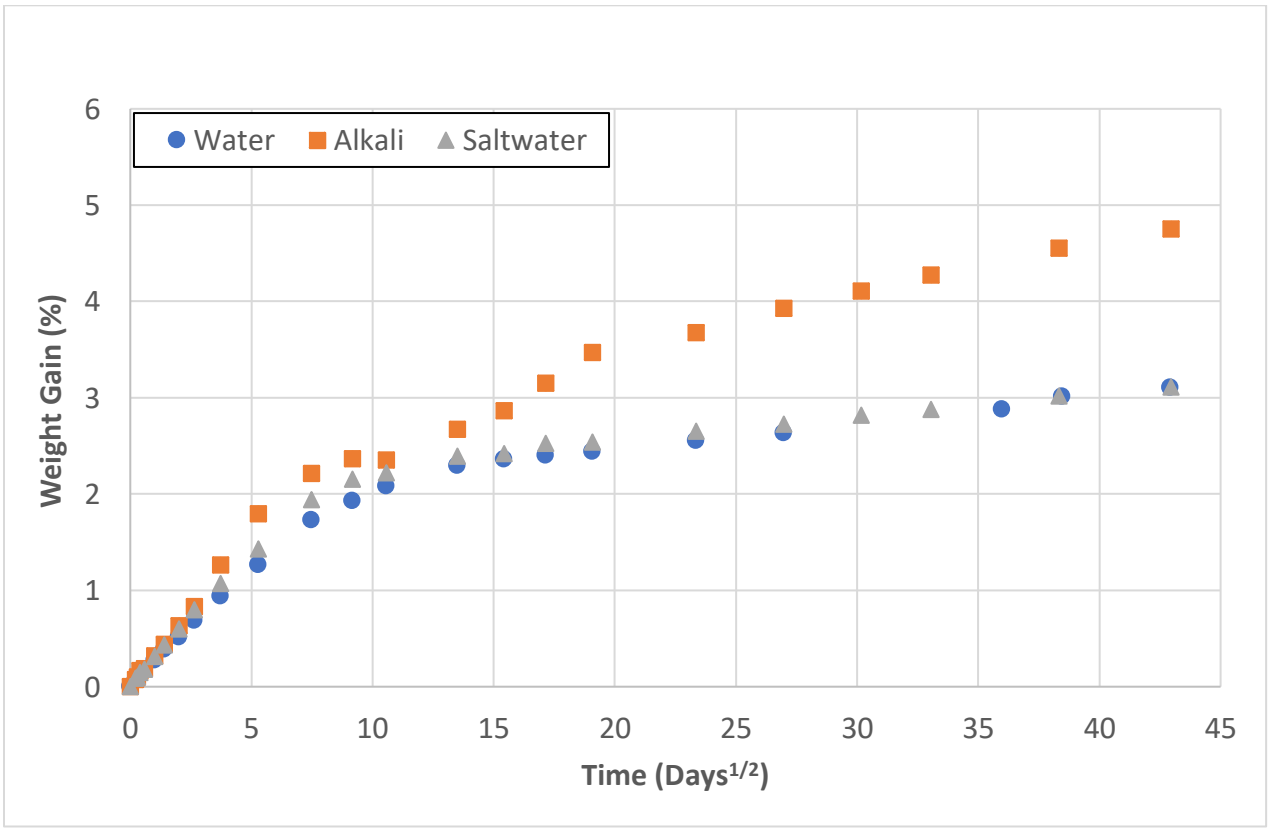
Water
Alkali
Saltwater
Weight Gain (%)
Time (Days^1/2)
0
1
2
3
4
5
6
0
5
10
15
20
25
30
35
40
45

Figure 5-1. *(a). Moisture uptake in the neat resin. (b). Moisture uptake in the single-layered composites. (c). Moisture uptake in the two-layered composites.*

Table 5-1. *Two-Stage Diffusion Parameters*

Specimen	**Solution**	**M_{max} (%)**	**M_∞ (%)**	**D ($x10^{-7}$ mm^2/s)**	**k ($x10^{-5}$ mm^2/s)**	**D_x ($x10^{-7}$ mm^2/s)**	**k_x ($x10^{-5}$ mm^2/s)**
Resin	**Water**	4.338	3.274	1.04	2.80	0.54	1.40
	Alkali	4.625	3.293	0.91	3.71	0.47	1.91
	Saltwater	4.229	3.415	1.02	2.09	0.53	1.08
1-Layer	**Water**	3.008	1.331	1.83	10.1	1.64	9.05
	Alkali	5.285	1.844	1.58	15.60	1.42	13.97
	Saltwater	2.855	1.530	1.14	7.22	1.02	6.47
2-Layers	**Water**	3.102	1.799	1.11	6.13	0.91	5.02
	Alkali	4.751	1.719	1.10	15.51	0.90	12.69
	Saltwater	3.110	1.800	1.11	6.13	0.91	5.02

It should be noted that the second coefficient, k, reflects the level of the glassy state with higher levels indicating greater disruption of the polymer network. Knowing the values of the two diffusion coefficients and the value of moisture uptake at the kink point of transition between diffusion and relaxation mechanisms provides insight into hygrothermal history and the moisture exposure conditions. Over long periods of exposure, as seen in the current investigation, the changes in the polymer network due to competing effects of adsorption, postcure, and plasticization effected deterioration, can be significant and may not be discernible through short term exposures used in most previous studies. The second kink as seen in Figures 5-1(b)-(c) for

the specimens immersed in concrete leachate is a point in this context and reflects changes that may not be discerned even through accelerated test protocols reinforcing the concerns reported earlier by Scott and Lees [7]. It is of importance to note the differences in moisture kinetics between the one and two layered composites through the two coefficients. In the case of the single layered composites the highest values of *D* are seen through immersion in water followed by the alkaline solution, while in the two layered systems the three values are similar. However, in keeping with the expectation of greater deterioration in the fiber matrix bond and hydrolytic degradation being enhanced due to the higher pH and presence of salts in concrete leachate, the values of k for the samples immersed in concrete leachate are substantially higher than that from the two other solutions. Also, given the expectation of similarity in mechanisms irrespective of the number of layers of reinforcement, it is important to note that the values of k for the two composites immersed in alkali solution are very similar, with k = 15.6 x 10-5 mm^2/s for the single layered composite and k = 15.51 x 10-5 mm^2/s for the two layered specimens. In comparison *k* values for the water and saltwater immersions, while similar, are lower for the two layered specimens as compared to the single layered ones suggesting relatively lower levels of relaxation and overall deterioration.

It should be emphasized that the higher levels of diffusion in the first stage can be correlated with the high void content and increasing levels of fiber matrix debonding which results in greater uptake as was reported earlier [25, 42]. Aqueous solutions absorbed into the specimens cause both plasticization of the resin and micro-cavitation type irreversible damage such as the deterioration of bond between the fiber and the resin resulting in the formation of cavities and pathways which can accelerate capillary movement of solution. Uptake at this level results in an increase in the free

volume and hence an increase in the molecular mobility of epoxy molecules resulting in consequent dissociation of hydrogen bonds between absorbed water molecules and active sites in the polymer network.

The differences in stage 1 and 2 coefficients, *D* and *k*, in the three solutions is a result of a number of factors such as effects of moisture uptake on resin morphology, osmotic pressure in the case of salts in solutions, and the effect of uptake through additional paths in the composite enabled by fiber matrix interface debonding and in interlayer regions [1, 9, 42]. Additionally, there are competing effects of increasing chain mobility due to moisture induced plasticization and increased crosslinking due to time dependent, and moisture accelerated, progression of cure in the uncured segments, as well as increased tortuosity of uptake flow due to the presence of fibers especially with multiple layers [1]. It is therefore of interest to assess, at least at a relative level, the response in the bulk resin within the composites with that determined from the unreinforced resin itself. Following Shen and Springer [36] for unidirectional composites the diffusion coefficient for the resin and the composite, *D*, can be determined from the corresponding coefficient for the composite as follows:

$$D_r = \frac{D}{\left(1-2\sqrt{V_f/\pi}\right)\left[1+\frac{h}{l}\sqrt{\frac{\left(1-V_f\right)}{\left(1-2\sqrt{\frac{V_f}{\pi}}\right)}}+\frac{h}{w}\right]^2} \tag{3}$$

where V_f is the fiber volume fraction, and *h*, *l*, and *w*, are the thickness, length, and width of the specimens. Values of the diffusion coefficient for the bulk resin determined through the use of equation (3) are given in Table 5-2. It can be seen that in all the cases the theoretical values are

significantly higher than those determined experimentally on the neat resin due to mechanisms of increased uptake with fiber-matrix debonding induced capillarity and micro-cavitation damage, and the consequent interactions of absorbed water with regions of the local polymerized epoxy network. This is in line with earlier reported results of water entering the interfacial region at rates as high as 450 times more rapidly than in the neat resin [43]. It can be seen that the effect of increased compaction and intermingling of fibers from layers decreases the difference in the two layered composites as can also be expected from lower levels of resin rich outer layers and the increased tortuosity of flow of solution within the two layered composites. It is also noted that the highest value of difference in the single layered composites are for the specimens immersed in water with the lowest being in saltwater confirming earlier reported mechanisms of sodium chloride salts acting to decrease the uptake in saturation level due to reverse osmosis occurring as the water is absorbed into the composite and forms an electrolyte as it dissolves water soluble elements within the polymer [44-46]. The differences in mechanisms as a result of increased tortuosity through multiple layers as well as the effect of solution salts can be further elucidated, at a level of relative comparison, through assessment of diffusivities in directions parallel (D_{11}) and normal (D_{22}) to the fibers through

$$D_{11} = \left(1 - V_f\right) D_r \tag{4a}$$

$$D_{22} = \left(1 - 2\sqrt{\frac{V_f}{\pi}}\right) D_r \tag{4b}$$

with values reported in Table 5-2. As would be expected through capillary induced mechanisms for water uptake $D_{11} > D_{22}$.

5.3.2. DMTA CHARACTERIZATION

Dynamic mechanical thermal analysis techniques provide a powerful tool for developing insight into changes in structure and viscoelastic response of polymers and polymer composites through changes in glass transition temperature (T_g), loss tangent (tan δ), storage modulus, and loss modulus. Moisture uptake is known to cause plasticization and depression in the glass transition temperature through disruption of Van der Waals force based interchain hydrogen bonds and increased macromolecular mobility. For the purposes of the current investigation the T_g was determined from the peak of the loss tangent curve. The use of this characteristic is advantageous both because it is easy to determine and is independent of specimen dimensions [47] ensuring that what is measured is a material characteristic rather than effected by details of the test setup. Figure 5-2 shows the depression in T_g as a function of moisture content. Variation in the standard deviation of values is between 1% and 7% with the least variation being noted at the beginning and end of the period of exposure. It should be noted that as shown in Figures 5-1(b)-(c) the time taken to attain a specified moisture content can be very different based on the solution type and number of layers of reinforcement. In all cases except that of immersion in water where T_g is noted to continue to decrease over the entire time period of immersion, T_g is seen to reach an initial minimum followed by fluctuations which are due to local differences in degree of polymerization and moisture uptake, among other factors, and small increases with an increase in the time of exposure.

Table 5-2. *Analytically Determined First Stage Diffusion Coefficients ($x10^{-7}$ mm^2/s)*

	Single Layered Composite			**Two Layered Composite**		
	Water	**Alkali**	**Saltwater**	**Water**	**Alkali**	**Saltwater**

$(D_r)_{expt}$	1.04	0.91	1.02	1.04	0.91	1.02
$(D_r)_{calc.}$	3.79	3.28	2.36	2.24	2.22	2.24
$\frac{(D_r)_{calc}}{(D_r)_{expt}}$	3.65	3.60	2.32	2.15	2.44	2.20
D_{11}	2.81	2.42	1.75	1.59	1.58	1.59
D_{22}	1.61	1.39	1.00	0.88	0.87	0.88

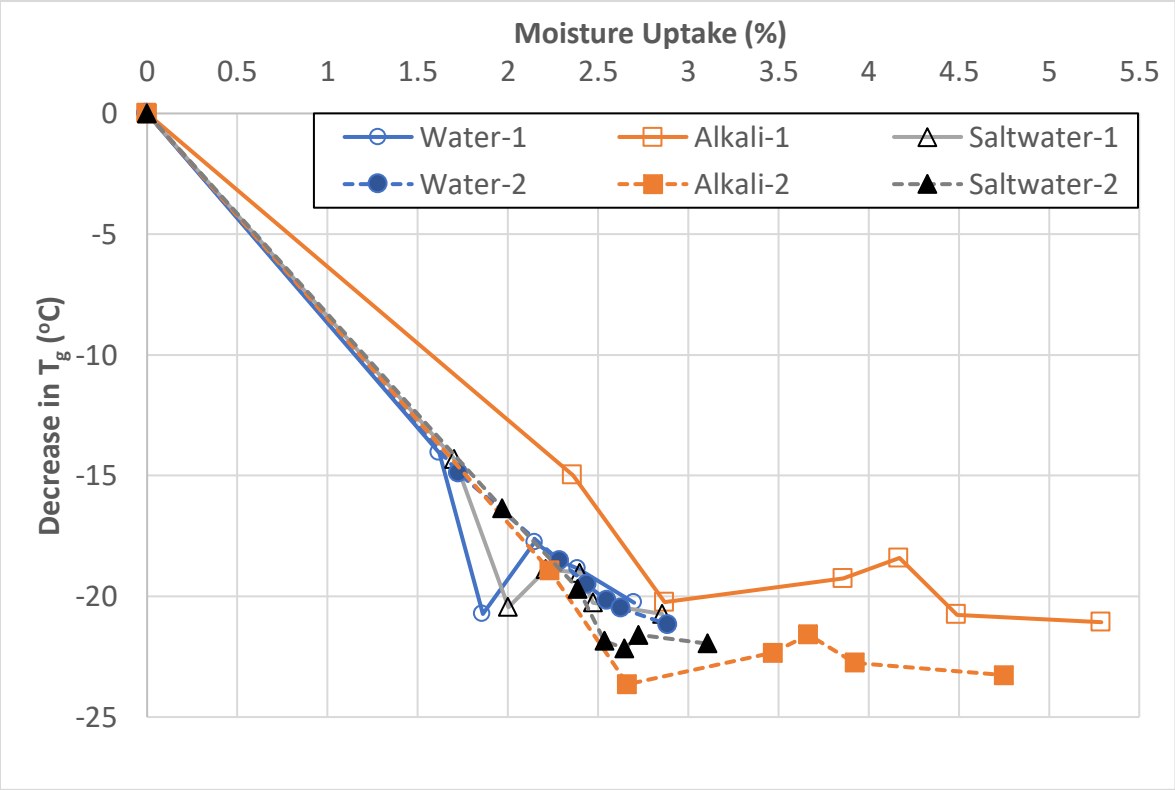

Figure 5-2. *Decrease in T_g as a function of moisture uptake (The notations of -1 and -2 relate to single layered and 2-layered composites, respectively)*

The initial drop is seen to coincide with the time periods that are largely diffusion dominated following trends reported by Zhao and Lucas [48]. The phenomenon of decrease of T_g with increasing time of exposure has been reported earlier for water [15, 18, 49-51]. Decreases of between 15 to 20^{o}C per percent of moisture uptake have also been reported [18, 50, 51]. The fluctuation and increase in T_g after attainment of a minimum are due to the effects of secondary crosslinking attributed to type 2 bound water interacting with hydrophilic groups such as hydroxyls and amines [52] as well as due to additional microdamage induced uptake and Type II water. As can be seen in Figure 5-2 the greatest drop in T_g is after immersion in concrete leachate with the minimum being as a result of immersion in water. The minimum level is attained within six months of immersion for all solutions with the single layered composites, whereas with the two layered composites the period is noted to extend, albeit with relatively minor further depression in T_g to 18 months in salt water and through the entire period of immersion for water. The drop in T_g in the initial linear segment in Figure 5-2 is between 8 and 8.7 ^{o}C per percent of moisture uptake for all specimens except the single layered composites in the concrete leachate solution which shows a lower rate of 6.8^{o}C per percent of moisture uptake, indicating a lower level of decrease from that reported for epoxies used in the aerospace sector, which have been reported to typically be at the level of 20^{o}C per percent of moisture uptake [20, 24, 43, 50].

While levels of decrease in T_g are similar as a result of immersion in all three solutions for the single layered specimens the difference is far greater in the two layered specimens where distinct differences can be seen at the six-month level with the greatest drop being in the specimens immersed in the concrete leachate. The specimens in saltwater show a drop of 6.3% greater than that in water which is close to the difference of 7% between water and seawater reported by

Kafodya and Xian [53], whereas the alkaline immersion shows a 27.5% greater drop. It is of importance to note, however, that at longer periods of time the differences are far less, 3.7% and 9.9%, for the salt and concrete leachate solutions, respectively, as compared to that in water. This has significance in terms of the higher initial stage-2 moisture uptake mentioned earlier for the specimens in concrete leachate. It is noted that the endpoint of the initial linear decrease in T_g with the increase in moisture uptake coincides with the first increase in uptake after initial saturation and the post-minimum T_g peak coincides with the initiation of the earlier mentioned third stage of uptake kinetics for the composites in the concrete leachate solution, emphasizing the complex interactions taking place in the network and at the fiber matrix interface. At the simplest level uptake can be considered to take place in two phases as related to effects on T_g and properties, as described later. The first phase is diffusion dominated and relates to attainment of an initial equilibrium and is largely reversible with the major effect being plasticization which also leads to a depression in T_g [9, 39]. Water absorbed into the polymer exists both as free water within microcavities and bound water which interacts within polar segments of the network. The second stage consists of largely irreversible effects and as a point of interest it would be valuable to have a multi-parameter model that differentiated between polymer network and morphology changes from those due to microstructure deterioration in the resin and composite. Both these are currently addressed through a single parameter, k [9, 33].

(a)

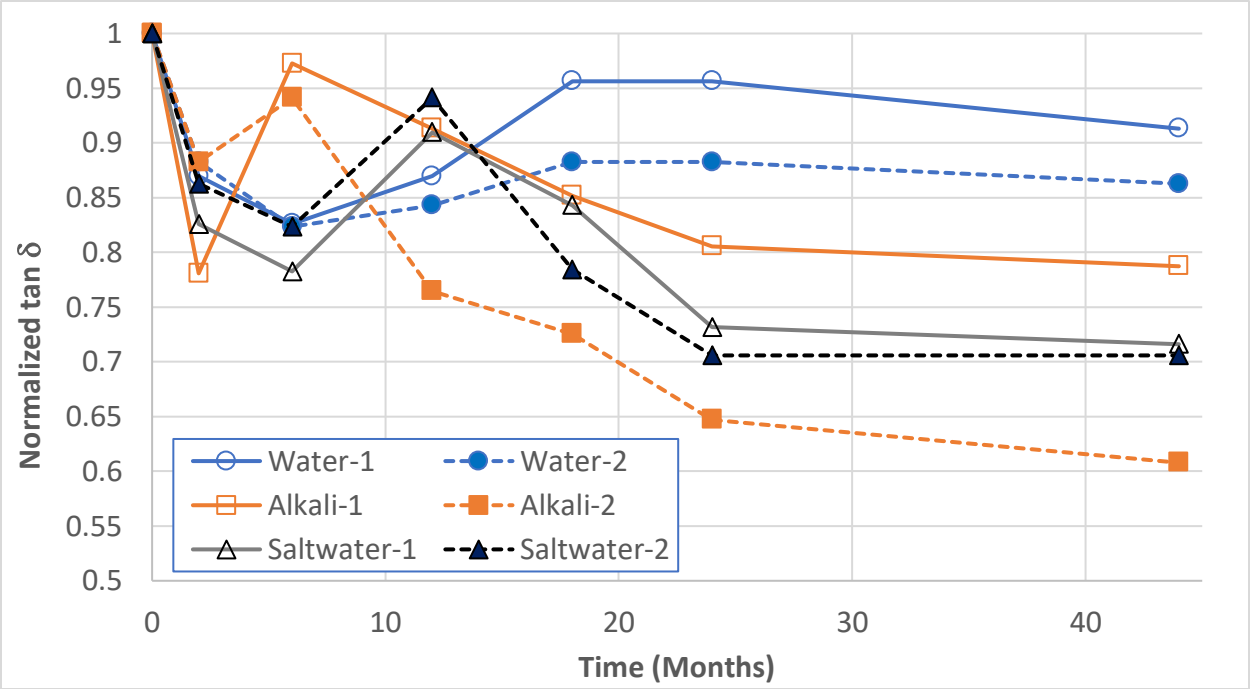
Normalized tan δ
1
0.95
0.9
0.85
0.8
0.75
0.7
0.65
0.6
0.55
0.5
0
10
20
30
40
Time (Months)
Water-1
Water-2
Alkali-1
Alkali-2
Saltwater-1
Saltwater-2

(b)

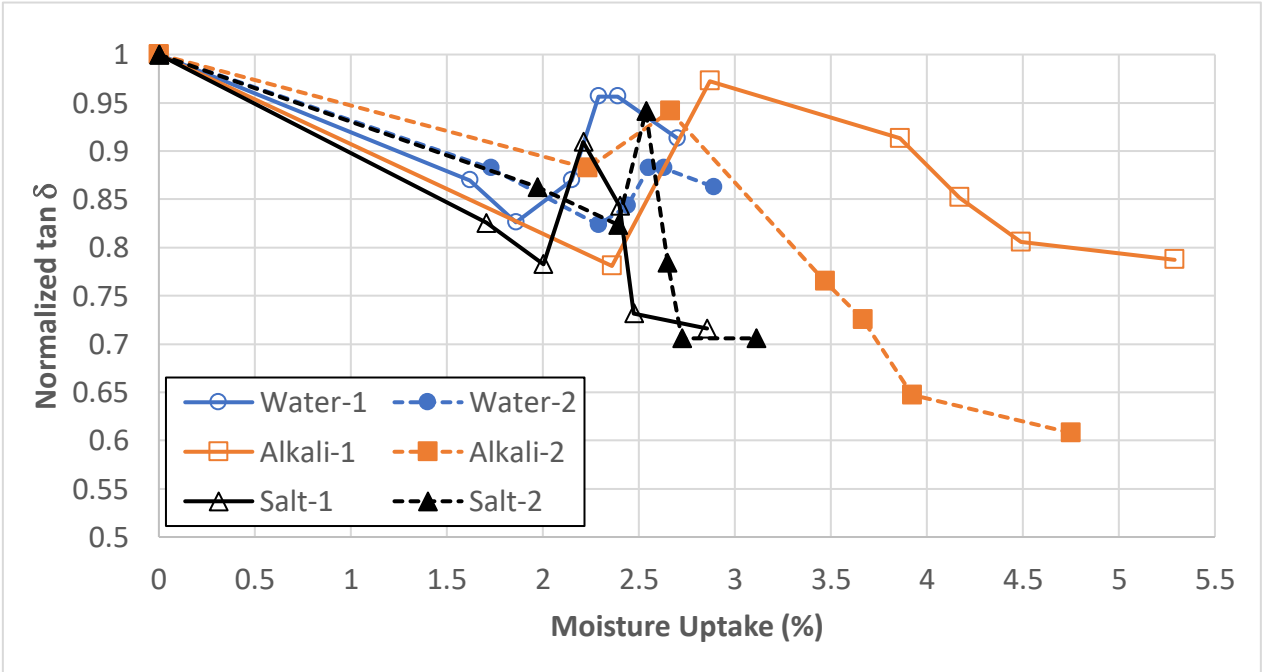
Normalized tan δ
1
0.95
0.9
0.85
0.8
0.75
0.7
0.65
0.6
0.55
0.5
0
0.5
1
1.5
2
2.5
3
3.5
4
4.5
5
5.5
Moisture Uptake (%)
Water-1
Water-2
Alkali-1
Alkali-2
Salt-1
Salt-2

Figure 5-3. *(a). Change in normalized tan δ height as a function of time of immersion (the notations of -1and - 2 relate to single-layered and two-layered composites, respectively). (b). Change in normalized tan δ height as a function of moisture uptake (the notations of -1 and - 2 relate to single-layered and two-layered composites, respectively).*

Nogueira et al. [15] noted that uptake within the free volume hinders chain mobility resulting in a drop in T_g and a reduction in the tan δ peak. Xian and Karbhari [33] in a study on the present resin system noted that hygrothermal aging resulted in a decrease in both the glass transition temperature and loss tangent peak. The loss tangent peak can be linked to the degree of molecular mobility and is hence indicative of changes in degree of cross-linking and network structure [15, 33]. The peak of the loss tangent occurs in the glass transition region and thus is directly related to movement and interactions of small groups and polymer chains due to the transition. The change in $tan\ \delta$ peak height normalized by the height of an unexposed specimen is shown in Figures 5-3(a)-(b) as a function of time of immersion, and level of uptake, respectively. As can be seen from Figure 5-3(a), $tan\ \delta$ height shows an initial decrease followed by an increase and then a continued decrease. Immersion in saltwater and concrete leachate solutions results in a larger drop than that from water. Given that the level of uptake over the 44-month period is significantly different in the three solutions it is more instructive to assess the drop as a function of uptake as in Figure 5-3(b). The initial drop in tan δ height is noted to occur between uptake levels of 1.86% (for the single layer composite in water) to 2.36% (for the single layered composite in concrete leachate) with the drop being linear with increase in moisture content. The single layered composites had the largest drops with the rate of decrease in tan δ being close for all three solutions. In comparison the drops for the two layered composites were less with the specimens

immersed in concrete leachate having the least drop. It is noted that the decrease extended to about 0.7-0.77 of M_∞ in the case of water and saltwater solutions and between 0.45-0.47 of M_∞ for concrete leachate signifying that while the initial uptake was largely in the diffusion dominated stage of uptake it continued into the second stage for the water and saltwater specimens. This drop was followed by an increase in tan δ height which is followed by a continuous decrease suggesting competition between mechanisms of moisture induced plasticization, postcure, and degradation through fiber matrix debonding and micro-cavitation level deterioration. The post peak drop in tan δ was the fastest in the case of saltwater immersion and the slowest, as well as the least in value, from immersion in water, again emphasizing the added role of salts in saltwater and concrete leachate on deterioration in the composite.

(a)

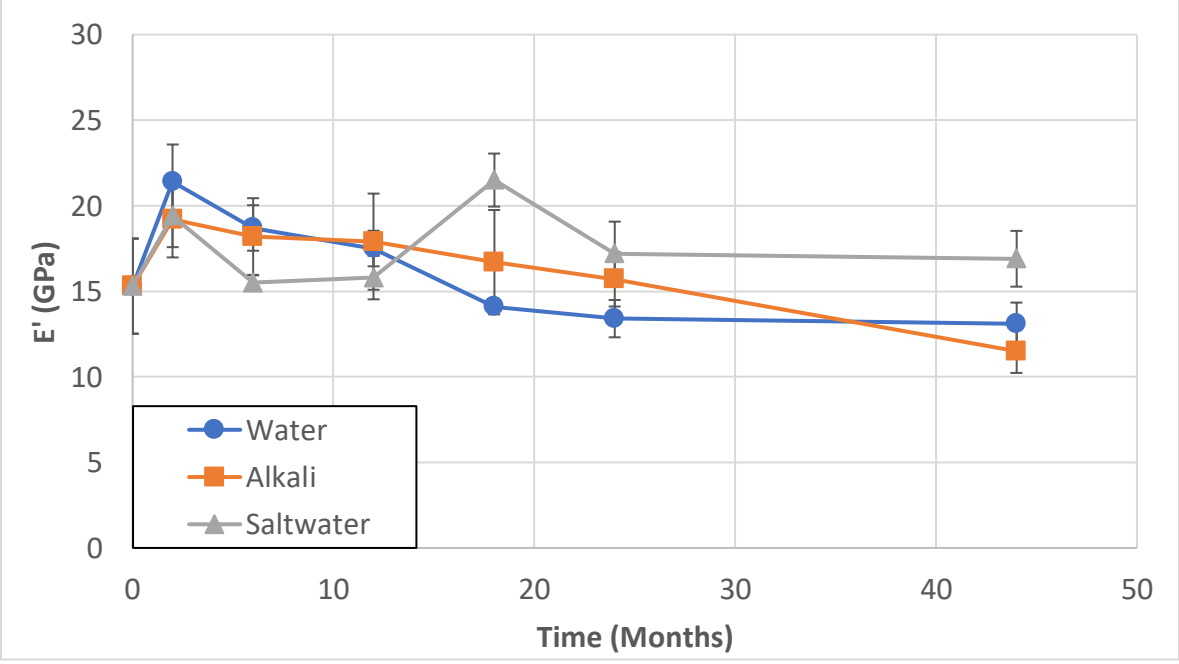

(b)

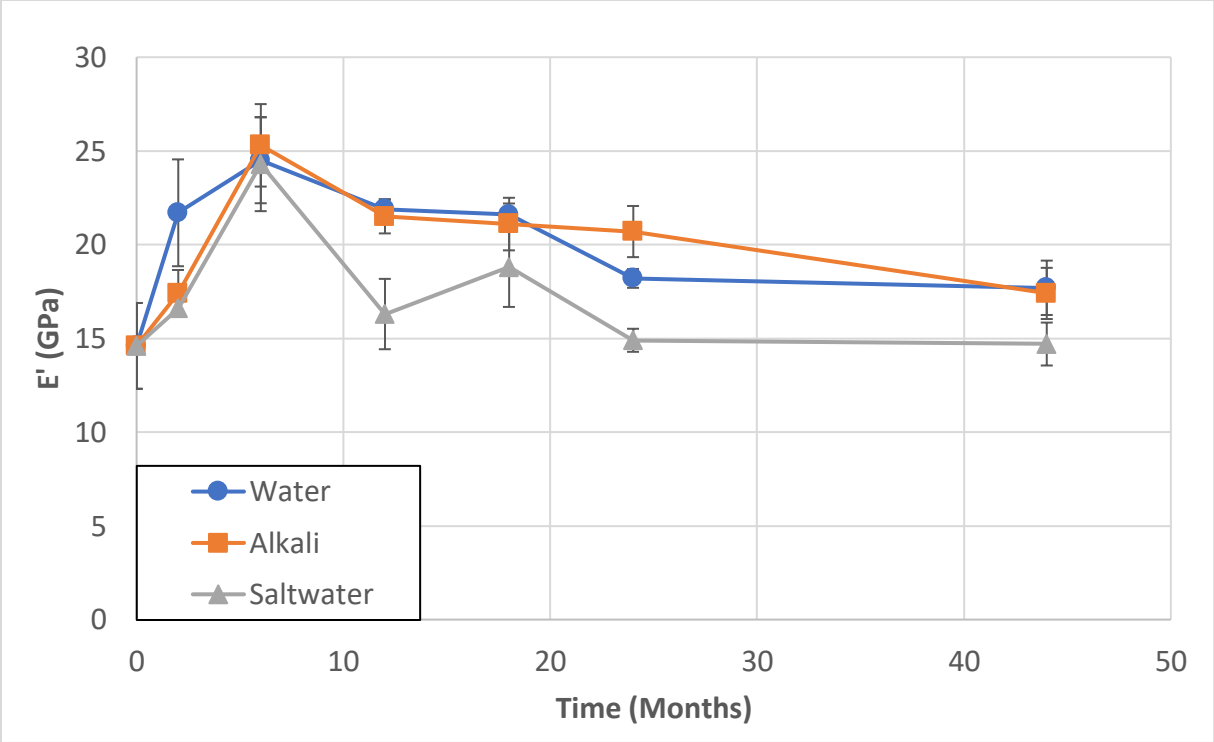

Figure 5-4. *(a). Change in initial storage modulus of the 1-layeredcomposites as a function of time of immersion and solution type. (b). Change in initial storage modulus of the2-layer composites as a function of time of immersion and solution type.*

As mentioned earlier the initial conditions for wet layup composites result in the degree of cure increasing with time and even being initially accelerated by moisture uptake. The competing effects of plasticization, postcure, and other deterioration can be elucidated through comparison of T_g and initial storage modulus (determined in the current investigation for uniformity at a temperature of T_g – 40 ^{o}C) as a function of time of immersion. An increase in storage modulus would indicate increased levels of crosslinking whereas a decrease would indicate plasticization

as can be seen from Figures 5-4(a)-(b). The overall response trend of the composites does not appear to differ significantly due to the number of layers except that the initial peak in storage modulus (indicative of postcure which results in a higher degree of crosslinking and stronger interfacial bonds) is attained at about two months for the single layered specimens and about six months for the two layered specimens. This can be attributed to the effect of thickness and the rate of attaining specific levels of moisture uptake such as that to reach the first stage in the two-stage uptake model. In addition, it is seen that immersion in the NaCl solution has a greater effect in the two-layer specimens. It is of interest to note that while time periods to reach the first stage in the resin were roughly the same after immersion in all three solutions, the effect of solution was clearly seen in the composites due to the effects on fiber-matrix debonding and associated damage which result in greater uptake through capillary action. The existence of two peaks in *E'* as a result of immersion in saltwater is thought to be due to the effects of the NaCl on the network structure and due to osmotic action but needs further investigation.

5.3.3. MECHANICAL CHARACTERIZATION

Changes in tensile strength and modulus of the single and two layered composites as a function of period of immersion in the three solutions is shown in Figures 5-5(a)-(d). The single layer composites show slightly greater deteriorative effects than the two layered ones which is in line with the higher values of the diffusion coefficients, *D* and *k*, as listed in Table 5-1 that indicate faster initial uptake and a greater effect of relaxation/deteriorative mechanisms. It is noted that the maximum deterioration in strength is through immersion in saltwater (18% in the one layer and 21% in the two layer composite) with the least being due to water (8% in the one layer and 6% in the two layer composite) which is in line with results reported earlier for wet layup carbon-epoxy

composites in a range of solutions [1, 2, 6, 32]. Alkali exposure results in drops of 11% for the single layered composite and 13% for the two layered composite. Jose-Trujillo et al. [54] reported a drop in tensile strength of 4.5% after 125 days in seawater, which compares well to the drops of 6 and 7% for the single and two layered composites at 180 days in saltwater. Over the 60-month period of immersion the drop in strength is largely seen to occur over the first 24-month period with a level of postcure extending up to the first six months in some cases. The initial increase in strength and stiffness was noted after immersion in water for both composite thicknesses, and in stiffness for the two layered composites after immersion in the concrete leachate. This phenomenon was also reported by Abanilla et al. [1], Marouani et al. [8], and Nogueira et al. [15], among others, and as described earlier is also seen through DMTA characterization. While the differences in effect due to the three solutions can be seen in strength characteristics, the response in terms of stiffness is not as clear since the results for the most part fall within the overall scatter bounds although the specimens immersed in water show the least deterioration with levels in fact being at a bit higher with immersion due to the aforementioned postcure effect. The maximum increase in stiffness is 7% for the 2-layered composites immersed in water. It is emphasized that even at the 60-month period the degradation in tensile strength is significantly less than predicted by accelerated test models in the literature with drops of 18-21% for the composites immersed in saltwater, 11-13% in concrete leachate, and 6-8% in water. This, again, emphasizes the need for longer testing and better predictive models.

Since the composites are unidirectionally reinforced, it can be expected that exposure would not result in significant drops in axial direction tensile characteristics although fiber matrix debonding, matrix microcracking, and resin plasticization and deterioration, do cause deteriorative effects especially at the lower fiber volume fractions representative of wet lay-up composites.

Flexure tests are known to be more sensitive to fiber matrix adhesion characteristics [55]. Figures 5-6(a)-(b) show results of the flexure tests in terms of flexural strength.

$$\sigma_f = \frac{3PL}{2bh^2} \tag{5a}$$

and shear strength.

$$\tau_f = \frac{0.75P}{bh} \tag{5b}$$

where P is the failure load, L is the span, and b and h are the specimen width and thickness, respectively, as a function of the solution type and time of exposure. Due to the large overlap in results standard deviations are not shown in Figures 5-6(a)-(b). The standard deviation for individual sets is less than 10% for all solutions and time periods considered. It can be seen that in all cases there is rapid degradation for an initial period followed by a slower rate of deterioration with longer time periods of immersion resulting in near asymptotic or extremely slow duration rate regimes. Immersion in water results in the least deterioration in the initial period after which all three solutions cause about the same level of final deterioration in both flexural and shear strengths similar to results reported earlier [1, 56, 57].

While unidirectional composites show good retention of tensile properties in the fiber direction, they are more susceptible to crack propagation and interlayer separation under flexural and shear loading. The interlaminar properties are dependent on resin characteristics which show greater susceptibility to moisture induced deterioration when processed using wet layup due to varying interlayer thicknesses, and higher void content [1]. Deterioration can thus be at the fiber matrix interface level through debonding and microcrack coalescence as well as in the resin rich zone between fabric layers, and due to resin hydrolysis.

(a)

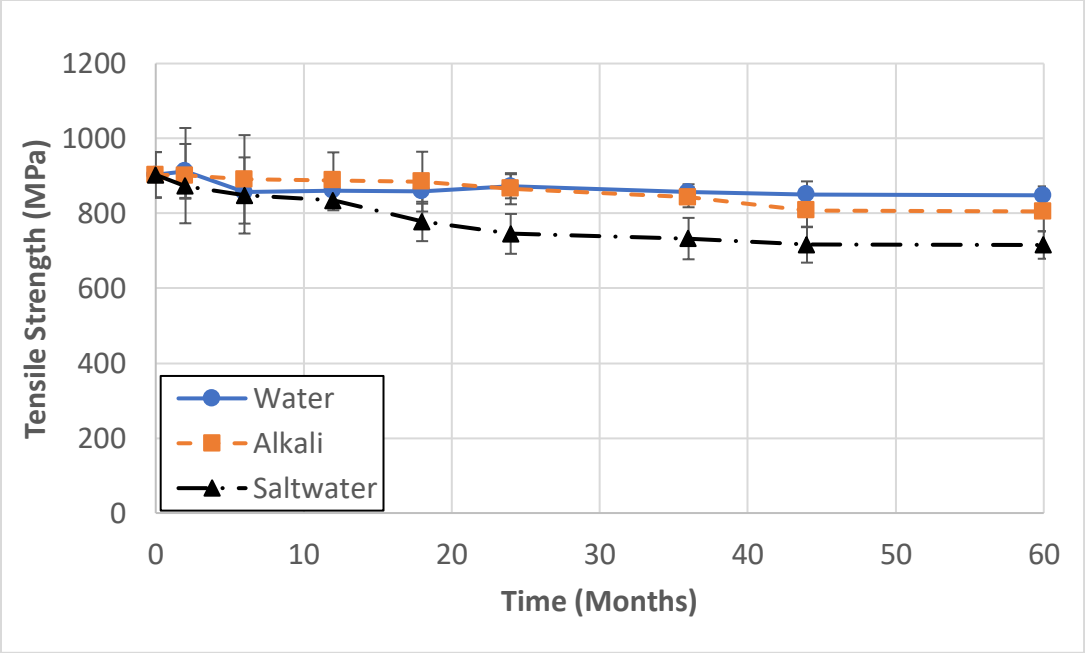
Tensile Strength (MPa)
1200
1000
800
600
400
200
0
0
10
20
30
40
50
60
Time (Months)
Water
Alkali
Saltwater

(b)

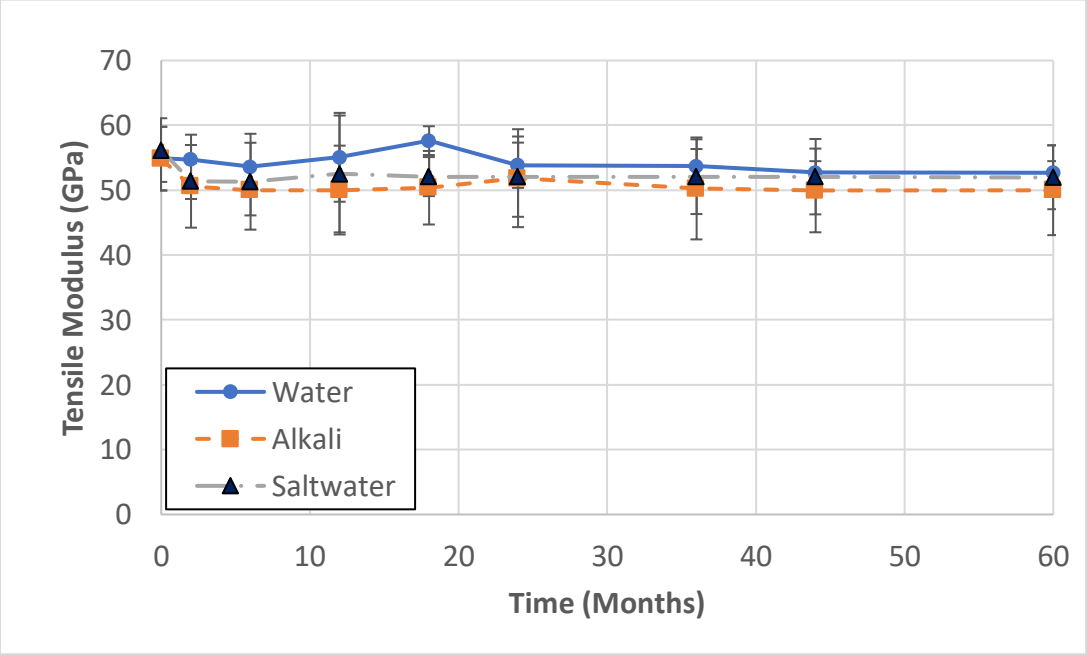
Tensile Modulus (GPa)
70
60
50
40
30
20
10
0
0
10
20
30
40
50
60
Time (Months)
Water
Alkali
Saltwater

(c)

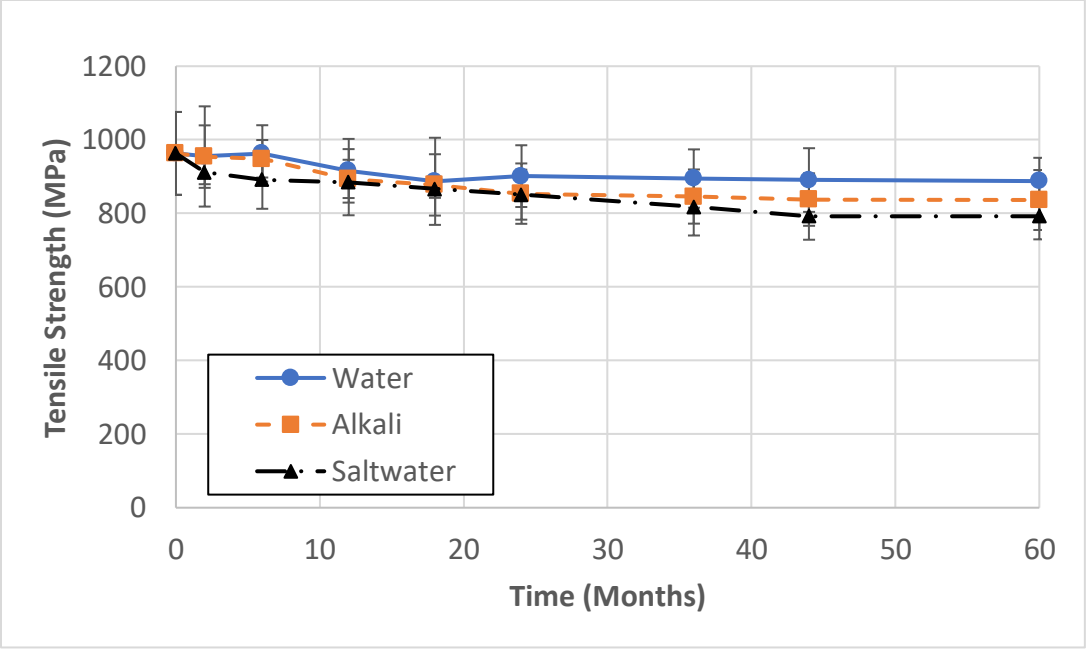

(d)

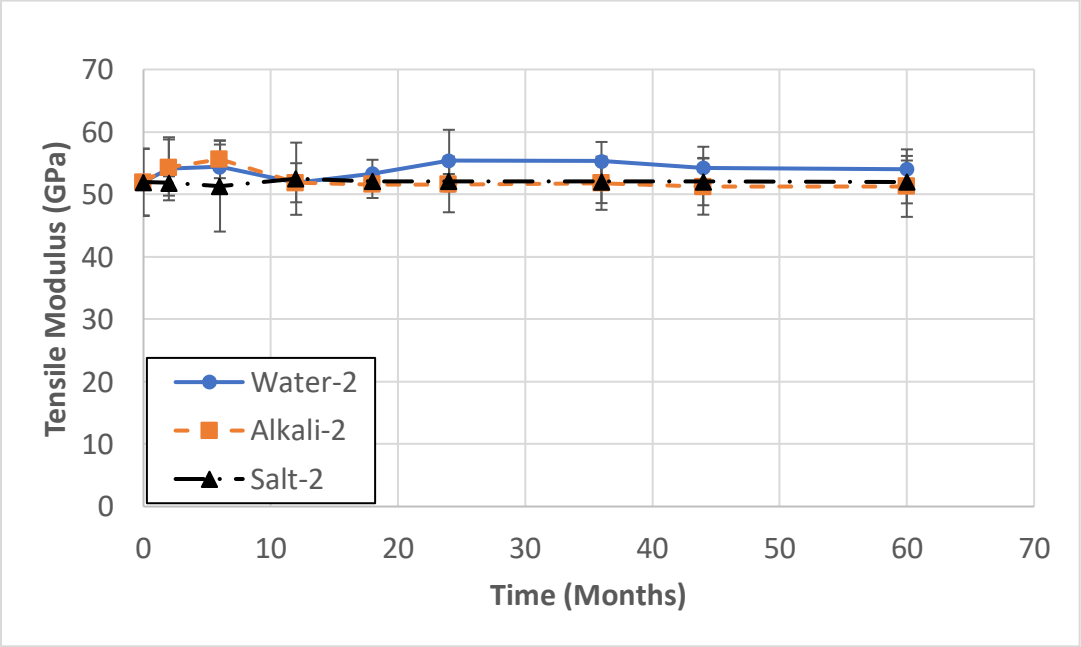

Figure 5-5. *(a). Change in tensile strength of the single-layered composites as a function of time of immersion and solution type. (b). Change in tensile modulus of the single-layered composites*

as a function of time of immersion and solution type. (c). Change in tensile strength of the two-layered composites as a function of time of immersion and solution type. (d). Change in tensile modulus of the two-layered composites as a function of time of immersion and solution type.

The two layered composites, as expected, do show a higher level of shear strength deterioration than the single layered composite specimens. It is of interest to compare the levels of deterioration of the specimens at a few specific time periods, as in Table 5-4, noting that the initial steep drops in strength occur within two months for the single layered specimens and six months for the two layered samples.

(a)

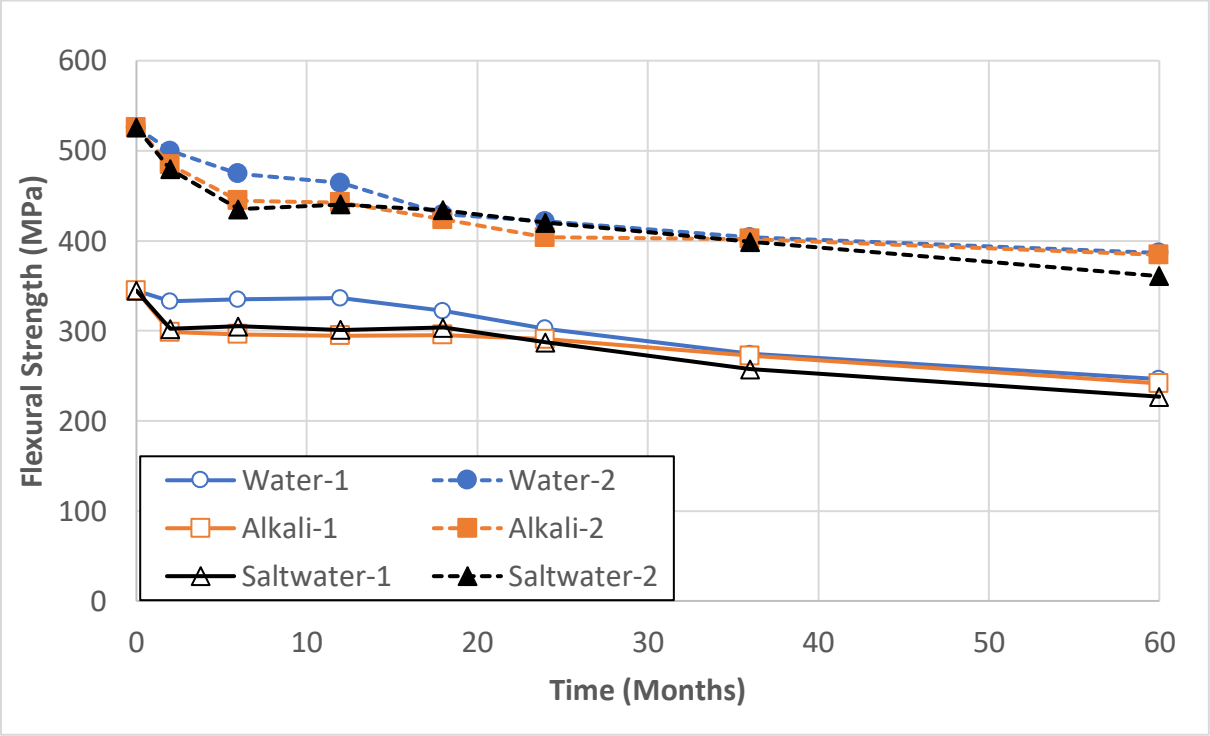

(b)

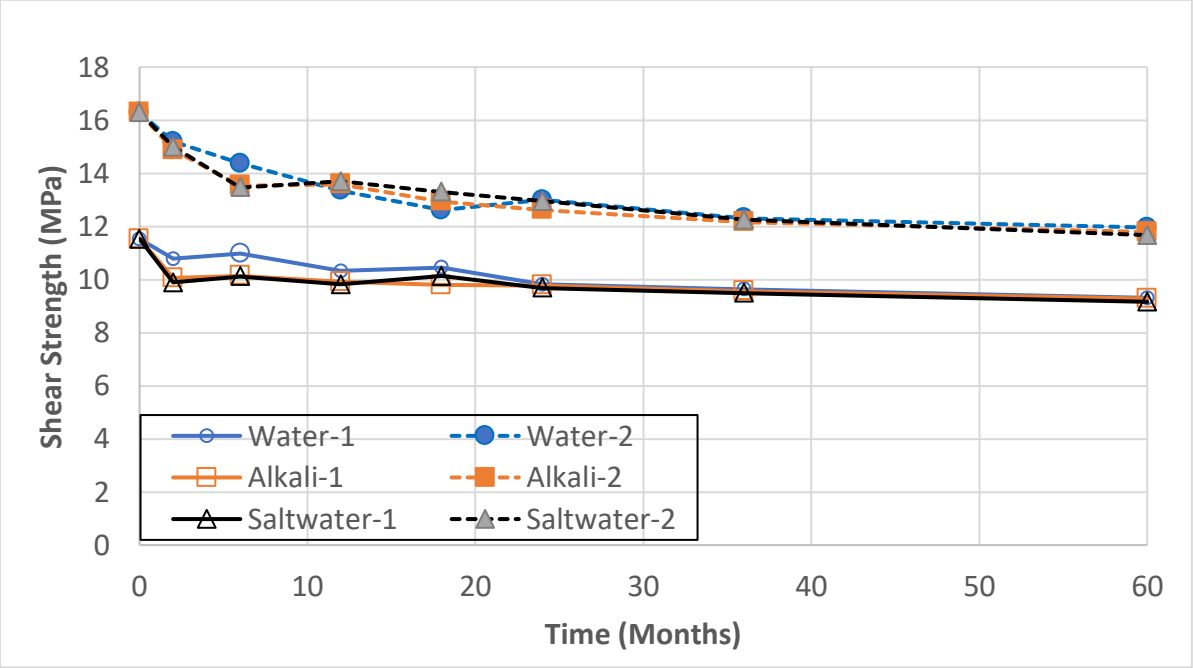

Figure 5-6. *Change in shear strength as a function of exposure (The notations of -1 and -2 relate to single layered and 2-layered composites, respectively). Change in shear strength as a function of exposure (The notations of -1 and -2 relate to single layered and 2-layered composites, respectively)*

Table 5-3. *Time (hours) to Attain First Stage Equilibrium Moisture Content as a Function of Solution and Number of Layers*

	Water	**Alkali**	**Saltwater**
Resin	11,400	11,267	13,095
Single Layered Composite	363	465	652
Two Layered Composite	1,586	624	1,160

Abanilla et al. [1] reported a drop of about 29% in interlaminar shear strength of a two layered wet layup carbon epoxy system after a hundred weeks of immersion in deionized water, 5% NaCl solution, and alkali solution, which is a bit higher than the level seen in this study after 24 months. Botelho et al. [58] reported a drop of 21% in interlaminar shear strength for carbon/epoxy exposed to high humidity at 40^{o}C and Jose-Trujillo [54] reported a drop of 20% in the strength of carbon/epoxy specimens after aging in seawater using specimens with the same span to depth ratio (16:1) used in this study whereas Murthy et al. [59] reported drops of 48% and 34% in flexural strength and tensile strength, respectively, after immersion in seawater covering the range reported in this study. It is noteworthy, however, that the time period of exposure is significantly longer in the current study as compared to previous studies reported in the literature. The development of near asymptotic response over longer periods of exposure strongly suggest that estimates made through models that extrapolate deterioration from shorter time periods of exposure may be overestimating effects leading to excessively high and erroneous predictions of property changes.

Table 5-4. *Percentage Drop in Flexural and Shear Strength*

(W: Water, A: Alkali/Concrete Leachate, S: Saltwater)

Period of Immersion		**Single Layered Composite**						**Two Layered Composite**					
		σ_f			**τ_f**			**σ_f**			**τ_f**		
		W	**A**	**S**	**W**	**A**	**S**	**W**	**A**	**S**	**W**	**A**	**S**
Initial Drop: 2 months		3	13	12	7	13	14	-	-	-	-	-	-
Initial Drop: 6 months		-	-	-	-	-	-	10	15	17	12	17	17
24 months		12	16	17	15	15	16	20	23	20	20	23	21
60 months		29	30	34	19	20	21	27	27	31	27	28	28

5.4. SUMMARY AND CONCLUSIONS

Fiber reinforced polymer matrix composites provide significant advantages for use in the rehabilitation of civil infrastructure. Their widespread use is, however, constrained due to a lack of a comprehensive understanding of long-term durability. Most durability studies are conducted over short-time periods which are not long enough to provide a basic understanding of the mechanisms of deterioration.

In the tests reported here, ambient cure wet layup carbon-epoxy composites used widely for the external strengthening of concrete structural elements were immersed in water, saltwater, and concrete leachate solution for periods between 44 and over 60 months. Moisture uptake was

shown to be best described using a two-stage model with coefficients D and k, describing the diffusion and relaxation/deteriorative stages, respectively. The values of k for the samples immersed in concrete leachate are substantially higher than that from the two other solutions due to greater deterioration in the fiber matrix bond and higher levels of hydrolytic degradation of the polymer network. In all cases except that of immersion in water where T_g is noted to continue to decrease over the entire time period of immersion, T_g is seen to reach an initial minimum followed by fluctuations and small increases with an increase in the time of exposure, with the initial drop coinciding with the time periods that are largely diffusion dominated. The largest drop in T_g is after immersion in concrete leachate with the minimum being as a result of immersion in water. The loss tangent peak can be linked to the degree of molecular mobility its changes are indicative of changes in degree of cross-linking and network structure. tan δ height shows an initial decrease followed by an increase and then a continued decrease. Immersion in saltwater and concrete leachate solutions results in a larger drop than that from water. This drop was followed by an increase in tan δ height which is followed by a continuous decrease suggesting competition between mechanisms of moisture induced plasticization, postcure, and degradation through fiber matrix debonding and micro-cavitation level deterioration. The post peak drop in tan δ was the fastest in the case of saltwater immersion and the slowest, as well as the least in value, from immersion in water, again emphasizing the added role of salts in saltwater and concrete leachate on deterioration in the composite. The maximum deterioration in tensile strength is through immersion in saltwater with the least being due to water which is in line with results reported earlier for wet layup carbon-epoxy composites in a range of solutions. In comparison there is very little change, or difference, in stiffness emphasizing the fiber dominated performance in this mode although there are initial increases due to progression of postcure. While unidirectional composites

show good retention of tensile properties in the fiber direction, they are more susceptible to crack propagation and interlayer separation under flexural and shear loading, and drops in both flexural and shear strength are noted over time although there are imperceptible differences over the long-term as a result of the type of solution. As in the case of tensile properties, and the glass transition temperature, the response is asymptotic over the longer term immersion periods suggesting that predictions based on short-term exposure may be overestimating effects leading to excessively high and erroneous predictions of property changes and the consequent use of overly conservative design factors to address durability.

The study emphasizes the need for the development of a comprehensive understanding of mechanisms, often competing, that affect the durability of ambient cure composites that are expected to have long service-lives in harsh environmental conditions. Results from short-term tests, including using accelerated approaches, may not provide reliable data especially when basic phenomena such as saturation of moisture uptake are not attained. The results show the need to differentiate between effects of post-cure, from those of relaxation and other reversible phenomena, and those related to irreversible changes in polymer and composite morphology and microstructure.

5.5. REFERENCES

[1] Abanilla MA, Li Y, Karbhari VM. Durability characterization of wet layup graphite/epoxy composites used in external strengthening. Composites: B. 2006; 37: 200-212.

[2] Uthaman A, Xian G, Thomas S, Wang Y, Zheng Q, Liu X. Durability of an epoxy resin and its carbon fiber-reinforced polymer composite upon immersion in water, acidic, and alkaline solutions. Polymers. 2020; 12, 614: 24 pp.

[3] Mosallam AS, Nasr A. Structural performance of RC shear walls with post-construction openings strengthened with FRP composite laminates. Composites: B. 2017; 115: 488-504.

[4] Quino G, Pellegrino A, Tagarielli VL, Petrinic N. Measurements of the effects of pure and saltwater absorption on the rate dependent response of an epoxy matrix. Composites: B. 2018; 146: 213-221.

[5] Tual N, Carrere N, Davis P, Bonnemains T, Lolive E. Characterization of seawater ageing effects on mechanical properties of carbon/epoxy composites for tidal turbine blades. Composites: A; 2015; 78: 380-389.

[6] Zafar A, Bertocco F, Schjodt-Thomsen J, Rauhe JC. Investigation of long term effects of moisture on carbon fibre and epoxy matrix composites. Composites Science and Technology. 2012; 72: 656-666.

[7] Scott P, Lees JM. Water, salt water, and alkaline solution uptake in epoxy thin films. Journal of Applied Polymer Science. 2013; 130(3): 1898-1908.

[8] Marouani S, Curtil L, Hamelin P. Ageing of carbon/epoxy and carbon/vinylester composites used in the reinforcement and/or repair of civil engineering structures. Composites: B. 2012; 43: 2020-2030.

[9] Karbhari VM. Long-term hydrothermal aging of carbon epoxy materials for the rehabilitation of civil infrastructure. Composites: A. 2022; 153: 106705.

[10] Karbhari VM, Abanilla MA. Design factors, reliability, and durability prediction of wet layup carbon/epoxy used in external strengthening. Composites: B. 2007; 38: 10-23.

[11] Xin H, Liu Y, Mosallam A, Zhang Y, Wang C. Hygrothermal aging effects on flexural behavior of pultruded glass fiber reinforced polymer laminates in bridge applications. Construction and Building Materials. 2016; 17: 237-247.

[12] Lettieri M, Frigione M. Natural and artificial weathering effects on cold cured epoxy resins. Journal of Applied Polymer Science. 2011; 119: 1635-1645.

[13] Adamson MJ. Thermal-expansion and swelling of cured epoxy-resin used in graphite-epoxy composite-materials. Journal of Materials Science. 1980;15(7): 1736-1745.

[14] Zhou JM, Lucas JP. Hygrothermal effects of epoxy resin. Part I: The nature of water in epoxy. Polymer 1999; 40(20):5505-5512.

[15] Nogueira P, Ramirez C, Torres A, Abad MJ, Cano J, Lopez J, Lopez-Bueno I, Barral L. Effect of water sorption on the structure and mechanical properties of an epoxy resin system. Journal of Applied Polymer Science. 2001; 80(1): 71-80.

[16] Hahn HT. Residual-stresses in polymer matrix composite laminates. Journal of Composite Materials. 1976; 10(Oct): 266-2678.

[17] Xiao GZ, Delamar M, Shanahan MER. Irreversible interactions between water and DGEBA/DDA epoxy resin during hydrothermal aging. Journal of Applied Polymer Science. 1997; 65(3): 449-458.

[18] Chateauminois A, Chabert B, Soulier JP, Vincent L. Dynamic-mechanical analysis of epoxy composites plasticized by water - artifact and reality. Polymer Composites. 1995; 16(4): 288-296.

[19] Mazor A, Broutman, LJ, Eckstein BH. Effect of long-term water exposure on properties of carbon and graphite fiber reinforced epoxies. Polymer Engineering and Science. 1978; 18(5): 341-349.

[20] Ellis TS, Karasz FE. Interaction of epoxy resins with water: The depression of glass transition temperature. Polymer. 1984; 25(5): 664-669.

[21] Lee MC, Peppas NA. Water transport in epoxy resins. Progress in Polymer science. 1993; 47: 1349-1359.

[22] Lee MC, Peppas NA. Water transport in graphite/epoxy composites. Journal of Applied Polymer Science. 1993; 47: 1349-1359.

[23] Loos AC, Springer GS. Moisture absorption of graphite-epoxy composites immersed in liquids and in humid air. Journal of Composite Materials. 1979; 13(2): 131-147.

[24] McKague EL, Jr., Reynolds JD, Halkias JE. Swelling and glass transition relations for epoxy matrix material in humid environments. Journal of Applied Polymer Science. 1978; 22: 1643-1654.

[25] Mijovic J, Lin K-F. The effect of hygrothermal fatigue on physical/mechanical properties and morphology of neat epoxy resin and graphite/epoxy composite. Journal of Applied Polymer Science. 1985; 30(6): 2527-2549.

[26] Chin JW, Nguyen T, Aouadi K. Sorption and diffusion of water, salt water, and concrete pore solution in composite matrices. Journal of Applied Polymer Science. 1999; 71: 483-492.

[27] Wang B, Li D, Xian G, Li C. Effect of immersion in water or alkali solution on the structures and properties of epoxy resin. Polymers. 2021; 13, 1902: 14 pp.

[28] Xin H, Liu Y, Mosallam A, Zhang Y. Moisture diffusion and hygrothermal aging of pultruded glass fiber reinforced polymer laminates in bridge application. Composites B, 2016; 100: 197-207.

[29] Marouni S. Curtil L, Hamelin P. Composites realized by hand lay-up process in a civil engineering environment: initial properties and durability. Materials and Structures. 2008; 41: 831-851.

[30] Helbling C, Abanilla M, Lee L, Karbhari VM. Issues of variability and durability under synergistic exposure conditions related to advanced polymer composites in the civil infrastructure. Composites Part A. 2006; 37(8): 1102-1110.

[31] Atadero RA, Lee L, Karbhari VM. Consideration of material variability in reliability analysis of FRP strengthened bridge decks. Composite Structures. 2005; 70(4): 430-443.

[32] Xian G, Karbhari VM. DMTA based investigation of hygrothermal ageing of an epoxy system used in rehabilitation. Journal of Applied Polymer Science. 2007; 104(2): 1084-1094.

[33] Xian G, Karbhari VM. Segmental relaxation of water-aged ambient cured epoxy. Polymer Degradation and Stability. 2007: 92:1650-1659.

[34] Karbhari VM, Murphy K, Zhang S. Effect of concrete based alkali solutions on short-term durability of E-glass/vinylester composites. Journal of Composite Materials. 2002; 36(17): 2101-2121.

[35] Browning CE. The mechanisms of elevated temperature property losses in high performance structural epoxy resin materials after exposures to high humidity environments. Polymer Engineering and Science. 1978; 18(1): 16-24.

[36] Shen CH, Springer GS. Moisture adsorption and desorption of composite materials. Journal of Composite Materials. 1976; 10: 2-20.

[37] Carter HG, Kibler KG. Langmuir-type model for anomalous moisture diffusion in composite resins. Journal of Composite Materials. 1978; 12(2): 118-131.

[38] Moy P, Karasz FE. Epoxy water interactions. Polymer Engineering and Science. 1980; 20(4): 315-319.

[39] Bao L-R, Yee AF, Lee CY-C. Moisture absorption and hygrothermal aging in a bismaleimide resin. Polymer. 2001; 42: 7327-7333.

[40] Diamant Y, Marom G, Broutman LJ. The effect of network structure on moisture absorption of epoxy resins. Journal of Applied Polymer Science. 1981; 26: 3015-3025.

[41] Maggana C, Pissis P. Water sorption and diffusion studies in an epoxy resin system. Journal of Polymer Science: B- Polymer Physics. 1999; 37: 1165-1182.

[42] Chateauminois A, Vincent L, Chabert B, Soulier JP. Study of the interfacial degradation of a glass-epoxy composite during hygrothermal ageing using water diffusion measurements and dynamic mechanical thermal analysis. Polymer. 1994; 35(22): 4766-4774.

[43] Tomblin JS, Salah L, Ng YC. Determination of temperature/moisture sensitive composite properties. DOT/FAA/AR-0 1/40. US Department of Transportation. Federal Aviation Administration. September 2001.

[44] Kahraman R, Al-Harthi H. Moisture diffusion into aluminum powder filled epoxy adhesive in sodium chloride solutions. International Journal of Adhesion and Adhesives. 2005; 25(4): 337-341.

[45] Tai RCL, Szklarska-Smialowska Z. Effect of fillers on the degradation of automotive epoxy adhesives in aqueous solution. Journal of Material Science. 1993; 28: 6199-6204.

[46] Yang Q, Xian G, Karbhari VM. Hygrothermal aging of an epoxy adhesive used in FRP strengthening of concrete. Journal of Applied Polymer Science. 2008; 107(4): 2607-2617.

[47] Hagen R, Salmen L, Lavebratt H, Stenberg B. Comparison of dynamic mechanical measurements and Tg determinations with two different instruments, Polymer Testing. 1994: 13: 113-128.

[48] Zhou J, Lucas JP. Hygrothermal effects of epoxy resin. Part II: variations of glass transition temperature. 1999; 40: 5513-5522.

[49] Birger S, Moshonov A, Kenig S. The effects of thermal and hygrothermal aging on the failure mechanisms of graphite-fabric epoxy composites subjected to flexural loading. Composites. 1989; 20(4): 341-348.

[50] Wright WW. The effect of diffusion of water into epoxy resins and their carbon fiber reinforced composites. Composites. 1981; 12(3): 201-205.

[51] Barton JM, Greenfield DCL. The use of dynamic mechanical methods to study the effect of absorbed water on temperature-dependent properties of an epoxy resin-carbon fibre composite. British Polymer Journal. 1986; 18(1): 51-56.

[52] DeNeve B, Shanahan MER. Water absorption by an epoxy resin and its effect on the mechanical properties and infra-red spectra. Polymer. 1993; 34(24): 5099-5105.

[53] Kafodya I, Xian G. Durability study of pultruded CFRP plates under sustained bending in distilled water and seawater immersions: Effects on the visco-elastic properties. International Journal of Materials and Metallurgical Engineering. 2015. 9(2): 137-143.

[54] Jose-Trujillo E, Rubio-Gonzalez C, Rodriguez-Gonzalez JA. Sea water ageing effect on the mechanical properties of composites with different fiber and matrix types. Journal of Composite Materials. 2019; 53(23): 3229-3241.

[55] Madhukar MS, Drzal LT. Fiber-Matrix adhesion and its effect on composite mechanical properties: II. Longitudinal (0^o) and transverse (90^o) tensile and flexural behavior of graphite/epoxy composites. Journal of Composite Materials. 1991; 25: 958-991.

[56] Schadler LS, Koczak MJ, Amer MS. Environmental effects on interface behavior in graphite/epoxy single fiber composites. Proceedings of the Materials Research Society Symposium, Vol. 385. 1995: 155-166.

[57] Weitsman YJ, Elahi M. Effects of fluids on the deformation, strength and durability of polymeric composites – an overview. Mechanics of Time Dependent Materials. 2000; 4: 107-126.

[58] Botelho EC, Pardini LC, Rozende MC. Hygrothermal effects on the shear properties of carbon fiber/epoxy composites. Journal of Materials Science. 2006; 41: 7111-7118.

[59] Murthy HNN, Sreejith M, Krishna M, Sharma SC; Sheshadri TS. Sea water durability of epoxy/vinylester reinforced with glass/carbon composites. Journal of Reinforced Plastics and Composites. 2010; 29(10): 1491-1499.

CHAPTER 6. CONCLUSION AND FUTURE WORK

This dissertation provides an examination of the long-term durability of fiber-reinforced polymer (FRP) composites, used in civil infrastructure, marine, and offshore applications. Through extensive literature review and analysis of experimental data, significant findings on the impact of moisture and environmental exposure on the performance and degradation of these materials have been identified.

In the first paper, the study underscores the significant impact of environmental exposure, specifically moisture in the form of humidity and immersion, on FRP composites. Moisture uptake in these composites is a complex process influenced by various factors such as exposure conditions, constituent materials, including interactions with the polymer matrix and sorption into the composite structure, which can be exacerbated by damage such as microcracks and fiber–matrix debonding. The rate and extent of moisture uptake vary significantly with environmental conditions, particularly temperature and humidity, as well as conditions of immersion and are not always adequately described by the commonly used Fickian diffusion model. The study highlighted the inadequacies of the traditional Fickian diffusion model, which fails to account for the complex, multi-phase nature of moisture uptake, necessitating more advanced multi-stage models that account for both diffusion and relaxation/deterioration mechanisms. Various models, such as Henry's law, Freundlich's relation, and Langmuir response, offer different approaches to describe the range of moisture uptake response. For example, the Langmuir model was not sufficient to take into account the long-term effects such as relaxation. As a result, alternative models—such as two-phased Fickian and structural modifications model —have been developed to better account for deviations from Fickian behavior. The paper emphasizes the importance of

selecting an appropriate model based on material characteristics, length of assessment, environmental exposure, and operative mechanisms. It also highlights the need for further research to develop a comprehensive understanding of moisture uptake mechanisms and to link these mechanisms directly to predictions of long-term durability.

The second study focused on changes glass transition temperature (T_g) in response to moisture serve as an indicator of both short-term and long-term performance shifts . Glass transition temperature is an important assessment for measuring durability, as it strongly influenced by phase morphology, and chemical composition, and it helps identify changes caused by moisture uptake. Due to the sorption of moisture/solution, the glass transition temperature decreases, which in turn lowers the threshold service temperature. Although numerous studies and models exist for prediction T_g , most assume a linear decrease and a rapid initial decline in T_g with temperature over time. However, extensive experimental data, including the long-term data used for this study and those of others, indicates a more complex behavior and different pattern. The data indicates that T_g initially declines rapidly with moisture uptake but then reaches a threshold beyond which the decrease slows significantly or plateaus, exhibiting asymptomatic behavior after a transition threshold. This transition threshold can be related to competing mechanisms of plasticization and postcure. The extent of this decrease is influenced by factors such as temperature, moisture content, polymer's molecular structure, cross-link density, and postcure reactions. The impact of this finding is significant for understanding the long-term behavior and durability of FRP composites. The impact of exposure temperature and moisture content on T_g, emphasizing the need for precise T_g measurements to assess the true state of the material over time.

Although Fickian models are widely used to study the moisture uptake behavior in composite materials, long-term data reveal that relaxation and deterioration processes must also be considered. The model presented in the third study distinguishes three distinct phases: a diffusion-dominated initial regime, a transition phase, and a longer-term phase where material relaxation/deterioration dominates. The relaxation-dominated phase, in particular, involves irreversible damage mechanisms that are often obscured when only a single relaxation constant k is used. Therefore, employing correction and modification factors is employed for accurately capturing these differences by inclusion of damage terms to the diffusion and relaxation coefficients. Moreover, the research demonstrated that both moisture uptake and glass transition temperature (T_g) responses are temperature-dependent, suggesting that accelerated aging tests conducted at high temperatures may not accurately replicate real-world conditions. Additionally, the study established a significant correlation between moisture-induced changes in T_g and flexural performance, indicating that both properties deteriorate in a similar manner under moisture exposure. These insights underscore the need for further investigation into how moisture affects material degradation at the fiber-matrix interface and within the polymer network.

The fourth study extended the investigation to various environmental exposures, including water, saltwater, and concrete leachate. It was observed that different environments lead to varying degrees of material deterioration, with saltwater and concrete leachate causing the most severe effects. The relaxation/deterioration effects are notably higher for samples in concrete leachate, reflecting greater deterioration in fiber-matrix bonds and increased polymer network hydrolysis. Glass transition temperature (T_g) initially decreased rapidly, followed by fluctuations and minor increases, with the most significant drop occurring in concrete leachate. The loss tangent ($tan\ \delta$)

showed a pattern of initial decrease, followed by an increase and continued decline, indicating interactions between moisture-induced plasticization, postcure, and degradation mechanisms. Saltwater and concrete leachates caused the largest decreases in T_g and $tan\ \delta$, while water caused the least. Tensile strength deteriorated most in saltwater, aligning with earlier findings, while stiffness changes were minimal, highlighting fiber-dominated performance. Unidirectional composites maintained tensile properties but showed reduced flexural and shear strength over time, with long-term responses suggesting that short-term predictions may overestimate property changes and lead to overly conservative design factors. The study emphasized the role of competing degradation mechanisms—such as plasticization, post-cure, and hydrolytic degradation—in influencing material performance. The findings advocate for a more refined approach to design and testing, considering long-term effects rather than relying solely on short-term accelerated tests.

Future work should extend the current research by incorporating the effects of fabric thickness and fiber areal weight into a more comprehensive model is essential. The behavior of composites with multiple fabric layers is not merely a summation of individual layer properties; instead, complex interactions between layers affect overall performance. Adding layers increases the fiber volume fraction due to compaction, which alters the composite's mechanical and physical properties. Compaction increases the tortuosity of moisture diffusion pathways, significantly impacting moisture uptake kinetics and consequently, affecting the glass transition temperature (T_g). Compaction and intermingling also influence delamination susceptibility and the homogeneity of moisture distribution. Understanding these effects is crucial for optimizing manufacturing processes, predicting moisture-related issues, and ensuring material performance

and durability. Future research should focus on developing multi-scale models that integrate both micro- and macro-scale phenomena, providing a more comprehensive understanding of how microstructural changes, moisture uptake, and T_g variations impact the mechanical properties of FRP composites.

In addition, a mechanistic model that incorporates both micro- and macromechanical principles should be developed. It must account for fiber-matrix bond degradation, changes in the resin network and morphology, moisture-induced plasticization, and postcure processes to predict long-term performance based on specific constituent materials and exposure conditions. It should also consider rate-dependent and relaxation/deterioration-dependent sorption mechanisms, degradation at interface levels, as well as capillary and wicking phenomena.

The relationship between changes in glass transition temperature (T_g) and degradation at the fiber-matrix interface also requires investigation. This research could provide insights into moisture-induced deterioration mechanisms and help refine predictive models by linking T_g changes to specific degradation processes. Additionally, studying the correlation between the fabric areal weight, glass transition temperature, and flexural strength is valuable. It has been observed that composites with higher fabric weight show greater decline in both T_g and flexural strength, indicating a correlation between these properties and increased deterioration at the interphasial and intralaminar regions. Future work should focus on expanding these findings to develop more detailed models and refine predictions for long-term performance under varying environmental conditions.

Finally, the long-term durability of FRP composites under cyclic environmental conditions, such as wet-dry cycles and temperature fluctuations, should be studied to better simulate practical scenarios. Addressing these areas will advance the understanding of FRP composite behavior, leading to effective predictive models and performance assessments.